UNIVERSITY OF SHEFFIELD -
DEPARTMENT OF BIOMEDICAL SCIENCES

# *Analysis of a fih Mutation in Zebrafish*

A thesis submitted for the degree of
Doctor of Philosophy

**Emma Clare Judson**

**01 September 2012**


# Abstract

Hypoxic signaling is involved in homeostatic and developmental angiogenic and neurogenic proliferation and differentiation as well as modulating many disease processes that result in or from restricted blood flow. A better understanding of this pathway and how other pathways interact with it is important for progression towards targeted therapeutics.

Von Hippel Lindau *(vhl-/-)* zebrafish embryos demonstrated hypoxic phenotypes such as hyperventilation, polycythemia and an altered vascular network (van Rooijen et al., 2009). The *fih-/-* embryos showed no morphological phenotype and the adults are fully viable and fertile. By combining the two lines it was possible to investigate the effect of a double knock out of these genes and the effect this had on downstream targets. The first hypothesis to test, the first observation to make, was to assess the effect of the loss of *fih* on both wild type embryos and on *vhl* null embryos. Given the roles of *fih* and *vhl* are independent of each other in regulating HIF function (FIH regulating HIF function, while VHL regulates HIF turnover), the hypothesis in this case would be that the loss of *fih* alone may not show dramatic phenotypes, however in the context of the loss of *vhl* it may alter or exacerbate phenotypes observed in the organisms where *vhl* was lost.

This was proved to be correct when it came to assessment of global and morphological phenotypes. The loss *fih* resulted in no significant changes compared with wild type embryos in initial observations; however the loss of both *fih* and *vhl* altered the known *vhl-/-* phenotype, which indicated a role for *fih*, under conditions of de-regulated hypoxia inducible factor (HIF), in enhancing hypoxic signaling. Expression levels of Hif targets, *phd3* and *vegfa*, were assessed and showed that these were elevated in the *vhl-/-* zebrafish line and further elevated in *fih-/-;vhl-/-* embryos, by *in situ* hybridisation. Further analyses of the downstream effects of the loss of *fih* were assessed using microarray analysis and further validated using qRT-PCR. Preliminary results suggested that on a transcriptional level, *fih* in isolation was not influencing expression and that *fih* functioned mainly through HIF.

Vascular branching was altered in the *vhl-/-* zebrafish line compared to wild-type siblings, and this was exacerbated in the *fih-/-;vhl-/-* embryos. This correlated with increased *vegf* expression and a corresponding increase in endothelial cell numbers.

The *fih-/-;vhl-/-* embryos exhibited decreased blood flow along the aorta, which ceased at 5dpf despite continuation of the heart beat. The *fih-/-* embryos exhibited an increase in blood velocity along the aorta with a corresponding increase in heart rate at the same stage. Our data suggested that Fih had an essential role in the regulation of heart rate in the zebrafish and, in combination with *vhl*; it influenced formation and functionality of blood vessels by affecting the hypoxic signaling pathway.

Also investigated were correlations between the zebrafish model of *fih* loss and those published in the mouse, and several connections and corroborations were made. However there was also scope, in the zebrafish, for the proposal of a potential mechanism of action which was not proposed in the mouse model. Microarray analysis revealed that, specifically in the *fih* null embryos, two key genes in the renin angiotensin system were down regulated. Since this is a mechanism by which fluid dynamics are regulated, and since there have been observations of altered blood flow dynamics in double mutants, further investigation as to the potential role of this homeostatic mechanism and its potential regulation by *fih* are needed to further investigate these findings.

A second hypothesis that was proposed was that lead by a study by Lee et al, which proposed a model whereby the three proteins, FIH, VHL and HIF are required to bind together with VHL acting as a functional bridge in order to result in downstream effects (Lee et al., 2003). In this case a loss of *vhl* would disrupt the hydroxylation of HIF-α by *fih* as well. The hypothesis in this case would therefore be that the loss of *fih* as well, in an individual that had lost *vhl* function, would result in no alteration in the phenotypes observed. This hypothesis was shown not to be supported by the data and further investigation into possible interactions between the proteins would need to be assessed in order to ascertain the discrepancy.

# Table of Contents

# Table of Figures

# Index of Tables

# Abbreviations and Nomenclature

| Abbreviation | Definition |
|---|---|
| **AAH** | Aspartyl-(Asparaginyl) B-Hydroxylase |
| **ACE2** | Angiotensin Converting Enzyme 2 |
| **ADAM** | A Disintegrin And Metallopeptidase Domain |
| **ADHD** | Attention-Deficit Hyperactivity Disorder |
| **ADIPOQL** | Adiponectin |
| **ADIPOR** | Adiponectin Receptor |
| **ADM** | Adrenomedullin |
| **AGT** | Angiotensinogen |
| **AHR** | Aryl Hydrocarbon Receptor |
| **ALAS** | Aminoelvulinase Δ-Synthase |
| **AMPK** | 5’ Adenosine Monophosphate-Activated Protein Kinase |
| **AMB** | Amphoteracin B |
| **AMY** | Amylase |
| **ANGPT** | Angiopoietin |
| **ANG** | Angiotensin I |
| **APAF** | Apoptotic Protease Activating Factor |
| **APE1** | AP Endonuclease |
| **APLN** | Apelin |
| **APPB** | Amyloid Beta Precursor Protein (Cytoplasmic Tail) Binding Protein |
| **AR** | Ankyrin Repeat |
| **ARD** | Ankyrin Repeat Domain |
| **ARD1** | Arrest-Defective Protein 1 |
| **ARNT** | Aryl Hydrocarbon Receptor Nuclear Translocator |
| **ASN** | Asparagine |
| **AT1AR** | Angiotensin II Type 1 Receptor |
| **ATP** | Adenosine – 5’- Triphosphate |
| **B-Actin** | Beta Actin |
| **BAD** | Bcl-2 Antagonist Of Cell Death |
| **BAG** | Bcl-2 Associated Athanogene |
| **BAXA/B** | Bcl-2 Associated X Protein |
| **BAT** | Brown Adipose Tissue |
| **BCL** | B-Cell Leukaemia/Lymphoma |
| **BDKRB** | Bradykinin Receptor |
| **bHLH** | Basic Helix-Loop-Helix Motif |
| **BIK** | Bcl-2 Interacting Killer |
| **BMF** | Bcl-2 Modifying Factor |
| **BNP3l** | Bcl-2/Adenovirus E1B Interacting Protein 3-Like |
| **CA** | Carbonic Anhydrase |
| **CAD** | C-Terminal Transactivtation Domain |
| **CASP** | Caspase |
| **CBP** | CREB Binding Protein |
| **CCRCC** | Clear Cell Renal Cell Carcinoma |
| **CDKN** | Cyclin-Dependent Kinase Inhibitor |
| **CDP/Cut/Cux** | Cut-Like Homeodomain Protein |
| **CEL** | Carboxyl Ester Lipase |
| **CHF** | Congestive Heart Failure |
| **ChREBP** | Carbohydrate Response Element Binding Protein |
| **CHYMO** | Chymotrypsinogen |
| **CKI** | Cytokeratin |

| | |
|---|---|
| **CNS** | Central Nervous System |
| **CO-IP** | Coimmunoprecipitation |
| **COX** | Cytochrome C Oxidase Subunit |
| **CPA** | Carboxypeptidase |
| **CTRL** | Chymotrypsin |
| **CYP11B2** | Aldosterone Synthase |
| **ΔΔct** | Delta-Delta Ct |
| **DDIT** | DNA-Damage-Inducible Transcript |
| **DAPT** | N-[N-(3,5-Difluorophenacetyl)-L-Alanyl]-S-Phenylglycine-*T*-Butyl Ester |
| **Dll4** | Delta-Like Ligand 4 |
| **DLV** | Dorsal Longitudinal Vessel |
| **DMSO** | Dimethyl Sulfoxide |
| **dpf** | Days Post Fertilisation |
| **EC** | Endothelial Cell |
| **ECM** | Extracellular Matrix |
| **EDV** | End-Diastolic Volume |
| **EFL1** | Elongation Factor 1 |
| **EGLN** | Egg Laying |
| **ELA** | Elastase |
| **ENO** | Enolase |
| **EPO** | Erythropoietin |
| **ESV** | End-Systolic Volume |
| **EXO** | Exonuclease |
| **FABP** | Fatty Acid Binding Protein |
| **FGA** | Factor I - Fibrinogen |
| **FII** | Factor II - Thrombin |
| **FIII** | Factor III - Tissue Factor |
| **FV** | Factor V - Proaccelerin, Labile Factor |
| **FVIIi** | Factor Viii - Proconvertin Stable Factor |
| **FVIII** | Factor VIII - Antihemophilic Factor A |
| **FIX** | Factor IX - Antihemophilic Factor B, Christmas Factor |
| **FX** | Factor X - Stuart-Prower Factor |
| **FXIIIal** | Factor Xiiia Like |
| **FIH** | Factor Inhibiting HIF |
| **FLI1** | Friend-Leukaemia Integration 1 Transcription Factor |
| **FLIM** | Fluorescence Lifetime Imaging Microscopy |
| **FNG** | Fibrinogen I |
| **FLT1** | Fms-Related Tyrosine Kinase 1 (VEGFR1) |
| **FLT4** | Fms-Related Tyrosine Kinase 4 (VEGFR3) |
| **FRET** | Fluorescence Resonance Energy Transfer |
| **G6Pase** | Glucose 6-Phosphatase |
| **GALR** | Galactin Receptor |
| **GAPDH** | Glyceraldehydes-3-Phosphate Dehydrogenase |
| **GATA** | Transcription Factor Specific To 'GATA' Sequences |
| **GCGA** | Glucagon A |
| **GCGR** | Glucagon Receptor |
| **GCK** | Glucokinase |
| **GCSF** | Granulocyte Stimulating Factor |
| **GF** | Growth Factors |
| **GFP** | Green Fluorescent Protein |
| **GlUT1** | Glucose Transporter 1 (Slc2a) |
| **GM-CSF** | Granulocyte Macrophage-Colony Stimulating Factor |
| **GO** | Gene Ontology |
| **GOF** | Gain Of Function |

| | |
|---|---|
| **GOI** | Gene Of Interest |
| **GPIB** | Phosphoglucose Isomerase |
| **HAS** | Hif Ancillary Sequence |
| **HDAC** | Histone Deacetlylase |
| **HDL** | High Density Lipoprotein |
| **HER** | Epidermal Growth Factor Receptor Family |
| **HES** | Hairy And Enhancer Of Protein Family |
| **HEY** | Hes-Related Repressor Protein Family |
| **HFD** | High Fat Diet |
| **HIF** | Hypoxia Inducible Factor |
| **HK1** | Hexokinase1 |
| **HO-1/Hmox** | Heme-Oxygenase |
| **HPX/HK** | Hemopexin |
| **HRE** | Hypoxia Response Element |
| **ICAM-1** | Intercellular Adhesion Molecule 1 |
| **ICD** | Intracellular Domain |
| **IGF** | Insulin Growth Factor |
| **IGFBP** | Insulin Growth Factor Binding Protein |
| **IGFR** | Insulin Growth Factor Receptor |
| **iHOP** | Information Hyperlinked Over Proteins |
| **IκB** | Inhibitor Of Kappa B |
| **IKBKG** | Inhibitor Of Kappa Light Polypeptide Gene Enhancer In B-Cells, Kinase Gamma |
| **IL** | Interleukin |
| **INS** | Preproinsulin |
| **ISV** | Intersegmental Vessel |
| **ISWI** | Imitation Switch |
| **JMJC** | Jumonjic |
| **KDA** | Kila Dalton |
| **KDM** | Lysine (K)-Specific Demethylase |
| **KDR** | Kinase Insert Domain Receptor (VEGFR2) |
| **KKS** | Kallikrein-Kinin System |
| **KNGI** | Kininogen 1 |
| **L-685458** | (5S)-(T-Butixycarbon-Ylamino)-6-Phenyl-(4R)Hydroxy-(2R)Benzylhexanoyl)-L-Leu-L-Pheamide |
| **LCM** | Laser Capture Micro-Dissection |
| **LDH** | Lactate Dehydrogenase |
| **LDL/VLDL** | Low Density Lipoprotein/Very Low Density Lipoprotein |
| **LOF** | Loss Of Function |
| **LPHN** | Latrophillin |
| **MCA** | Middle Cerebral Artery |
| **MCL1** | Myeloid Cell Leukaemia Sequence 1 |
| **MCP-1** | Monocyte Chemoattractant Protein 1 |
| **MEF** | Mouse Embryonic Fibroblast |
| **MMP** | Matrix Metalloproteinases |
| **MPH** | Methylphenidate/Ritalin |
| **NAD(P)H** | Nicotinamide Adenine Dinucleotide Phosphate |
| **NCARE** | Negative Calcium-Response Element |
| **NICD** | Notch Intracellular Domain |
| **NID** | Nidogen |
| **NFKB** | Nuclear Factor Of Kappa B |
| **NFKBIA** | Nuclear Factor Of Kappa Light Polypeptide Gene Enhancer Of B-Cells Inhibitor Alpha |
| **NLS** | Nuclear Localisation Sequence |
| **NOS** | Nitric-Oxide Synthase |

| | |
|---|---|
| **NRARP** | Notch Regulated Ankyrin Repeat Domain Protein |
| **NRP** | Neuropillin |
| **NTC** | Non-Template Control |
| **ODDD** | Oxygen-Dependent Degradation Domain |
| **P300** | 300kd Co-Activator Protein |
| **PAI-1** | Plasminogen Activator Inhibitor-1 |
| **PAPASS** | 3'-Phosphoadenosine 5'-Phosphosulfate Synthase |
| **PARP** | Poly (ADP-Ribose) Polymerase Family |
| **PAS** | Per/Arnt/Sim |
| **PBS** | Phosphate Buffered Saline |
| **PCR** | Polymerase Chain Reaction |
| **PDGF** | Platelet-Derived Growth Factor |
| **PEPCK** | Phosphoenolylyruvate Carboxykinase |
| **PER** | Period |
| **PFA** | Para-Formaldehyde |
| **PFKFB** | 6-Phosphofructo-2-Kinase/Fructose-2,6-Biphosphatase |
| **PGC-1A** | Peroxisome Proliferator Activated Receptor Gamma Co-Activator Gene |
| **PGK1** | Phosphoglycerate Kinase |
| **PGAM1** | Phosphoglycerate Mutase 1 |
| **PGM1** | Phosphoglucomutase 1 |
| **PHD** | Prolyl Hydroxylase Domain |
| **PKMA** | Phosphofructokinase |
| **PKM2A** | Pyruvate Kinase |
| **PKCZ** | Protein Kinase C Z |
| **PKM** | Pyruvate Kinase |
| **PLG** | Plasminogen |
| **PPARG** | Peroxisome Proliferator Activated Receptor |
| **PRCP** | Polylcarboxypeptidase/Angiotensinase |
| **PROC** | Protein C |
| **PTH1A** | Parathyroid Hormone 1a |
| **PYGL** | Phosphorylase - Liver Glycogen |
| **QRT-PCR** | Quantitative Real-Time Polymerase Chain Reaction |
| **RAAS** | Renin-Angiotensin Aldosterone System |
| **RBC** | Red Blood Cell |
| **RBPJ** | Recombination Signal Binding Protein For Immunoglobulin Kappa J |
| **RBPSUH** | Recombining Protein Suppressor Of Hairless |
| **RCC** | Renal Cell Carcinoma |
| **RUNX1** | Runt Related Transcription Factor |
| **SAP** | Shrimp Alkaline Phosphatase |
| **SCLC** | Small Cell Lung Cancer |
| **SDF** | Stromal Cell Derived Factor |
| **SERPINDI** | Heparin Cofactor II |
| **SEI/SNF** | Switch/Sucrose Nonfermentable |
| **SHH** | Sonic Hedgehog |
| **SIM** | Single-Minded |
| **SIRNA** | Small Interfering RNA |
| **SM** | Smooth Muscle |
| **SMARC** | SWI/SNF, Matrix Associated, Actin Dependent Regulator Of Chromatin |
| **STAT** | Signal Transducer And Activator Of Transcription |
| **STIL** | Tal1 (Scl) Interrupting Locus |
| **TAD-N/TAD-C** | N- And C-Terminal Transactivtation Domain |
| **TAC** | Tachykinin |
| **TACR** | Tachykinin Receptor |
| **TAL** | T-Cell Acute Lymphocityic Leukaemia |

| | |
|---|---|
| **TAM** | Tumour-Associated Macrophages |
| **TCA** | Total Coagulation Assay |
| **TF** | Tissue Factor |
| **TG** | Triglycerides |
| **TGF** | Transforming Growth Factor |
| **TIE** | Tyrosine Kinase Receptor |
| **TILLING** | Targeting Induced Local Lesions In Genome |
| **TNFA** | Tumour Necrosis Factor A |
| **TNNT** | Troponin-T |
| **TPI1** | Triosephosphate Isomerase |
| **UCP** | Uncoupling Protein |
| **UPAR** | Urokinase Plasminogen Activator Receptor |
| **VEGF** | Vascular Endothelial Growth Factor |
| **VEGFR** | Vascular Endothelial Growth Factor Receptor |
| **VHL** | Von Hippel Lindau |
| **VLP/VHLH** | VHL-Like Protein |
| **VPF** | Vascular Permeability Factor |
| **VSMC** | Vascular Smooth Muscle Cell |
| **VVO** | Vesicular-Vacuolar Organelles |
| **WT** | Wild Type |
| **XIAP** | X-Linked Inhibitor Of Apoptosis |
| **XSU(H)** | Suppressor Of Hairless |
| **ZGC** | Zebrafish Gene Collection |

**Table 1:** *Abbreviations*

| ***Gene*** | **Homozygous wild type** | **Heterozygous mutant** | **Homozygous mutant** |
|---|---|---|---|
| ***fih*** | +/+ | +/- | -/- |

**Table 2:** *Notation of Genotype*

| Species | **Gene** | **Protein** |
|---|---|---|
| **Zebrafish** | *Fih* | Fih |
| **Human** | *FIH* | FIH |
| **Mouse** | *Fih* | FIH |

**Table 3:** *Notation Gene and Protein abbreviations for different species*

# Acknowledgements

I would like to acknowledge the support of my supervisor Dr Freek van Eeden along with the co-supervision of Dr Stephen Renshaw.

My advisors, Tim Chico and Tanya Whitfield have provided support where needed and challenged my understanding to prepare me for the in depth discussion and interpretation of the literature and my data.

I should also mention the members of my lab; Dr Robert Wilkinson, Dr Kiran Santhakumar, Dr Stone Elworthy, Dr Rosemary Kim, David Greenald, Eleanor Markham, Dr Oliver Watson and Dr Peter Novodvorsky for troubleshooting opportunities along with thoughtful discussion of the data in lab meetings.

Further support has come from Dr Sarah Walmsley and all the other members of our monthly Hypoxia Meetings.

I would like to mention the contribution of Dr Martin Gering in providing the *Tg(csl-venus)qmc61* notch reporter line and Dr Christopher Schofield in providing the *fih* specific inhibitors.

For the microarray I would like to acknowledge Dr Paul Heath for training in microarray techniques and his performing of the bioanalysis of the microarray samples, and Mr Andrew Platts for providing the use of the Agilent Microarray Scanner

For the high speed imaging, a microscope and camera owned by Dr Tim Chico, was used, and I would like to acknowledge that contribution, along with training in the use of the equipment and the processing of kymograph data by Caroline Grey.

I would also like to acknowledge Dr Martin Loxley for helping to optimise the zebrafish cholesterol assay.

I would also like to thank all the members of the CDBG Aquaria Staff for their support in the Zebrafish Facilities in keeping the fish healthy.

I would like to thank the Centre for Developmental Biology for funding the project.

I would also like to extend my heartfelt gratitude to my parents, siblings and friends for their ever present love and support throughout.

# 1 General Introduction

## 1.1 Causes and Consequences of Hypoxia

Decreases in environmental oxygen, or disruption of local metabolism by an imbalance between oxygen supply and consumption (Nangaku and Eckardt, 2007), can all cause hypoxia. The latter can have a variety of reasons; hypoventilation, restriction of ventilatory systems, reduced alveolar surface size or diffusion barriers (Uenoyama et al., 2010). In mammalian species, these changes in environmental oxygen are detected by the carotid body, which picks up acute changes in arterial blood oxygen levels and initiates systemic cardiac, vascular and respiratory responses to these changes (Prabhakar and Semenza, 2012). The carotid bodies are bilateral sensory organs located at the bifurcation of the common carotid artery (Prabhakar, 2000). They are made up of glomus type 1 chemoreceptor cells which, upon challenge with hypoxia, release neurotransmitters that set the level of electrical activity in the afferent fibers of the carotid sinus nerve (Rocher et al., 1988). The response to decreases in environmental oxygen is a highly regulated process that plays a role in normal physiology and initially leads to increased ventilation and cardiac output. In addition to these metabolic physiological adaptations, hypoxia prompts cells to induce vascular growth and haematopoiesis in order to maximise the body's access to available oxygen during hypoxia.

Systemic hypoxia is defined as an inadequate oxygenation of blood and tissues when demand exceeds supply leading to the need for corrective measure (Fahling and Persson, 2012). Distinct types of hypoxia can be defined by different manifestations of the process and different tissues in which it occurs. Anemic hypoxia occurs in response to reductions in hemoglobin levels or when hemoglobin is abnormal and cannot bind oxygen. This results in a reduction of oxygen-carrying capacity (Kertscho et al., 2012). The mechanism for detecting the difference between normal arterial oxygen and lowered venous oxygen that occurs in these cases is unknown (Fahling and Persson, 2012). Ischemic hypoxia can be the result of limited flow to a particular tissue or organ that means insufficient oxygen/blood supply is available, and this type of hypoxia can be associated with several disease processes, but also more simply with a

response to exercise (Edvinsson and Povlsen, 2011, Thijssen et al., 2011). This can result in limited glucose delivery and accumulation of metabolites that can also then go on to affect the cellular response (Fahling and Persson, 2012). Histotoxic hypoxia could indicate problems in peripheral gas exchange, meaning that cells can't absorb or utilize oxygen and carbon monoxide or cyanide poisoning could each be causes for this (Choi et al., 2010).

Molecular sensors to detect these changes in oxygen availability need to have low oxygen affinity and the method employed can be different under the different hypoxic conditions discussed (Bunn and Poyton, 1996). These can be potassium channels, mitochondria, members of the NAD(P)H oxidase family and prolyl hydroxylases (Fahling and Persson, 2012). On a cellular level hypoxia induces a systematic signaling cascade known as the hypoxic signaling pathway, leading to stabilisation of hypoxia inducible factor α (HIF-α) as the central transcription factor. This results in the activation of transcription of genes, which initiate the body's response to the reduced oxygen availability. This signaling pathway, along with downstream effects such as angiogenesis, plays a role in many vascular diseases in humans, including ischemic heart disease, stroke and cancer. For example, in cases such as in ischemic heart disease where a blockage has occurred in a vessel (Semenza, 2004), developing collateral vessels to remodel the blood vessels surrounding the blockage to re-route the supply can be seen to be beneficial. However, if HIF-α levels are allowed to accumulate, inappropriately in the heart, this can lead to these responses occurring aberrantly, which can lead to defective cardiac homeostasis and cardiomyopathy (Holscher et al., 2012).

Several studies have shown that vascular response can be enhanced by an increase in vascular endothelial growth factor (VEGF) mRNA expression, a hypoxic signaling target, with increased hypoxia inducible factor 1α (HIF-1$\alpha$) activity (Sung et al., 2005, Alidoosti et al., 2011, Ong and Hausenloy, 2012). To name a few examples, it has also been shown that HIF-1$\alpha$ was accumulated following renal ischemia and also in reperfusion in human proximal tubule cells after hypoxia/reperfusion (H/R), in rat kidneys after ischemia/reperfusion (I/R) and in human biopsies after transplants. This induction of HIF-1α expression was reported to be crucial for proxial tubule epithelial cell survival and recovery (Conde et al., 2012). Other reports describe the various effects of

stabilisation of HIF-1α on angiogenesis in skeletal muscle (Pajusola et al., 2005) and hind limb ischemia (e.g.((Patel et al., 2005b)).

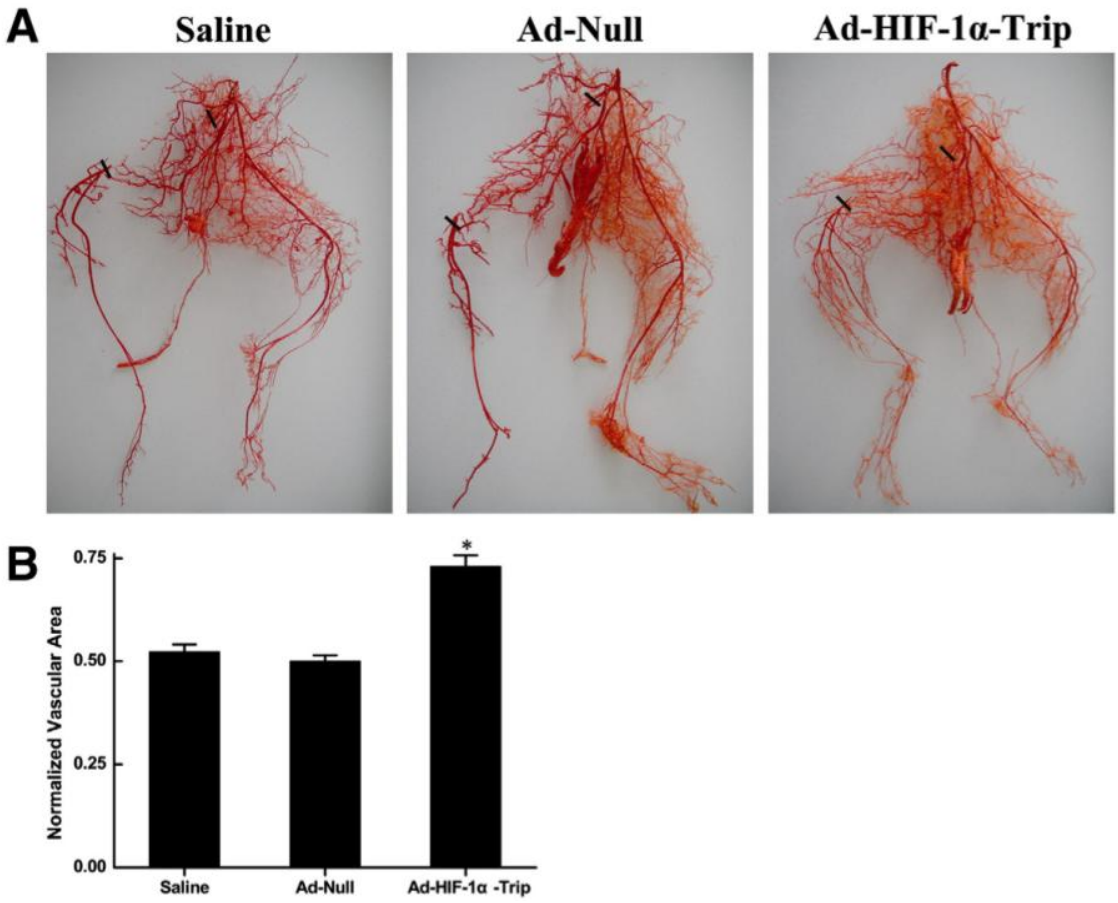


**Figure 1 Dominant active HIF results in increased branching angiogenesis in the hind limbs of rabbits**

T*aken from (Li et al., 2011a) to demonstrate the stimulating effect of dominant active HIF-1α expression (Ad-HIF-1a-Trip) on angiogenesis in ischemic hind limbs evaluated by vascular casting.* ***A)*** *Shows the representative vascular casts of the hind limbs of rabbits in Saline (mock), Ad-Null (empty adenovirus vector) or Ad-Hif-1a-Trip (without the full target sites of PHD and the specific target site of FIH-1) on day 28 following transfection, where the lines indicate the location of the femoral artery stump.* ***B)*** *Shows the quantification of the normalized vascular area of the ischemic hind limbs, *P<0.05 vs. saline. Mean values and SEM are shown and each group had 3 rabbits.* Reprinted with permission from Elsevier, also Lancet special credit with permission from Elsevier

Findings from Li et al., 2011 **(Figure 1)** demonstrate that the animals transfected with functionally dominant active form *HIF-1α*, which possesses both stability and effective

transcriptional activity under normoxic conditions, showed the best re-vascularisation response to the induced hind limb ischemia (Li et al., 2011a). This suggests that the induction of HIF signaling and the consequence of inducing downstream transcription of vascular inducing genes such as VEGF are involved in collateral vessel formation following ischemia.

According to the British Heart Foundation figures from 2010 1.5 million people had a myocardial infarction, with over 900,000 of these being under the age of 75. Similarly 1.2 million people in the UK had a stroke, with around 600,000 of these being under the age of 75 (BHF, 2010). The incidence of new cases of cancer was around 309,500 in 2011 (excluding non-melanoma skin cancer) according to Cancer Research UK (CRUK, 2011). Statistics such as these make it easy to visualise the impact that diseases of these kinds have on the human population worldwide and demonstrate how important a better understanding of the underlying mechanisms are to the way that we tackle them.

In cancer HIF signaling is associated with several characteristics of solid tumour, allowing them to expand and become a threat. These effects include; 1) expansion of cancer cells, which depends on enhanced glucose transport and glycolysis (the Warburg effect). 2) Tumours can't grow larger than several $mm^3$ without angiogenesis, and the degree of vascularisation has been inversely correlated with patient survival. 3) The probability of invasion, metastasis and death are positively correlated with the degree of intra-tumoural hypoxia, regulated by immature/defective microcirculation so that cells adjacent to neo-vessels can still be hypoxic. 4) Tumour hypoxia has been associated with resistance to chemotherapy, immuno-therapy and radiotherapy, and therefore associated with tumour survival (Zhong et al., 1999). Several solid tumours have been shown to be angiogenesis dependent (Folkman, 1985, Sugimachi et al., 2002) and will co-opt the body's own mechanisms of blood vessel development and re-modelling for its own gains at the expense of the patient, using HIF activation to induce expression of VEGF, stromal-cell derived factor (SDF1), Angiopoietin etc (Fahling and Persson, 2012, Isobe et al., 2012). Many studies have been performed in order to assess levels of HIF-1α protein as a predictive tool across several different carcinomas (Yohena et al., 2009, Semenza, 2010, Zhong et al., 1999). In a review in 2010, Semenza identified a largely positive

correlation between levels of HIF-1α with clinico-pathological factors and the subsequent influence on prognosis. Semenza also compiled a list of xenograft models looking at HIF-1 and HIF-2 loss of function (LOF) and gain of function (GOF) models in various tissues have shown that LOF correlates with decreased growth of the xenograft, while GOF xenografts demonstrate the opposite effect (Semenza, 2010). Over-expression of HIF-1α in a human PCA (prostate cancer) cell line derived from bone metastasis was found in normoxic culture conditions (Zhong et al., 1999). Semenza suggested that in certain tumours (breast, cervical, endometrial), high levels of HIF might be used as an indicator for more aggressive therapy in patients (Semenza, 2010).

## 1.2 Overview of the Hypoxic Signaling Pathway

The cellular response to hypoxia is a highly regulated process that plays a role in normal physiology and is driven by the HIF family of transcription. These responses to hypoxia are conserved across metazoans from worms to humans, aiming to increase glycolysis to compensate for energy loss and improve oxygenation through erythropoiesis and angiogenesis (Fong and Takeda, 2008). The human response to hypoxia is also initially to increase pulmonary ventilation, cardiac output and heart rate (Semenza, 2004).

Active HIF is a heterodimer-complex of HIF-α and HIF-β, which together regulate the transcription of a large number of effector genes (Wenger et al., 2005, Manalo et al., 2005). HIF-1 was identified as a hypoxia-inducible nuclear factor that bound to the 3' hypoxia-response enhancer element (HRE) of the Epo gene (Semenza and Wang, 1992, Marti, 2004, Semenza et al., 1991, Smith et al., 2008), which has been characterised as a haematopoietic factor (Krantz, 1991) that is produced in response to tissue hypoxia (Jelkmann, 1992). Since then, three HIF-α isoforms have been identified in humans, *HIF-1α, HIF-2α* and the relatively uncharacterised *HIF-3α* (Heikkila et al., 2011), although the latter, in fact, may have an inhibitory role in HIF signaling (Makino et al., 2007). For this section, these will be referred to collectively as *HIF-α*.

In a normoxic environment there are several control mechanisms on the activation of the hypoxic signaling pathway (for a review (Masson and Ratcliffe, 2003) and see

**Figure 2**). Prolyl hydroxylase domain containing proteins (PHDs) hydroxylate two specific proline residues on the HIF-α protein and this hydroxylation leads to Hypoxia-Inducible Factor (HIF)-α recognition and ubiquitination by von Hippel Lindau protein (VHL) complex (VHL, elonginC, elonginB, cullin2, rbx1) and subsequent degradation by the proteasome. Factor inhibiting HIF (FIH) hydroxylates HIF-α at a specific asparagine residue ($Asn^{803}$ on HIF-1α), a residue within the binding site for HIF complex co-activators in the nucleus, impairing the activity of the HIF-α protein.

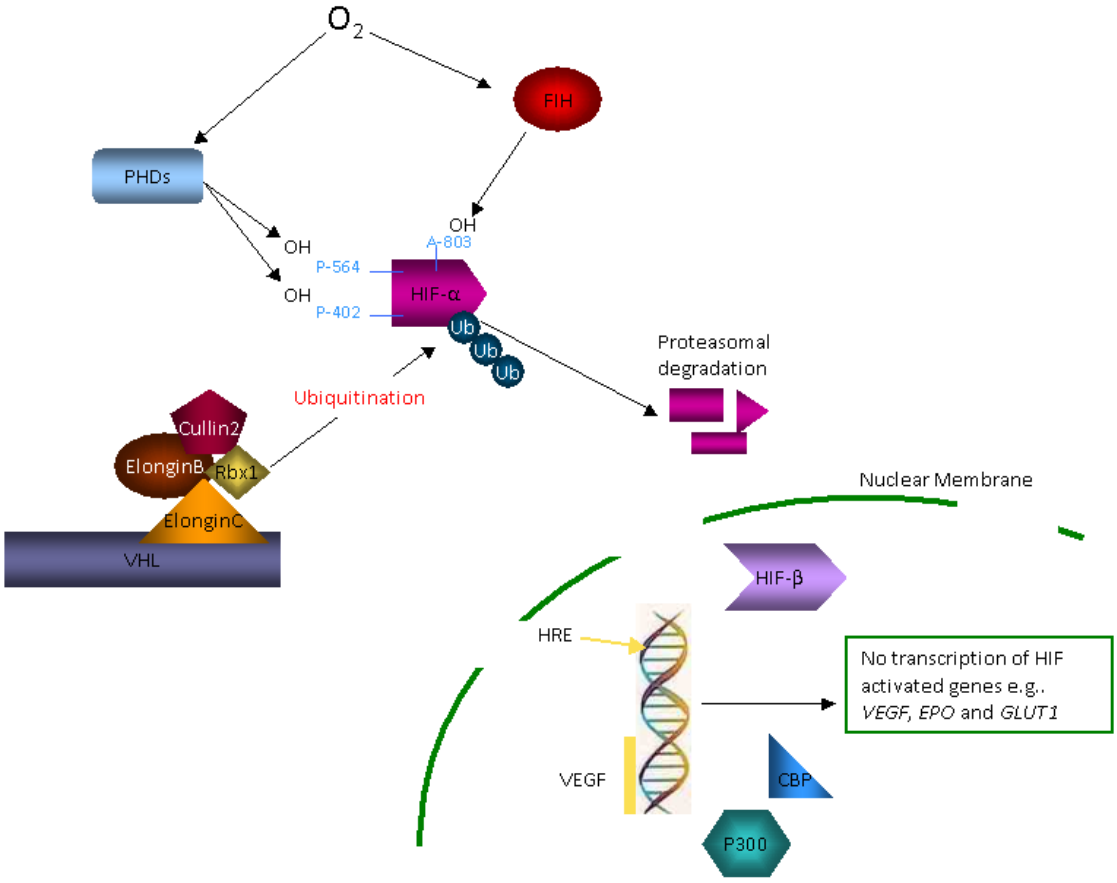


**Figure 2 HIF signaling pathway in normoxia**

*In normoxia HIF-α levels are regulated by hydroxylation. PHDs hydroxylate specific residues inducing the recognition by an ubiquitination complex including VHL, targeting it for proteasomal degradation. Simultaneously FIH hydroxylates a distinct residue in a key region necessary for the binding of co-activators, such as p300.*

In hypoxia the hydroxylation events that regulate HIF-α levels and activity in normoxia don't occur. This ensures the VHL complex is not triggered to and ubiqutinate HIF-α, allowing HIF-α to accumulate and translocate into the nucleus, where it binds with HIF-

β, to form an active transcription complex, including p300 and CBP co-activators, see **Figure 3**.

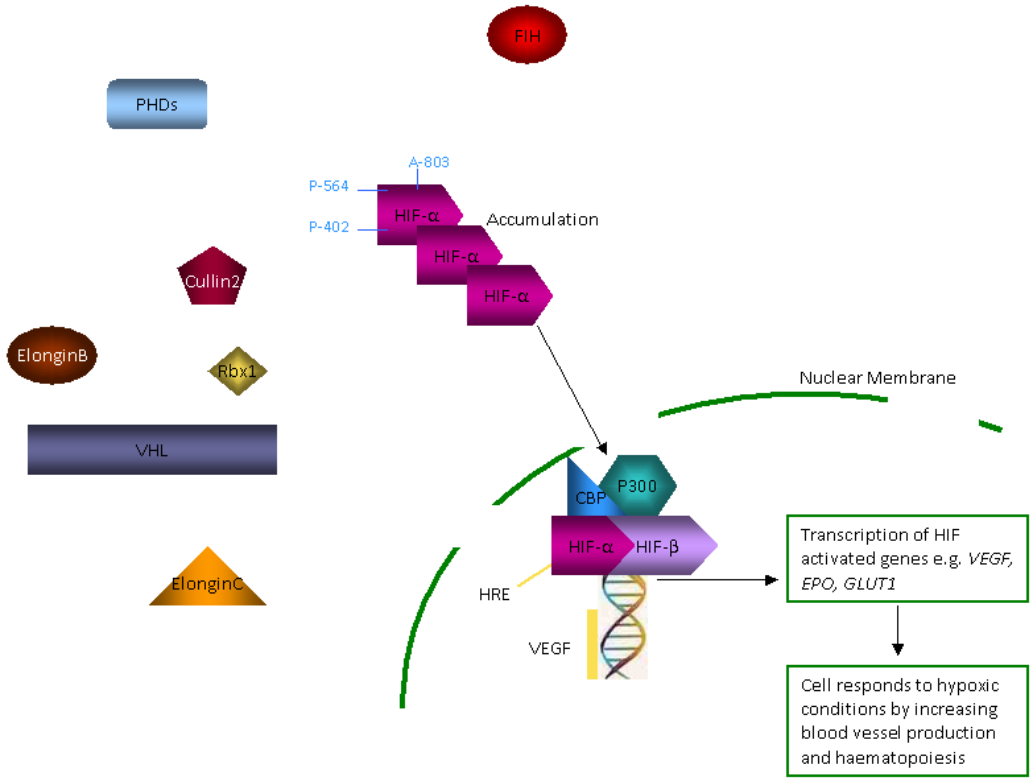


**Figure 3 HIF signaling pathway in hypoxia**

*In hypoxia the hydroxylase enzymes (PHDs and FIH) are inhibited, HIF-α is not hydroxylated and the levels accumulate. It then translocates into the nucleus where it forms a transcriptional active complex with HIF-β and co-activators p300 and CBP. This complex binds to HREs in the genome, activating transcription. A negative feedback loop also exists where PHD2 & 3 are both known targets of HIF-activated transcription, once up-regulated they can then regulate levels of HIF-α.*

Normal and or pathological activation of the HIF pathway results in a variety of effects, some examples have been illustrated in **Figure 4.**

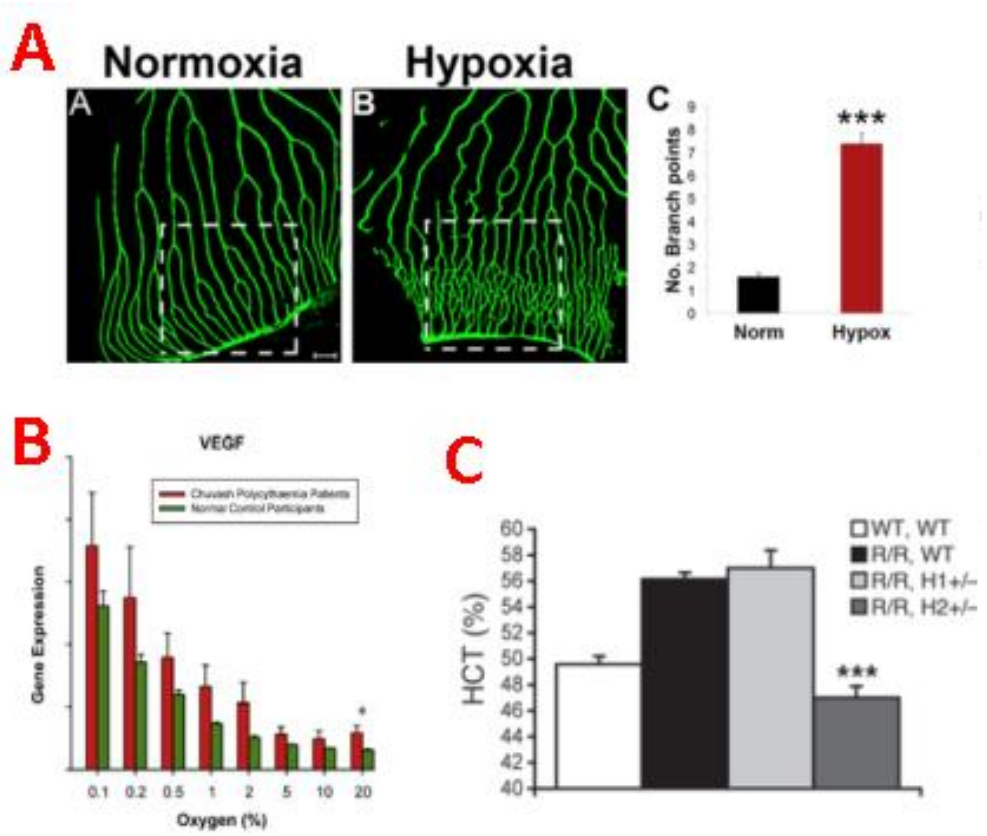


**Figure 4 Distinct phenotypes of increasing hypoxia and/or HIF-signaling are observed in the branch points of blood vessels, the expression of VEGF and by assessing the hemoatocrit.**

***A)*** *Increased branching angiogenesis in adult Tg(Fli1;eGFP) zebrafish (a GFP reporter line tagged to the friend-leukemia factor transcription factor, which labels the endothelium (Lawson and Weinstein, 2002b)), where the hypoxic group were exposed to 10% air saturation for 12 days. Taken from Figure 1 of (Cao et al., 2008).* ***B)*** *Vegf mRNA isolated from lymphocytes taken from venous blood from Chuvash Polycythemia (CP) (see main text) patients as well as normal control participants was incubated at eight different levels of oxygen tension prior to RNA isolation. The expression of Vegf at different oxygen tensions, from 0.1% (where Vegf mRNA is highest) to 20% (where Vegf mRNA is lowest) was compared against CP patients, who exhibit higher levels of Vegf mRNA compared to normal control patient samples at each of the oxygen tensions tested (Smith et al., 2006).* ***C)*** *Polycythemia (illustrated by an increase in hemoatocrit (HCT)) exhibited in R/R mice (Vhl mutation in mice that models Chuvash Polycythemia). Loss of 1 allele of Hif-2α but not Hif-1α resulted in HCT levels reverting to WT levels in R/R mice (Hickey et al., 2010).*

Some of these phenotypes have been shown to be phenotypes in *HIF-2α* gain of function (GOF) mutants and Chuvash Polycythemia (CP) models, which is a heritable autosomal-recessive disease caused by germline homozygosity for the 598C-T mutation in exon3 of von Hippel Lindau (*VHL),* which mutation causes inappropriate

activation of HIF signaling (Formenti et al., 2011, Hickey et al., 2007). The common phenotypes observed in CP patients and *HIF-2α* GOF suggest a role for HIF-signaling in controlling these phenotypes (Formenti et al., 2011). CP patients differ from those with VHL disease, as these patients are not predisposed to cancers (highly vascularised tumours and cysts including thrombosis, haemangioblastomas, pheochromocytomas and clear cell renal cell carcinoma (CCRCC)) (van Rooijen et al., 2009, Gordeuk et al., 2004). Instead, phenotypes of CP include increased hemoglobin and hematocrit levels, with patients also exhibiting elevated respiratory and pulmonary vascular regulation along with elevated responses to acute hypoxia. Patients experience cerebral vascular events or peripheral thrombosis, which leads to premature mortality (van Rooijen et al., 2009, Gordeuk et al., 2004).

## 1.3 Hypoxia-Inducible Factor (HIF)

The HIF heterodimer along with cofactors (p300 and CBP) forms a complex that acts as a transcription factor, initiating expression of target genes, containing HREs (Wenger et al., 2005, Kaluz et al., 2008). The human HIF-1 consensus sequence has been described by the DNA motif 5'-TACGTGCT'3' (Varma and Cohen, 1997, Wang and Semenza, 1995) and many genes with these sequences in their enhancer regions have been shown to be involved in adaptation to the hypoxic environment, including those involved in pathways such as angiogenesis, haematopoiesis and the glycolytic pathway.

Protein sequence homology was found between the *Drosophila Melanogaster* period (Per) single-minded (Sim) and the mammalian aryl hydrocarbon receptor (AHR) and aryl hydrocarbon receptor nuclear translocator (ARNT(=HIF-β)), which all contain a 200-350aa sequence that constitutes the PER-ARNT-AHT-SIM (PAS) domain (Wang et al., 1995). The PAS domain is present in both HIF-α and -β and is required for the accurate formation of the HIF protein heterodimer, as well as for DNA binding (Lee et al., 2004, Wang et al., 1995). Active HIF is a heterodimer of HIF-α (of which there are three in humans) and HIF-β proteins (of which there are also three in humans) (Lee et al., 2004, Lisy and Peet, 2008). The HIF-α proteins contain both an N- and C-terminal transactivtation domain (TAD-N and TAD-C), bridged by an inhibitory domain (ID) at residues 576-784 in HIF-1α, which is thought to be the interaction region for FIH (Lee

et al., 2004). The TAD-N (residues 531-575) in this protein overlaps with the oxygen-dependent degradation domain (ODDD). The TAD-C (residues 786-826) interacts with co-activators 300kd co-activator protein (p300) and CREB binding protein (CBP) an action that is required for the function of HIF after the dimer forms in the nucleus (Lee et al., 2004, Lisy and Peet, 2008), see **Figure 5**

HIF-α although constitutively expressed in cells, has a very short half-life (less than 5mins) in normoxia and has been shown to be as little as 1 minute in re-oxygenated ferret lungs (Huang et al., 1996, Yu et al., 1998, Lisy and Peet, 2008). The levels of HIF-α in the cytoplasm are controlled by oxygen dependent regulatory elements within the pathway, and its stability is negatively regulated by hydroxylation by PHDs and FIH (Bruick and McKnight, 2001, Epstein et al., 2001, Jaakkola et al., 2001, Lisy and Peet, 2008), **see Figures 5 and 6**. It has been shown, using a hydroxylation specific antibody, that the proline residues 564 on HIF-1α and 531 on HIF-2α protein are the key residues irreversibly hydroxylated in normoxia and that this hydroxylation is diminished in hypoxia, regardless of the presence of VHL (Chan et al., 2002). The hydroxylation events by the PHDs leads to the bringing together of a ubiquitin ligase complex containing VHL, which interacts with residues within the ODDD of the HIF-α protein, initiating ubiquitination and subsequent degradation in the proteasome.

Other modifications, besides hydroxylation, of HIF have been identified as well although their relevance for hypoxic signaling is less clear. Acetylation of lysine residues has also been identified on the HIF-1α protein, $Lys^{532}$ and $Lys^{674}$. The acetylation at $Lys^{532}$ can induce VHL-dependent HIF-α protein degradation, while acetylation at $Lys^{674}$ is required for HIF-1α transcriptional activity (Geng et al., 2011). Phosphorylation events have also been described on the HIF-α protein through activation of p42/p44 mitogen-activated protein kinases (MAPK), which has been shown to promote transcriptional activity of HIF and is proposed to indicate a cooperation between hypoxic and growth factor signals (Richard et al., 1999). Subsequent studies have shown phosphorylation of Threonine-296 ($Thr^{796}$) is involved in transactivation of the HIF-α protein (Gradin et al., 2002). The phosphorylation at $Thr^{796}$ has also been shown to interrupt the hydroxylation at $Asn^{803}$ initiated by FIH, ensuring HIF-α activity by allowing the binding of co-activators in the nucleus (Lancaster et al., 2004).

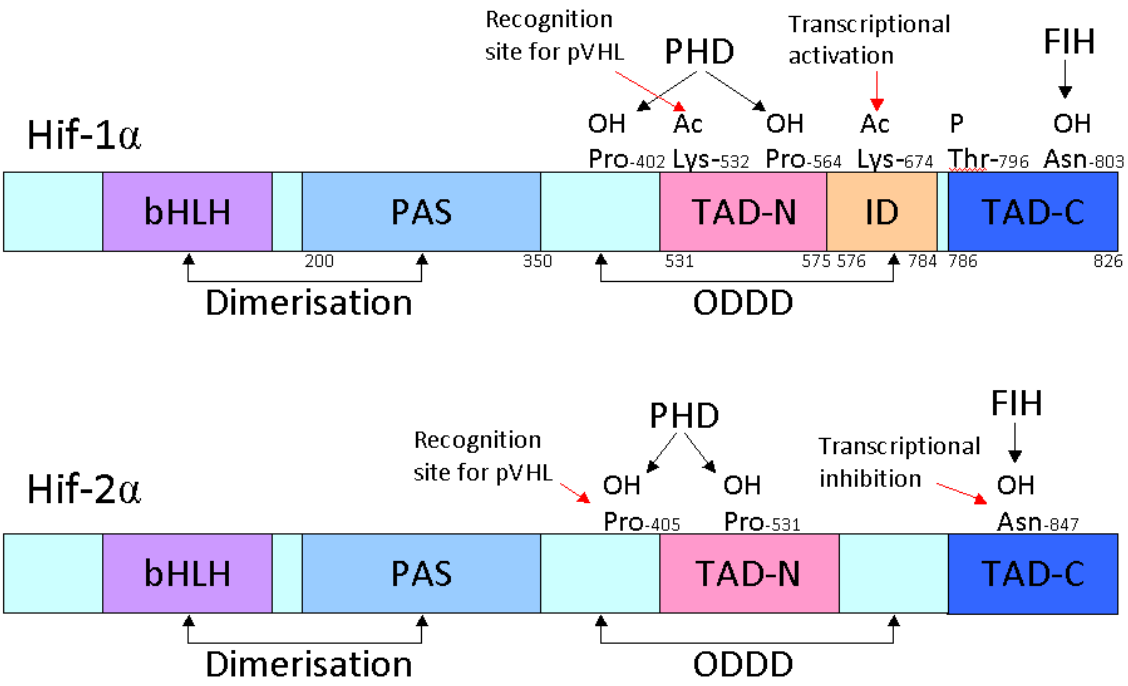


**Figure 5 Key residues on the HIF-α proteins are indicated in their roles and in their interaction with other proteins such as PHDs and FIH.**

*The hydroxylation of two proline residues ($P^{402}$ and $P^{564}$ on HIF-1α, and $P^{405}$ and $P^{531}$ on HIF-2α) earmarks the protein for degradation. The hydroxylation (OH) of an asparagine residue ($N^{803}$ on HIF-1α and $N^{847}$ on HIF-2α) blocks the transcriptional functions of the HIFα protein (Keith et al., 2012). Acetylation (Ac) of $Lys^{532}$ is involved in pVHL-dependent Hif-α regulation, whereas Ac of $Lys^{674}$ is required for HIF transcriptional activity (Geng et al., 2011). The Lys regulation of HIF-2α has not been described on a residue level. In the figure bHLH = basic helix loop helix, two transcriptional activation domains (TADs) at the NH(2) terminal and COOH terminals, both of which are important for the optimal transcriptional activity. The TAD-N and ODDD or oxygen-dependent-degradation domain overlap. $Thr^{796}$ is phosphorylated (P) ensuring transactivation of the protein by preventing FIH hydroxylation at $Asn^{803}$ (Gradin et al., 2002, Lancaster et al., 2004). Figure adapted from (Nangaku and Eckardt, 2007).*

The downstream effects of each of the HIF-α hydroxylation events described in **Figure 5** are described below (See **Figure 6**) in more detail.

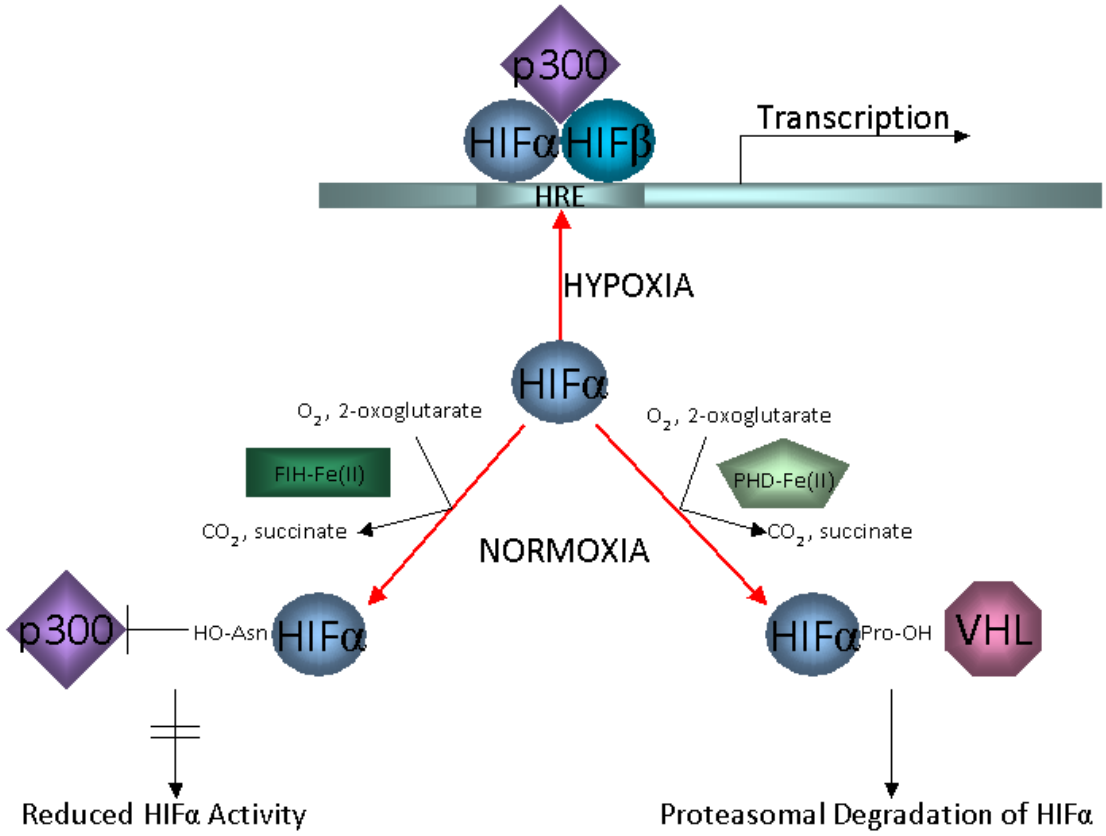


**Figure 6 There have been different outcomes, demonstrated by Lancaster et al, of different hydroxylation events of the HIF-α protein by either PHDs or FIH (Lancaster et al., 2004).**

*PHD hydroxylation induces VHL mediated ubiquitination and subsequent proteasomal degradation, whereas, FIH hydroxylation blocks the binding of p300, a co-activator, and simply may blunt the proteins activity. Abbreviations: hypoxia inducible factor (HIF), von hippel lindau (VHL), factor inhibiting HIF (FIH), iron (Fe), prolyl hydroxylation domain containing protein (PHD), nuclear co-activator (p300), proline hydroxylation (Pro-OH), asparagine hydroxylation (Asn-OH)*

The differential nature of HIF-α regulation by VHL and FIH in the homeostasis of the pathway means that the loss by inhibition or mutation of the regulators can have distinct downstream effects in normoxia. The loss of VHL leads to the accumulation of HIF-α, aberrant signaling and an increase in HIF target gene expression such as *VEGF*, *EPO* and *GLUT-1*. This is tempered by the presence of FIH, which will continue to impair HIF-α activity in the nucleus. The loss of FIH will mean that HIF-α will be able to function, should any accumulate, however this will be attenuated by the presence of VHL instigating HIF-α breakdown. The loss of both of these proteins in combination can cause a further amplification of the downstream effects of loss of either of the two proteins individually. The various effects of the loss of each of these genes constitute

the subject of the current study in the zebrafish and will be described further in the remainder of the thesis.

The different HIF isoforms have been shown to correlate with particular functions (Loboda et al., 2010), for example HIF-1α is a key regulator of neutrophil function and life span (Elks et al., 2011). In mice this has also been shown, where HIF-1α has been shown to be predominant during mouse embryogenesis and HIF-2α (under physiological and stress conditions in adult mice) for *Epo* regulation in mice (Gruber et al., 2007). In vascular development as well HIF-1α and HIF-2α have also been shown to play distinct roles, here HIF-1α regulates endothelial cell proliferation, migration and vascular sprouting, while HIF-2α is more responsible for controlling vascular morphogenesis, integrity and assembly. HIF-1α has two zebrafish homologs Hif-1αa and Hif-1αb (Elks et al., 2011) and HIF-2α also has multiple zebrafish homologs Epas1a, Epas1b and possible ortholog Hif1al2 (Ensembl, 2012).

HIF-$\alpha$ protein stability and activity is regulated by PHD containing proteins and FIH, hydroxylating distinct residues on the HIF-$\alpha$ protein, which then leads to VHL-dependent ubiquitination, see **Figure 5**. There appears to be quite some complexity in the precise regulation. For instance, HIF-α stabilisation could also be achieved using either a constitutively active Akt (Protein Kinase B/PKB) or the introduction of v-Src or Ras V12 oncogenes, which resulted in the loss of $Pro^{564}$ hydroxylation (Chan et al., 2002). In acute hypoxia MCF7 cells react by suppressing PHD2, which has been shown to have a smaller effect on inducing HIF-2α compared to HIF-1α. Suppression of PHD1 and PHD3, independently or in combination with other PHDs had more significant effects on HIF-2α than on HIF-1α (Appelhoff et al., 2004).

The HIF-1β subunit on the other hand, is also known as an aryl hydrocarbon receptor nuclear translocators (ARNTs) and is constitutively present in the nucleus (Li et al., 1996, Lee et al., 2004). Cells lacking functional HIF-β have been used to assess and confirm the necessity of this protein in DNA-binding and transcriptional activation of HIF-complex (Wood et al., 1996). This component of the HIF pathway will not be discussed in isolation in this thesis.

Iyer et al showed that *Hif-1α-/-* mouse embryonic stem cells (ESCs) showed reduced levels of glucose transporters (GLUT) mRNAs, glycolytic enzymes and vascular

endothelial growth factor (VEGF), along with reduced cellular proliferation, which are known to be induced by hypoxia/HIF signaling, (Iyer et al., 1998). Complete deficiency of *Hif-1α* in mouse embryos resulted in embryonic lethality by E11, which is the time at which *Hif-1α* is expressed, with the embryos demonstrating neural tube defects, cardiovascular malformations and marked cell death within the cephalic mesenchyme. Mice lacking *Hif-2α* have also been investigated and many of those that were born alive also developed vascular abnormalities including hemorrhages (Scortegagna et al., 2003, Peng et al., 2000) and demonstrated congested blood in the liver (Tian et al., 1998). The deaths of *Hif-2α-/-* embryos was suggested to be due to circulatory failure, indicating a fundamental role for this protein in the control of cardiac output (Tian et al., 1998).

In the zebrafish, little is known about *in vivo* HIF function, Elks et al describes the generation of a series of dominant active and negative constructs analogous to the zebrafish homologs Hif-1αa and Hif-1αb, by mutating the residues where the PHDs and FIH have been shown to bind, see **Figure 5** (Elks et al., 2011). Dominant-negative Hif-1αa blocked the activation of the HIF pathway usually seen by treatment with the pan-hydroxylase inhibitor DMOG as late as 56hpf (hours post fertilisation), as indicated by an increase in *phd3* expression (a known Hif target) (Elks et al., 2011). It was also shown that in the zebrafish dominant-negative Hif-1αb alone was sufficient to block DMOG regulated delay in resolution of neutrophilic resolution, while dominant-negative Hif-1αa had no effect on inflammation (Elks et al., 2011).

### 1.4 Von Hippel Lindau (VHL)

In 1993, von Hippel Lindau was identified as the gene causing VHL disease; a dominant genetic disorder, which was first described in 1936 (Maher et al., 2011) and is associated with tumours in a variety of organs, including the kidneys (Maranchie et al., 2002). The gene encodes a 30kDa protein (Latif et al., 1993) on chromosome 3p25.5 and was cloned using a genetic linkage-based positional cloning approach (Seizinger et al., 1988, Gnarra et al., 1995). The VHL gene product exists in two forms in humans, a larger p30 protein and a smaller p19 protein, the latter generated by internal translation initiation at the second methionine (Iliopoulos et al., 1998, Schoenfeld et

al., 1998). Subsequently it was shown that VHL is a critical component in the HIF signaling pathway (Ohh et al., 2000, Cockman et al., 2006, Maxwell et al., 1999) and It has been shown that this interaction between VHL and HIF is iron dependent (Maxwell et al., 1999).

VHL responds directly to the hydroxylation of HIF-α by PHDs by forming a protein complex with HIF, to target it for degradation. Several studies have been done to assess the components of the complex (also known as the VBX complex) with VHL and elonginC (Kibel et al., 1995), along with elonginB (Kibel et al., 1995), cullin2 (cul2) (Pause et al., 1997) and ring-box 1 (rbx1) (Kamura et al., 1999), have been shown to be involved, with VHL acting as the substrate recognition component of the complex, see **Figure 7** (Iwai et al., 1999, Koth et al., 2000, Kinoshita et al., 2007, van Rooijen et al., 2011).

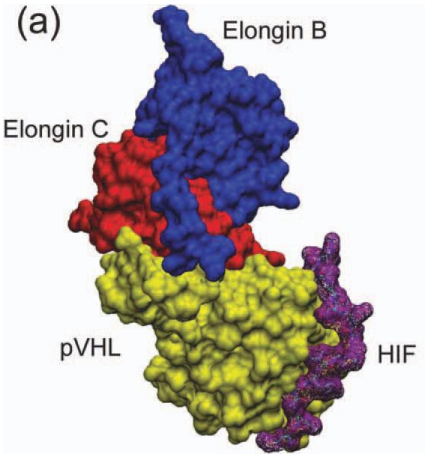


**Figure 7 A computational model of the ElonginB/C-Vhl-Hif complex demonstrates the interaction of the various proteins involved.**

*Taken from (Domene and Illingworth, 2012) Permissions were granted from Publishers the Wiley Company for the republication of this figure*

VHL has been shown to move between the cytosol and the nucleus, with most of the protein concentrated in the cytosol (Kaelin 2002). Although VHL's function in HIF-signaling is the best studied, a number of additional functions have been described, **see Figure 8**; for example in regulation of microtubules (Thoma et al., 2009, Thoma et al., 2010), cilia (Esteban et al., 2006) and extracellular matrix (ECM) deposition (Tang et

al., 2006, Lai et al., 2011). It is likely that some of these functions also contribute to the tumour suppressor function of VHL.

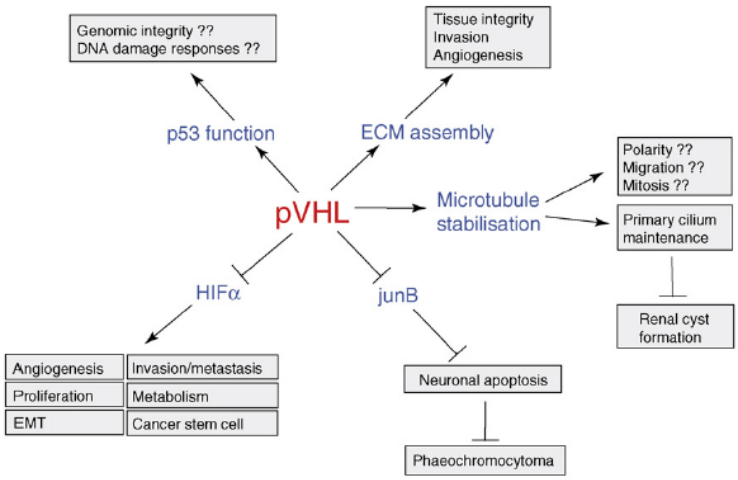


**Figure 8 There are multiple HIF-α-dependent, as well as independent, functions of pVHL that could contribute to tumour suppression.**

*Arrows (↘) indicate positive or activating effects and the symbol* (⊢) *represents inhibitory effects. Abbreviations include ECM-extracellular matrix, EMT-epithelial to mesenchymal transition. Figure taken from (Frew and Krek, 2007)* and reprinted with permission from Elsevier, also Lancet special credit with permission from Elsevier

The function of the VBX complex is to ubiqutinate HIF-α and this process then targets it for proteasomal degradation upon cues from HIF-1α hydroxylation in normoxia (**Figures 2 and 3**). VHL forms the substrate recognition part of this complex, with direct binding between VHL and HIF-1α within the complexes (Lai et al., 2011, Ohh et al., 2000, Tanimoto et al., 2000), see **Figure 9**. In addition Li et al showed that VHL mediates an oxygen-dependent interaction between FIH and HIF-1α potentially explaining the unexpected inhibitory effects of moderately low oxygen concentrations of FIH hydroxylase activity towards HIF. FIH has a high affinity for oxygen and would be expected to be inhibited only in near anoxia (Li et al., 2011b).

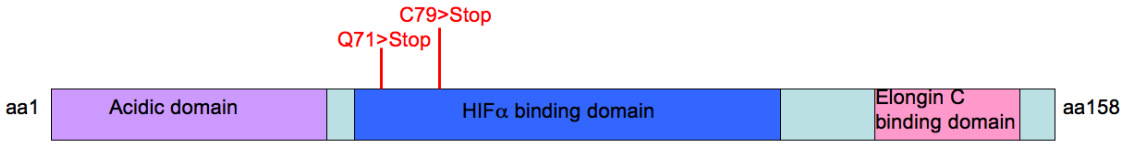


**Figure 9 A schematic of the longest form of the Vhl protein has been highlighted in terms of its active domains. Also highlighted are two points where mutations have been found in the zebrafish.**

*Q71 and C79 stop indicate equivalent residues that have been mutated in the zebrafish lines vhlhu$^{2117}$ (Q23X) and vhlhu$^{2081}$ (C31X) that were identified following F1 N-ethyl-N-nitrosurea (ENU)- induced mutagenesis in a Targeting induced local lesions in Genomes (TILLING) screen (van Rooijen et al., 2009).*

Heterozygous loss-of-function (LOF) *Vhl* mutations are relatively common in the human population, with about 1 in 36,000 individuals affected (Kaelin 2002) and a penetrance of 90% of patients by the age of 65 years (Lonser et al., 2003). Homozygous loss of *Vhl* is linked to a subset of human tumours, suggesting that the role of *Vhl* in tumourigenesis is tissue dependent (Kaelin, 2002) with cause of death in many patients being typically metastases from renal cell carcinoma (RCC) or symptoms related to central nervous system (CNS) haemangioblastomas (Lonser et al., 2003, Maranchie et al., 2002). Importantly, sporadic kidney cancer is usually also the result of biallelic loss of VHL. Levels of *Hif-1α* and *Hif-2α* have been shown to be elevated in RCCs and haemangioblastomas lacking functional VHL protein, but HIF-2α is thought to be critical for tumour formation (Raval et al., 2005). *Hif* expression has been linked to the regulation of angiogenesis and erythropoiesis (Krieg et al., 2000), for instance, patients with *Vhl* LOF tumours can show responses to elevated levels of *Epo* that are produced in the serum and can result in polycythemia (Pastore et al., 2003). Chuvash polycythemia patients, which are homozygous for a R200W missense mutation in *VHL* exhibit phenotypes, such as elevated Epo levels and elevated respiration rate that can be independent of tumour production, and are phenocopied in *vhl-/-* zebrafish embryos and *VhlR/R-/-* mice, which are homozygous for the "Chuvasch allele" (van Rooijen et al., 2009, Hickey et al., 2010).

Heterozygous *Vhlh* mice appear phenotypically normal; however *vhlh* knockout mice don't survive, dying at E10.5-12.5. The development of the null embryos appeared normal up to this time, at which point placental dysgenesis developed. Surprisingly,

the placenta was found to demonstrate failed vasculogenesis with hemorrhagic lesions, followed by hemorrhage in the embryos causing necrosis and death of the embryos (Gnarra et al., 1997). VEGF protein levels were shown to be high in the placental labyrinth trophoblasts of normal E10.5 embryos, while, contrary to predictions, it was greatly reduced in the same cells in the VHL-deficient placentas. Since VEGF family member null mice demonstrate similar phenotypes in impaired vasculogenesis as well as blood island development, along with embryonic lethality at around the same stage as was observed in the *Vhlh* mice, the decreased VEGF levels in these mice may play a contributory role in embryonic lethality (Gnarra et al., 1997).

Several mutant zebrafish lines have been generated, each carrying a null mutation in *vhl*, see **Figure 9**. The zebrafish provides an alternative model for studying the downstream effects of loss of *vhl* because, unlike the mouse models, homozygous null zebrafish embryos survive through embryogenesis and out to 8-11 days post fertilisation (dpf) (van Rooijen et al., 2009). This survival is due to a combination of factors that distinguish the mouse and zebrafish models, namely the zebrafish are externally fertilised and are therefore not reliant on placentation/mother's blood supply, they are small enough to survive a lack of circulation and they benefit from a certain level of maternal gene expression/rescue in the early stages of development. Furthermore, a second homolog of *VHL* named *vhl-like* is present, this gene is inactive towards HIF but may exert certain HIF independent functions of human VHL (FvE pers. Comm.). The *vhl* null zebrafish line has been characterised (van Rooijen et al., 2010, van Rooijen et al., 2009) and demonstrates several hypoxic phenotypes such as polycythemia, increased circulation, hyperventilation and they exhibit a vascular phenotype (see **Figure 10**). Zebrafish *vhl-/-* embryos exhibit elevated levels of *vegf* expression and hyper-branched vascular network, visualised using the *Tg(fli1;eGFP)* transgenic zebrafish line, which labels the endothelium throughout development (Lawson and Weinstein, 2002b), see **Figure 10Error! Reference source not found.**.

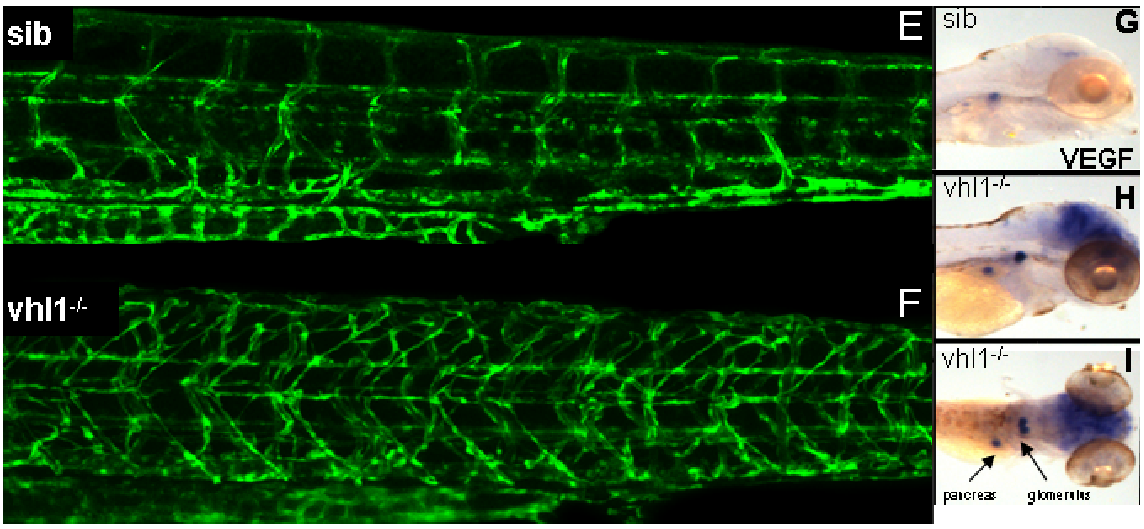


**Figure 10 The vascular network of *Tg(fli1;eGFP)* labeled *vhl-/-* zebrafish and siblings demonstrates the hyperbranching and concurrent increase in VEGF expression in the mutant embryos.**

*The altered vessel network is highly apparent, with many more, disorganized and sprouting vessels in the mutant. The VEGF in situ photographs in the right hand panel show that VEGF expression levels increase in the mutant. This figure has been taken from (van Rooijen et al., 2009).*

An ortholog of VHL, *Vhl*-like protein *(VLP)* has also been predicted from human genome sequence data (Qi et al., 2004), however it is not thought to be related to the fish *vhl-like* gene. It has so far not been proven to be functional, and therefore its *in vivo* role remains unclear. In the study by Qi et al it was shown that expression of *vlp* increased in the absence of *vhl* attenuated ubiquitination of *hif-1α* resulting in a decrease in expression of Hif target genes, which was used to propose that *Vlp* functions as a dominant-negative *Vhl* as protector of *Hif-α* (Qi et al., 2004).

### 1.5 Prolyl Hydroxylase Domain Containing Proteins (PHDs)

PHDs were originally identified in both *Drosophila*, the first known as *Drosophila* Hif Prolyl Hydroxylase (dHPH) (Bruick and McKnight, 2001) and *C. Elegans*, known as egg laying nine (*Egln* or *Egl-9*) (Epstein et al., 2001). Four have been identified in humans and they have been shown to hydroxylate the HIF-α proteins, resulting in recognition by VHL and ultimately causing its breakdown. The family shares approximately 55% sequence homology among their catalytic domains and are able to hydroxylate all three HIF-α subunits using oxygen as a donor for the oxygen atom in the hydroxyl

group (Fong, 2008). PHDs hydroxylate proline residues 402 and 564 on human HIF-1α subunit under normoxic conditions, thus lending oxygen sensitivity to the HIF pathway (Appelhoff et al., 2004, Berra et al., 2003) (**Figures 2 and 3**). Although they have been shown to hydroxylate HIF in order to regulate its function, they are also known to have other substrates (Cummins et al., 2006).

Extended and aberrant signaling through this pathway could lead to uncontrolled proliferation of vascular and haematopoietic cell lineages, where the implications are vascular diseases and cancers. To this end HIF-α also negatively regulates itself by up-regulating *PHD3* under hypoxia (Fong, 2008) (see **Figure 3**) to switch off the hypoxic response after oxygen concentrations are restored and the tissues are no longer at risk is a critical mechanism. *PHD3* has been shown to have a functional HRE, located within a conserved region of the first intron, 12kb downstream of the transcription initiation site (Pescador et al., 2005). Using the sequence to drive reporter gene expression was successful under hypoxic conditions (Pescador et al., 2005). Pescador et al also showed that HIF was necessary and sufficient to induce gene expression following this enhancer sequence. *PHD2* has also been shown to have functional HREs in its promoter regions (Pescador et al., 2005, Metzen et al., 2005), and it is induced by hypoxia *in vitro* (Marxsen et al., 2004). Induction of *PHD2* by hypoxia was absent in *vhl-/-* RCC4 cells, suggesting that hypoxic induction of *PHD2* and *PHD3* is critically dependent on HIF-α and that degradation of HIF-1α after re-oxygenation was accelerated (Marxsen et al., 2004) to control the duration and sensitivity to change of the hypoxic response (Marxsen et al., 2004, D'Angelo et al., 2003, Rantanen et al., 2008).

The chemical reaction, 2-oxoglutarate-FeII+ (2OG-FeII+), connects the key hydroxylases that regulate HIF mRNA levels and activity in the hypoxic pathway and forms the basis of a number of chemical inhibitors of these hydroxylases. Cobalt chloride ($CoCl_2$), dimethyloxalylglycine (DMOG) and desferrioxamine (DFO) have been used in various studies to chemically mimic hypoxia (Groenman et al., 2007), see **Figure 11**. DMOG is a nonspecific 2-oxoglutarate-dependent dioxygenase inhibitor which has been shown to inhibit the PHD family as well as FIH resulting in up-regulation of HIF-α as well as the induction of downstream gene expression (Groenman et al., 2007, Shen et al., 2009). DFO on the other hand removes intracellular iron in order to stabilise HIF-α, since the

enzymatic activity of PHDs and FIH are reliant on both molecular oxygen and iron (Groenman et al., 2007, Shen et al., 2009). $CoCl_2$, a transition metal chloride, has been shown to be a strong inhibitor of FIH, while having only a weak effect on the PHDs (Groenman et al., 2007, Hirsila et al., 2005).

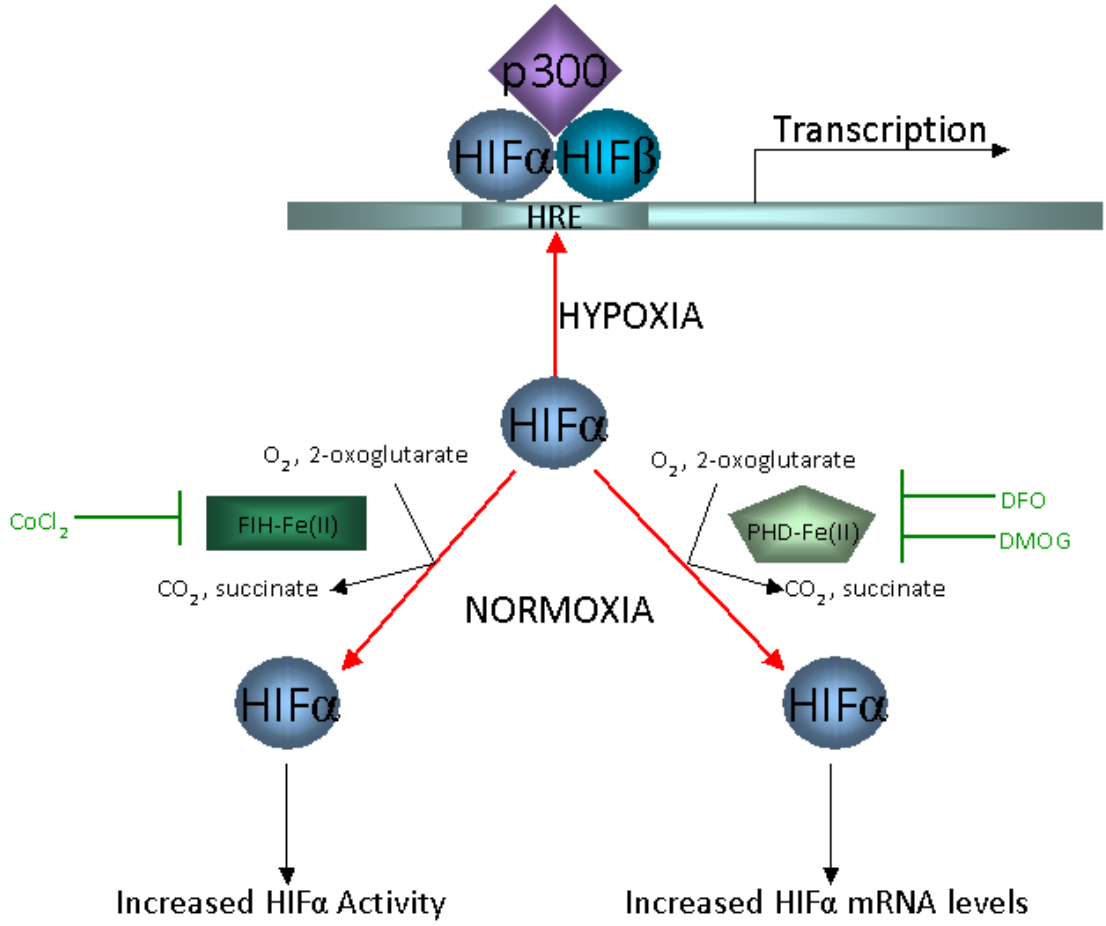


**Figure 11 The effects of a number of inhibitors of the various hydroxylases have been highlighted to demonstrate the ways in which they have been shown to regulate HIF mRNA levels and activity.**

*The figure, adapted from (Lancaster et al., 2004) and again from* ***Figure 6****.* ***Abbreviations:*** *hypoxia inducible factor (HIF), von hippel lindau (VHL), factor inhibiting HIF (FIH), iron (Fe), prolyl hydroxylation domain containing protein (PHD), nuclear co-activator (p300), proline hydroxylation (Pro-OH), asparagine hydroxylation (Asn-OH), cobalt chloride (*$CoCl_2$*),* dimethyloxalylglycine (DMOG) and desferrioxamine (DFO)

Fluorescent fusion proteins were used to assess the subcellular localisation of the three PHD proteins and FIH. Metzen et al showed distinct localisation of the different proteins, with PHD1 exclusively being present in the nucleus, PHD2 and FIH mainly localised in the cytoplasm and PHD3 spread between both locations. They also

showed that hypoxia was not capable of influencing the localisation of any of the enzymes they looked at *in vitro* (Metzen et al., 2003, Lee et al., 2003, Soilleux et al., 2005). PHD1 being present exclusively in the nucleus along with suggestions that it has a lower affinity for HIF-1α compared with PHD2 and PHD3 put it as the least dominant enzyme for HIF-α degradation (Metzen et al., 2003).

A fourth PHD protein was identified in 2002 by Oehme et al, which was found to be associated with the endoplasmic reticulum, which differentiated it from the other PHDs, which are localised to the nucleus or cytoplasm or both (Oehme et al., 2002). Over-expression of PHD4 *in vitro* did suppress HIF activity, dependent on the consensus ODDD proline residues, which correlated with a decrease in HIF protein, suggesting that it might also be involved in oxygen sensing (Oehme et al., 2002).

In a review by Fong and Takeda in 2008 the various biological roles of the various PHDs were collated, from the initial finding the egg-laying function in *c. elegans* was lost upon the loss of EGL-9 (Epstein et al., 2001, Trent et al., 1983) to the role in cell growth in the fat bodies and wing discs of *Drosophila* (Frei and Edgar, 2004). The use of short interfering RNAs (siRNAs) allowed Berra et al to demonstrate that the PHD proteins have distinct functions, with PHD2 as the critical oxygen sensor, which is also up-regulated by hypoxia, providing a HIF-α dependent auto-regulatory mechanism driven by the oxygen tension (Berra et al., 2003). They showed that silencing *Phd2* alone was sufficient to stabilise HIF-α in normoxia *in vitro*, but silencing of *Phd1* or *Phd3* was not (Berra et al., 2003). Following 5-6 days of *Phd2* siRNA treatment with constitutive expression of *Hif-1α* in normoxia they showed a successive decline in *Hif-1α* despite the lack of *Phd2*, and it was under these conditions that simultaneous *Phd1* siRNA could re-establish the high levels of *Hif-α*. This suggested that when one PHD protein was suppressed a HIF-dependent mechanism was in place to activate other members of the family to compensate (Berra et al., 2003).

Phd function has been explored *in vivo* in mouse knock out models. In mice, knock out of *Phd2* resulted in embryonic lethality between embryonic days 12.5 and 14.5, whereas *Phd1-/-* and *Phd3-/-* mice were viable. The *Phd2-/-* embryos showed severe placental and heart defects, which preceded their deaths, phenotypes that are similar to those in *Vhlh-/-* mice. These embryos showed global increases in *Hif-1α* protein

levels throughout the placenta and the embryo, albeit not in the heart (Takeda et al., 2006). Although *Phd1* and *Phd3* mutants are viable more detailed analysis has shown that all *Phd* deficient mice showed some degree of polycythemia with over-expression of *Hif-1α* in the liver and *Epo* in the kidneys, with *Phd2-/-* alone giving the strongest phenotype. For instance, double knock-out of both *Phd1* and *-3* lead to moderate erythropoiesis with elevated levels of *Hif-2α* in the liver (Takeda et al., 2008). A reciprocal experiment, assessing the over-expression of *Phd1,* revealed that this suppressed *Hif-1α* accumulation and tumour growth (Erez et al., 2003) and immortality of human endometrial cancer cell, often associated with *Phd2* (Kato et al., 2006).

Information on the *phd* genes in the zebrafish has not been published except for (Santhakumar et al., 2012) and (van Rooijen et al., 2009). The Ensembl genome browser was used to assess the zebrafish *phd* gene family and shows that the human *PHD2* gene has undergone gene duplication in the zebrafish whereas the *PHD1* and *PHD3* genes are each represented by a single homolog.

### 1.6 Factor Inhibiting HIF (FIH)

FIH, also known as HIF-1an, is an asparagine hydroxylase enzyme with a length of 349 amino acids (**See Figure 12**). FIH catalyses the splitting of dioxygen, using one oxygen atom for hydroxylation of an asparagine residue on target proteins, and the other for oxidising the cofactor 2-OG(α-ketoglutarate) to succinate, releasing $CO_2$ (Lisy and Peet, 2008, Lando et al., 2002a, Mahon et al., 2001). It has therefore also been described as an α-ketoglutarate dependent non-heme iron dioxygenase, with substrate binding as a prerequisite for oxygen activation and substrate hydroxylation (Saban et al., 2011b, Iwai et al., 1998, Hanson et al., 2003). Saban et al suggest that this tight control over $O_2$-reactivity was a distinguishing feature and was due to strong hydrogen bonding (Saban et al., 2011b).

Leucine-795 ($Leu^{795}$) (in human HIF-1α) is conserved on HIF-α proteins and can bind FIH close to its dimerisation interface (Lando et al., 2002a, Mahon et al., 2001, Lancaster et al., 2004) and this HIF-$\alpha$ binding pocket is unique to FIH within its enzyme family (Lancaster et al., 2004). FIH hydroxylates a conserved aspargine-803 ($Asn^{803}$) within the C-terminal domain (TAD-C) of HIF-1α proteins under normoxic conditions,

attenuating HIF activity by blocking its interaction with p300/CBP co-activators (Rantanen et al., 2008, Lando et al., 2002a, McNeill et al., 2002). The HIF $Asn^{803}$ hydroxylation event may be subject to further regulation in addition to oxygen levels as phosphorylation of HIF threonine-796 ($Thr^{796}$) enhances transcriptional responses of HIF in hypoxic conditions by preventing hydroxylation of $Asn^{803}$ (Lee et al., 2004, Mahon et al., 2001), **see Figure 5**.

### 1.6.1 Regulation of HIF hydroxylation by oxygen

Lee et al showed that the $K_m$ values of FIH and PHDs for molecular oxygen have been reported to be roughly 90 and 250μM, respectively *in vitro* (Lee et al., 2004), where the $K_m$ is the Michaelis-Menton constant at which a substrate concentration at which the reaction rate is half of its $V_{max}$ (maximum velocity). Since physiological oxygen concentrations are below this estimated $K_m$ value (around 4-40μM) the PHD and FIH proteins are not saturated with oxygen and can thus respond to physiologically relevant changes in intracellular $O_2$ and decreases in $O_2$ concentrations are likely to reduce the catalytic rate of the PHDs before that of FIH (Lee et al., 2004). Precise regulation may be more complex however, for instance VHL has been indicated to promote the $O_2$-dependent interaction between FIH and hydroxylated HIF-1α, to promote the FIH-mediated $Asn^{803}$ hydroxylation (Li et al., 2011b). Li et al went on to demonstrate *in vitro* that FIH repression of HIF-TAD-C was indeed released under severe hypoxia. On its own FIH has a very low rate of ROS production because FIH only binds oxygen when it is bound to its substrate HIF (Saban et al., 2011b). The differences in chemical sensitivity kinetics and the different oxygen concentrations that are required to activate the PHD proteins as opposed to FIH support the hypothesis that their roles in regulating HIF-α were also distinct (Saban et al., 2011a, Saban et al., 2011b). A mutation was identified in the *fih* gene in a zebrafish line at Sheffield University, the mutation resulted in a premature stop codon at Y94, prior to any of the functional domains in the resulting protein, and it was designated as allele number i217, as shown in **Figure 12**.

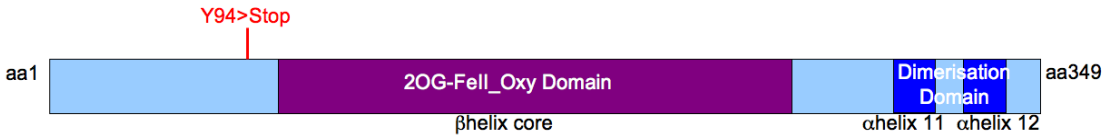


**Figure 12 A schematic of the FIH protein has been highlighted in terms of its active domains. Also highlighted is the point where a mutation has been found in the zebrafish.**

*It is made up of 349 amino acids (Mahon et al., 2001) and contains a β-helix core domain that contains its 2OG-FeII-Oxy domain (Lando et al., 2002a). Y94 stop indicates the residue that has been mutated in the zebrafish line that was identified at Sheffield University, allele number i217.*

FIH functions as a homodimer, the C-terminus comprises (right hand of **Figure 12**) 2 α-helical dimerisation domains (see **Figure 13**) (Lando et al., 2002a, Lando et al., 2002b, Lancaster et al., 2004). The protein structure contains a mixture of α and β strands, with 14 β-strands arranged into two sheets, one with 9 and the other with 5 strands. The central core is a C-terminal 8 β-strand jellyroll (double-stranded β-helix), which is homologous to other 2-OG-dependent oxygenases and the cupin protein family. The N-terminus is formed of another 6 strands. The helical structures are interspersed, with several helix-helix interactions in the center, at an apparent FIH dimerisation interface (Dann et al., 2002, Elkins et al., 2003).

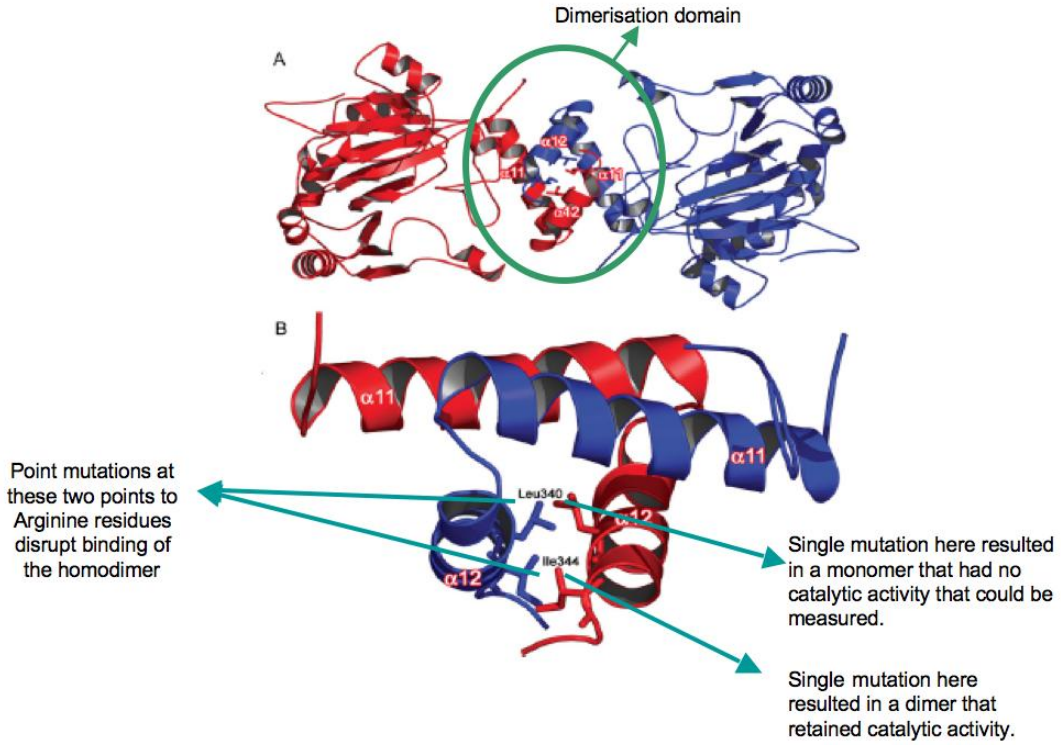


**Figure 13 The FIH protein has been shown to function as a dimer and Lancaster et al demonstrated the binding domain and included research into key residues that were crucial to functional binding of the dimer.**

This figure *has been adapted from (Lancaster et al., 2004) and describes:* ***A)*** *the positions of FIH protein dimerisation between two α-helical domains and* ***B)*** *the positions of point mutations that were made in the protein sequence, mutations that interfere with the dimerisation and or catalytic activity of the complex*

The two C-terminal helices of each monomer of FIH have been shown to form a tight interaction, producing an anti-parallel helix bundle (see **Figure 13**). Deletion of the C-terminal 47aa FIH residues prevents the truncated protein's ability to hydroxylate the HIF-TAD-C, whereas deletion of the N-terminal 33aa of FIH did not affect FIH activity. This combined with several other individual deletion studies suggested that the FIH homodimer is a functionally relevant structural form, in solution (Dann et al., 2002). Valine-802 ($Val^{802}$) within the TAD-C of the HIF-1α protein, has been shown, through targeted mutations, to be essential for the efficient hydroxylation of HIF-α by FIH (Linke et al., 2004). This is proposed to be due to the alteration of the positioning of the FIH hydroxylated asparagine residue, resulting in impaired catalysis (Linke et al., 2004).

FIH was first identified to be a HIF-1α interacting protein (Mahon et al., 2001) and this interaction has been shown to be enhanced by VHL expression, and diminished by VHL knockdown (Li et al., 2011b). If HIF escapes ubiquitination by VHL complex, it should remain inactive due to $Asn^{803}$ hydroxylation by FIH. Using tagged peptides Li et al demonstrated a direct interaction between the three peptides, FIH, VHL and TAD-C, and showed that they assemble correctly in normoxia and less so in hypoxia, with VHL interactions with TAD-C and FIH diminished. HIF was therefore proposed as a chaperone of FIH-VHL interaction as FIH was found to associate with VHL regardless of presence of HIF but this interaction was markedly reduced in hypoxia (Li et al., 2011b), see **Figure 14**.

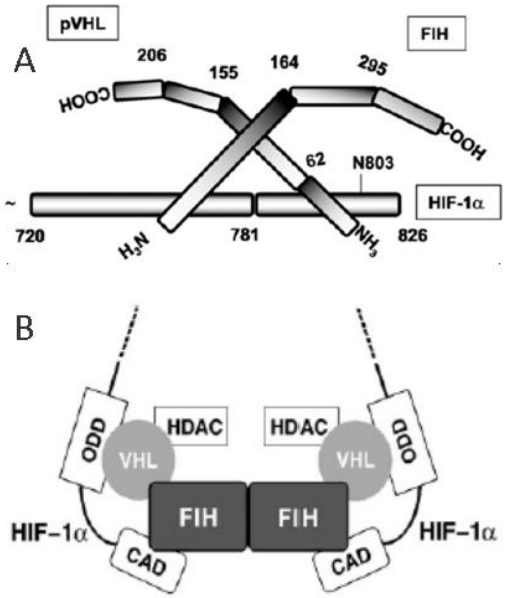


**Figure 14 Several models have been proposed for the orientation and interaction of the complex of HIF-VHL-FIH, this figure demonstrates two of these.**

**A)** *Figure from (Li et al., 2011b) provides a schematic representation of interplay among HIF-1α TAD-C, FIH, and VHL proposed by in vitro study. They show the HIF-1α CT2 (aa782-826) bound to VHL, HIF1α CT1 (aa720-781) bound to FIH; VHL NT (aa1-62) bound to CT2, VHL middle portion (aa63-155) bound to FIH; and FIH NT (aa1-164) bound to either VHL or CT2. Abbreviations: full-length (FL), C-terminus-COOH (CT), N-terminus-$NH_3$ (NT)* ***B)*** *Figure from (Lee et al., 2003) provides a hypothetical model of a complex formed between the FIH dimer, VHL and HIF-1α. Hypothesis indicates FIH acting as a bridge in the association between VHL and the HIF-α C-TAD and associated HDACs.* ***Abbreviations:*** *Histone deacetylases (HDAC), C-terminal domain (CAD), oxygen-dependent domain (ODD)*

It has been shown *in vitro* that FIH hydroxylation of HIF occurs independently of the presence of VHL or PHD hydroxylation (Lando et al., 2002a), however, as stated above, in cells, PHD dependent hydroxylation of HIF will promote the interaction with VHL, which in turn may promote HIF-FIH interaction (Li et al., 2011b). This can be seen when looking at tumour models, VHL loss of function (LOF) in CCRCC has been attributed to hyper-vascularity and poor prognosis due to increased levels of HIF even in normoxia (Iliopoulos et al., 1996). If only VHL is lost, however, FIH would still be present and it has remained unclear how VHL deficient RCC express functional HIF (Li et al., 2011b). Lee et al suggest that it is the interaction between VHL and FIH that ensures that when VHL is induced to bind HIF-α in normoxia, following proline hydroxylation by the PHDs its association with FIH brings this alongside the TAD-C where it performs Asn-hydroxylation to inhibit binding of co-activators (Lee et al., 2003). Li et al proposed therefore, that the HIF TAD-C was activated in the absence of VHL due to a decrease in the interaction between FIH and the TAD-C, however have also acknowledged that they were unable to identify the $O_2$ dependent FIH modifications that regulate their proposed VHL-FIH interaction (Li et al., 2011b).

The Li et al study proposes a model whereby decreasing $O_2$ levels induces sequential process optimising activity of HIF to a level required for cellular adaptation to hypoxia and that VHL acts as an adaptor molecule to couple FIH and HIF-1α (Li et al., 2011b). In moderate hypoxia the PHDs lose activity and this stabilises HIF by blocking VHL binding and the proposed FIH-VHL complex disassembles leading to partial activation of TAD-C by decreasing FIH-TAD-C binding. However, in severe hypoxia FIH and the PHDs are nonfunctional so both HIF TADs are fully activated (Li et al., 2011b).

Questions remain as to whether, in the absence of VHL, expression of FIH would be increased to maintain regulation of HIF. FIH has been shown to be present in *vhl-/-* mouse embryonic fibroblasts (MEFs) although to a lesser extent than in wild type MEFs, see **Figure 15.**

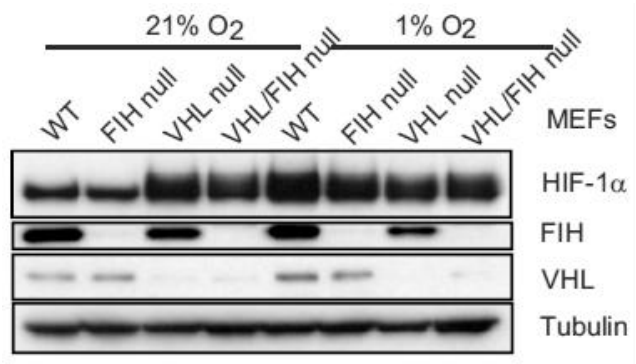


**Figure 15 FIH Expression under different oxygen tensions alters depending on the presence or absence of VHL, in mouse embryonic fibroblasts (MEFs)**

*Figure taken from Zhang et al shows immunoblotting for HIF-1a, FIH, and VHL from whole-cell lysates of immortalized WT, FIH null, VHL null, and VHL/FIH double null mouse embryonic fibroblasts (MEFs). Cells were treated under normoxia or hypoxia for 16 hr before harvest. Tubulin was used as the loading control. Figure republished from (Zhang et al., 2010)* with permission from Elsevier, also Lancet special credit with permission from Elsevier

The immunoblot revealed that the loss of VHL did not induce increased expression of FIH in the MEFs either in normoxia or hypoxia, although it was present. These studies have largely been performed *in vitro,* Mahon et al used *in vitro* peptides in binding assays (Mahon et al., 2001) and Li et al used *in vitro* peptides expressed in various cell lines (Li et al., 2011b). The loss of VHL though, did result in increased expression of HIF-1α in these MEFs in normoxia. In hypoxia, the expression of HIF-1α was elevated in all of the mutants as well as, and almost especially, in the wild type MEFs. These *in vitro* studies indicate binding interactions between the proteins, however Tanimoto et al could not demonstrate the interaction between the HIF TAD-C (aa778-826) and VHL in immunoprecipitation (IP) assays (Tanimoto et al., 2000). More investigation is therefore necessary to enquire as to the functional interactions between these proteins *in vivo*.

FIH is a well-conserved gene in vertebrates and the zebrafish genome has a single homolog. In more primitive animals FIH cannot be unambiguously identified, in *c.elegans* it is most closely related to a *jmjd-5* gene. Expanding the "FIH gene tree" in ENSEMBL (www.ensembl.org) revealed three distinct clusters of genes, the *jmjd* family, the *tyw (jmjc) family* and the *hif1an (fih)* family. The most primitive organism containing an *hif1an (fih)* family gene is the *ciona savigni* (sea squirt), suggesting it

evolved in the chordate lineage.

JumonjiD (*JMJD)* homology, and crystal structures of *FIH* and other members of the cupin family have since been used to suggest that *FIH* may in fact be a member of this super-family (Yang et al., 2009, Hewitson et al., 2002). There is also clear sequence and structural similarity of FIH with JumonjiC (JMJC) domain proteins (Trewick et al., 2005, Mahon et al., 2001, Clissold and Ponting, 2001). The JmjC domain-containing histone demethylases have been shown to be induced by HIF-α dependent mechanism in hypoxia (Yang et al., 2009). However a role as a histone demethylase has not so far been shown for FIH.

### 1.6.2 Transcriptional Regulation of FIH

Published reports show that FIH protein is ubiquitously expressed, having been detected in all tissue culture cell lines examined to date by western blotting techniques, and at similar levels (Lee et al., 2004, Lee et al., 2003, Stolze et al., 2004). It has also been shown in multiple murine tissues by western blotting, from brain, heart and lung, through reproductive organs such as ovary and uterus, as well as in the skin and salivary glands (Zhang et al., 2010).

Melvin et al proposed a mechanism of *FIH* transcriptional regulation involving a member of the chromatin-remodeling complex switch/sucrose nonfermentable (SEI/SNF) family, imitation switch (ISWI). They demonstrated *in vitro* that reductions in the levels of ISWI was correlated with reductions in *FIH* mRNA levels, and also connected ISWI with levels of RNA polymerase II on the *FIH* promoter, affecting protein levels (Melvin et al., 2011). They propose this as a mechanism of regulation of FIH in order to subsequently regulate HIF-α levels and downstream transcriptional responses to hypoxia. They went on to investigate ISWI in negative regulation of two HIF target genes, carbonic anhydrase 9 (*CA9)* and BCL2/adenovirus E1B (*BNIP3)*, and showed that mRNA and protein levels of these genes was reduced in response to ISWI, just as FIH responded and that despite these changes levels of HIF were not altered (Melvin et al., 2011, Zhang et al., 2010). This suggests that absolute levels of FIH might be important.

Despite an extensive search through renal cell carcinoma (RCC) cell lines, a disease where mutations in *VHL* are known to be causative, and primary tumour samples no evidence was found to suggest that germline or somatic mutations in *FIH* contribute to RCC, although the chance that epigenetic regulation of might play a role has not been ruled out. Polymorphic variants were identified that might be useful in further investigation of the role of FIH in modifying the hypoxia response (Morris et al., 2004). There is some indirect indication that Cut-like homeodomain protein (CDP) may reduce FIH mRNA in RCC cells and CDP is associated with metastatic progression of tumours (Li et al., 2007a) but proof for a function of FIH is currently lacking.

### 1.6.3 Other FIH Substrates: a role of Hypoxia/FIH in Inflammation

FIH was first identified as a negative regulator of HIF by interacting with the TAD-C of HIF-α protein by yeast two-hybrid assays (Hewitson et al., 2002, Mahon et al., 2001, Wilkins et al., 2012) but has since been shown to have other substrates, including the ankyrin repeat domain (ARD) containing proteins such as Notch (Zheng et al., 2008) and p105/nuclear factor kappa B (NFκB1), Inhibitor of Kappa B (IκBα) (Wilkins et al., 2009) and myosin phosphatase target subunit 1 (MYPT1) (Webb et al., 2009). Importantly, proteomics experiments suggest it may be generally hydroxylate ARD containing proteins **(see also Chapter 6.6.4)** (Cockman et al., 2009).

Through a series of *in vitro* assays and by mass spectrometry analysis of FIH-transfected cells an interaction was shown between FIH and the ankyrin repeat domains (ARD) in the IκB family. Co-IP studies have shown a direct association between endogenous FIH and IκB-ARD proteins (Cockman et al., 2006), and several groups have shown that FIH hydroxylates IκBα at $Asn^{210}$ and $Asn^{244}$, but that the one at $Asn^{244}$ is preferential, with a mass spectrometry profile that suggests the $Asn^{244}$ residue is 100% hydroxylated while the $Asn^{210}$ residue is 50% hydroxylated (Devries et al., 2010). It has also been illustrated that these interactions occurred more readily than those between FIH and HIF-α (Cockman et al., 2006). The role of IκB hydroxylation by FIH has been shown not to be directly relevant to IκB stability, degradation or activity of IκB and this observation led to the hypothesis that these regulations and

stoichiometric competition could indicate a method of regulating the FIH-HIFα interaction (Devries et al., 2010).

On the other hand degradation of FIH or inhibition by siRNA was sufficient to reduce NF-κB activity (Cockman et al., 2006). A complex has been shown to form between FIH and IκB *in vitro*, which has been shown for FIH and other ARD-containing proteins (Devries et al., 2010). IκBα activated HIF-1α by sequestering FIH away from HIF-1α although these effects on HIF activity were only observed in low oxygen environments (Shin et al., 2009), possibly due to the continued function of PHD protein hydroxylation and VHL ubiquitination of HIF-1α in normoxia. Knock down of IκBα resulted in inhibition of HIF-1α, and this was rescued by subsequent inhibition of FIH, but IκBα is thought to be able to activate the HIF-1α TAD-C independently of $Asn^{803}$ and this might be through positive regulation of p300 recruitment to HIF-1α protein (Shin et al., 2009). IκBα was also found to positively regulate HIF-1 transcriptional activity by antagonising FIH and positively regulating the recruitment of p300 to HIF-1α, in acute but not severe hypoxia (Shin et al., 2009). Shin et al use these findings to suggest that IκBα plays a pivotal role in the cross-talk between the HIF-1 and NF-κB signaling pathways (Shin et al., 2009). In this context they propose that IκBα acts a mediator, allowing cellular responses to switch between NF-κB-mediated inflammation to HIF-1-mediated hypoxic adaptations (Shin et al., 2009)(see **Figure 16**). However, this is difficult to reconcile with the data from Cockman 2009, which suggests that IκBα is just one of many FIH binding proteins (Cockman et al., 2009).

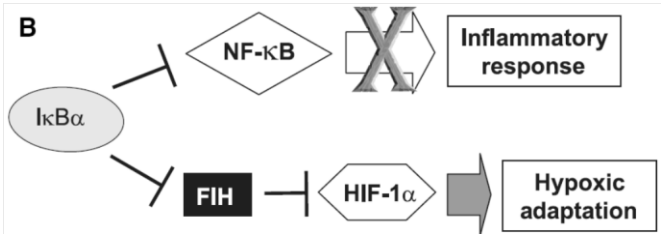


**Figure 16 Two pathways with proposed cross talk are those of hypoxic adaptation and the inflammatory response, with IκBα as a key mediator.**

*Figure is taken from (Shin et al., 2009) to describe their model of cross-talk between the HIF-1 and NF-κB pathways. Permissions were granted from Publishers the Wiley Company for the republication of this figure.*

In a study assessing the behaviour and function of neutrophils in response to hypoxia and HIF regulation, hypoxia is able to increase NF-κB protein expression and activity, and this is thought to mediate neutrophil survival (Walmsley et al., 2005). Observations that enhanced survival of peripheral blood neutrophils was observed in patients with VHL diseases, along with studies of *HIF-1α-/-* murine neutrophils resulted in both reductions in NF-κB message and anoxia-stimulated cell death (Walmsley et al., 2005). Hypoxia driven stabilisation of NF-κB is proposed to be a link between oxygen deprivation and cell survival, however the mechanism of the interaction remains to be elucidated (Walmsley et al., 2005).

Sakamoto et al have since shown that FIH may be regulated by other proteins in addition to ankyrin domain proteins. They described that FIH was suppressed in macrophages by the c-terminal tail of a membrane bound matrix metalloproteinase (MT1-MMP/MMP-14). They proposed that this suggested a role for MT1-MMP expression in macrophages as a significant role in regulating HIF-1 activity. The cytoplasmic tail (CPT) of MT1-MMP in the membrane of the macrophage has been implicated in glucose metabolism, and It has this process that's been connected to FIH. The CPT is proposed to bind to FIH, inducing the interaction with MINT3 (an FIH inhibitor) (Hara et al., 2011, Sakamoto and Seiki, 2009, Sakamoto and Seiki, 2010), abrogating the interaction between FIH and HIF. Inhibition of FIH is then what leads to increased HIF activity and the induction of glycolytic metabolism of macrophages even in areas of low HIF expression in normoxia (Sakamoto et al., 2011). In cell line studies it has been demonstrated that tumour cells where MT1-MMP was expressed exhibited increased glycolytic activity. These effects mimic the Warburg effect, the observation that most cancer cells predominantly produce energy by a high rate of glycolysis followed by lactic acid fermentation in the cytosol observed in solid tumours (Sakamoto et al., 2011). Macrophages lacking MT1-MMP exhibit reduced glycolysis and a 60% reduction in ATP levels and that these macrophages show defects in motility, cytokine production and phagocytosis.

### 1.6.4 Other FIH substrates: a role of FIH Hydroxylation in Notch Signaling

A complex cross-talk may exist between the Notch and HIF pathways and this has been suggested to occur at various levels, either globally with oxygen levels affecting the binding of particular components and direct cross-talk between components of the two pathways including Notch and FIH.

The Notch mutation was first identified by John S. Dexter in 1914 who noticed a notched pattern in the wings of *Drosophila melanogaster*, and the alleles of the gene were identified a few years later in 1917 by Thomas H. Morgan (Brou et al., 2000). The molecular cloning of *Drosophila* Notch locus followed in 1982 by Artavanis-Tsakonas et al (Artavanis-Tsakonas et al., 1983).

The pathway has since been shown to affect developmental changes by changing the gene transcription repertoire of the receiving cell. The notch pathway is a cell-cell communication mechanism controlled by direct binding of receptors (Notch) and ligands (Delta/Delta-like/Jaggged) in the membrane of two cells (Lai, 2004). Notch is a single pass transmembrane protein, 2703 amino acids long (4 homologs have been identified in vertebrates) that serves as a receptor for Delta/Delta-like/Jagged proteins (3 Delta and 2 Jagged homologs have been identified in vertebrates) (Kidd et al., 1986, Ohishi et al., 2000). Importantly, the notch receptor contains ankyrin repeat domains and the crystal structure of the *Drosophila* Notch receptor ARD has been developed to a 2.0Å resolution by Zweifel et al. The architecture of the domain consists of an elongated array of anti-parallel six α-helices and a putative seventh C-terminal sequence repeat (Zweifel et al., 2003). The structure of the mouse and human Notch proteins have been shown to be homologous to Drosophila Notch, see **Figure 17** (Lubman et al., 2005, Ehebauer et al., 2005).

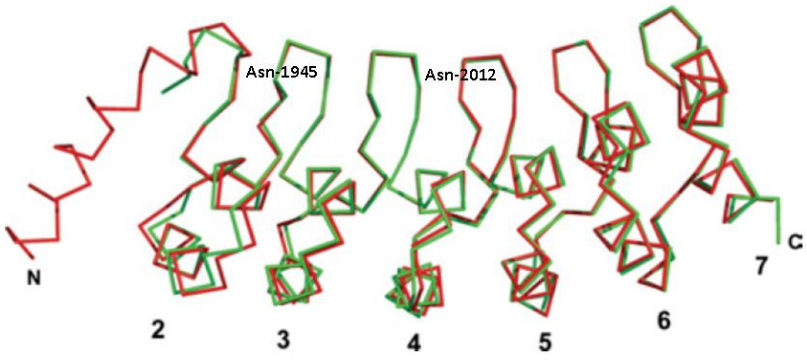


**Figure 17 There are multiple points of homology between Drosophila and Human Notch proteins**

*Shows the superimposed structures of the Drosophila Notch and the human Notch1 ANK domains, taken from (Ehebauer et al., 2005). The Asn residues marked are indicated are the indicated positions of those where FIH hydroxylation takes place (Zheng et al., 2008).*

The notch pathway describes a cell-cell communication mechanism controlled by direct binding of receptors (Notch and Delta/Delta-like/Jagged respectively) in the membrane of two cells (Lai, 2004) (see

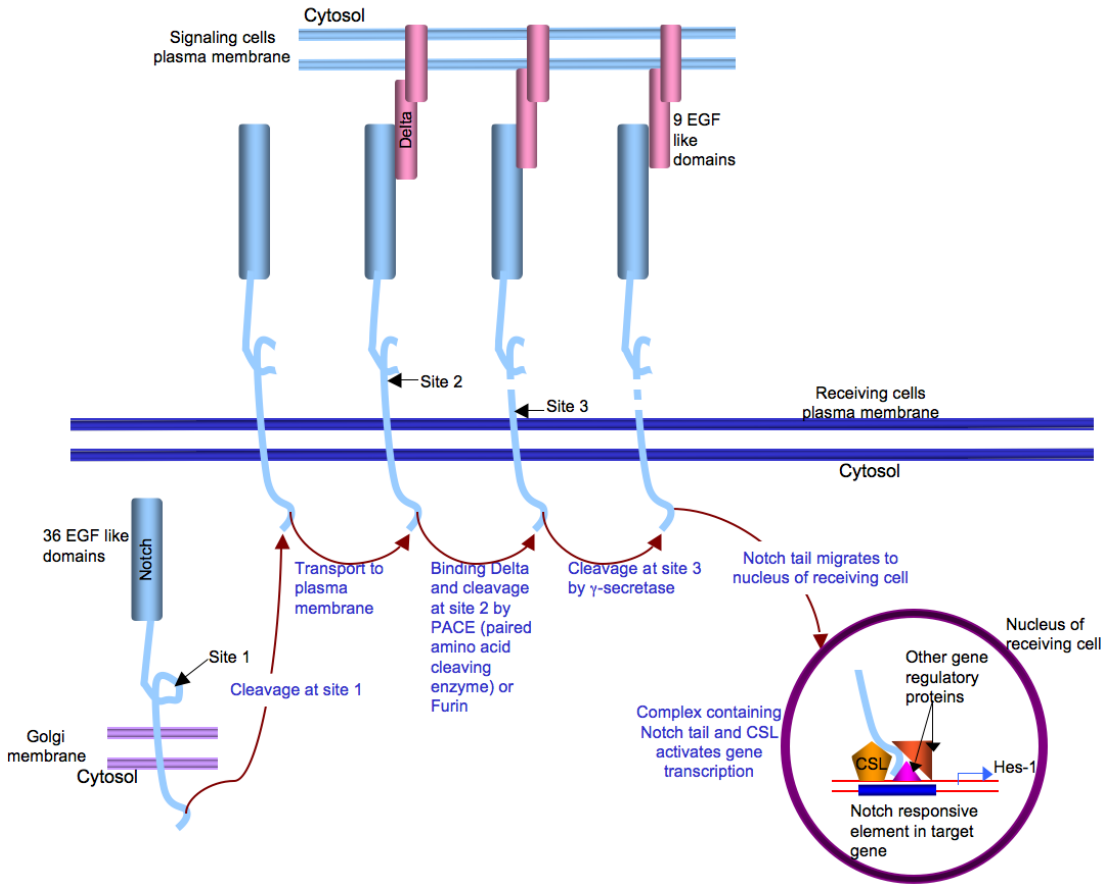


**Figure** 18).

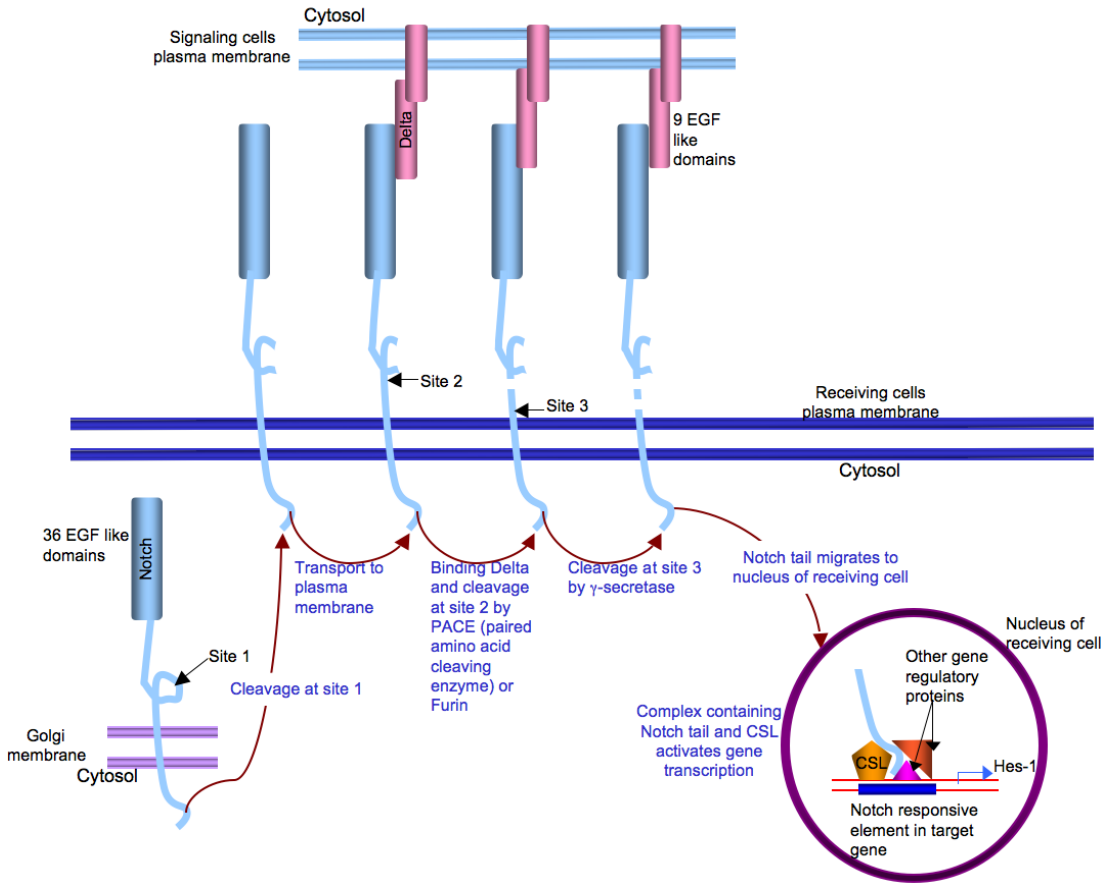


**Figure 18 The notch signaling pathway.**

*The notch protein is cleaved at the Golgi membrane and transported to the plasma membrane. Signaling is initiated when the extracellular domain of Notch is internalized by the delta presenting cell. A second cleavage event then occurs, initiating the cleavage at the plasma membrane by γ-secretase enzymes. This releases the notch intracellular domain (NICD) to migrate into the nucleus where it binds a complex of other proteins to activate gene transcription (Lai, 2004) by binding a complex of proteins including CSL (CBF1, Suppressor of Hairless, Lag-1), a transcription factor (Pursglove and Mackay, 2005)*

Notch target genes include Hairy and Enhancer of Split (Hes) family members and Hes-related repressor protein (Hey) family members or the Epidermal growth factor (EGFR) receptor family (Sjolund et al., 2008, Lai, 2004). The Hes and Hey family members are transcriptional repressors (Pfaffenroth and Linehan, 2008) that control Notch signaling output (Sjolund et al., 2008).

The NICD interacts directly with HIF-1α, and this has been shown to be recruited to Notch-responsive promoters following hypoxia driven Notch activation (Gustafsson et

al., 2005, Pear and Simon, 2005) leading to increase in expression of notch target genes. Hypoxia has been shown to stabilise the NICD as well as increase its activity, through interactions with HIF-1α rather than pVHL (Gustafsson et al., 2005). FIH has been shown to interact with both full length Notch, within the ankyrin repeat domain folds that are cleaved to release the NICD (Coleman et al., 2007) as well as the cleaved NICD (Zheng et al., 2008), alongside the proposed interaction between HIF-α and the NICD (Gustafsson et al., 2005). For simplicity, the diagram in **Figure 19** indicates the interaction between HIF-α and NICD proposed by Gustafsson et al.

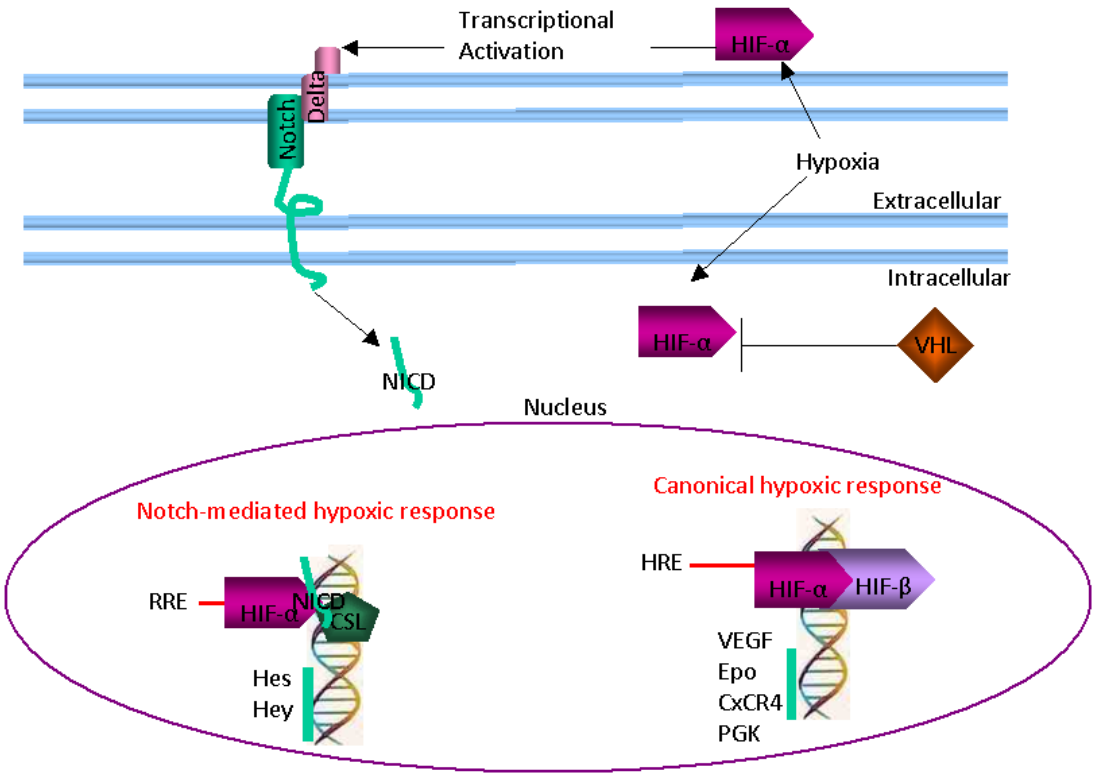


**Figure 19 There is proposed cross-talk between Hypoxia and Notch signaling pathways**

*This figure has been adapted from one in (Gustafsson et al., 2005) to illustrate the cross-talk between hypoxia and Notch signaling. Abbreviations:- Notch intracellular domain (NICD), hypoxia inducible factor (HIF), von hippel lindau protein (VHL), (CSL), hairy and enhancer of split (HES), hairy and enhancer of split with YRPW motif (HEY), vascular endothelial growth factor (VEGF), erythropoetin (EPO), C-X-C chemokine receptor type 4 (CXCR4), phosphoglycerate kinase (PGK), HIF response element (HRE), rev response element (RRE). Reprinted with permission from Elsevier, also Lancet special credit with permission from Elsevier*

In addition, FIH has been shown to interact directly with endogenous Notch receptors by hydroxylating highly conserved asparaginyl residues within the ankyrin repeat (AR) domains (ARDs) (Coleman et al., 2007, Zheng et al., 2008). Zheng et al also went on to show that FIH hydroxylation of the NICD occurs at two residues $N^{1945}$ and $N^{2012}$, before the β-hairpin turns separating the ICD ANK 2nd and 3rd repeats and 4th and 5th repeats respectively (Zheng et al., 2008), see **Figure 20**. These residues are critical for the function of the NICD as a transactivator in neurogenesis and myogenesis *in vivo*, as well as for the mediation of Notch complexes. This is a common feature of the Asn residue that is targeted within ARD proteins that are also hydroxylated by FIH (Wilkins et al., 2012). The results of several reports have demonstrated conflict over the effect of FIH hydroxylation of different substrates. Several studies have shown that the hydroxylation stabilises localised regions of the ankyrin fold (Yang et al., 2011b, Hardy et al., 2009, Kelly et al., 2009), enhancing notch signaling. Other studies have questioned the importance of the actual hydroxylation and suggested the binding of FIH itself might be inhibitory when over-expressed (Coleman et al., 2007). These discrepancies could be due to cell type specific or even context specific elements within individual studies, making comparison between them difficult and leading to the need for further investigation.

Several features do combine to describe a consensus sequence required for FIH hydroxylation, which Wilkins et al have compiled. The consensus sequence shows that there isn't a single amino acid that is conserved at every residue and that recognition is therefore reliant on a few individual positions, (Wilkins et al., 2012). These findings are consistent with Asn hydroxylation by FIH, although also identified are histidinyl residues within the ankyrin repeat domain of tankyrase-2 that can also be hydroxylated by FIH *in vitro* (Yang et al., 2011a). Binding studies performed by Coleman et al showed that FIH had a higher binding affinity for these ARDs of the notch protein than it did for HIF-α (Coleman et al., 2007), see **Figure 20.**

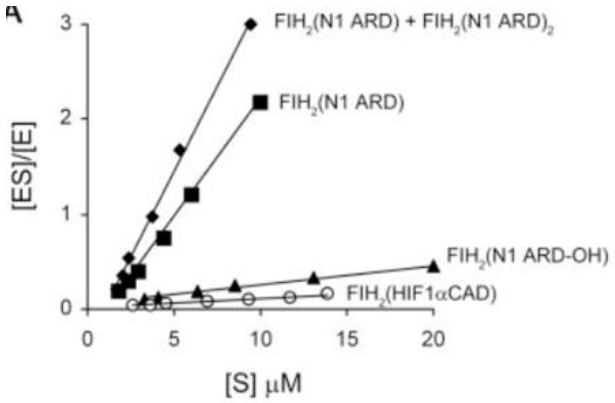


**Figure 20 The binding of FIH to both HIF and notch components have been shown to have different binding efficiency**

*Figure describes mild ionization electrospray mass spectrometry (MS); Kd or Scatchard plot was used plotting the specific binding on the X-axis and the specifc binding divided by free ligand concentration on the Y-axis. The Kd is then described as the negative reciprocal of the slope to assess binding efficiencies. The binding of the Fih dimer ($Fih_2$) with N1 (including data for $FIH_2$-$(N1)_2$, $FIH_2$ and N1 (excluding data for $FIH_2$-$(N1)_2$, $FIH_2$ and N1 ART(OH), and $FIH_2$ and His-HIF-1αCAD were assessed. Equimolar Fih plus substrate were mixed and analysed in the absence of Fe/2OG. [E]=enzyme concentration [S]=substrate concentration. It demonstrates stronger binding of Fih dimer to the notch proteins that were tested than to the c-terminal domain of HIF-α. Figure from (Coleman et al., 2007).*

Fih hydroxylation of the NICD stabilises the ankyrin repeat domain, resulting in an increase in Notch signaling, whereas Fih binding of the NICD has an inhibitory role on the NICD when Fih is over expressed. The preferential binding of FIH to Notch and also other ankyrin repeat domain containing proteins (of which there are over 200 in the genome) may provide an explanation as to how HIF protein, once stabilised in the absence of VHL, can escape hydroxylation and be highly active even in the presence of FIH (Coleman et al., 2007, Wilkins et al., 2012). The affinity of FIH for TAD-C could be influenced by residues in close proximity to the Asn that FIH has been shown to hydroxylate, but appear to be unaffected by increases in length of the unfolded TAD-C (Wilkins et al., 2009, Cockman et al., 2009). Zheng et al suggest that FIH provides a link between these two pathways, with differential regulation of the proteins having impact on the overall signaling (Zheng et al., 2008). The affinity of FIH for Notch has been shown to decrease upon hydroxylation and this has been proposed to influence the ability of Notch to sequester FIH away from HIF-α and regulate transcriptional output from TAD-C (Wilkins et al., 2009).

The combined effect, in hypoxia, of decreased $O_2$ inhibiting FIH function (stopping FIH inhibition of Notch/NICD) and the increased stability of HIF-1α (stabilising the NICD after cleavage) can lead to increased stabilisation and function of the Notch signaling pathway and downstream targets. Where Notch protein levels are low, FIH will bind HIF-α and hydroxylate it, which inhibits its function. However, increasing levels of FIH or Notch induce sequestering of NICD by FIH in preference to HIF resulting in de-repression and subsequent signaling (Zheng et al., 2008).

More research is needed to assess whether or not FIH has a preference for binding Notch-ARD (inactive) or the NICD (active), since the literature simply indicates that both interactions are possible (Zheng et al., 2008, Coleman et al., 2007). It is also curious that studies have suggested sequestration of FIH away from HIF by specific proteins such as Notch/NICD where FIH has been shown to preferentially bind the latter over HIF. If FIH is truly able to interact with multiple pathways where ankyrin repeat domain proteins are present, as has been shown by Cockman et al (Cockman et al., 2009) then the sequestering of FIH away from HIF-α by Notch/NICD should not be specific to this interaction. The ARD domain is one of the most common amino acid motifs in nature, is present in over 300 proteins in the human genome and is conserved in all kingdoms of life (Cockman et al., 2009). This being the case, and with FIH having been shown to interact with several of these proteins, including IκB and Notch receptors (Cockman et al., 2009), more research is therefore required in order to clarify the relationship between these interactions and the specific effect they have on different signaling pathways.

The complexity of the cross-talk between HIF and Notch signaling becomes relevant when the downstream effects of each pathway are assessed. Downstream targets of HIF signaling include those involved in angiogenesis, and Notch signaling has been reported to be involved in the decision whether to become tip or stalk cells. Outside the vascular system, Notch influences some cell cycle control mechanisms, differentiation in neural and haematopoietic cell fates in the developing embryo as well as the differentiation of arterial and venous cells by lateral inhibition (Bentley et al., 2009). With respect to sprouting angiogenesis DLL4 expression in a developing tip

cell inhibits the expression of DLL4 in neighbouring cells, where Notch is expressed. This sets up a lateral inhibition mechanism, which in turn regulates the number of tip cells that are identified and therefore the number of developing branch points on a particular blood vessel (see **Figure 21**)(Hellstrom et al., 2007, Caolo et al., 2012, Leslie et al., 2007).

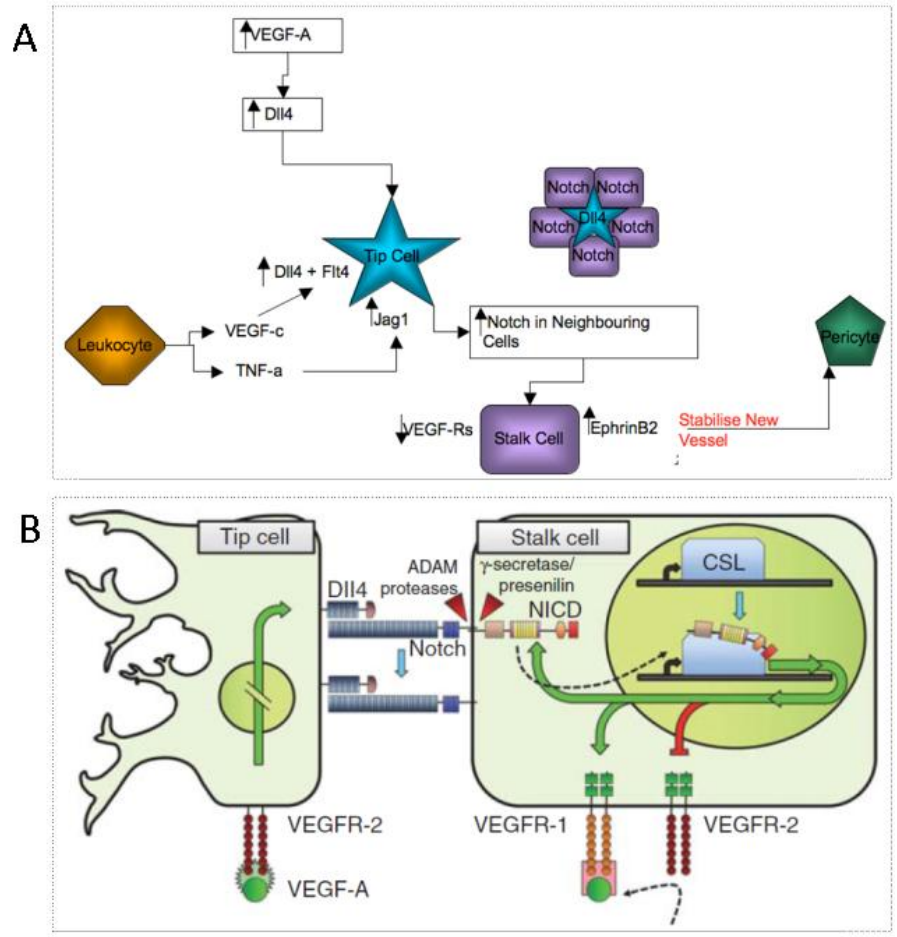


**Figure 21 Some of the links in different pathways involved in the branching morphogenesis that allows new blood vessels to form from pre-existing ones**

***A)*** *Describes the sources of different signals that dictate the identity of tip cells versus stalk cells. VEGF-A (a hypoxic signaling target) induces the expression of DLL4 (a notch ligand) in a newly designated tip cell. The expression of DLL4 in one cell induces lateral inhibition preventing surrounding cells from taking on this fate and inducing the expression of Notch and Jagged in these cells, designating these stalk cells. The tip cell reads cues such as Vegf, guiding the migration of the newly forming vessel as the stalk cells below it proliferate and drive progress forward.* ***B)*** *Provides a clearer indication of the direct cross talk between adjacent cells through the Dll4 (on the tip cell) and Notch (on the stalk cell) providing further downstream signaling through VEGF receptors, figure taken from (Tung et al., 2012).*

The recombining binding protein suppressor of hairless (RBPSUH) encodes the RBP-Jκ protein, otherwise known as CSL after mammalian, *Drosophila* and *C. elegans* homologs (Miele, 2011), which acts as a transcription factor recognising the mouse sequence C(T)GTGGGGA (Oka et al., 1995). It has been shown to interact with all four of the mouse Notch receptors, making it important for transcriptional control of canonical Notch signaling (Kato et al., 1996, Souilhol et al., 2006, Fortini and Artavanis-Tsakonas, 1994). In the mouse, the loss of RBP-Jκ leads to embryonic lethality before 10.5 days of gestation (Oka et al., 1995). In the zebrafish its loss leads to an increase in the sprouting of ISVs (Siekmann and Lawson, 2007). By decreasing notch expression, or indeed by decreasing expression of just the ligand *dll4*, there is an increase in the tip-cell behaviour and therefore an increase in sprouting (see **Figure 22**).

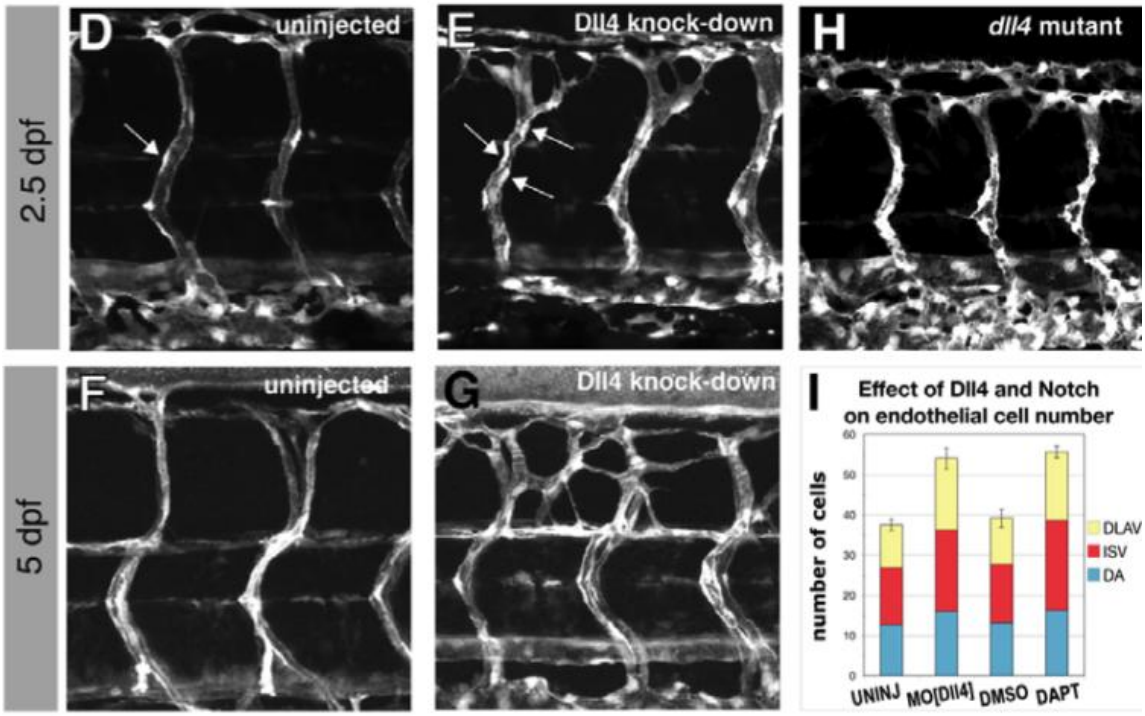


**Figure 22 Dll4 knock-down results in increased endothelial cell number and increased vessel branching**

*(D-G) Tg(fli1:EGFP) embryos at 2.5 dpf (D,E) or 5 dpf (F,G) either uninjected (D,F) or injected with 10 ng MO[Dll4] (E,G). White blobs (arrows in D,E) are endothelial cell nuclei. (H) Similar region of a 2.5-dpf dll4-homozygous- mutant embryo (carrying the fli1:EGFPtransgene). (I)Endothelial cell counts in the DAs, ISVs and DLAVs of embryos at 3 dpf. Embryos lacking Dll4 or treated with 100 m DAPT have more cells than uninjected or DMSO- treated control siblings. Both effects are significant at the P=0.001 level (t-test; n6 specimens for each treatment; error bars represent s.e.m.). Figure taken from (Leslie et al., 2007). Reproduced with persmissions.*

In normoxia, increasing expression of DLL4 ligand increases levels of Notch signaling in receiving cells, in a non cell-autonomous manner, induces lateral inhibition, ensuring individual tip cells are surrounded by stalk cells and an organised development of the vasculature (Siekmann et al., 2008). This means that a decrease in Notch signaling leads to an increase in sprouting blood vessels due to the loss of lateral inhibition and the increase in cells taking on tip cell identity.

Hypoxia increases expression of VEGF-A, which binds VEGFR-2 on an endothelial cell, inducing tip cells and resulting in increased expression of Notch ligands jagged-1 and delta-4 in the nearest cells, thereby desensitising those cells to Notch signaling (Jakobsson et al., 2010, Sainson and Harris, 2006, Bedogni et al., 2008) in a cell-

autonomous manner through *cis*-inhibition (Wang et al., 2011) but at the same time inhibiting adjacent cells from adopting the same fate through activation of Notch. The down-regulation of *dll4* by MO injection **(Figure 22)**, results in increased branching of the vessels because it ensures that this lateral inhibition mechanism is not initiated and this results in the tip-cell fate being taken on by an increased number of cells.

At the same time HIF might more directly promote Notch signaling, by a transcriptional up-regulation of notch protein via HIF (Sainson and Harris, 2006). As mentioned before, HIF-α can also act more directly on Notch, stabilising the NICD after cleavage (directly or indirectly), which can enhance expression of notch target genes (Sjolund et al., 2008, Zeng et al., 2005, Zheng et al., 2008). The interaction between HIF and Notch signaling is complex and *in vivo* models may help to resolve major and minor effects.

### 1.6.5 Role for Fih in Regulating Metabolism

Cell culture data, such as that described for the interactions between FIH and its substrates, made strong predictions on role of FIH in inflammation, Notch and more importantly hypoxia. The release of a paper describing the generation and initial characterisation of an *Fih-/-* mouse, however, demonstrated some surprising phenotypes. This puts all previous data into perspective and provides a contrast and new emphasis that requires clarification. Zhang et al published the study of the *fih*-/- mouse model, following the start of this project to assess the *fih217/217* zebrafish, and demonstrated that Fih played a normoxic role in regulating metabolism (Zhang et al., 2010) and phenotypes relating to inflammation/notch signaling were not described. This does not mean that these interactions were not present; it simply indicates that they were not obvious phenotypes as the mice were viable. It was shown instead that on *Fih*-/- mice displaying increased cellular ATP and suppression of AMPK, along with a hyper-metabolic state. This was characterised by looking at the elevated oxygen consumption and increase in heat production in the embryos along with an increased heart rate. It corresponded with a decreased body mass and adiposity, along with protection from high-fat-diet-induced weight gain.

Zhang et al also showed that the *Fih-/-* mice also showed that, consistent with the lack of HIF-related changes in vascularisation the basal levels of *Epo* were not altered,

however they demonstrated a decrease in both plasma and renal *Epo* levels in response to hypoxia. Given that *Epo* is a HIF-target, the decrease in expression is surprising, since in an *Fih-/-* mouse there would be a loss of *Hif-α* regulation and if anything an up-regulation of target genes could be expected. They propose that these alterations are not due to direct effects on *Epo* expression, but rather on the correlation with altered respiration during hypoxia. The findings of Zhang et al. together led to the conclusion that *fih* was playing a role that is not directly connected to its role in regulating HIF activity, and that this was connected to a metabolic rather than hypoxic phenotype. These data were not released when the current PhD project was begun and this provided a change in the course of the investigations that were subsequently pursued.

### 1.7 Use of the Zebrafish as a Model Organism for Hypoxic Signaling

Zebrafish (*Danio rerio*) provide many key features that make it a desirable model for the study of vertebrate development, and more recently it has also become a popular model to model human diseases and processes that are highly relevant to human disease. The zebrafish provide a real time model for studying the development of tissues that are inaccessible in other mammalian models. Taking blood vessels as a relevant example there are several different models that have been developed for the assessment and visualisation of vascular growth *in vivo,* with different accessibility and opportunities, (Norrby, 2006), see comparison in **Figure 23.**

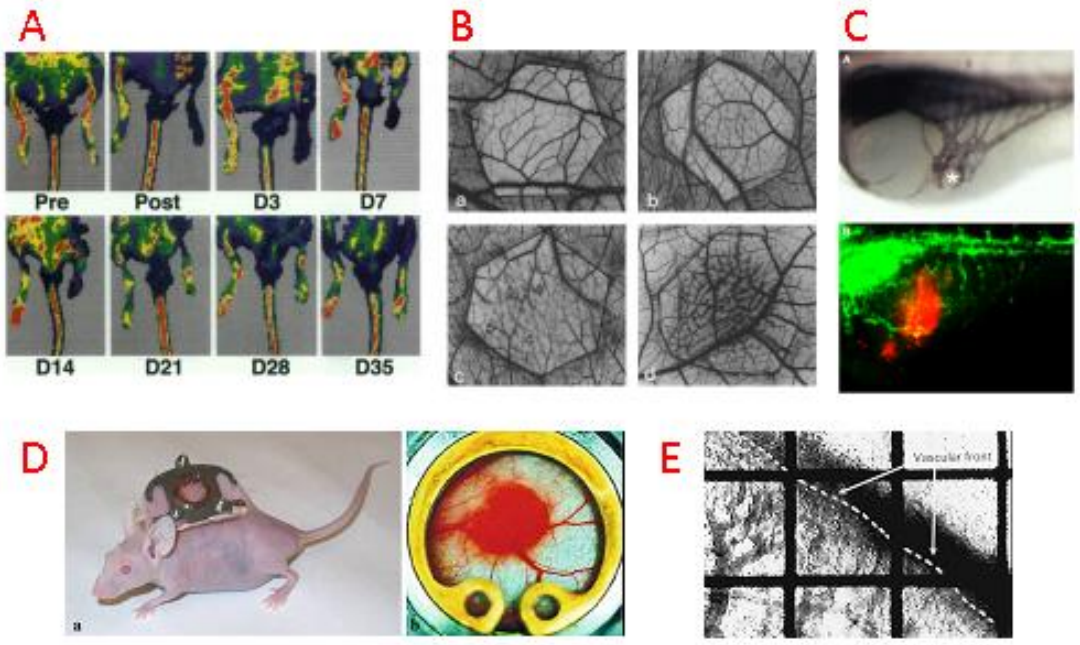


**Figure 23 There are multiple animal models for observing vascular growth, from laser Doppler perfusion to window chamber assays.**

***A)*** *Hindlimb blood flow monitored serially in vivo by laser Doppler perfusion imaging (LDPI), false colours represent normal baseline perfusion (Pre) in red, followed by marked reduction in blood flow post excision of one femoral artery (Post) in blue. Perfusion then sequentially monitored to return to near normal levels by 28days post (Couffinhal et al., 1998).* ***B)*** *Chick chorioallantoic membrane (CAM) assay used to visualise effect of VEGF on vascular growth, a) control - with neither vascular growth or vascular patterning b) effect of 0.5µg VEGF$^{165}$, showing weak angiogenic response in region of pre-capillary vessels c) effect of 1µg VEGF$^{165}$ d) effect of 3µg VEGF$^{165}$ where brush-like vessels have formed (Wilting et al., 1993).* ***C)*** *Illustrates the zebrafish as a model of tumour angiogenesis at 48hours where injection with tumour cells, where a) shows 24hours post injection, embryos were stained with alkaline phosphatase activity to visualise newly formed blood vessels b) GFP-tagged blood neovessels (green) penetrate the tumour cell graft loaded with Dil fluorescent dye (red) (Tobia et al., 2011).* ***D)*** *Window chambers used to visualise vasculature in dorsal skin-flap (Hak et al., 2010).* ***E)*** *In a window chamber in the rabbit ear, a dotted line indicates the vascular front, so observations and measurements can be made of wound healing assays (Ichioka et al., 1997).*

Each model provides a method for accessing the vasculature, using Doppler imaging to visualise flow through vasculature, or cutting windows to access the vessels beneath the skin. The zebrafish model has several strengths, allowing visualisation of the vasculature without invasive procedures, with the help of particular GFP transgenics. Due to their small size at early stages, diffusion of oxygen occurs through the embryo and the developing vasculature and blood cells are not necessary for the delivery of

oxygen to internal organs (Pelster and Burggren, 1996, Gray et al., 2007). This means that manipulations of the developing vasculature and circulatory system can be studied without seriously compromising development of the embryo as a whole, as it does continue to be oxygenated through diffusion. The zebrafish heart has been shown to regenerate following damage, making it a useful model for the mechanisms by which this could be achieved (Lien et al., 2012, Poss et al., 2002, Raya et al., 2004).

Zebrafish are naturally found in still or slow moving streams, river basins or around rice agriculture around the Ganges and Brahmaputra in north-eastern India, Bangladesh and Nepal (Spence et al., 2008). In the wild spawning appears to be seasonal, or in relation to food availability that might be a consequence of seasonal changes. In spite of this, breeding can be maintained year round in the laboratory and females will spawn every 2-3 days in the presence of males (Spence et al., 2008). Growth rate is the most rapid in the first three months and decreases to the time the adults are eighteen months old, although this has been observed to be faster in captivity, see **Figure 24.**

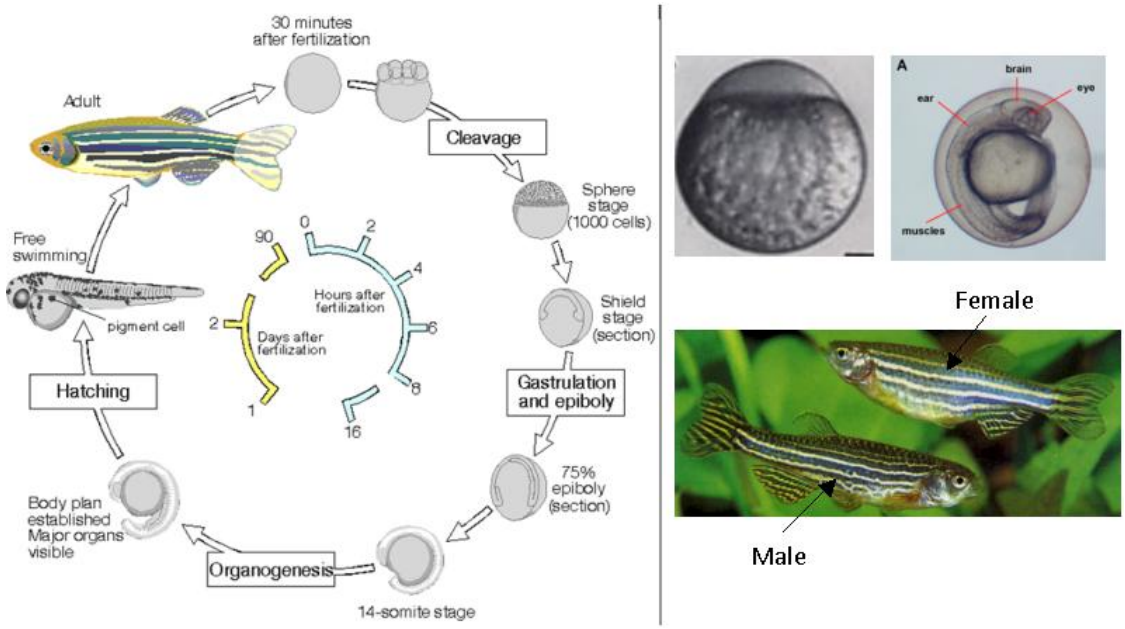


**Figure 24 The natural life cycle of the zebrafish, described with photographs at three stages; 1 cell, just prior to hatching and adult**

*Including time, along with photographs taken at three stages of the live process. The figure has been taken from various internet sources including: (DanioRerio.com, 2012, Fleming, 2007, Nusslein-Volhard, 2008).*

The generation time is short, often between 3-4 months, and a pair of mating adults can produce a clutch of several hundred eggs, enough for large-scale assays. The embryos are small, approximately 0.7mm in diameter after fertilisation, transparent and easily manipulated. External fertilisation and the embryos transparency allows visualisation of developmental changes over time; as the organs develop, as the heart starts to beat and as blood cells begin to circulate (Spence et al., 2008). This also allows for genetic manipulation of the embryos from the moment of fertilisation by the injection of constructs to disrupt or enhance particular genes' function and study the effects (Dodd et al., 2000, FFS, 2011). TILLING studies use mutagens to generate random mutations in large numbers of individual fish, progeny from mutated fish are studied to identify the causative gene of any phenotype chosen for study. The biomedical advantages of the fish are found in their systemic similarities to human, with circulatory, inflammatory and nervous systems being three examples.

Kimmel et al., have described the stages of normal development of the zebrafish embryo, providing a useful tool for the study both of changes over time but also of alterations to the normal pattern (Kimmel et al., 1995). The rapidity of their development, 36 hours to have precursors to all major organs, along with startle responses and food seeking within five days, allows for the study of development in real time (Spence et al., 2008). These features combined made them candidates for the first large scale random mutagenesis screens in vertebrates (Spence et al., 2008, Granato and Nusslein-Volhard, 1996).

Zebrafish are a naturally shoaling fish, and even if raised in isolation take up a shoaling behaviour when they are placed together (Buske and Gerlai, 2011). They are therefore being used for many behavioural assays due to their characteristic patterns of behaviour and their small size (Norton and Bally-Cuif, 2010).

### 1.8 The Development of the Vasculature

The formation of the vasculature is one of the earliest and most important events during organogenesis in the developing embryos of many species and is essential for the provision of oxygen and nutrients, along with the removal of waste products. The

diffusion distance for oxygen is between 0.1 to 0.2mm, and this necessitates the body's production of an extensive network of blood vessels (Heinke et al., 2012). In 1628 William Harvey first described the connection between arteries and veins filled with blood to form a circulatory system, despite the fact that he couldn't visualise it. The process of forming the vascular system is divided in two, with vasculogenesis forming the initial development and angiogenesis forming the process of expansion and remodeling of the network.

### 1.8.1 Vasculogenesis

Vasculogenesis, the physiological process of *de novo* endothelial differentiation from mesodermal precursors, by necessity occurs before the onset of circulation and results in the formation of the extra-embryonic yolk sac vasculature, the paired aortas, the endocardium and the primary vascular plexus (Flamme et al., 1997, De Val and Black, 2009).

In the mouse, differentiation of endothelial cells (angioblasts) occurs from mesodermal precursor cells in the embryonic yolk sac around E6-E6.5 and then later in the embryo itself (Drake and Fleming, 2000). The angioblasts form into cord-like vascular structures before generating vascular lumens and the subsequent organisation of vascular networks. Angioblasts have been defined as being *tal-1+/-;flk-1+/-*, with the expression of *tal-1* decreasing as the endothelial cells mature (Drake and Fleming, 2000, Gering et al., 1998).

VEGF has been shown to be expressed in the endothelium in regions where it can support vessel growth, and over-expression causes anomalous vessel formation *in vivo* (Fouquet et al., 1997). The VEGF isoforms, of which six have been identified in humans, are all secreted as covalently linked homodimers, with monomers associating through hydrophobic interactions. The three most well-described VEGF receptors (vegf-r) are receptors 1 (c-fms-like tyrosine kinase - *flt-1),* 2 (kinase insert domain-containing receptor - *kdr/flk-1)* and in the fish a second gene *kdrl* (Bussmann et al., 2008) and 3 (fetal liver kinase 4 - *flt-4)* (Quinn et al., 1993). The zebrafish *kdr-l* gene has been proposed, at different stages in the literature, to be either a gene duplication of the human *KDR* gene or a fourth class of vertebrate VEGF receptor and therefore a

true orthologue. Bussmann et al propose that *kdr/flk1* is the prominent VEGF-A receptor in the zebrafish and indicate it should be called *kdr-like* as a separate ortholog of the gene rather than a gene duplication, while the second *kdr* gene (the one that most similar to human *KDR* should remain *kdr* in the zebrafish (Bussmann et al., 2008).

Three acidic residues ($Asp^{63}$, $Glu^{64}$ and $Glu^{67}$) and three basic residues ($Arg^{82}$, $Lys^{84}$ $His^{86}$) have been identified in VEGF that are essential for binding to *Flt-1* and *Flk-1* (Robinson and Stringer, 2001). *Flt-1* and *Flk-1* have been shown to have differential expression, with *Flt-1* implicated in vessel organisation and *Flk-1* expression early on in the intra-embryonic angioblasts in the mouse as well as different affinities for VEGF (Waltenberger et al., 1994, Dumont et al., 1995). Following vessel formation *Flk-1* expression is reduced while *Flt-1* expression, along with other endothelial tyrosine kinases remains (Fouquet et al., 1997, Dumont et al., 1995, Waltenberger et al., 1994). An inhibitory mechanism exists utilising a soluble truncated form of *Flt-1* (*sflt-1),* which has been shown to bind to VEGF as strongly as full length *Flt-1* and acts by inhibiting VEGF activity by sequestering it from other receptors and forming non-signaling heterodimers with *Flk-1* (Robinson and Stringer, 2001). In the zebrafish *flt-4, kdr and kdr-like* are co-expressed in the blood vessels, except in the dorsal aorta. Here *flt-4* is down-regulated as development proceeds, indicating that *flt-4* is not required for arterial differentiation of endothelial cells in the dorsal aorta (Covassin et al., 2006). It is proposed that developmental stage and spatial expression patterns of *vegf-a* and *vegf-c* are responsible for the ligand accessibility and therefore receptor sensitivity in the various vessels in the zebrafish (Covassin et al., 2006). Differences are observed between the phenotypes of loss of function (LOF) of *flk-1* in the zebrafish and in the LOF of *Flk-1* and *Flt-1* in the mouse. In the zebrafish LOF of *flk-1* has been shown to only disrupt angiogenic sprouting from pre-existing vessels leaving the initial vasculogenesis and haematopoiesis unaffected, where in the mouse more initial disruptions are observed (Habeck et al., 2002). These differences are ascribed, by Habeck et al, to be down to the fact that in the mouse the primary vascular plexus is formed and remodeled whereas the zebrafish vascular system forms initially without apparent remodeling (Habeck et al., 2002, Isogai et al., 2001).

The different vegf ligands have been shown to interact with distinct vegf receptors, albeit with some level of overlap. VEGF-A interacts with FLT-1 as well as FLK-1/KDR,

sFLT-1 and Neuropilin (NRP-1), VEGF-B interacts with FLT-1, sFLT-1 and NRP-1, VEGF-C and VEGF-D interact with both KDR/FLK-1, FLT4 as well as Integrin αvβ3 and VE-Cadherin (VEC) (Neufeld et al., 1999, Veikkola et al., 2000). While signaling through FLT-1 and FLK-1/KDR as well as NRP-1 and Integrin αvβ3 has been implicated in angiogenesis, signaling through FLT-4 and VEC has been implicated in developmental angiogenesis and lymphangiogenesis (Veikkola et al., 2000, Neufeld et al., 1999, Shibuya, 2006, Vlahakis et al., 2005).

In the zebrafish, endothelial cells that line the various vessels in the developing zebrafish embryo have arterial and venous identity before circulation starts. A hierarchical signaling cascade was established leading these fate choices (Lawson and Weinstein, 2002a, Weinstein and Lawson, 2002), although alternative pathways may exist (Wilkinson et al., 2012, Nicoli et al., 2008) (See **Figure 25**).

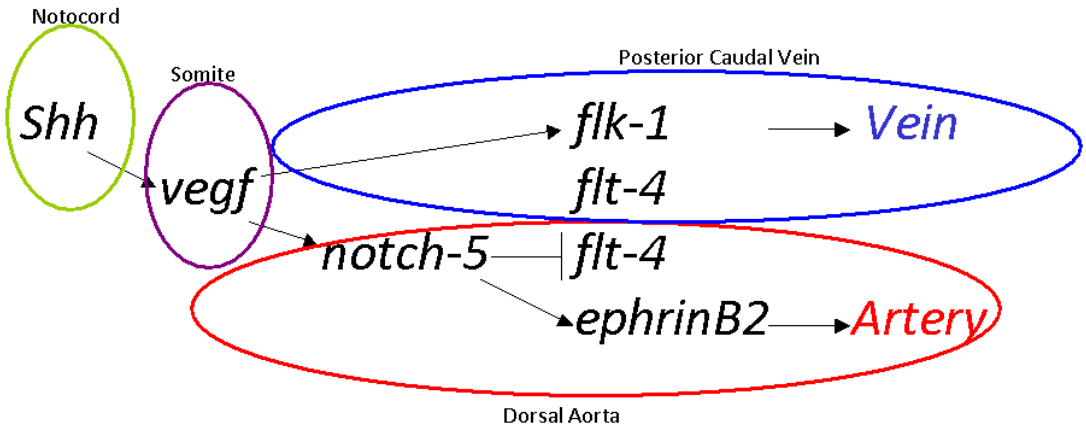


**Figure 25 Signaling in artery-vein differentiation is distinct in order to generate distinct tissue**

*This flow chart indicates the hierarchy of signaling that induces the difference between early arteries and veins (Lawson and Weinstein, 2002a, Lawson et al., 2002).*

This signaling cascade is probably also involved in the migration of endothelial progenitors (Lawson and Weinstein, 2002a) and lays down the basis for the vascular and haematopoietic lineages, as well as in distinguishing between arteries and veins (Wang et al., 1998, Adams et al., 1999, Gerety et al., 1999, Herbert et al., 2009). As the endothelial cells migrate under the somites and later, when they reach the midline,

dorsally towards the notochord, they are exposed to a variety of signals that is likely to determine their final fate choices (See **Figure 26**).

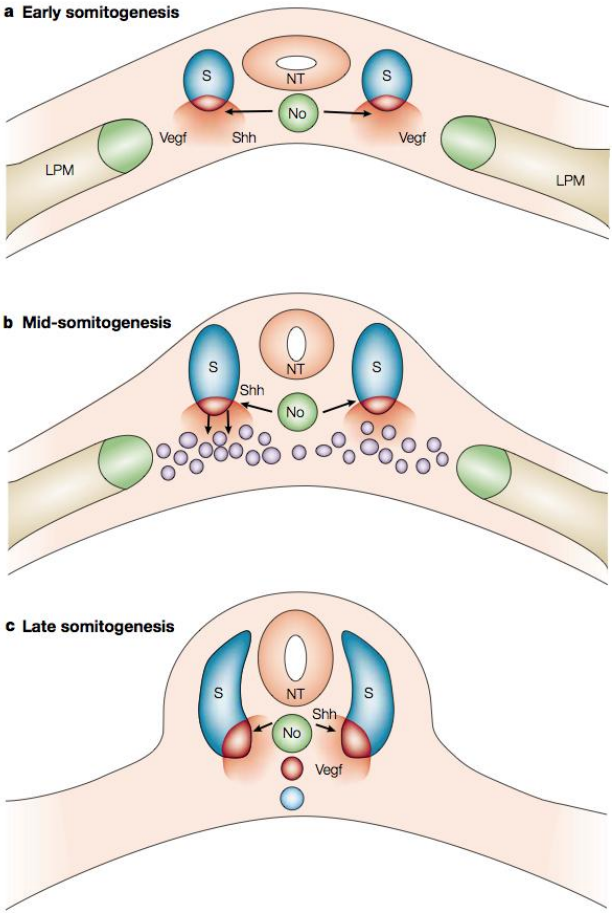


**Figure 26 Migration of vascular progenitors in the zebrafish has been described and followed in detail, responsive to levels of different cues.**

**A)** *Shh expression in the notochord has been shown to drive the expression of vegf in the surrounding somatic tissue, inducing angioblasts from the dorsal lateral mesoderm (green), which are then in close proximity to the Vegf.* ***B)*** *Later in mid-somitogenesis, local Vegf activates the Notch pathway, potentially through induction of notch5 in the developing dorsal aorta, which goes on to induce expression of ephrinB2a. Vascular progenitors then migrate towards the midline, with arterial progenitors leading the way (purple).* ***C)*** *In late somitogenesis distinguishing the artery from the vein is induced by the down-regulation of vein markers (eg. flt4 becomes restricted to the posterior cardinal vein (blue circle), and is actively repressed by the Notch pathway) in the arteries (red circle = artery). Reprinted by permission from Macmillan Publishers Ltd:* Arteries and veins: making a difference with zebrafish (Lawson and Weinstein, 2002a) *copyright (2002)*

The pruning, maturation and remodeling of this initial plexus is then initiated and termed angiogenesis (ten Dijke and Arthur, 2007).

### 1.8.2 Angiogenesis

Angiogenesis is the physiological process, which occurs in response to tissue hypoxia, disease and developmental alterations (Carmeliet, 2003). It allows the adaptation of the blood vessel network with the branching of new blood vessels from pre-existing ones. This process is implicated in multiple disease processes such as wound healing, ischemic myocardial infarction, atherosclerosis, rheumatoid arthritis and tumour angiogenesis (Fong, 2008).

Non-sprouting (intussusceptive) angiogenesis allows for rapid formation of new blood vessels under flow, within minutes to hours of the initiation of the process, without proliferation of endothelial cells (Risau, 1997). Sprouting angiogenesis on the other hand is a slower process with an invasive component, expanding the blood vessel network into un-vascularised tissues (Burri et al., 2004).

Sprouting angiogenesis is largely dependent on, and regulated by, the downstream targets of the hypoxic signaling pathway, such as *VEGF* (Fong, 2009). The process is initiated when a cell within the vascular wall is induced to become a tip cell. This is a process that depends on the activation of the VEGF receptor (Gerhardt et al., 2003, van Rooijen et al., 2010). A tip cell becomes pro-migratory, extending filopodia into the surrounding tissue to aid directional migration. Behind this tip cell, stalk cells proliferate extending the new vessel before it is lumenised and becomes competent to carry flow (**Figure 27** shows a schematic representation).

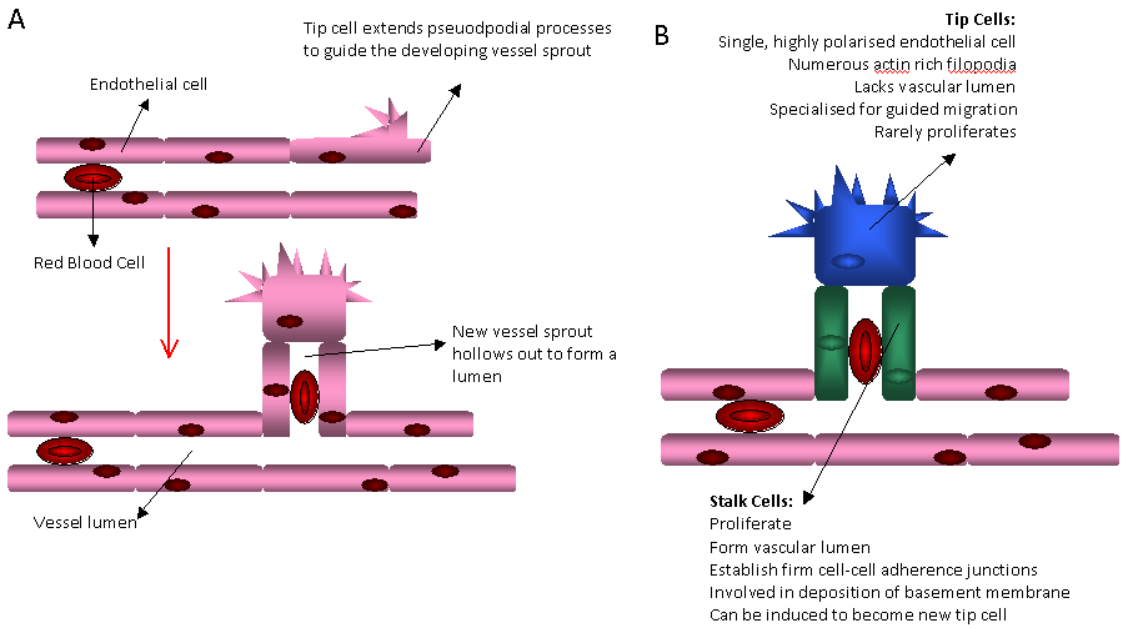


**Figure 27 The process of adaptive angiogenesis in a schematic diagram**

***A)*** *The induction of the tip cell, followed by the proliferation of stalk cells and the eventual lumenisation of the new vessel, adapted from various sources, including (Liman and Endres, 2012, Lammert and Axnick, 2012).* ***B)*** *Figure adapted from Figure in (Phng and Gerhardt, 2009) review on the role of Notch in angiogenesis, describes the different features of endothelial tip and stalk cells in the vasculature.*

These processes are complex and involve the co-operation of multiple signaling pathways in addition to VEGF and Notch, which play roles not only in the developing of the vessels but in distinguishing their fate from arteries and veins (Nunes et al., 2011). The migratory cues to guide the new branching have been linked to the expression of cytokines and their receptors, such as stromal-cell-derived factor 1 (Sdf1)/Cxcl12, reviewed by Ho et al (Ho et al., 2012). Motility of neuronal cells can then be shown to be enhanced by the presence of Aspartyl-(asparaginyl) β-hydroxylase (AAH), which in turn has been shown to hydroxylate Notch in a HIF independent manner (Lawton et al., 2010), this could also be possible as a mechanism in the vasculature. Along with the migratory nature of the new tip cells, in order to invade into novel tissues the extracellular matrix is remodeled (Foskett et al., 2011). A list of other genes involved in both vasculo- and angiogenesis is tabulated in a review by Heinke et al, along with the phenotypes of the various knock-out mice models that have been generated (reviewed in (Heinke et al., 2012)). This collates findings from *Vegfa-/-* mice, which demonstrate abnormal blood island formation and reduced embryonic vasculature, to

*Ang2-/-* mice, which also have impaired lymphatic vessel formation and patterning as well as defects in the development of the vascular bed. Notably, *Hif-1α-/-* mice demonstrate malformed hearts, yolk sacs and embryonic vasculature and have been shown to be embryonic lethal at E11 (Heinke et al., 2012, Patel-Hett and D'Amore, 2011). The common feature of the null models that are described in this table is that they result in embryonic lethality between E6.5 and E13.5, indicating the necessity of these processes of vascular control in the development of the embryos.

The process of angiogenesis has been modeled in several different *in vitro*, *in silico* and in *vivo* systems (Geudens and Gerhardt, 2011, Guidolin et al., 2011). Most importantly, the mouse retina and the zebrafish trunk have both been used to assess sprouting angiogenesis, along with studies of vascular patterning in the mouse hindbrain, hindlimb and the cornea.

### 1.8.3 Tumour Angiogenesis and Vasculogenic Mimicry

A solid tumour can only reach a critical dimension before hypoxia in its center up-regulates mediators such as HIF and downstream targets like VEGF (Nagy et al., 2009, Chung et al., 2010, Evans et al., 2012), which is where tumour angiogenesis resembles normal developmental angiogenesis (Persson and Buschmann, 2011, Helfrich and Schadendorf, 2011). In development though, the restoration of oxygen as the tissue is sufficiently vascularised leads to the down-regulation of angiogenic initiators such as VEGF, allowing the vessels to mature. In tumour growth the proliferation of vascular tissues is unlimited and uncoordinated, see **Figure 28** (Chung et al., 2010).

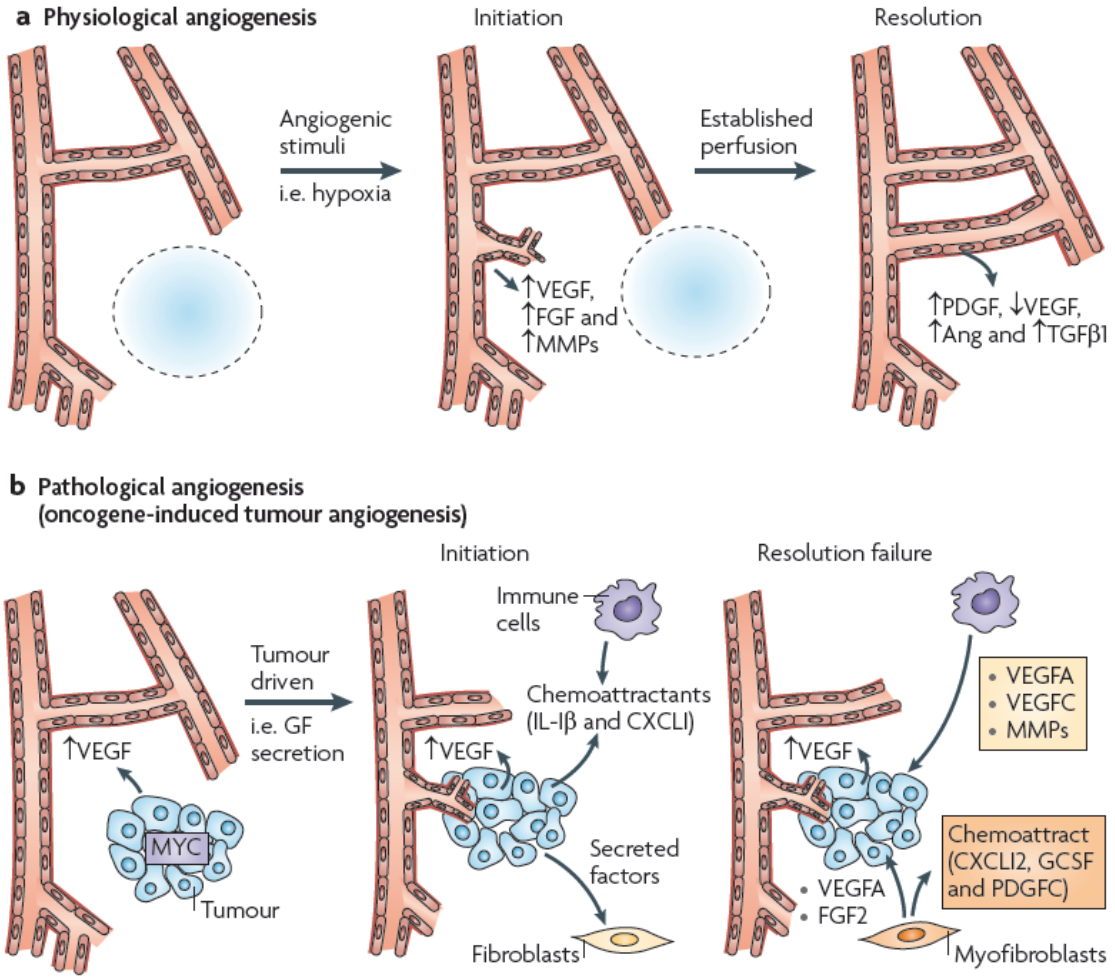


**Figure 28 Failure to resolve the angiogenesis cascade results in pathological angiogenesis.**

***A)*** *Shows the process of physiological angiogenesis following a stimulus such as hypoxia. The increase in growth factors (GFs) such as VegfA causes vessel destabilization and initiates vascular sprouting. Matrix metalloproteinases (MMPs) facilitate remodeling of the extracellular matrix (ECM). On vessel stabilisation Vegf levels drop and platelet-derived growth factor (PDGF), angiopoietins (Ang) and transforming growth factor β1 (TGF-β1) levels increase to begin the resolution phase responsible for stabilisation and recruitment of smooth muscle cells to the new vessels.* ***B)*** *Shows how under pathological conditions, tumour-secreted VegfA can initiate the angiogenesis cascade. The tumour cells have also been shown to increase expression of soluble factors responsible for activating fibroblasts and attracting immune cells, and these stromal cell types are capable of sustaining the angiogenic process resulting in a failure to resolve and the continued development of immature vessels. Other abbreviations include GcsF (Granulocyte stimulating factor) and IL-1β (interleukin-1β). Reprinted by permission from Macmillan Publishers Ltd: (Chung et al., 2010)* Targeting the Tumour Vasculature: Insights into Physiological Angiogenesis *copyright (2010)*

Due to high levels of VEGF and other oncogene driven factors, tumour vessels are enlarged, disorganized (Persson and Buschmann, 2011, Nagy et al., 2009) and tend to

be leaky (Nagy et al., 2012, Weis and Cheresh, 2005, Maeda, 2001) and in this they resemble and respond to similar signals and cues as collateral vessels. Vascular density tends to be highest at the interface between the tumour and the host, in both the tumour and the host tissue, with uneven distribution, flow directions and shunts throughout the network, leading to decreased blood flow in the tumour compared to the host (Persson and Buschmann, 2011, Halin et al., 2009).

### 1.8.4 Vascular Patterning of the Zebrafish

Vascular development has been largely studied in vertebrate models, despite techniques that often require that the animal be sacrificed for imagining, which often affects the number of time points that can be studied. However the zebrafish provide advantages to established techniques in higher vertebrates. Many have been described in the previous section, including their small size and the oxygen availability through diffusion in the embryos. An extensive study of the normal development of the zebrafish blood vessel network was undertaken, using confocal imaging and micro-angiography to map the network over development, by Isogai et al 2001 (Isogai et al., 2001).

The predictable patterning of the vasculature of the zebrafish and the extent of the information that is available provides an invaluable tool for the study of defects to this patterning. See **Figure 29** for a schematic simplification of the key trunk vasculature in the zebrafish embryo.

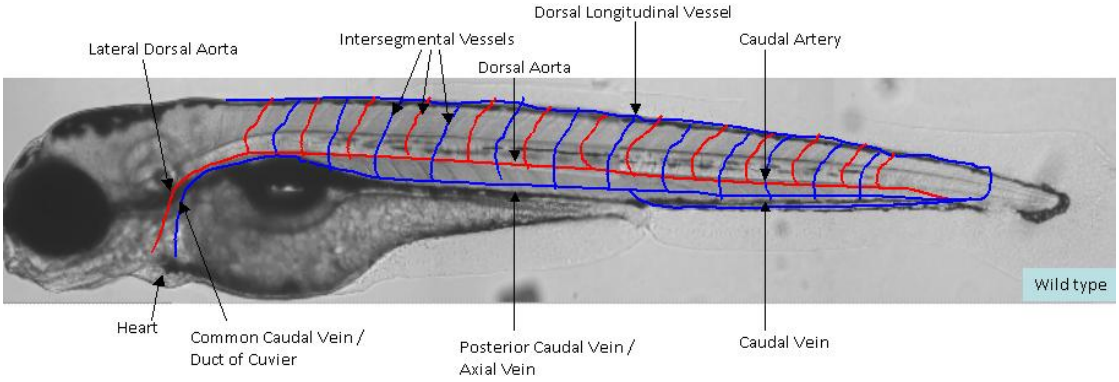


**Figure 29 A simplified representation of key blood vessels in the zebrafish at late embryonic stages demonstrates the regularity of the network**

*A greyscale image of a 5dpf wild type zebrafish embryo has been shown here with a schematic simplification of some of the key blood vessels and their nomenclature.*

The time scale of various assays including the application of vascular inhibitors and the appearance of alterations to the vasculature are shown to their comparison when in the context of the other animal models. For example in the study of angiogenesis inhibitors (24-48hours) to observe a response in the zebrafish compares with the chick (3-4 days) and the murine matrigel plug assay (5-7days), murine (1week) and rabbit (2-3days), or the mouse xenograft model (several weeks) (Tobia et al., 2011).

## 1.9 Thesis Aim

This thesis aims to test the hypothesis that FIH functions in both the HIF/Notch pathways focusing on blood vessel development and patterning, and to possibly identify further targets, either via transcriptome analysis or detailed phenotypic characterisation exploiting a recently created *fih* null zebrafish line.

# 2 Materials and Methods

## 1 Zebrafish

### 2.1.1 Fish Maintenance and Feeding

Zebrafish were fed live artemia brine shrimp, which was hatched in aerated hatchers of salted water once a day and a supplement food (flake or pellet) once a day. They are maintained on a 14hour day:10hour night cycle, to simulate sunrise and ensure a consistent time for first-light, the time at which the zebrafish will lay eggs. The water temperature is maintained at 28$^{o}$C and pH 7.

### 2.1.2 Genetic Crosses

Individual pairs of adult fish were mated in boxes with mesh for the embryos to fall through and collected in a lower box. Dividers were used overnight and removed the following morning where the timing of the lay was important and wanted at some point after 8am. Embryos were collected and the adult fish are returned to their tanks. Fertilised eggs were sorted from un-fertilised ones into Petri dishes and the aquarium water was replaced with E3 medium. The embryos developed in incubators kept at 28$^{o}$C.

### 2.1.3 Zebrafish Lines

Wild type strains used included LWT zebrafish strain (where out-crossing mutant lines) and Nacre (where embryo imaging would be enhanced by lack of pigmentation).

Mutant strains included single mutant adults (*vhl+/-* adult fish, fih+/- and *fih217/217* adult fish), as well as double mutant adults (*fih+/-;vhl+/-* and *fih217/217;vhl+/-* adult fish). For assays comparing *fih217/217* embryos to wild type, in order to increase the number of embryos that could be imaged without the need for post-assay genotyping, *fih+/-* adult fish were crossed to LWT adult fish, resulting in *fih+/+* and *fih+/-* embryos, for this study these were interpreted as being wild type.

*Fih;vhl x Tg(csl-venus)qmc61-* (Gering, M. pers. Comm.) provided a GFP read-out of cells expressing Notch. *Fih;vhl x Tg(Fli1:eGFP)* line allows for the visualisation of the vasculature (Motoike et al., 2000, Lawson and Weinstein, 2002b). *Fih;vhl x Tg(Flk1:eGFP-NLS)* line allows for quantification of endothelial cells as the GFP is nuclear localised (Blum et al., 2008). *Fih;vhl x Tg(Phd3:eGFP)* line developed by Santhakumar et al provides a read-out for *phd3* expression and a surrogate read-out of hypoxic signaling (Santhakumar et al., 2012).

## 2.2 Embryo Handling and Genotyping

### 2.2.1 De-chorionating Embryos

Chorions can be removed manually using watchmen forceps to gently release the embryos from the chorions. Alternatively embryos were treated with 1mg/ml Pronase in E3 media for 10 minutes at room temperature to degrade the chorions and aid removal.

### 2.2.2 Fixing Embryos

Embryos were anaesthetised using tricaine in the E3 medium and transferred to labeled tubes. The medium was removed and replaced with 4% para-formaldehyde (PFA) in PBS to cover and fix the embryos. The tubes were stored at 4$^{o}$C overnight and then the PFA was washed off using PBS. If required embryos were then transferred through a series of methanol solutions in PBS; 25%, 50%, 75% and 100% methanol to protect the embryos and then stored in the freezer at -20$^{o}$C.

### 2.2.3 DNA Preparation from Embryos or Fin Clips

Embryos/fins were collected in methanol to dehydrate the tissue before the methanol was evaporated off at 80$^{o}$C. 25ul of TE tween was added and heated to 98$^{o}$C for 15 minutes in a PCR machine and the block cooled completely before 5ul of 10mg/ml proteinase K was added and the samples left at 55$^{o}$C overnight with the lid at 110$^{o}$C. The proteinase K was deactivated by heating the block to 98$^{o}$C for 15 minutes and the block was cooled again. The samples were made up with 25ul of TE.

REDExtract-N-Ampt Tissue PCR Kit (Sigma Aldrich) was also tested for extraction of DNA. Individual embryos could be placed in 0.2ml PCR tubes. 25µl of extraction solution was added followed by 6.25µl of tissue preparation solution. The sample was initially incubated at room temperature for 10 minutes and then incubated at 95$^{o}$C for 3 minutes. 25µl of neutralising solution was added to the sample before vortexing and storing at 4$^{o}$C.

#### 2.2.4 Genotyping from Embryos or Fin Clips

Genotyping PCR solutions were set up by making a master mix as per the recipe in **Table 4,** before being placed in a thermal cycler for the PCR reaction. See **Tables 5 and 6** for PCR program parameters. The PCR products were then stored at 4$^{o}$C.

| Reagent | FIH/VHL PCRs - Volume (µl) | Gal4/NICD PCRs - Volume (µl) |
|---|---|---|
| **2x Biomix (Qiagen)** | 10 | 10 |
| **Forward Primer** | 0.1 | 1 |
| **Reverse Primer** | 0.1 | 1 |
| **dd$H_2O$** | 8.8 | 6 |
| **DNA** | 1 | 2 |
| **Total** | **20** | **20** |

**Table 4** *Reagents and volumes of the PCR reaction mixture used to amplify fih and vhl (column 1) and gal4 and NICD (column 2)*

FIH genotyping primers:
F – 5’ TGTAGGAGCCTGTTGTACTGA 3’
R – 5’ GAGTTTGTGGACAAGATGCA 3’

| Step | Process | Temperature ($^{o}$C) | Time (minutes) | Cycles |
|---|---|---|---|---|
| **1** | Denaturation | 94 | 4 | 1 |
| **2** | Extension | 92 | 0.5 | 35 |
| **3** | Annealing | 56 | 0.5 | |
| **4** | Elongation | 72 | 0.5 | |
| **5** | Final Elongation | 72 | 10 | 1 |
| **6** | Hold | 10 | Forever | |

**Table 5** *PCR program used for FIHexn genotyping*

VHL genotyping primers:
F – 5’ CCGACTCTCACAAGATTACGC 3’
R –5’ CTC CGAGGAAGTTGATCCAG 3’

| Step | Process | Temperature ($^{o}$C) | Time (minutes) | Cycles |
|---|---|---|---|---|
| **1** | Denaturation | 94 | 4 | 1 |
| **2** | Extension | 92 | 0.5 | 39 |
| **3** | Annealing | 56 | 0.5 | |
| **4** | Elongation | 72 | 0.6 | |
| **5** | Final Elongation | 72 | 10 | 1 |
| **6** | Hold | 10 | Forever | |

**Table 6** *PCR program used for vhl1exn genotyping*

The PCR programs were run using 1ul of the DNA extracted from the embryo or fin clip to be identified. Running 5µl out on a 1% agarose gel checked the PCRs had worked (226bp for FIH PCR and 412bp for VHL PCR). To identify mutants from siblings diagnostic digests were performed. For FIH PCRs a digest of 5µl of the PCR using MseI enzyme and for VHL PCRs a digest of 5µl of the PCR product using BciVI enzyme, see **Table 7** for reagents and volumes used for the digestion.

| Reagent | FIH - MseI Mixture Volume (µl) | VHL - BciVI Mixture Volume (µl) |
|---|---|---|
| **Buffer** | 1.8 (2) | 1.8 (4) |
| **BSA** | 0.1 | 0 |
| **Enzyme** | 0.1 (MseI) | 0.2 (BciVI) |
| **dd$H_2O$** | 13 | 13 |
| **PCR product** | 5 | 5 |
| **Total** | **20** | **20** |

**Table 7** *Reagents and volumes used for digestion of PCR products in diagnostic digests in fih and vhl genotyping*

The digests were performed at 37$^{o}$C overnight and the whole digest was run out on a 1% agarose gel for VHL PCR/digest and 3% agarose gel for FIH PCR/digest. See **Figure 30** for representation of agarose gel post digestion.

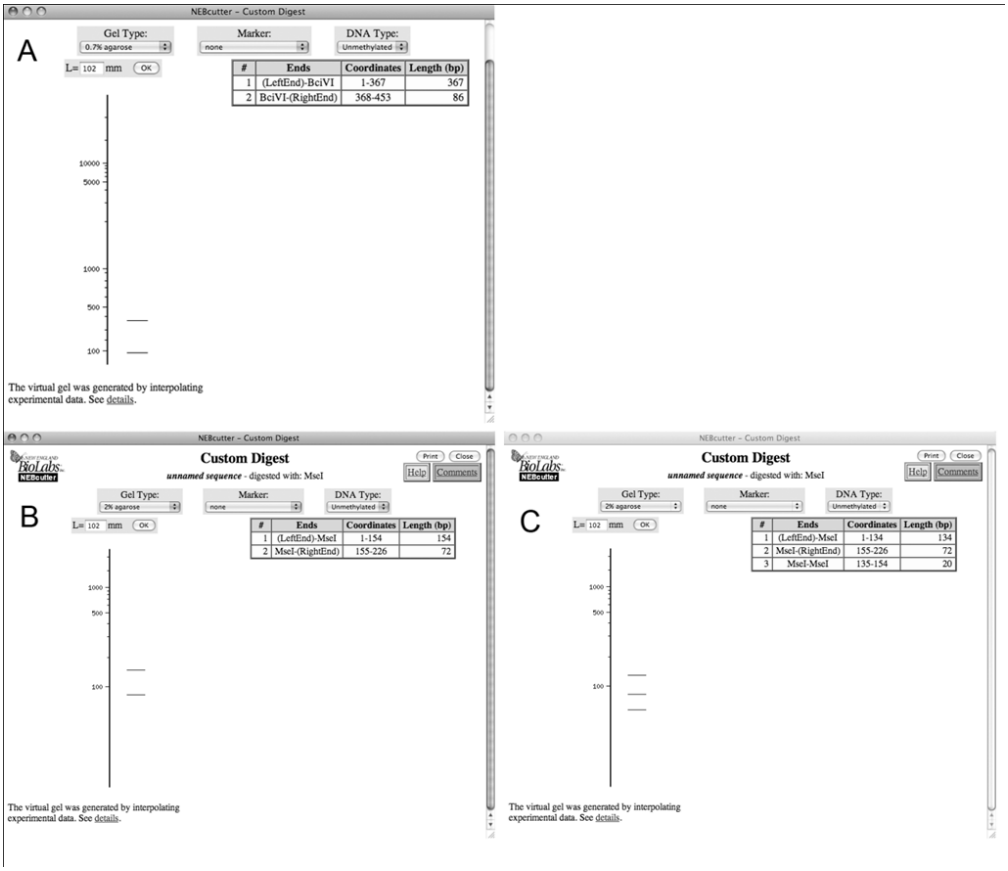


**Figure 30 Indicates expected band sizes following diagnostic digestion**

*A) Indicates the expected band sizes of VHL PCR product after digestion with BciVI enzyme in a wild type embryo (367bp and 80bp). In the VHL mutant embryos the BciVI enzyme site is lost and the enzyme won't cut, leaving one band. In the vhl-/+ embryos there will also be the presence of a third band at the uncut size 412bp. B) Indicates the expected band sizes of FIH PCR product after digestion with MseI enzyme for a wild type embryo (72bp and 154bp). C) Indicates the expected band sizes of FIH PCR product after digestion with MseI enzyme for an fih217/217 embryo (134bp, 72bp, 20bp).*

A transgenic line for the gal4-heat shock driven induction of notch signaling (*hsp70:Gal4;UAS:mycnotch1a-intra)* (Scheer et al., 2002) was also used to test the *Tg(csl-venus)qmc61* transgene, below are primers and PCR programs for the identification of the gal4 and NICD components of this line during genotyping.

Primers for identification of Gal4:
F - 5' CGCTACTCTCCCAAAACCAA 3'
R - 5' CAGTCTCCACTGAAGCCAATC 3'

| Step | Process | Temperature (°C) | Time (minutes) | Cycles |
|---|---|---|---|---|
| **1** | Denaturation | 94 | 3 | 1 |
| **2** | Extension | 94 | 0.5 | 30 |
| **3** | Annealing | 55 | 0.5 | |
| **4** | Elongation | 72 | 0.5 | |
| **5** | Final Elongation | 72 | 3 | 1 |
| **6** | Hold | 8 | Forever | |

**Table 8** *PCR program for identifying Gal4*

Primers for identifying NICD:
F - 5' CATCGCGTGTCAGCCTCAC 3'
R - 5' CGGAATCGTTTATTGGTGTCG 3'

| Step | Process | Temperature (°C) | Time (minutes) | Cycles |
|---|---|---|---|---|
| **1** | Denaturation | 9 | 3 | 1 |
| **2** | Extension | 94 | 0.5 | 34 |
| **3** | Annealing | 61 | 0.5 | |
| **4** | Elongation | 72 | 0.75 | |
| **5** | Final Elongation | 72 | 5 | 1 |
| **6** | Hold | 8 | Forever | |

**Table 9** *PCR program for identifying NICD*

Unlike the FIH and VHL PCRs, the Gal4 and NICD PCRs would only amplify in a positive sample, so negative controls were run each time, with no DNA, to confirm that positive amplification was the result of a positive PCR.

#### 2.2.5 Gel Electrophoresis

Amplified gDNA product following PCR process was run on a 1% agarose gel for 15 minutes at 100 volts. 1% agarose was made up using 1g agarose dissolved in 100ml 1xTAE (242g of Tris Base, 57.1ml acetic acid and 100g 0.5mM EDTA, made up to 1 litre of $dH_2O$) and 50µl of Ethidium Bromide. 5µl of PCR product was loaded into each well on the agarose gel with 5µl of an appropriate hyperladder in the first lane to assess the size of the DNA bands. The gel was imaged under ultraviolet light using a Uvitec lightbox. For 3% agarose gels, used for *fih*-mseI digests in order to separate smaller

fragments, a 1:1 ratio of standard agarose and low-melt-point agarose was used and the agarose added to TAE and left on a roller for 1 hour, in order to aid in the melting and prevent boiling over.

### 2.2.6 Purification of PCR Products

Prior to sequencing a PCR product the sample must be purified to remove residual nucleotides. Two hydrolytic enzymes are used for this process, Exonuclease 1 (Exo) and Shrimp Alkaline Phosphatase (SAP), which are mixed and added to the PCR product in a total volume of 10µl using the volumes shown in Table 5. The mixture is vortexed and placed in a thermal cycler and incubated at 37$^{o}$C for 45 minutes followed by inactivation of the enzymes at 95$^{o}$C for 15 minutes.

| Reagent | Volume |
|---|---|
| Exo1 (20 U/µl) | 0.15 |
| SAP (1 U/µl) | 0.90 |
| PCR Product | 7.00 |
| Water | 1.95 |
| **Total Volume** | **10** |

**Table 10** *Volumes of reagents in EXO/SAP mixture used to purify PCR products prior to sequencing*

10µl of purified PCR product are required to send to the Core Genomic Facility at Sheffield University, along with 10µl of 1pmol/µl forward primer for DNA sequencing.

### 2.2.7 Mounting Embryos

Embryos were mounted in 0.7% low melting point agarose (LMPA) in E3 containing 400µl of tricaine in 10mls. For confocal microscopy, embryos were mounted on a coverslip on the bottom of a 35mm petri dish. For standard compound microscopy, embryos were mounted on a coverslip.

## 2.3 Vascular Assays

### 2.3.1 Vascular Imaging

Two key endothelial transgenic lines were crossed into the mutant lines. The *Tg(Fli1:eGFP)* line allows for the visualisation of the vasculature (Motoike et al., 2000, Lawson and Weinstein, 2002b) and the transgenic line *Tg(Flk1:eGFP-NLS)* line allows for counts to be made of the cells in the endothelium since the GFP label is nuclear localised within the endothelial cells (Blum et al., 2008). The Perkin Elmer Ultraview Vox Spinning Disc confocal microscope and various objective lenses was used to observe the blood vessel network of the various mutants at various stages and treatments to observe changes in vascular patterning and endothelial cell number.

Automated method for counting endothelial cells involved imaging the embryos with the *Tg(Flk:eGFP-NLS)* transgene in the background, importing Z-stacks of images at maximum intensity. The images were converted to type 8-bit, and then adjusted to maximise the brightness and contrast until only the endothelial cells remain (white) on a black background. Using the process tool bar, the image was then converted to binary, and analysed to count the particles.

### 2.3.2 Angiograms

Using the 16x objective on the Olympus IX81 microscope with a Basler high-speed camera images were taken of embryos with the aorta horizontal along the image. Images were taken at a rate of 200-500 frames per second and each image saved individually. The images were processed using ImageJ by importing the sequence of images and then removing half of the images from the other half of the images, leaving a trace of the pixels that had moved between the two sets. The resulting image was processed in order to maximise the contrast between the trace and the background and coloured using the Fire lookup table in the ImageJ program. This was then overlaid onto a single image from the original photographs to act as a reference (Chico et al., 2008).

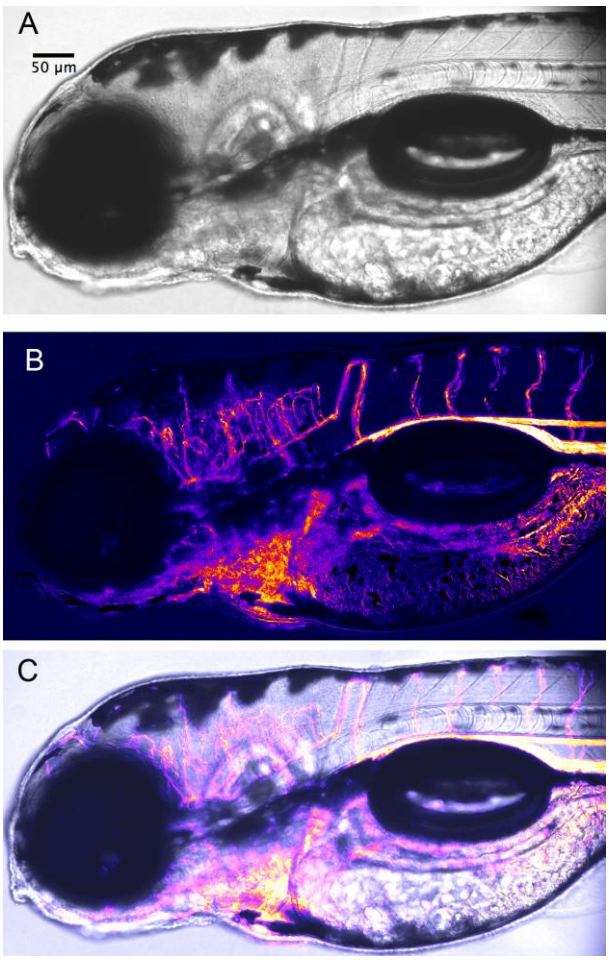


**Figure 31 Image deletion angiograms generated from high-speed imaging.**

***A)*** *represents a single frame for the overlay of the angiogram, to give representative orientation for the vasculature* ***B)*** *single frame image-deletion angiogram* ***C)*** *an overlay of greyscale image with the image-deletion angiogram.*

### 2.3.3 Vascularisation Index

Three parallel lines were drawn from the pigment line to the notochord over the top of vessel bed images, from the first to the eighth somite. A count was made of the number of vessels that intersected with each of the lines, and the sum of these counts was plotted to represent the vascularisation index of the embryos (Pelster et al., 2003, Yaqoob and Schwerte, 2010), see **Figure 32**.

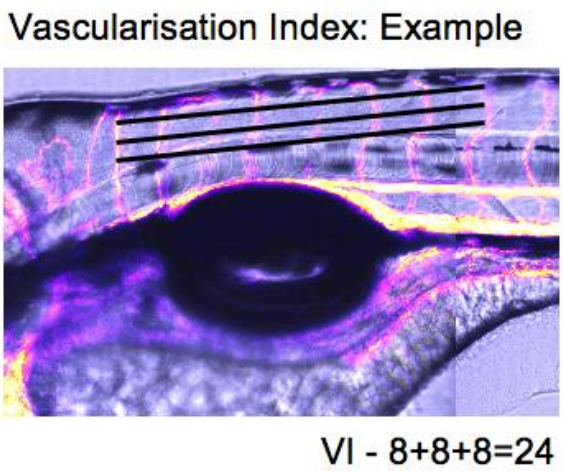


**Figure 32 Method for assessing vascularisation index**

*Counts made of the number of vessels that cross over each line.*

### 2.3.4 Haemodynamics

Using the 16x objective on the Olympus IX81 microscope with a high-speed camera and Video Savant software, images were taken of mounted embryos, ensuring the aorta horizontal along the image. Images were taken at a rate of 300 frames per second and each image saved individually. The images were imported and processed using ImageJ by importing the sequence of images and using the select tool to draw a rectangle along the length of the aorta 1 pixel high and the length of 3 somites either side of the anus (to maintain consistency). This was then cropped and saved as a raw data file. The raw data file was then imported, ensuring that the width was adjusted to the width of the line that had been drawn, to create a visual kymograph of the aorta with the path of individual erythrocytes demonstrated as individual traces. The height of the kymograph is representative of the amount of time that had passed while the width of the kymograph represents the distance along the aorta. The scales were adjusted accordingly and the width and height of individual erythrocytes were measured using a rectangle drawn in ImageJ, allowing velocity to be calculated using the formula:

$$\textbf{Velocity (µm/s)} = \frac{\textbf{Distance (µm)}}{\textbf{Time (s)}}$$

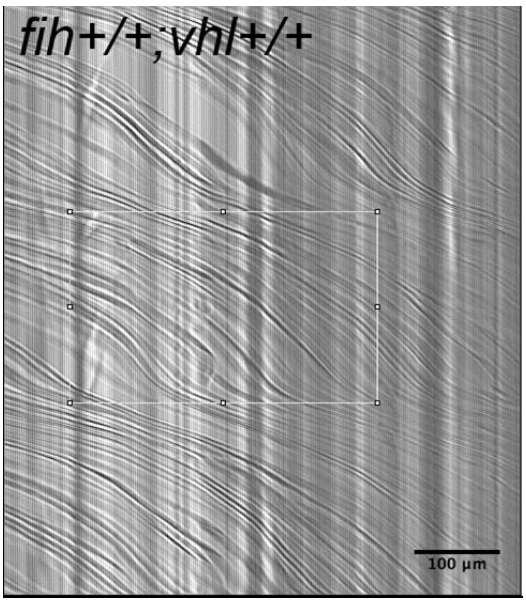


**Figure 33 An example of a kymograph that was derived from imaging a wild type embryo**

*The box indicates the tracking of an erythrocyte from the start to the end of a heart beat, the measurements of which are used to calculate its rate.*

The width and height of this rectangle were then put into a spreadsheet and the height converted to time and the distance and time used to calculate speed of the pixel that curve represented. 3 measurements were taken from each kymograph, so the speed recorded was an average for each fish.

### 2.3.5 Heart Image Analysis and Cardiac Output

Using an Olympus IX81 microscope connected to a high speed camera, images of the heart were taken at 300 frames per second, through a 20x objective lens. Analysis of the images was performed using ImageJ software. The number of frames to complete two heart beats was used along with the frame rate of the recordings to calculate the heart rate in beats per minute. The perimeter of the ventricles was outlined for the end-diastolic (EDV) and end-systolic (ESV) volumes. The software utilises a 'Fit Ellipse' algorithm, calculating the center of mass and the major and minor axes of the ellipse, with the same volume as the perimeter drawn around the ventricle. These measurements were transferred into an Excel spreadsheet and used along with the formula of a prolate spheroid;

**Ventricular volume = 4/3 x π x *a* x *b*$^2$,** where *a* and *b* refer to half of the long and short axes of the ventricle.

The mean stroke volume (µl$^3$) was calculated from the difference between the end systolic volume (eSV) and end diastolic volume (eDV) (across two ventricular eDV and eSV);

**Stroke volume (µl$^3$) = eSV (µl$^3$) - eDV (µl$^3$)**

**Ejection volume (µl$^3$) = $\frac{\text{stroke volume (µl}^3\text{)}}{\text{eDV (µl}^3\text{)}}$**

**Cardiac output (µl$^3$/min) = stroke volume (µl$^3$) x heart beats (beats per minute)** as described in (van Rooijen et al., 2010).

### 2.3.6 Erythrocyte Density

Using an Olympus IX81 compound microscope connected to a high speed camera, images were taken at 300 frames per second, through a 40x objective lens of the sixth to tenth somite with the aorta horizontal in the frame. Analysis of the images was performed using ImageJ software. In a 200µm section of the aorta a count was made of the number of erythrocytes. Three measurements were taken of the diameter of the aorta and the diameter of erythrocytes. Based on the volume of a cylinder being $\pi r^2 xl$ (where r = radius and l=length), and the volume of an erythrocyte being $\pi r^2 x0.3$ (Schwerte et al., 2003). These calculations were used to produce a volume of the aorta in µm$^3$ and converted into nl to give a final figure of erythrocytes/nl.

### 2.3.7 Vascular Competence

Embryos carrying the *Tg(Fli1:eGFP)* were collected and mounted, at 4dpf. Using a micro-injector needle 2,000,000MW tetramethylrhodamine dextran (TAMRA) dye (Invitrogen Molecular Probe) was injected into the common caudal vein, see **Figure 34**.

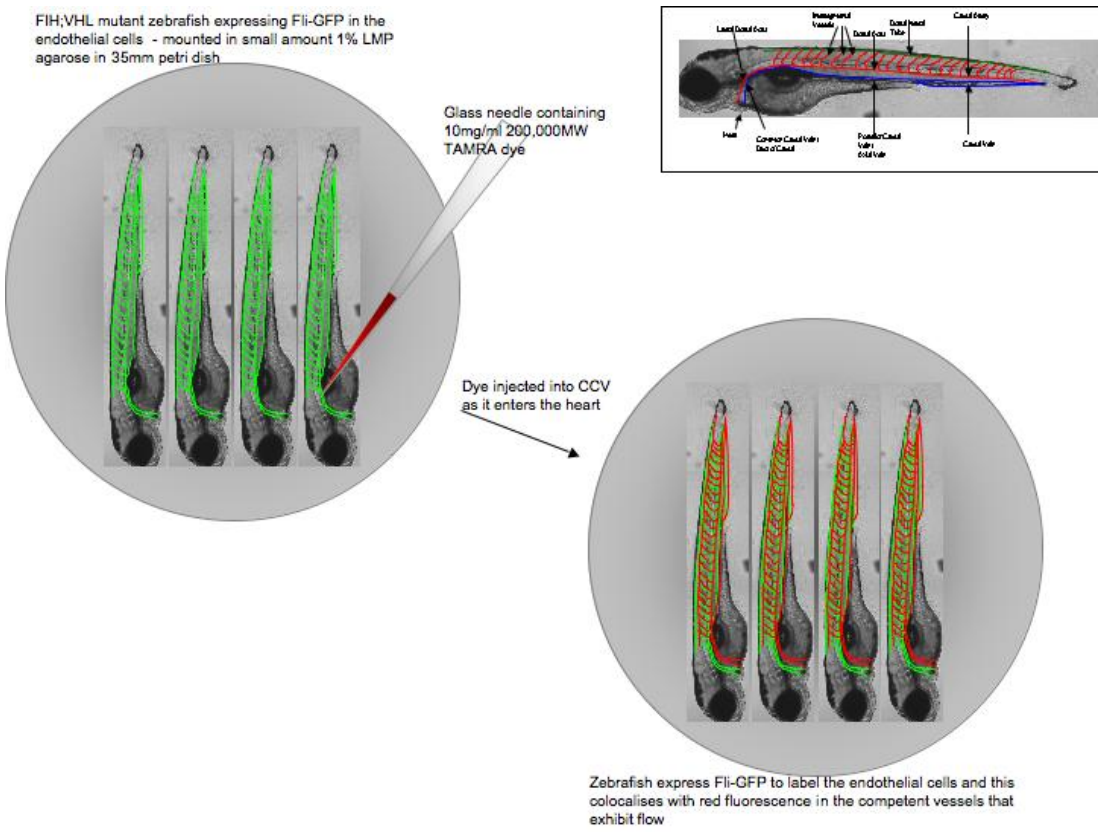


**Figure 34 Method plan for the injection of dye into the zebrafish embryos to study the integrity of the blood vessels**

These embryos were imaged overnight using the Perkin Elmer Spinning Disc confocal microscope to observe the movement of the dye within the circulation (E. Van Rooijen et al. 2010)( http://products.invitrogen.com/ivgn/product/D7139).

## 2.4 Molecular and Genetic Analysis

### 2.4.1 *In situ* Hybridisation

The protocol was an adaptation of (Thisse and Thisse, 2008), as described in (van Rooijen et al., 2010, van Rooijen et al., 2009).

### 2.4.2 Microarray

Agilent Two Colour 4x44k Zebrafish Version 1 Microarrays were selected for the comparison of the gene expression patterns. Four sets of comparisons were designed to compare:

| | | | |
|---|---|---|---|
| Slide 1 | *fih+/-; vhl +/+* | vs | *fih217/217*; *vhl+/+* |
| Slide 2 | *fih+/-; vhl+/+* | vs | *fih+/+; vhl-/-* |
| Slide 3 | *fih+/-; vhl+/+* | vs | *fih217/217; vhl-/-* |
| Slide 4 | *fih+/+; vhl-/-* | vs | *fih217/217; vhl-/-* |

For the purposes of the Microarray wild type embryos were those from a *fih*-/+ x LWT cross. For each comparison samples were stage matched at 3dpf, identified by phenotype for mutation and snap frozen in liquid nitrogen, in triplicate, and stored at -80$^{o}$C. Several individual embryos from each cross were preserved in methanol for genotyping to confirm the ID of the frozen embryos.

Sample preparation was performed on batches of whole embryos, with a minimum of 10 embryos in each sample, attempting to keep the number of embryos in each group the same wherever possible to remove bias. Whole embryos were selected rather than specific tissues/regions in order to assess global alterations in gene expression in the embryos. Each group, wild type and mutant alike, was going to be assessed in triplicate so sample preparation occurred over several batches, with embryos collected, sorted, and prepared at the same time of day in order to maintain consistency between the samples. RNA Extraction of the samples was performed using an Invitrogen mirVana RNA isolation kit, and the RNA concentrations were quantified using a Thermo Scientific Nanodrop 1000.

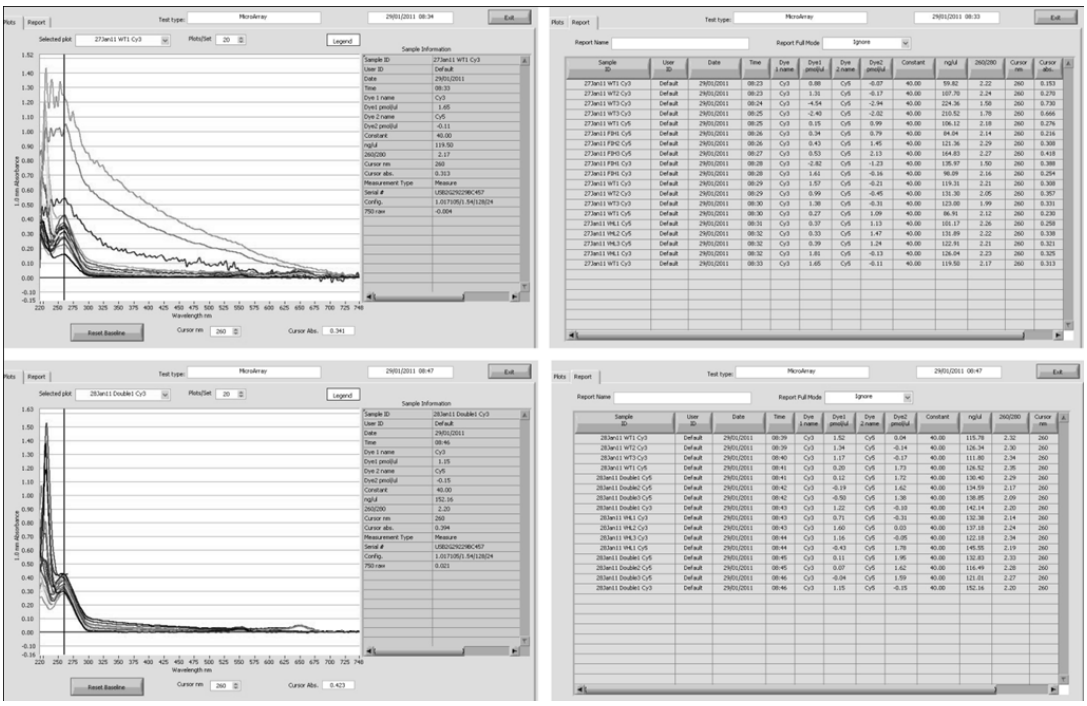

**Figure 35 Nanodrop data following labeling**

*Data used for quantifying the amount of labeled RNA in each sample, and in the calculations for loading the two samples for comparison onto microarray slides (see (Agilent) for calculations).*

In order to assess the quality of the RNA the samples were run through an Agilent 2100 Bioanalyser, to assess for break-down products and integrity and all the samples were deemed to have sufficient integrity to proceed with the microarray. An Agilent RNA 6000 Nano kit was used to load small aliquots of the RNA samples into a gel for quantification and analysis of the samples.

The RNA was labeled with Cy3 or Cy5 dye using an Agilent Low RNA Input Labeling Kit as per the protocols designated by Agilent. The concentration of RNA to use was limited by the sample with the lowest concentration and a total input volume in the kit of 1.5ul. The dye incorporation and final concentration of the RNA sample was quantified again on the Thermo Scientific Nanodrop 1000.

The microarrays were run by continuing the follow the Agilent protocol (Agilent) for two-colour microarray-based exon analysis (low input quick amp labeling). The samples were mixed and loaded onto gasket slides before the array slides were clamped onto them and the slides hybridized overnight in an Agilent Hybridisation

Oven at 65$^{o}$C. The slides were then removed from the gasket slides and washed before being loaded into the Agilent Microarray Scanner and analysed. The data from the microarrays was fed into GeneSpring software for analysis of genes with altered expression compared to WT. Gene expression changes that indicated a fold change above log 1 (2 fold) in the mutants compared to the wild type siblings were considered to be a hit.

### 2.4.3 Quantitative Real Time PCR (qRT-PCR)

Primers were designed to span neighbouring exons in the cDNA of each gene of interest (GOI). Standard gradient PCRs were performed over a range of annealing temperatures in order to test the primers. The product from the optimised band was cleaned up with an EXO/SAP reaction and sent for sequencing in order to confirm the correct section of the GOI was being amplified specifically.

| Abbreviation | Gene Name | GenBank Accession Number | Primer sequence (5' – 3') |
|---|---|---|---|
| Agt | Angiotensinogen | NM_198063.1 | GGGCGTAACTCCAAAGACTG<br>CATGAACGTCCTCTTGCTGA |
| Ace1 | Angiotensin 1 Converting Enzyme 1 | wu:fb81h03-201 | GGAGAAACCCACTGATGGAA<br>TTCTGAAGCTCACTGGCTGA |
| Ace2 | Angiotensin 1 Converting Enzyme 2 | NM_001007297.1 | GCCAAGCTCAACAACTACGA<br>GCAAATGTGCTGGAAGACAG |
| Cyp11b2 | Aldosterone Synthase | NM_001080204.1 | GAGAGACACGCAGACACAGC<br>ACTGGGGTCAAGGGTCAGT |
| Renin | Renin | NM_212860.1 | TCTCTCTCAGCGATCAGC<br>TCTGAGCTGGTGAACCAATG |
| Phd3 (Egln3) | Prolyl Hydroxylase Domain Containing Protein 3 | NM_213310.1 | CGCTGCGTCACCTGTATT<br>TAGCATACGACGGCTGAACT |
| Vhl | Von Hippel Lindau | NM_001080684.1 | ATGTCGGCTGTCTGGAGATT<br>GATGCACAGGTGTGCTCAGT |
| Vegfab-201 | Vascular Endothelial Growth Factor A | NM_001044855.2 | CAGTGTGAGCCTTGCTGTTC<br>CCATAGGCCTCCTGTCATTT |
| Vegfc | Vascular Endothelial Growth Factor C | NM_205734 | AAGAAGCTGGATGAGGAGACG<br>GAGGTTGACTCCTCGGACAC |
| Kdr/Flk1 | Kinase Insert Domain Receptor (VegfR2) | NM_131472 | CGCGCAACAGGTCACTATT<br>GTGAGGAGGATGTCGAGGAG |
| Flt4 | FMS Rleated Tyrosine Kinase 4 (VegfR3) | NM_130945 | TCTCGTTAGTGCCGTATCCA<br>GATGATGTGTGCTGGCTGTT |
| EphrinB2 | EphrinB2a Receptor | NM_131023 | ACCACGTTGTCACTCAGCAC<br>AGATGTTTGCTGGGCTCTGT |
| Amy2a | Amylase2a | NM_213011.1 | CAAACGGCAATCTCTGACC |

| | | | |
|---|---|---|---|
| | | | ATGGAGCTGGAACTCCTTCA |
| Ctrb1 | Chymptrypsinogen | NM_212618.1 | CTGGCCACTCCTGCTAAGAT<br>TGCAGTCTTCATTGGTCAGC |
| Glut1 | Glucose transporter 1 | NM_001039808 | ACTGCTGTGATTGGCTCCTT<br>TGGCCACTGATACAGACCAG |
| Hk1 | Hexokinase1 | NM_213252 | TGGATCTGGGTGGCTCTAAT<br>AGGTGAAGCCCACAGGAA |
| Prepro | Preproinsulin | NM_131056 | AGTGTAAGCACTAACCCAGGC<br>TGCAAAGTCAGCCACCTCAGT |
| Pepck | Phosphoenolpyruvate carboxykinase | NM_214751 | GAGAATTCTCACACACACACA<br>GTAAAAGCTTTCCGCCATAAC |
| Alas2 | Aminolevulinate synthase 2 | NM_131682.2 | GCTCTCAGGTGTCTGTGTGG<br>TAGACGGGCCAGTTCATTCT |
| Her12 | Hairy Related Protein 12 | NM_205619 | GCTGAGGAAGCCGATAGTTG<br>GCGAGAGGAAGTGGACAGAC |
| Notch3 | Notch3(Notch5) | NM_131549 | CGGCCTGGTTATATTGGTTC<br>TCTAAAGCCTCGCTGACACA |
| Nrarpa | Notch-regulated ankyrin repeat-containing protein | NM_181495 | AGCTGCTTCGGACTCGTTAC<br>CGAGGTAGCTGATGCAGAGA |
| Dll4 | Delta like ligand 4 | NM_001079835 | GCTTGGCTCACCTTTCTCAT<br>CGGAAGAAAGTCCTGCAGTC |
| Cxcr4a | C-X-C chemokine receptor type 4a | NM_131882 | TTGTGCTCACTCTGCCATTC<br>ACCGGTCCAAACTGATGAAG |
| Bactin2 | β actin 2 | NM_181601 | GCAGAAGGAGATCACATCCCTGGC<br>CATTGCCGTCACCTTCACCGTTC |

**Table 11** *QRT-PCR primer abbreviations, Genbank numbers and Primer sequences for all the genes that were validated from the microarray.*

QRT-PCR assays were optimised following guidelines described by Nolan et al (Nolan et al., 2006). A range of cDNA concentrations were selected, a 1/10 dilution series, and each line on the graphs in **Figure 36** represents a different cDNA concentration. The graphs in A and B indicate the amplification curve and melt curve for a pair of primers that were re-designed due to the production of primer dimers. The amplification curve (A) indicates a range of threshold values for the range of cDNA concentrations, as would be expected, however B) indicates two different peaks in the melt curve and this is indicative of the production of primer dimers. In C and D however, the range of threshold values on the amplification curve is more evenly spaced and the melt curve (D) indicates only one peak. These primers would have been deemed successful and the assay would have continued.

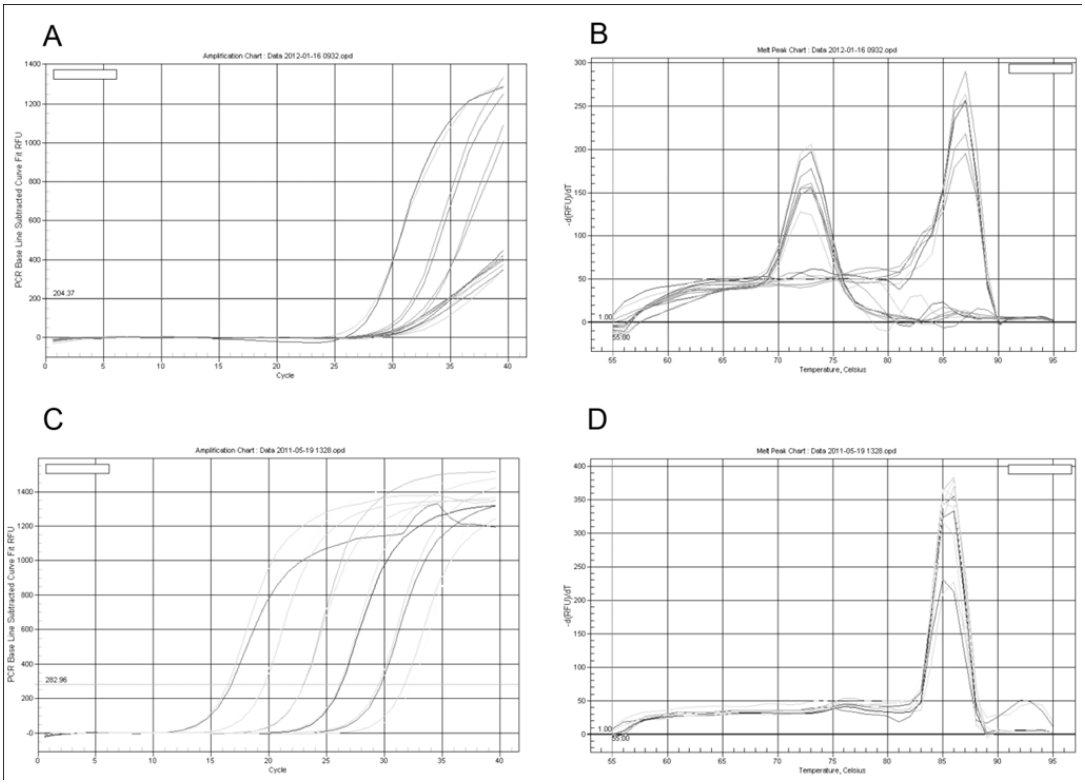


**Figure 36 Primer pair optimising**

***A)*** *Amplification curve, appear success* ***B)*** *Melt peak, ensure failure, second peak to the left indicates potential primer dimer or secondary products* ***C)*** *Amplification curve across a cDNA range, peaks provide different ct values and therefore range of ct range in correlation with range of cDNA concentration* ***D)*** *Melt peak reveals that despite range of cDNA concentrations the single peak indicates consistent product size.*

The results of each optimisation were analysed by plotting the threshold ct value (where the amplification of product had crossed a computer generated threshold number of cycles) against the log of the cDNA concentration in GraphPad software program. The gradient of the line was then calculated using the same software, for repeats of each gradient. The % efficiency was calculated as the average gradient divided by -3.3 and multiplied by 100, where -3.3 is the gradient of the line assuming 100% efficiency, see **Figure 37**.

Once this was confirmed a range of cDNA concentrations were run in a qRT-PCR reaction. Starting from 1ug and performing 1/10 dilution series, it was possible to observe the linear sensitivity range for each primer pair.

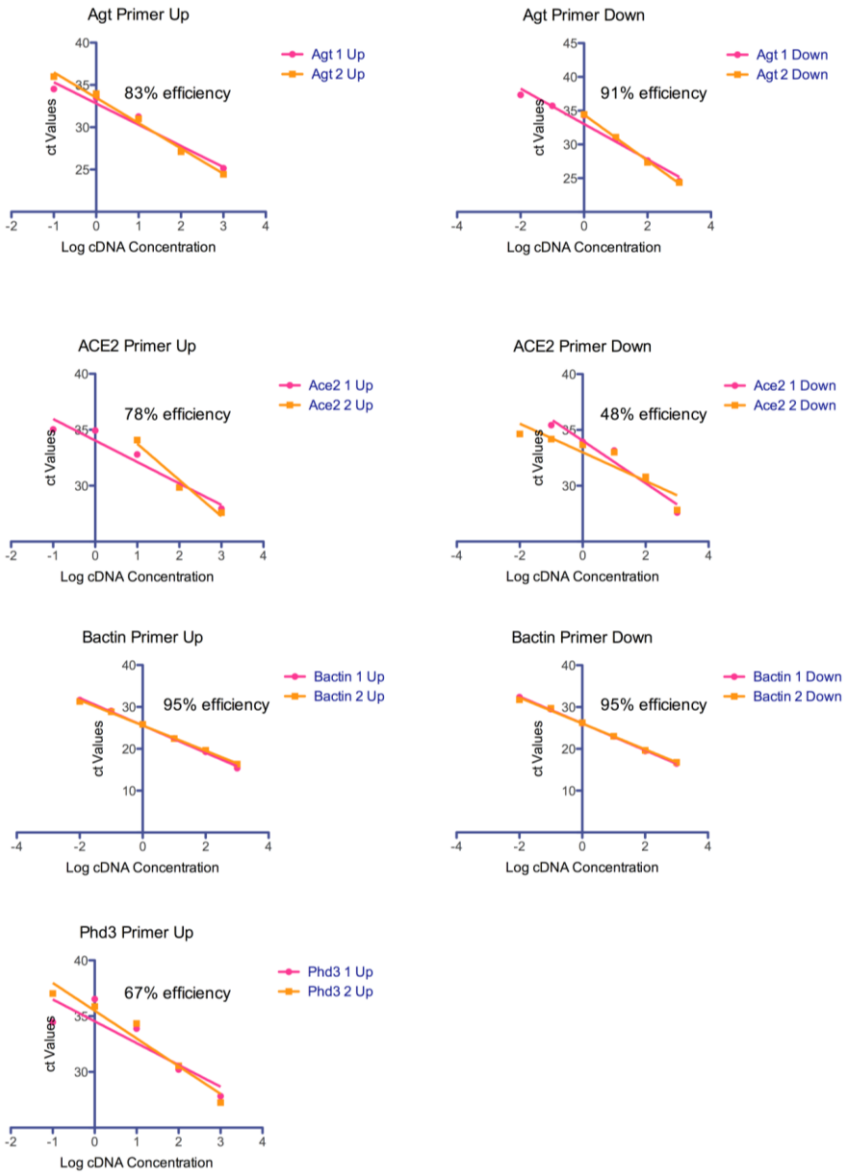


**Figure 37 Primer Optimisation**

*Graphs show the log cDNA concentration plotted against the ct values for each sample for7 primer pairs at two different primer concentrations. Primer Up refers to a 1µl volume of 10ng/µl stock of primer added to each reaction, while primer down refers to a 0.5µl volume of primer added to each reaction.*

This information was used to calculate the primer efficiencies for each pair, and the fold changes that will be detectable between wild type and mutant samples for the GOI. The ΔΔct analysis method assumes a primer efficiency of 100%, so +/- 10% of this was aimed for with each primer pair before continuing in order to avoid building in errors. By plotting the log of the cDNA concentration against the ct values and performing linear regression analysis it was possible to get the slope of the lines within

the linear range of the primers. Efficiency was then equal to (the slope of the line/-3.3)x100, where -3.3 is the slope of a line with 100% efficiency. Once the primer concentrations were optimised and a cDNA concentration was established within the center of the linear range of each primer pair, qRT-PCR reactions were set up over three biological replicate samples for each of the mutant lines. Initially the same samples were used as for the microarray.

Within a 96 well plate it was possible to run between 6 and 7 primer concentrations over the cDNA gradient with 6 concentrations, therefore between 3 and 4 genes and where possible two concentrations of primer were tested simultaneously, in order to know whether a decrease or increase in primer concentration would aid optimisation when each plate was analysed. The analysis of the 96 well plate shown in **Figure 37** showed that 0.5µl per reaction of primer at 10ng/µl stock concentration was optimal for angiotensinogen (*agt*) as well as *β-actin* and that the concentration of primer for angiotensin converting enzyme 2 (*ace2*) and prolyl hydroxylase enzyme (*phd3)* needed to be increased from 1µl per reaction.

The table below (**Table 12**) shows a summary of all of the optimisation that was performed for each gene that was validated by qRT-PCR for the microarray.

| Abbreviation | Sequenced | Fragment Size (bp) | cDNA Concentration (ng/reaction) | Primer Volume (µl/reaction – 10µM stock) | Primer Efficiency (%) |
|---|---|---|---|---|---|
| **Agt** | X | 229 | 10 | 0.5 | 91.18 |
| **Ace1** | X | 185 | 10 | 0.75 | 101.53 |
| **Ace2** | X | 228 | 10 | 1.75 | 95.97 |
| **Cyp11b2** | X | 224 | 10 | 1 | 108.64 |
| **Renin** | X | 173 | 10 | 1.5 | 102.74 |
| **Phd3 (Egln3)** | X | 181 | 10 | 0.5 | 96.58 |
| **Vhl** | X | 189 | 10 | 1 | 96 |
| **Vegfab-201** | X | 230 | 10 | 0.5 | 102.7 |
| **Vegfc** | X | | 10 | 0.5 | 95 |
| **Kdr/Flk1** | X | | 20 | 1 | 91 |
| **Flt4** | X | 164 | 20 | 0.5 | 92 |
| **EphrinB2** | X | 205 | 10 | 1 | 93.3 |
| **Amy2a** | X | 167 | 10 | 0.5 | 103 |
| **Ctrb1** | X | 184 | 10 | 0.75 | 91.95 |

| | | | | | |
|---|---|---|---|---|---|
| **Glut1** | X | 193 | 10 | 0.25 | 91 |
| **Hk1** | X | 234 | 10 | 0.5 | 93 |
| **Prepro** | X | | 20 | 1.5 | 94 |
| **Pepck** | X | | 20 | 1.5 | 97 |
| **Alas2** | X | 176 | 10 | 0.5 | 97.56 |
| **Her12** | X | 248 | 20-25 | 1.25 | 111 |
| **Notch3** | X | 138 | 20 | 1.5 | 116 |
| **Nrarpa** | X | 229 | 100 | 1 | 95.3 |
| **Dll4** | X | 155 | 10 | 1 | 92.15 |
| **Cxcr4a** | X | 144 | 20 | 0.5 | 90 |
| **Bactin2** | X | 322 | 10 | 0.5 | 95.70 |

**Table 12** *Each primer pair used for qRT-PCR was optimised and the parameters are indicated in this table. X indicates that a standard PCR was run and the product sequenced in order to confirm amplification of the gene of interest. The optimised cDNA concentration and volume of primer, given a 10ng stock concentration, that was ascertained for each primer set for each gene that was validated by qRT-PCR. The sequences of each primer pair can be found in* ***Table 11.***

Further optimised were the non-template control samples. Within each qRT-PCR run samples were run with no cDNA, these constitute non-template control samples (NTCs) and allow a true baseline to be gleaned from the comparison between expression in wild type cDNA and expression in the mutant cDNA. The ideal trace for the NTC was to see no amplification of product in the amplification curve, and to see no breakdown of product in the melt curve. **Figure 38** demonstrates the traces that would be seen if a NTC had contamination that was allowing the primers to generate a product (A and B), these results would infer that any difference seen between expression of that gene in the wild type samples compared to the mutant samples could be contaminated by background DNA and this run would be repeated. If the NTC had no contamination and the primers were unable to generate a product, the traces would appear as in C and D. Here the axes have been amplified and the resulting trace shows only the noise within the baseline for both the amplification and melt curves. These samples indicate that true differences can be interpreted between the wild type and mutant samples being compared and these samples would not need to be repeated.

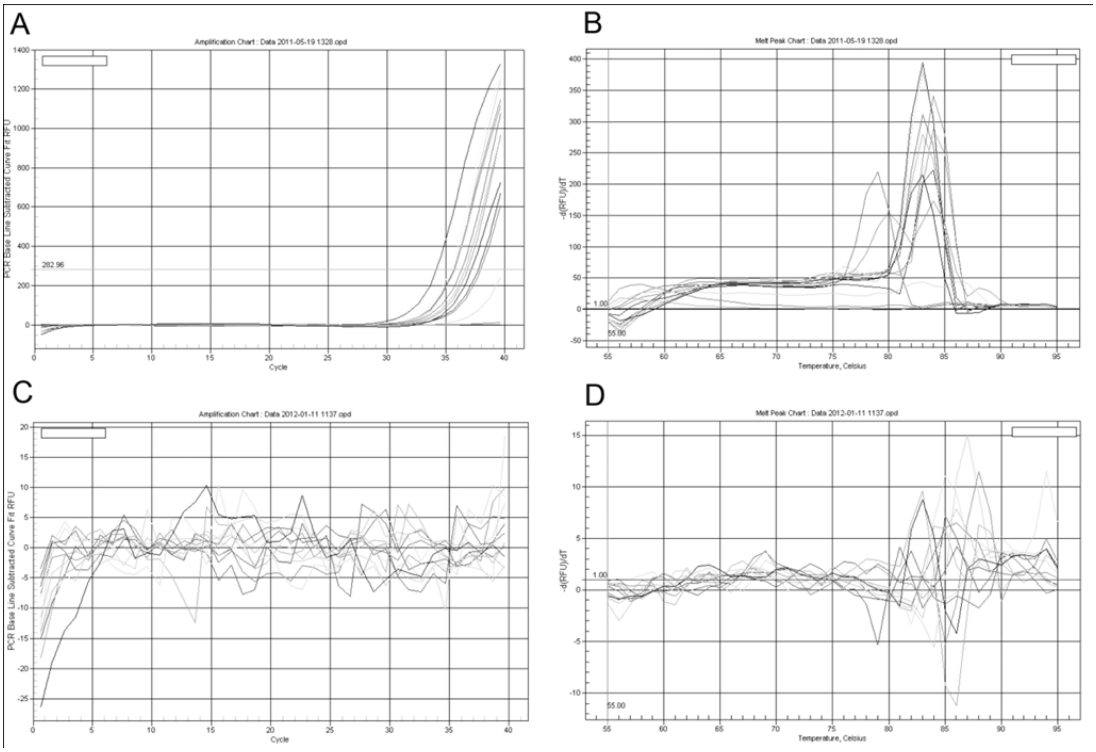


**Figure 38 Non-template control Examples**

***A** and **C)** are examples of amplification curves for two sets of non template controls (NTCs) that passed (**A**) and failed (**B**). **B** and **D)** are examples of melt curves for two sets of NTCs that passed (**B**) and failed (**D**).*

Optimisation of these protocols to ensure the quality of the no template control (NTC) samples ensured when comparing differences between control and mutant samples these were truly the result of these differences and were not obscured by external cDNA contamination in any of the reagents used in the master-mix.

### 2.4.4 In Situ Hybridisation Probe Preparation

Plasmid would be linearised using an appropriate enzyme, followed by a phenol chloroform extraction. Transcription of the probe was performed by mixing 1µg of linear plasmid DNA (where possible) and 10x transcription buffer supplied with enzyme, with 2µl 10x DIG labeling mix, 2µl of T7/SP6/T3 RNA polymerase, with "x"µl RNase free $H_2O$ to make up a final reaction volume of 20µl. This would be incubated for 2 hours at 37$^{o}$C. 1µl run out on a gel allows the relationship between DNA and RNA to be assessed to confirm the transcription success, before adding 2µl (40 units) DNase and incubating for 30minutes at 37$^{o}$C to remove remaining plasmid DNA. This reaction

is then stopped using 2µl EDTA (optional). RNA is precipitated with 2.5µl 4M LiCl and 75µ of pre-chilled ethanol for 30minutes on dry ice, at which point a pellet should be visible. Pellets are spun down and dissolved in 100µl RNase free water and stored at -20$^{o}$C.

### 2.4.5 Cloning *fih* into PCS2+ (Expression construct)

Bluescript plasmid containing *fih* gene: Primers were designed to clone up the *fih* sequence and add BamH1 and Xho1 sites on to the ends of the PCR product. Phusion Taq PCR performed (4 x 20µl reactions) followed by Dpn1 digestion to remove excess plasmid DNA. Following pooling of the 4 reactions, PCR purification was performed using the protocols within the Qiagen QiAquick PCR Purification Kit. Half resulting eluted volume was kept on ice/in freezer and the other half was mixed in a 1:1 ratio with BioRad PCR Ready Mix in order to T-Tail the DNA for 30minutes at 72$^{o}$C. This was PCR purified again following the same protocol from the same kit. A gel was run to check this had worked before setting up a ligation of the T-Tailed *fih* into PGEM-T Easy vector, ligation left overnight at 4$^{o}$C. Transformation was set up using NEB High Efficiency Transformation Protocol for Chemically Competent Cells and plated out onto agar plates with Carbenicillin and X-Gal and left at 37$^{o}$C overnight. Colonies were picked and grown up overnight in 6ml cultures of LB broth (cell media) containing Carbenicillin. Qiagen MiniPrep was performed, holding 1ml of the culture back for future inoculation, and a small sample was run on a gel. An Xho1/BamH1 digest was performed for 1 hour and run on a gel to check the band sizes (PGEM-T Easy (3kb), FIH (1kb)), and at this stage a sample was sent off for sequencing of the *fih* to confirm. 100ml cultures were set up from a single colony and left to grow overnight before performing Qiagen MidiPrep according to the manufacturers' protocol. Xho1/BamH1 digest was performed of both the PGEM-TEasy-FIH construct and an empty PCS2+ vector, cutting 10µg, for 1 hour. These were run on a SYBRSafe gel and visualised on a DNA safe UV light before cutting out the PCS2+ band and the smaller *fih* band, these were then gel purified using a Qiagen Gel Purification Kit to the manufacturers' protocols. A ligation was set up between the *fih* fragment and the PCS2+vector and left overnight. The ligation was transformed and plated out, colonies were selected

and grown up, mini preps were performed to check the final size of the product before larger cultures were set up to perform midi prep.

### 2.4.6 Microarray Validation and Target Analysis

In places microarray targets were analysed due to correlations between pathways that they were involved in or direct correlations in the literature between expression and function in similar models. For completeness and clarity of these, the references and a brief explanation of the potential relevance of the gene/pathways expression in this current project are tabulated below for reference.

| Gene/Family/Process | Relevance to this project and reason for investigating expression in microarray dataset. | Reference(s) |
|---|---|---|
| **Fih** | Role in high-fat-diet-induced weight gain and hepatic steatosis | (Zhang et al., 2010) |
| **NF-κB**<br>**Iκ-B**<br>**HIF-1** | Mediated cross-talk between inflammation and hypoxic adaptations through sequestering FIH away from HIF-1 | (Shin et al., 2009)<br>(Cockman et al., 2006) |
| **PFKFB3** | Glycolytic enzyme induced by hypoxia | (Calvo et al., 2006)<br>(Rider et al., 2004) |
| **HK1** | Glucose sensor, involved in the conversion of glucose to pyruvate as well as playing non-enzymatic roles in glucose sensing and signaling<br>Heme-binding plasma glycoprotein produced in the liver after stimulation by pro-inflammatory cytokines and maintains heme in soluble monomeric state | (Cho et al., 2006)<br><br>(Krikken et al., 2010) |
| **LDH** | Shown to have a Hif response element, up-regulated in hypoxia, catalysing the conversion of pyruvate to lactate in anaerobic cells | (Firth et al., 1995)<br>(Zehetner et al., 2008) |
| **Insulin** | Binds to insulin receptor kinase, results in autophosphorylation of multiple cytoplasmic tyrosine residues, also has an HRE | (Tornqvist et al., 1988)<br>(Ellis et al., 1986)<br>(Taylor, 1991)<br>(Zelzer et al., 1998)<br>(Yim et al., 2003)<br>(Maltepe et al., 1997)<br>(Zhang et al., 2010) |
| **PEPCK** | Lyase enzyme in gluconeogenesis pathway | (Zhang et al., 2010)<br>(Kucejova et al., 2011)<br>(Elo et al., 2007) |
| **Preproinsulin** | Primary translation product of insulin gene, expression up-regulated post exogenous glucose exposure | (Alarcon et al., 1998)<br>(Elo et al., 2007) |
| **Glut-1** | Expression found to be increased in *vhl-/-* zebrafish embryos | (van Rooijen et al., 2009) |
| **Fabp1a** | Involved in intracellular fatty acid trafficking as well as metabolism in the zebrafish<br>Zebrafish fabp1a correlates with human liver-type fabp, implicated in acute coronary syndrome | (Her et al., 2003)<br><br>(Matsumori et al., 2012) |

| | | |
|---|---|---|
| **UCP** | Increased $O_2$ consumption caused by changes in uncoupled mitochondrial respiration, surrogate | (Zhang et al., 2010) |
| **CA** | Zinc metalloenzyme catalyses reversebile reactions of $CO_2$, surrogate for $CO_2$:$O_2$ ratios | (Gilmour et al., 2009)<br>(Perry and Gilmour, 2006)<br>(Rummer and Brauner, 2011)<br>(Gilmour et al., 2004)<br>(Lin et al., 2008)<br>(van Rooijen et al., 2009) |
| **EPO and EPO-R** | Vhl-/- zebrafish embryos have elevated levels as well as exhibit polycythemia | (van Rooijen et al., 2009) |
| **Alas2** | Stimulated by hypoxia, catalyses rate-limiting step in heme biosynthesis | (Hofer et al., 2003) |
| **VEGFR-2, Dll4, PDGF-B, VEGFR-3** | Genes shown to be expressed in tip cells in the retina | (Strasser et al., 2010)<br>(del Toro et al., 2010) |
| **CXCR-4** | Gene shown to be expressed in stalk cells | (Strasser et al., 2010) |
| **Notch1, VEGF-VEGFR1/R2, Dll4** | Notch activation influences responses to *vegf*, and influence in turn the branching nature of blood vessels | (Williams et al., 2008)<br>(Leslie et al., 2007)<br>(Phng and Gerhardt, 2009)<br>(Patel et al., 2005a)<br>(Hellstrom et al., 2007)<br>(Liu et al., 2003)<br>(Li et al., 2007b) |
| **FIH, HIF, Notch-NICD** | Loss of *fih* is expected to positively regulate Notch activity, and HIF is expected to up-regulate Notch by stabilising NICD | (Zheng et al., 2008)<br>(Gustafsson et al., 2005) |
| **Delta-C** | Notch ligand shown in early zebrafish embryos in the epidermal cells that make up intersomitic vessels, dorsal aorta and aortic (branchial) arch arteries | (Smithers et al., 2000) |
| **Notch-3** | Shown to be involved in vascular tone and blood flow. Decreased expression resulted in vascular thickness and deficient contractile response to angiotensin II. Expression limited to vascular cells, fundamental to arterial specification of systemic vascular smooth muscle cells | (Boulos et al., 2011)<br>(Merrill et al., 2011)<br>(Ghosh et al., 2011) |
| **NRARP, NICD, Xsu(H)** | Over-expression of Nrarp shown to resemble loss of Notch signaling models. Zebrafish have two paralogues of nrarp gene. Expression shown to be connected to the inhibition of the Notch signaling pathway, and connected to increases in tip-cell differentiation and vascular branching | (Lamar et al., 2001)<br>(Topczewska et al., 2003)<br>(Leslie et al., 2007) |
| **Her and Hey family genes and Her12, Her15, Her2, Her 4.1, Her4.2, Hes 5** | Notch target family genes with similar expression to mouse Hes5, assessed in microarray to ascertain downstream Notch signaling effects and levels | (Katoh, 2007)<br>(Fischer et al., 2004a, Fischer et al., 2004b)<br>(Shankaran et al., 2007) |
| **Apoptotic Genes** | Hypoxia shown to induce expression of pro-apoptotic genes | (Li et al., 2007c)<br>(Greijer and van der Wall, 2004)<br>(Yu et al., 2011) |
| **FABP** | Correlation between increased circulating levels of *fabp* and increased levels of cholesterol/triglycerides and LDL | (Xu et al., 2007) |
| **Hypoxia and** | Hypoxia shown to induce increased cardiac output, | (Yaqoob and Schwerte, |

| | | |
|---|---|---|
| **ISVs** | stroke volume and end diastolic volume along with increased ISV vascularisation index. Heart rate in hypoxic fish shown to be decreased until 6dpf and then elevates, correlated with model of loss of *vhl* | 2010)<br>(van Rooijen et al., 2009) |
| **RAAS and Inhibitors** | Pathway plays critical roles in cardiovascular control and disease pathogenesis<br><br>Captopril (ACE inhibitor) known not to directly influence ace2 activity | (Basso and Terragno, 2001)<br>(Jacoby and Rader, 2003)<br>(Donoghue et al., 2000) |
| **Agt** | Produced in the liver and released and cleaved into active Agt1 by Renin, produced in the kidneys | (Bader, 2010) |
| **Ace1 and 2** | Enzymes which cleave angiotensin I to release angiotensin II and other breakdown products, binding to different receptors in different tissues | (Bader, 2010) |
| **KKS** | Kallikrein-Kinin system (KKS) shown to be connected with glucose homeostasis and bradykinin stimulation in isolated cells, promoting glut4 translocation | (Barros et al., 2012) |

**Table 13** *This table comprises a list of genes (or pathways), expression of which was investigated in this current project due to the possible correlations with existing literature.*

## 2.5 Treatments/Mechanism Assays

### 2.5.1 Fih Inhibitor Treatment

Embryos were treated from 1 cell stage with KKC396, a hypothesized Fih specific inhibitor. The drug was made up in E3 and added to the embryos at 1 cell stage at various concentrations in order to test the dose response of the compound. In order to ascertain the function of the compound kymographs were generated in order to calculate the velocity of the blood along the aorta. The compound was considered to be toxic above 3µM, but was re-tested at 1 and 3µM, exchanging the solution every day (Schofield, C. pers. Comm.).

### 2.5.2 Viewpoint Activity Assay

Embryos were selected and placed into multi well plates in a small amount of E3 media (1ml for 24 well plates, 2ml for 12 well plates) and allowed to habituate both to the well plate and the view point scanner for an hour. The settings in the software were optimized to select the number of wells in the plate and then the experimental parameters were added. Initial experiments had the lights on a 15 minute cycle of 100-0%, to test the startle response to the lights being switched off. The software is capable of picking up different classes of movement based on selected settings. A

range of movement was considered by the software to assess the movement of each fish to define freezing movement (0 pixels), mid-range movement (0-10 pixels) and burst movement (>10 pixels).

These experiments were repeated over 24 hours with the lights on the same cycle as the adults are exposed to in the aquaria, lights on between 8am-10pm and lights off between 10pm-8am to test the embryos natural circadian dictated swimming patterns (Blanco-Vives and Sanchez-Vazquez, 2009).

In conjunction with data and suggestions from Bally-Cuif laboratory a secondary assay was performed, assessing total distance swum over 5 minute period following 1 hour rest period following placing the embryos in the well plates and in the Viewpoint platform. These assays were performed at 6dpf. Methylphenidate (MPH/Ritalin) was tested in the assessment of hyperactivity in the *fih217/217* embryos, also in conjunction with data from Bally-Cuif laboratory. The embryos were first placed in 12 well plates and allowed to acclimatise for 1 hour and imaged for 5 minutes to assess total distance swum. The embryo media was removed and replaced with either Ritalin (various concentrations made up in DMSO) in E3 or E3 only or DMSO only and left for 1 hour before imaging again for 5 minutes.

$$\textbf{Activity was assessed as a \% activity} = \frac{\textbf{Post-treatment distance}}{\textbf{Pre-treatment distance}} \times 100$$

#### 2.5.3 ATP Assay

An ATP quantification assay (ATPLite) from Perkin Elmer, was used in conjunction with an Invitrogen CyQuant - NF cell proliferation assay kit to provide ATP quantification normalised to DNA concentration (as a surrogate for cell number). This allows for variations in cell number created by homogenising whole embryos to be accounted for.

**ATPLite protocol:** Sort and pool embryos into batches of 10 in eppendorfs and add tricaine for 20 minutes, aiming for triplicate samples where possible. Embryos were washed twice in PBS before adding 250µl of lysis buffer and homogenizing with a needle (4 dpf embryos require 30 passes through the needle). Add 1.25µl lysis buffer to get to working concentration. 50µl of PBS was added to wells of 96 well plate, 25µl

sample solution was added, along with 25µl of ATP substrate (achieving technical triplicates as well as biological triplicates). The plate was shaken for 5 minutes followed by 10 minutes in the dark before reading the fluorescence.

**CyQuant protocol:** 1.1ml buffer was added to 4.4ml miliQ (MQ) water and 22µl CyQuant dye. 50µl was placed in each well alone with 50µl of sample (technical triplicates as well as biological triplicates). Plates are incubated in the dark for 40 minutes to an hour before reading the fluorescence.

#### 2.5.4 Cholesterol Assay

Roche produce a Cobas enzymatic, colourimetric assay that is used to assess cholesterol levels in blood samples in the screening process for atherosclerotic risk factors as well as the diagnosis and treatment of disorders involving elevated cholesterol. The system is in place at the Medical School at Sheffield University and the samples were sent to them for analysis. 50-100 embryos (wt and *fih217/217* embryos) were isolated in sterile eppendorf tubes at 6dpf following tricaine treatment. The E3 media was removed and replaced with 100µl of PBS before the embryos were macerated using a plastic pestle (Sigma Aldrich) designed to fit in the end of the eppendorf tube. The tubes were centrifuged for 1 minute at maximum speed to spin down the tissue debris, and the supernatant was removed and placed in a clean tube and transferred to the Medical School team for performing the Cholesterol assay.

## 2.6 Statistics

Experiments were repeated a minimum of three times, and the data was pooled to provide an average of the results. Where embryos were obtained through marbled zebrafish tanks, this would constitute a single batch of embryos; therefore multiple set-ups were required to acquire repeat data sets. In order to obtain sufficient numbers of embryos with the double mutant phenotype (*fih-/-;vhl-/-*) it was necessary on occasion to pool embryos from multiple parent pairs, meaning that repeated data sets were obtained through multiple pair mated set ups.

Statistical analysis of each data set was performed using the Prism Graph Pad software program to obtain the graphs, as well as the statistical features such as averages and significance factors.

# 3 Morphological and Structural Analysis of the *fih* Mutant Zebrafish

## 3.1 Introduction

The transcriptional output of the hypoxic signaling pathway is controlled at several levels and is subject to a number of feedbacks. The effect of the loss of *vhl*, in the zebrafish, has been characterised in the past, both as a model of vascular response to hypoxia and as a model of Chuvash disease (van Rooijen et al., 2010, van Rooijen et al., 2009). This chapter aims to characterise the phenotypes, in the zebrafish, caused by the loss of *fih* gene function. Analysis began with the observation of embryos with a range of genotypes; from *fih+/+;vhl+/+* to *fih217/217;vhl-/-*.

## 3.2 Observations of the effect of loss of *fih*

### 3.2.1 *fih* is expressed in a variety of tissues and activated by the loss of *vhl*

In mouse tissues and cell lines that have been tested, FIH protein has been shown to be expressed at similar levels (Zhang et al., 2010). A zebrafish *fih* null mutant line was generated by TILLING, prior to the publication of data on the *Fih* knockout mouse, to characterise the role of *fih in vivo*. The mutation results in a C to A conversion resulting in a premature stop codon and a functional null mutant.

Initial morphological observations of the *fih* homozygous mutant phenotype did not detect obvious morphological abnormalities. Homozygotes could be raised to adulthood, were present in normal mendelian ratios, showed normal fertility, and no maternal effects were detectable in embryos derived from matings of homozygous mutant parents. To address the effect of the hypoxic signaling pathway and also the *fih* mutation itself on its own transcript *fih* mRNA expression patterns and levels were assessed in the zebrafish embryos; by *in situ* hybridisation (**Figure 39**) and microarray/qRT-PCR (**Chapter 9**).

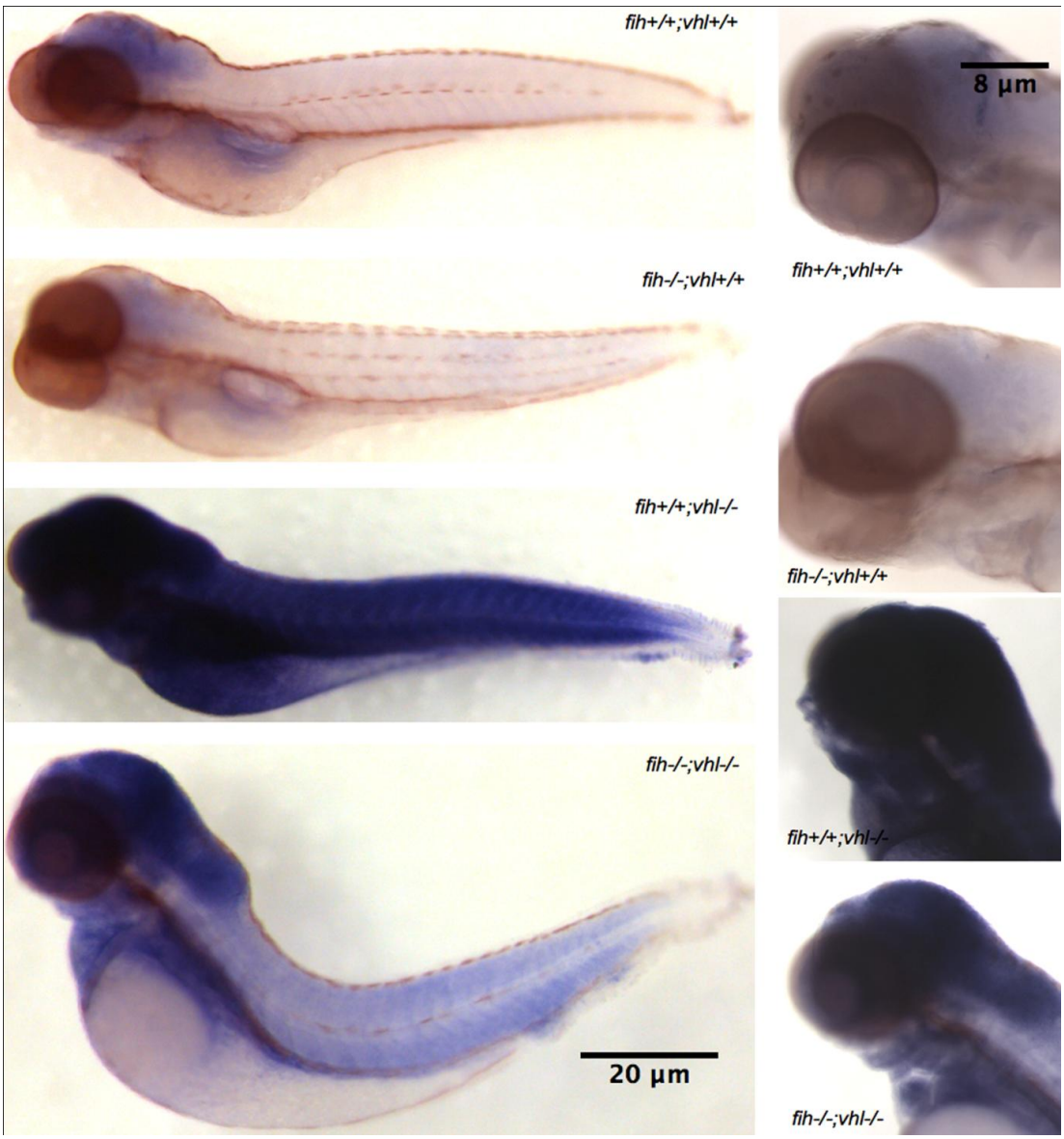


**Figure 39 Expression of *Fih* assessed by *in situ* hybridisation at 4.5dpf**

*Fih mRNA expression in wild type, fih217/217, vhl-/- and fih217/217;vhl-/- embryos at 4.5dpf. Left shows whole body images to show global expression patterns. Right shows isolated images of the heads at higher magnification to show details.*

*Fih* mRNA message appears in wild type embryos to be localised to the brain in general, heart and trunk/internal organs. Its expression in *vhl-/-* embryos is up-regulated throughout the whole body, suggesting that it acts as a negative feedback regulator acting on *hif-α* in the face of accumulation that occurs due to the loss of *vhl* (Santhakumar et al., 2012), although this is so far an assumption. There is some expression of *Fih* message in both the *fih217/217* embryos and the *fih217/217;vhl-/-* embryos, higher in these latter. The reduction of expression was unexpected, as loss

of *fih* would be expected to increase the activity of HIF-α to some degree, thus an increase in expression would be expected; either weaker or similar to that seen in *vhl* mutants. A possible explanation for this might be nonsense mediated decay of the message due to the early stop codon in *fih*$^{i217}$ fish. Further investigation of *fih* expression at various developmental stages is necessary in order to answer questions such as the time at which these differences/increases can be observed. Further investigation of *fih* expression has been performed by qRT-PCR, which will be discussed later in this thesis.

### 3.2.2 The *fih* mutation can enhance the *vhl-/-* phenotype

Since *fih* is induced in *vhl* mutants and can act *in vitro* to hydroxylate and inactivate HIF independently of the presence/absence of VHL, we expected that loss of *vhl* might not represent a full activation of the HIF pathway.

To test whether *fih* is capable of enhancing or otherwise altering the *vhl* mutant phenotype the *fih* and *vhl* mutant zebrafish lines were crossed together it was possible to observe a range of phenotypes that were changed from the known characteristics of the *vhl-/-* embryos. In a blind observation of known *vhl-/-* embryos with mixed *fih* backgrounds, phenotypes were sorted from the strongest to the weakest and subsequently genotyped it was revealed that the strongest phenotypes were exhibited by *fih217/217;vhl-/-* embryos **(see Figure 40 for examples of the phenotypes).**

These results showed that although loss of *fih* on its own does not have easily detectable morphological consequences, the loss of *fih* in the context of the loss of *vhl* may lead to further up-regulation of HIF signaling, see **Figure 6 and 11** in Introduction. The combined loss of both of these genes results in accumulation of functional *HIF-1α* protein in normoxia, a hypothesis that has been proposed by Li et al (Li et al., 2011b) since it will be neither ubiquitinated (by VHL) and broken down, or hydroxylated (by FIH) and inhibited. The observed phenotypes ranged from what has been characterised for *vhl-/-* embryos, including enlarged heart and decreased yolk usage through to *fih217/217;vhl-/-* embryos which exhibited further enlargement of the heart region and associated oedema along with dorsal curvature of the body axis. The loss of one copy of *fih* did not detectably alter the phenotype of *vhl-/-* embryos and for

this reason and for the remainder of this thesis where wild type embryos are being referred to these could include a small mixture of genotypes, see **Table 14**.

| WT | FIH Null | VHL Null |
|---|---|---|
| *fih+/+;vhl+/+* | *fih217/217;vhl+/+* | *fih+/+;vhl-/-* |
| *fih-/+;vhl+/+* | *fih217/217;vhl-/+* | *fih+/-;vhl-/-* |
| *fih-/+;vhl-/+* | | |

**Table 14** *Table describes various different genotypes collectively referred to as wild type, FIH Null or VHL Null, from this point forward in the thesis*

For closer inspection, higher magnification images of the embryos were taken to assess the influence of the loss of *fih* in *vhl-/-* embryos. The *fih217/217;vhl-/-* phenotypes, at first sight, included features such as smaller eyes, an increased curvature of the body axis, as well as a larger amount of remaining yolk compared to wild type siblings, see **Figure 40.** The reduction in yolk usage has been hypothesised to be due to developmental delay rather than a direct result of an altered rate of metabolism, and as such will require additional experimentation.


**Figure 40 Key elements of the various phenotypes in the zebrafish embryos at 4.5dpf**

*The red arrow head indicates the enlarged heard and heart cavity, the red diamond indicates the smaller eye observed in the fih217/217;vhl-/- embryos. The blue arrows illustrate the development of vascular loops in the tail. The green arrow indicates an area of sluggish circulation in the double mutant embryos. A high quality image of fih217/217 embryos was not obtained and these embryos were indistinguishable from wt embryos and are not shown. The composite images were taken on multiple focal planes.*

The human eye was used to sort the different morphological features described above, at least as far as distinguishing between *vhl* null and *fih;vhl* double null embryos, as compared with each other or compared with wild type phenotype. In order to more accurately test how good the human eye is at this sorting, fish could be sorted by multiple operators into classes and individual embryos from the classes could be independently genotyped to find out the exact error rate, false positives and negatives within each class. For the purposes of this thesis that error rate is not known, however genotyping of embryos was constant to ensure results were attributed to the correct class of embryo.

ImageJ was used to quantify morphological parameters such as fish length and the number of functional ISVs (see **Figure 41)**. At 4dpf the differences were small, however at 5dpf the *vhl-/-* and *fih217/217;vhl-/-* embryos did appear to have decreased total fish length compared to wild type and *fih217/217* embryos. The total number of functional ISVs was also decreased at 5dpf in the *fih217/217;vhl-/-* embryos.

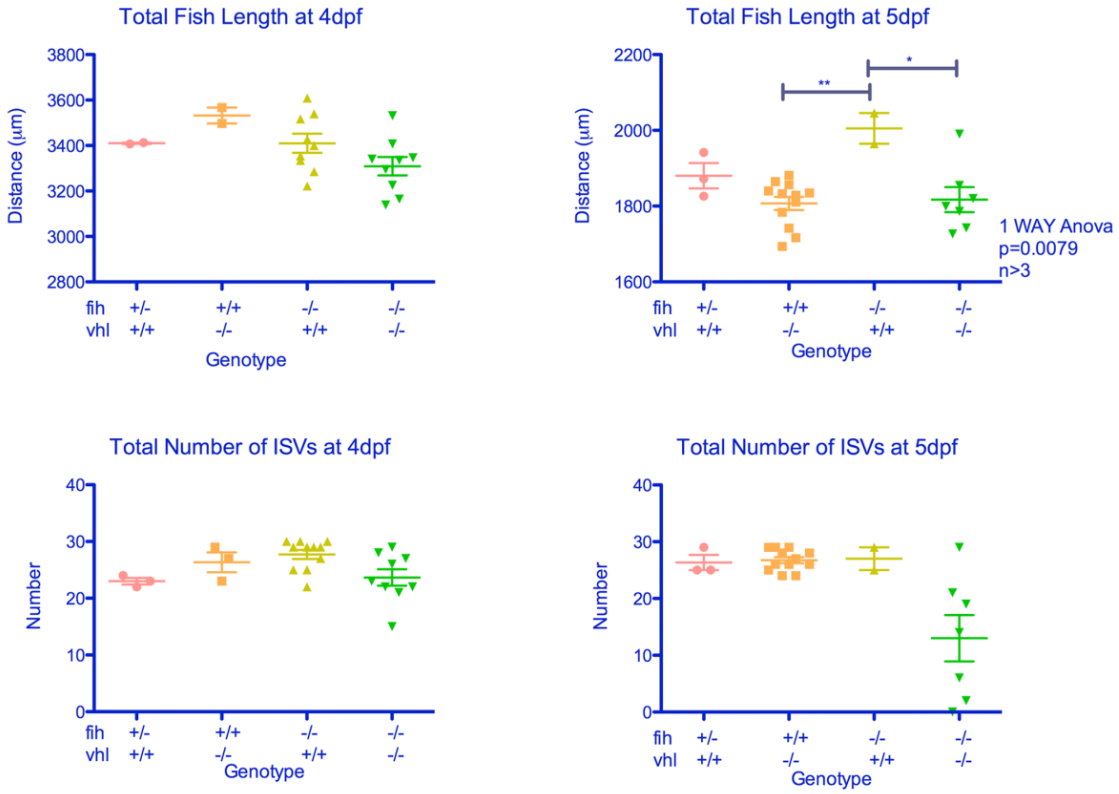


**Figure 41 Quantification of total vessel length and ISV number was performed in order to assess possible differences in these characteristics between the different mutant classes.**

*Measurements taken from image deletion angiograms using ImageJ to assess whole length and the total number functional of ISVs at different stages of development in the various mutants, showed little change although a slight increase in total fish length in the vhl-/- embryos was observed at 5dpf.*

To further characterise the observed phenotypes in the heads of the *vhl-/-* and *fih217/217;vhl-/-* embryos in comparison with wild type, image deletion angiograms

were used to illustrate blood flow and in so doing highlight the blood vessels and heart regions, see **Figure 42.**

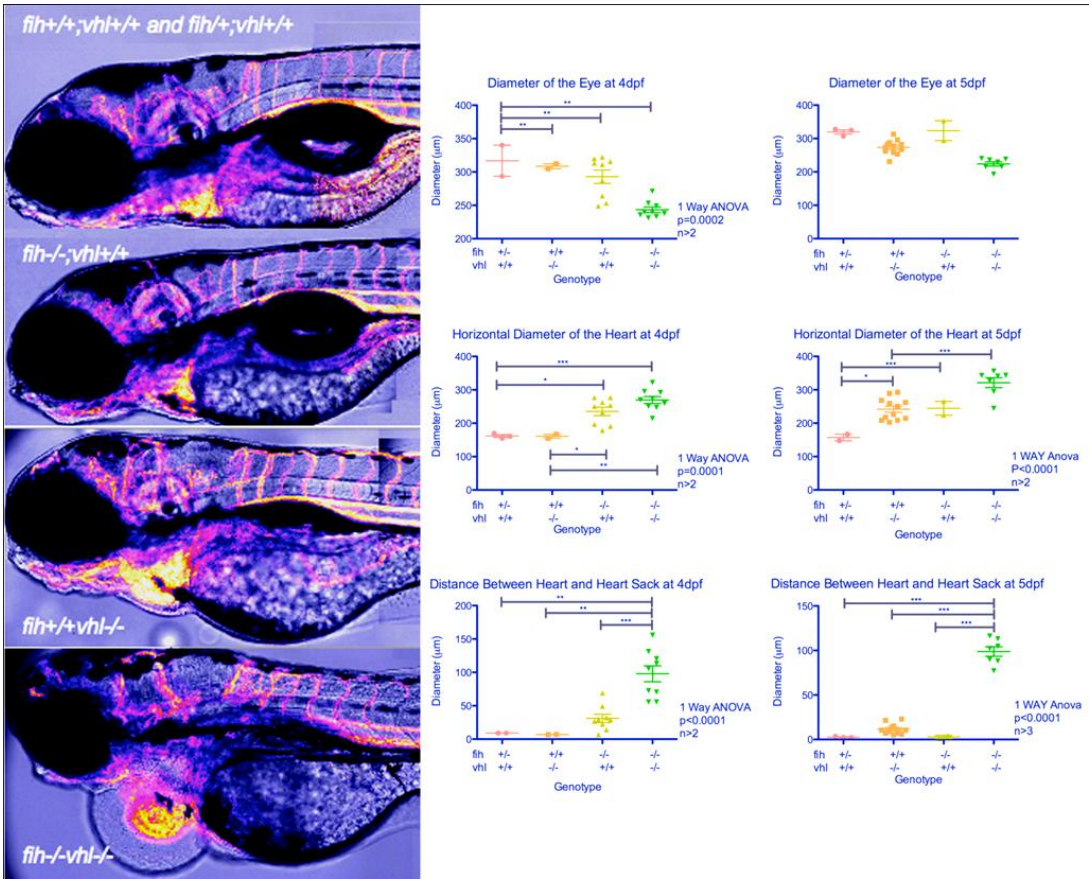


**Figure 42 Features such as the diameter of the eye, the horizontal diameter of the heart and the development of a space between the heart and the heart sack were measured to quantify changes in these features in the different classes of embryo**

***Left)*** *Illustrates the heads of embryos imaged using image deletion angiography at 4.5dpf.* ***Right)*** *Illustrates quantification of the eye diameter, heart diameter and distance between the heart and heart sack at both 4 and 5dpf*

The eye diameter of the *fih217/217;vhl-/-* embryos is decreased compared to the non double mutant siblings. The heart diameter in the *vhl-/-* and *fih217/217;vhl-/-* embryos is increased, and these latter also have a measurable increase in central oedema surrounding the hearts. In terminal cardiac failure, as well as some cancers, where low levels of oxygen are reaching the tissues, peripheral oedema can be caused both by decreased venous return and an increase in *Vegf* (Bates, 2010, Chin et al., 2003), so these were factors that were investigated in this model to assess their roles

in this phenotype. These early observations and quantification showed that differences between wild type and *fih217/217* siblings were minimal or absent suggesting that Fih has only a weak effect on Hif as compared to Vhl, and that it does not significantly impact on embryonic morphology. For this reason the focus of the investigation remained on the ways in which the *vhl-/-* phenotypes were altered by the loss of *fih* as well.

### 3.2.3 Loss of *fih* increases expression of HIF target genes compared to *vhl-/-* embryos

Expression patterns of several HIF signaling targets were examined by *in situ* hybridisation. The levels of *phd3* were shown to be elevated in the *vhl-/-* embryos (van Rooijen et al., 2010, van Rooijen et al., 2009). These finding were confirmed through repetition of the *in situ* hybridisation, including *fih* mutant embryos and post-assay genotyping allowed for the effect of the loss of *fih* to be assessed simultaneously. A further increase in *phd3* expression was seen in *fih217/217;vhl-/-* embryos whereas expression was unchanged in the *fih217/217* embryos, **see Figure 43 and Figure 44**.

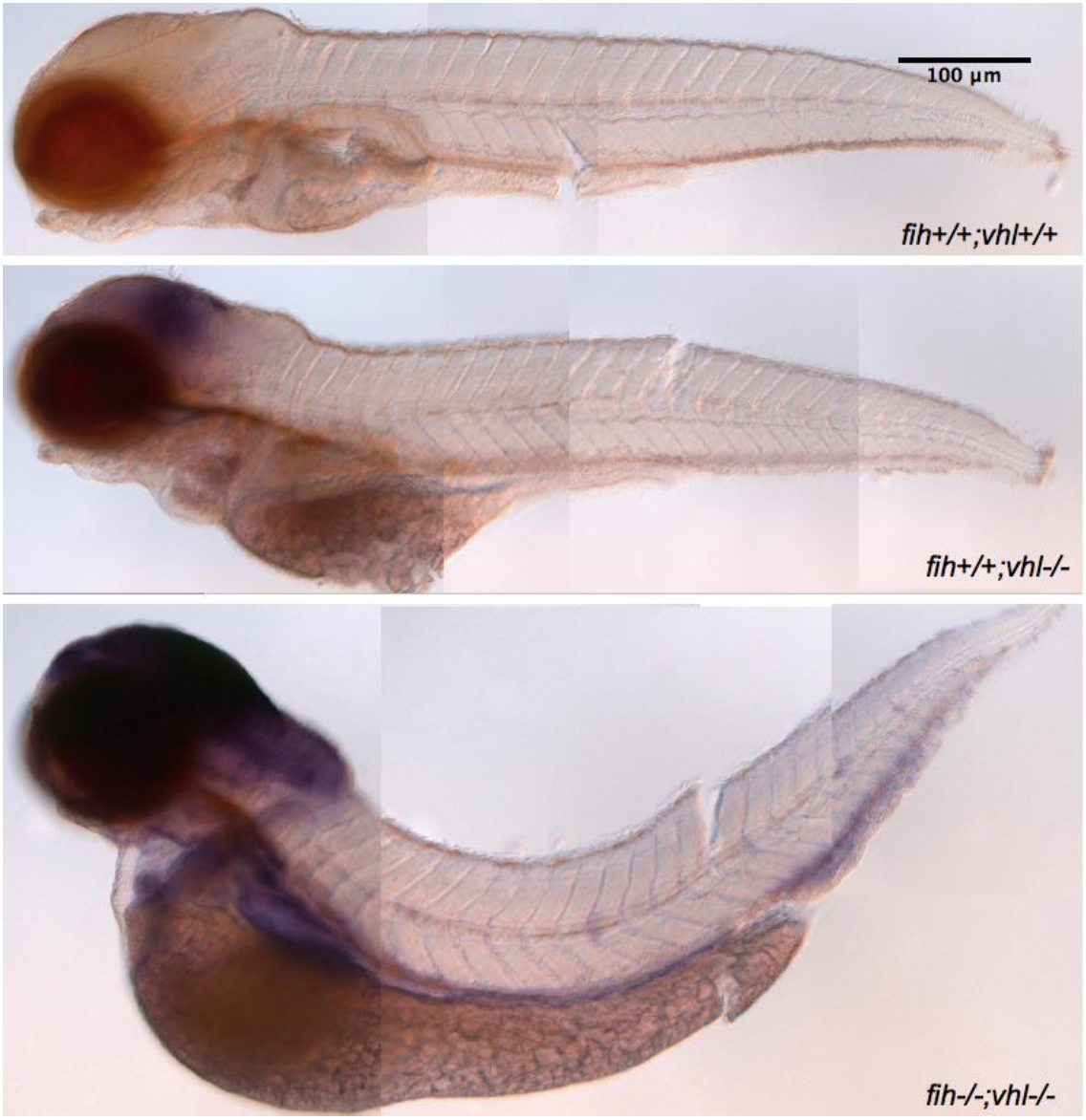


**Figure 43** ***in situ*** **hybridisation of** ***phd3***

*Phd3 mRNA is found in the brain, heart, internal organs, kidney pronephros and blood island in the tail, to differing degrees in the vhl-/- embryos and more in the fih217/217;vhl-/- embryos. A high quality image of fih217/217 embryos was not obtained and these embryos were indistinguishable from wt embryos and are not shown. The composite images were taken on multiple focal planes.*

A *Tg(Phd3:eGFP)* transgenic line, expressing GFP under the Phd3 promoter (Santhakumar et al., 2012), has been used to provide a live read-out of areas of hypoxic signaling, given that *phd3* is a strongly responding target of HIF-driven transcription with very low expression in normoxic embryos. The transgenic line was

crossed in to the *fih;vhl* mutant backgrounds in order to assess levels of hypoxic signaling in the live embryos, see **Figure 44**.

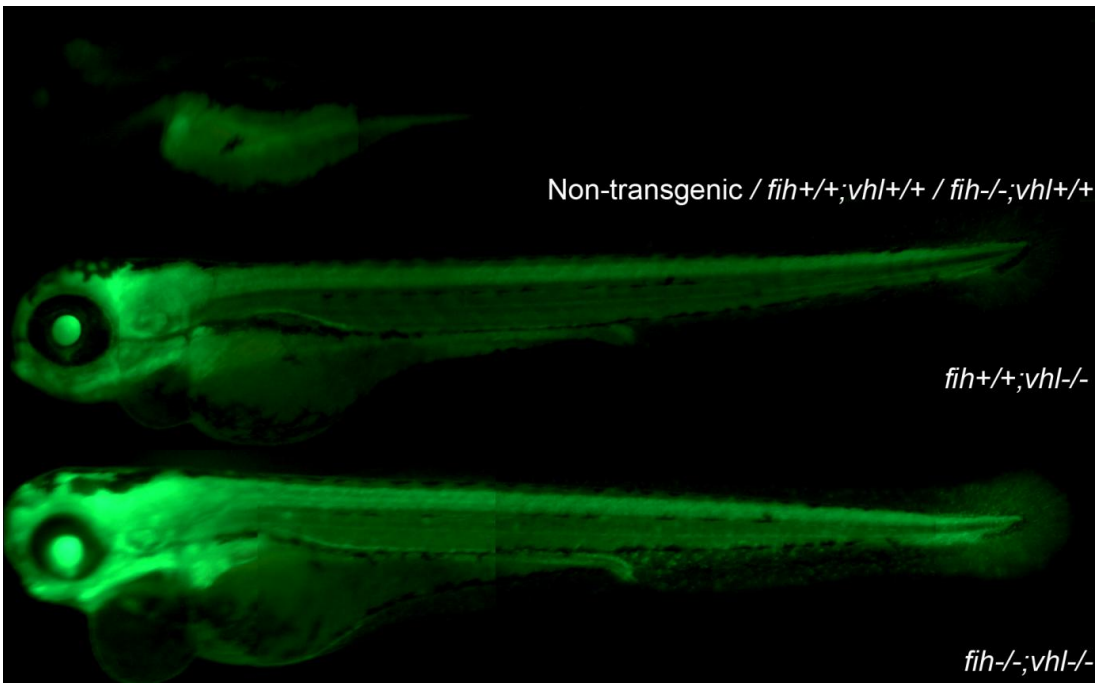


**Figure 44** ***Tg(Phd3:eGFP)*** **zebrafish line crossed into the** ***fih*** **and** ***vhl*** **mutant zebrafish lines provides an** ***in vivo*** **method for visualising the levels of** ***phd3*** **expression**

*Tg(Phd3:eGFP) expression demonstrates varying degrees of regulation in the different mutant backgrounds, from low/no expression in wild type and fih217/217 embryos to increased levels in vhl-/- embryos and then a further increase in fih217/217;vhl-/- embryos. A high quality image of fih217/217 embryos was not obtained and these embryos were indistinguishable from wt embryos and are not shown. Images were taken at 4dpf and consist of composite images taken on multiple focal planes.*

As described in the introduction *phd3* has a HRE in the promoter, the transcription of the gene can therefore be seen as a surrogate read-out of HIF signaling. *phd3* is necessary to keep HIF-α hydroxylated and the pathway switched off, however it is also a target and is therefore being amplified when the pathway is on. The low levels of expression in the absence of HIF signaling are therefore more difficult to explain and may be down to the difference in role of the different Phd proteins, for example *phd2* could be the regulator that keeps the baseline HIF activity low. It is currently unclear what the low level of *phd3* expression in wild type is caused by, it might be HIF independent, and these investigations are ongoing (Santhakumar unpublished data).

The increase in HIF signaling in normoxia in these *fih217/217* and *vhl-/-* embryos allows for the study of the downstream effects of this pathway without the need to maintain depleted oxygen levels. These data show that *fih* can modulate the phenotype of *vhl* mutants and is consistent with the expectation that loss of *fih* further enhances HIF signaling in a *vhl* mutant background. It also argues against a purely *vhl* dependent role of *fih* on HIF as might be predicted from Li et al (Li et al., 2011b).

## 3.3 Vascular Branching Phenotype

Hypoxia is known to initiate vascular gene expression along with vascular proliferation and remodeling in order to ensure adequate supply of lowered oxygen availability to the tissues. For this reason, along with knowledge of known vascular defects in the *vhl-/-* embryos, the vascular network in the *fih217/217* and *fih217/217;vhl-/-* embryos was assessed. The phenotypes that were observed in the *fih217/217* and *vhl-/-* zebrafish embryos distinguish each mutant from the other, apart from the *fih217/217* embryos from their wt siblings. These phenotypes include hyper-branching of the network, alterations in remodeling along with changes in gene expression.

### 3.3.1 Loss of *fih* causes further branching of the blood vessels in *vhl-/-* background

Confocal imaging of the blood vessels using transgenic zebrafish line of a fusion of the friend-leukemia integration 1 transcription factor to GFP *Tg(fli1;eGFP)* was performed (Cha and Weinstein, 2007, Lawson and Weinstein, 2002b), see **Figure 45.**

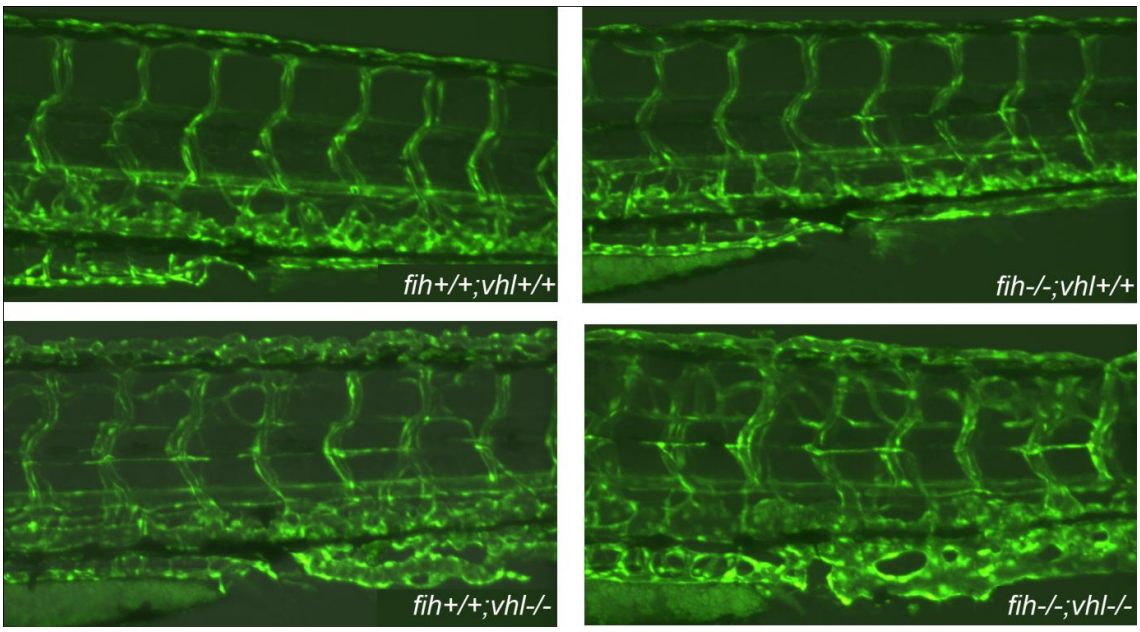


**Figure 45 Vascular patterning in the different embryos using *Tg(Fli1;eGFP)* transgenic to highlight the vasculature**

*Images were taken at 4.5dpf using a Spinning Disk Confocal microscope. The wild type and fih217/217 embryos show the expected patterning of the posterior caudal vein, the dorsal aorta and the intersegmental vessels (ISVs) connecting at the top at the dorsal longitudinal vessel. The patterning of both the vhl-/- and fih217/217;vhl-/- embryos showed distinct levels of branching of the vasculature.*

A hyper-branched blood vessel network in the *vhl-/-* embryos was shown by Dr Van Rooijen (van Rooijen et al., 2010) with associated increase in expression of vascular endothelial growth factor (*vegf-a)* a gene associated with the stimulation of angiogenesis and vasculogenesis and a target of HIF signaling. The hypothesis was that the further up-regulation of *vegf-a* due to the dual loss of *fih* and *vhl* in these embryos resulting in the further loss of negative control of Hif in the *fih217/217;vhl-/-* compared to the *vhl-/-* only embryos would lead to further complications in the blood vessel networks. The *fih217/217* embryos showed no observable change in the blood vessel patterning compared with *fih+/+* siblings. However the patterning in the *fih217/217;vhl-/-* embryos was altered compared with *vhl-/-* embryos, with many additional branches in the vascular structure.

The extra complexity of the vasculature led to the assessment of how many of the new connections were functional. Using image deletion angiography as a tool for assessing the competence of the vessels it was shown that many of these additional branches in

the blood vessels were lumenised and competent to carry flow (Chico et al., 2008). These differences were quantified using a vascularisation index technique (Yaqoob and Schwerte, 2010, Schwerte et al., 2003) and showed that there was statistical significance to the differences, **Figure 46**.

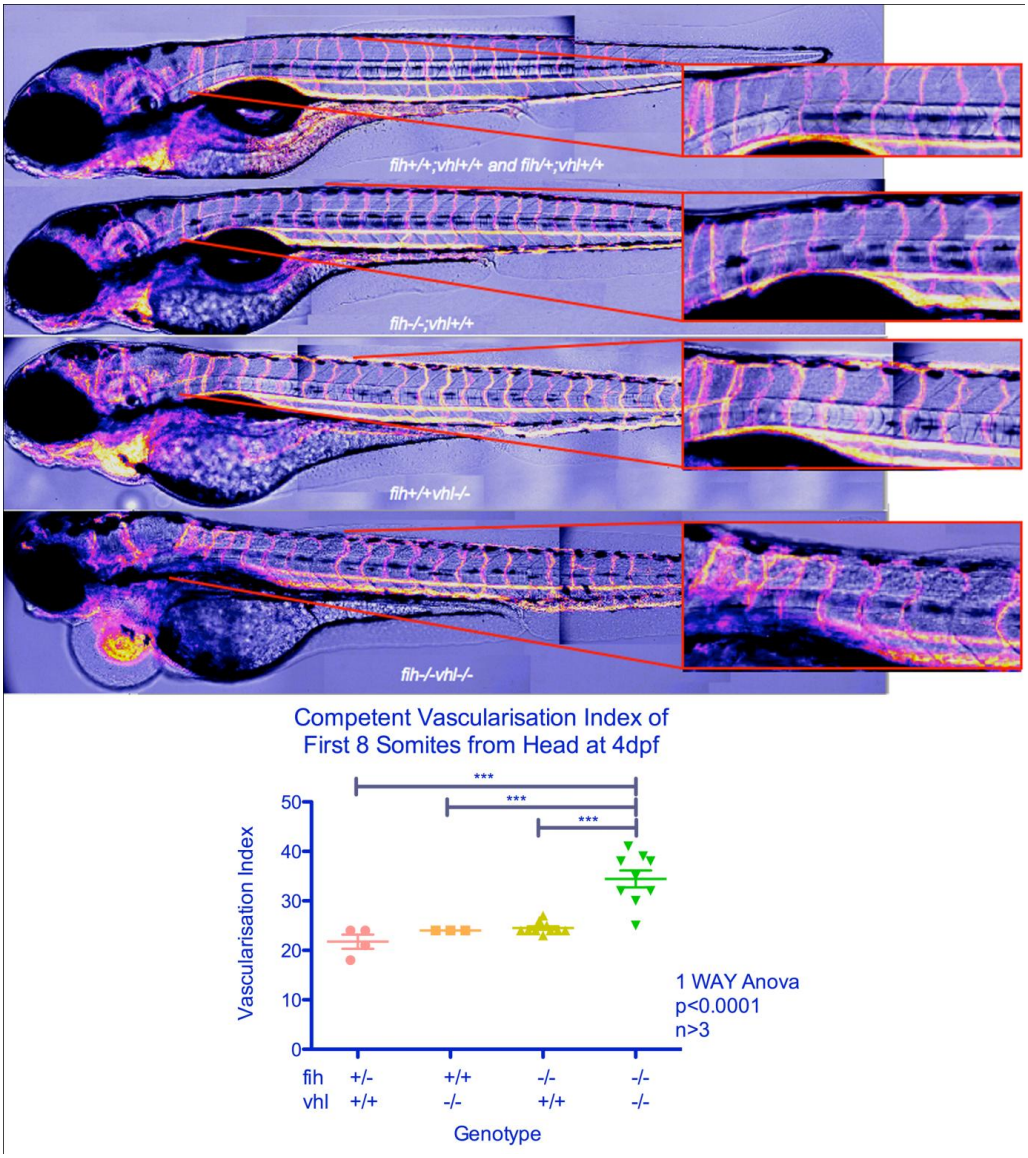


**Figure 46 Quantification of vascular index**

*The image deletion angiograms illustrate the level to which branches in the blood vessel network are competent to carry flow. Vascularisation index taken across the first eight somites back from the head illustrate that this is most striking in the fih217/217;vhl-/-.*

This increase in vascular density observed using the *Tg(fli1;eGFP)* transgenic line revealed the hyper-branching of the vascular network in both the *vhl-/-* and the *fih217/217;vhl-/-,* the image deletion angiograms revealed that several of these neo-vessels and extra branches were also competent to carry flow. These were particularly evident in the region behind the head, in the first 8 somites, in the *fih217/217;vhl-/-* embryos. Vascular index provides one tool for assessing complexity of branching. However it may be seen to provide confounding results, in relation to extra branching versus the result of branches being missing. Alternative assays will need to be investigated to confirm these findings.

### 3.3.2 Loss of *fih* causes a small increase in endothelial cell number in *vhl-/-* background

To assess the way in which these new vessels form, and assess the contribution that endothelial cell proliferation, rather than vascular remodeling, had on the complexity, the transgenic zebrafish line *Tg(flk1:eGFP-NLS)* was used (Blum et al., 2008). The transgenic line leads to GFP contained in the nuclei with a translational link to a nuclear localisation sequence (NLS) in the endothelial cells within the embryo, allowing for a physical count of the cells. A count of the endothelial cells in particular regions of interest; firstly behind the head where the additional bundle of blood vessels showed in the image deletion angiograms **(Figure 31)**, and secondly in the tail above the anus, see **Figure 47**.

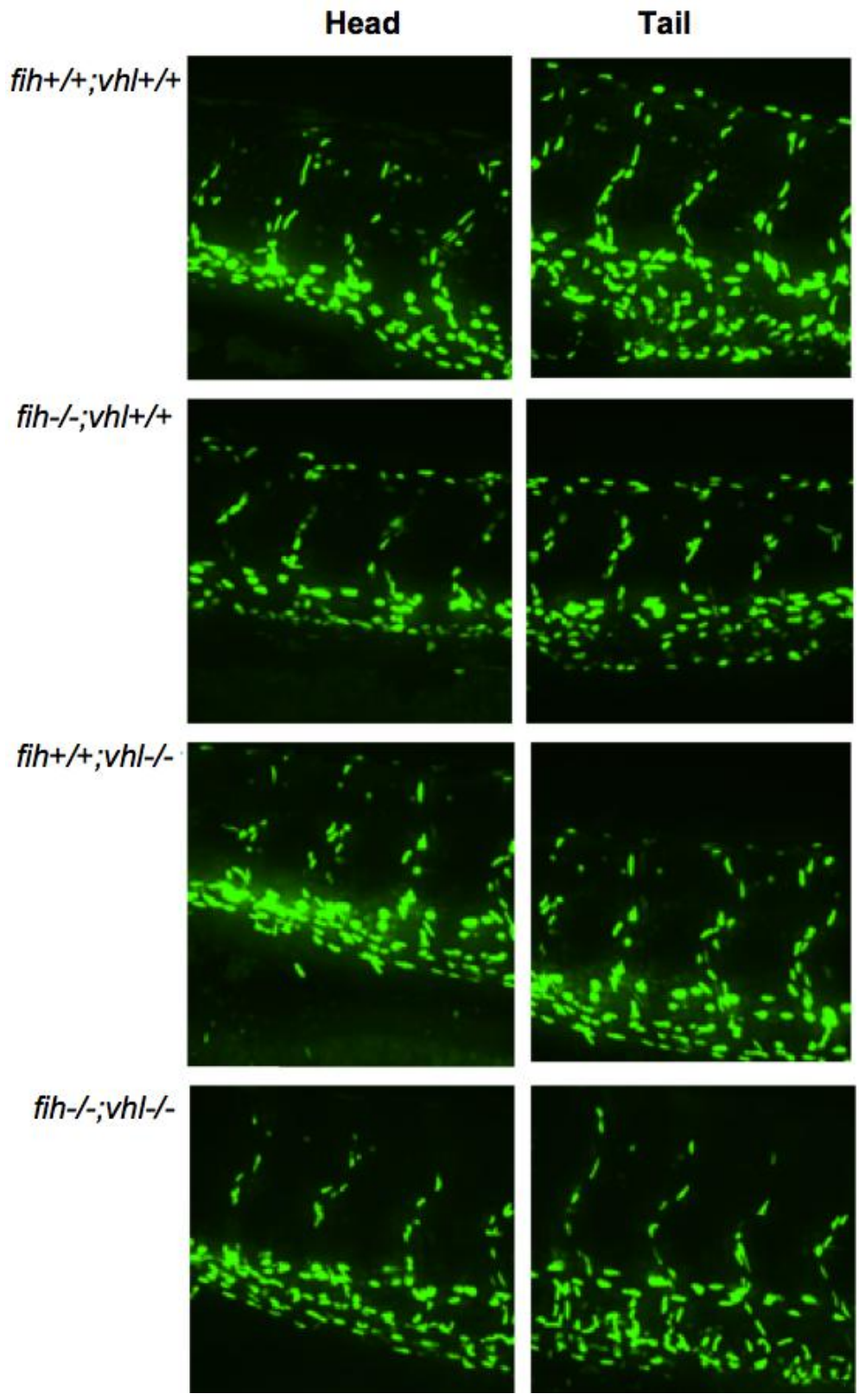


**Figure 47 Endothelial cells were imaged in order to assess proliferation**

*Images taken using spinning disc confocal microscopy of fih;vhl;Tg(Flk1:eGFP-NLS) embryos at 5dpf and displayed as z-projections of the z-stacks taken through the embryo.*

The images displayed in this way make the assessment of endothelial proliferation too ambiguous to judge, however using counts through the z-stacks and representing these numbers graphically it was possible to see trends that were more difficult to see from the images alone, see **Figure 48.** These were taken from the same batch of embryos, maintaining consistency.

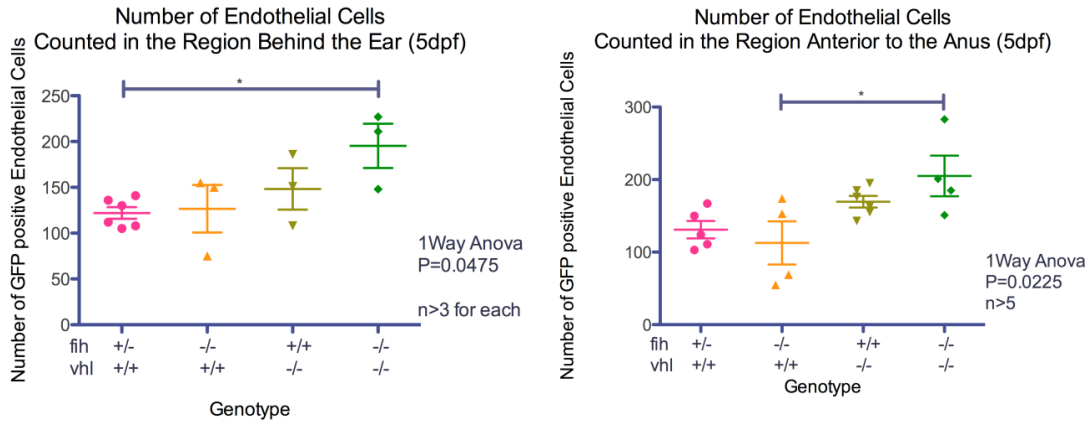


**Figure 48 Quantification of endothelial cell number**

*Quantification of the number of endothelial nuclei observed in the z-stacks demonstrated an increase between the wild type embryos and the fih217/217;vhl-/- embryos in both regions that were counted. Comparisons besides those marked were not significantly different.*

The trend increase in cell number in these regions at 5dpf was not extensive, it did however suggest that a combination of proliferation of the endothelium along with remodeling of the existing vasculature could be used to explain the branching of the blood vessels in the *fih217/217;vhl-/-* embryos. The loss of *fih* did not materially affect the number of endothelial cells, compared with wild type. The limitations of this data set are human error in the counting of the endothelial cells and could be combated by the inclusion of multiple operators counting the same samples and comparing the results, this is ongoing. The investigation of alternative methods, of generating algorithms for making the counts, was also ongoing at the time of writing this thesis.

### 3.3.3 Loss of *fih* causes an increase in Vegf family expression in the *vhl-/-* embryos

*Vegf*, like *phd3* has been shown to be a target of hypoxic signaling, which has been shown to respond to hypoxia via HIF (Forsythe et al., 1996) and contain both a Hif binding site (HBS) and a Hif ancillary sequence (HAS) within the HRE. The core sequences for the HBS and HAS were determined as TACGTG and CAGGT, respectively, with these elements offering an imperfect inverted repeat that is crucial for the function of the promoter (Kimura et al., 2001).

An *in situ* hybridisation revealed the same pattern of up-regulation of *vegf* in these zebrafish embryos as had been shown for *phd3,* with no detectable change in expression in the *fih217/217* embryos, see **Figure 49**.

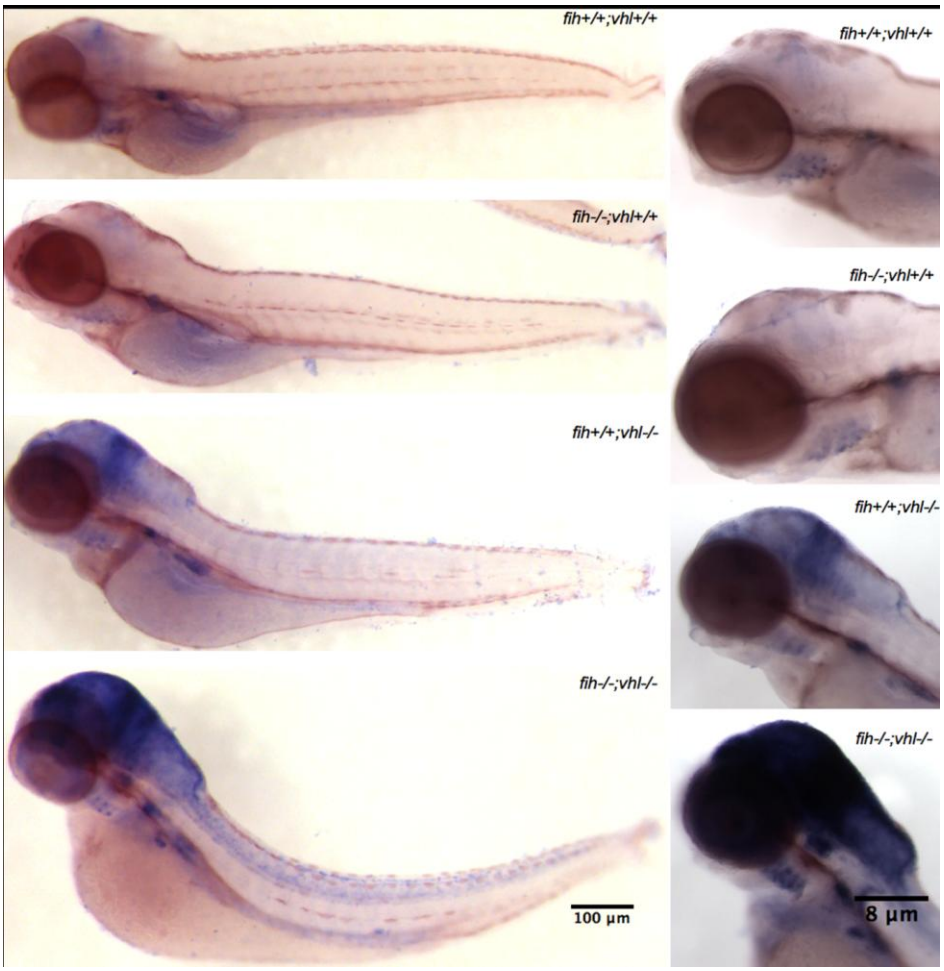


**Figure 49 *in situ* hybridisation of *Vegfaa* at 4.5dpf**

*Vegfaa mRNA expression in wild type, fih217/217, vhl-/- and fih217/217;vhl-/- embryos at 4.5dpf.* ***Left)*** *whole body images to show global expression patterns* ***Right)*** *isolated images of the heads at higher magnification to show details.*

The systematic up-regulation of *vegf* in conjunction with both the individual loss of *fih* and then *vhl* and then both correlates with the roles each of these genes plays in regulating Hif-α.

### 3.3.4 Role of Vegf in vascular permeability in the zebrafish embryo

The increase in *vegf-a* has been illustrated in **Table 15 and Table 16**, in the *vhl-/-* embryos as well as in the *fih217/217;vhl-/-* embryos. In the zebrafish it is possible to inject high molecular weight dye or quantum dots (Q-dots) and observe the vasculature microscopically in real time provides an opportunity to assess the immaturity and permeability of the vessels.

With the increased levels of *vegf* it could be hypothesised that the vessels in the *fih217/217;vhl-/-* embryos would be benefiting from pericyte recruitment, however they may also be experiencing increased vascular leakage. To test this in the *fih217/217;vhl-/-* embryos the same functional angiograms were attempted and imaged over time in order to observe the competence of the blood vessels, see **Figure 50**.

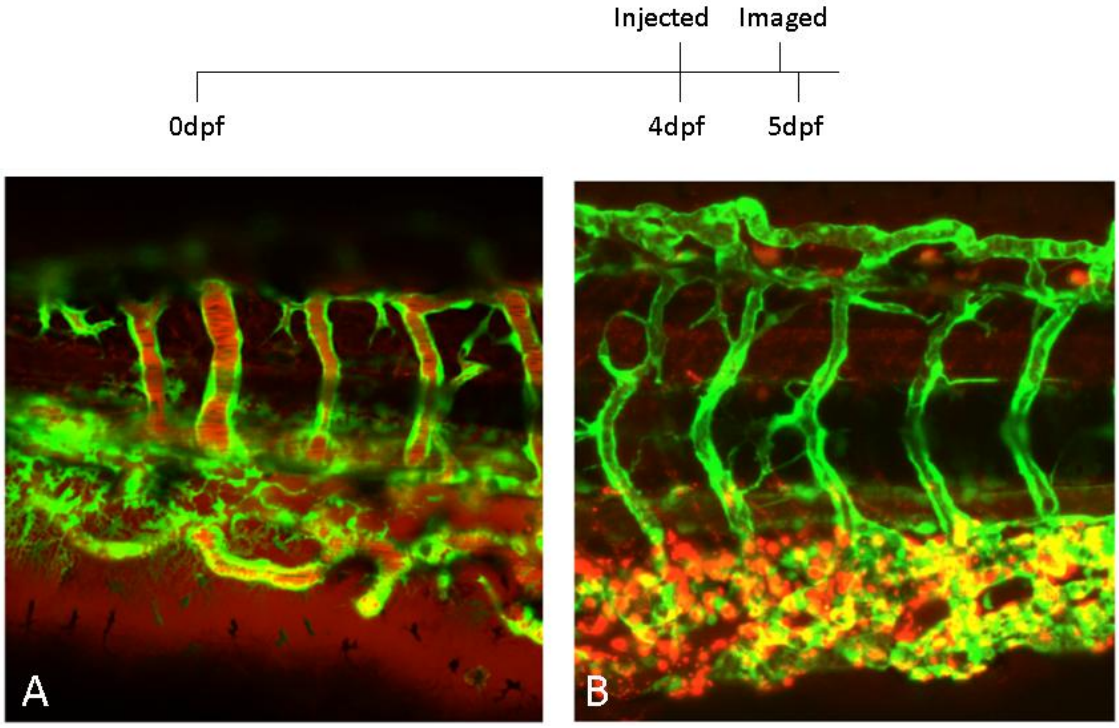


**Figure 50 An attempt to assess vascular competence by injection of high molecular weight dye into the circulation**

**A)** d*emonstrates the TAMRA dye within the vessels on day of injection* ***B)*** *demonstrates the TAMRA dye diffused out of the vessels by 5dpf. This pattern was observed in all embryos regardless of their genotype.*

The experiment was impossible to repeat exactly in the *fih217/217;vhl-/-* embryos due to their shorter survival times. These embryos experience cardiac contraction but blood ceases to circulate following 4.5dpf. This necessitated attempting to repeat the injections at much earlier stages, when the vessels in all the embryos including the wt siblings were several days more immature.

## 3.4 The loss of *fih* does not enhance all phenotypes observed in *vhl-/-* embryos

One of the phenotypes observed in the *vhl-/-* embryos, from around 3dpf, is observable looping of the ISVs over and above the pigment line and dorsal longitudinal vessel.

For the most part, to this point, the loss of *fih* in the *vhl-/-* embryos has lead either to further branching of blood vessels or stronger up-regulation of gene expression. One vascular phenotype of the *vhl-/-* embryos that did not conform to this trend was this looping of the ISVs in the tail of the embryos up above the dorsal longitudinal vessel (DLV) and the pigment line, see **Figure 51.**

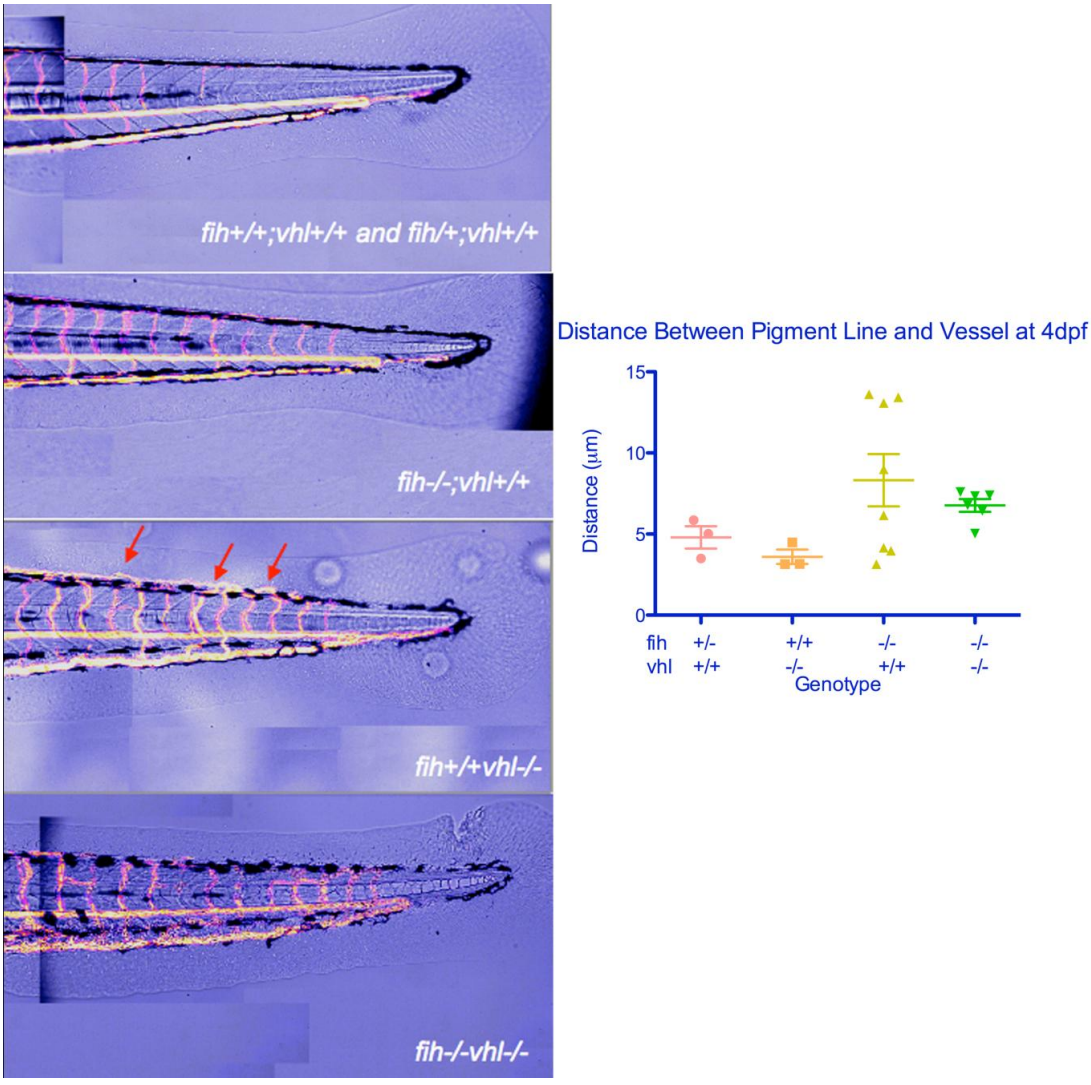


**Figure 51 Resolution of vascular looping (*vhl-/-)* in the tail vasculature in the *fih217/217;vhl-/-***

*The loops in the top of the ISVs occur in all the embryos, but in the vhl-/- embryos the loops extend higher above the dorsal longitudinal vessel. This was quantified using ImageJ to measure the distance between the pigment line and the inner curve of the loop in the ISV. Each mark is equal to one fish, n numbers for this assay are 3 to 8 per genotype and requires repetition.*

The looping of the ISVs wasn't observed in any of the other mutants by this technique, despite the lack of *vhl* in both the *vhl-/-* and the *fih217/217;vhl-/-* embryos. The observation that this is one phenotype that isn't exacerbated by the loss of both *fih* and *vhl*, despite the fact that these embryos do demonstrate excessive branching of the blood vessel network and increased vascular factors, suggests that other factors play a role in controlling this phenotype specifically. Shear stress presented itself as a possible mechanism for this control as it was recently found that flow is an important prerequisite for the development of the angiogenic phenotype by *vhl* mutants however this hypothesis has not been tested in these double mutants at this time, the preferred method would be to restore flow in these mutants to check whether the phenotype could be enhanced. In the absence of a reliable method for this the injection of the *tnnt2*-MO (silent heart) or the use of measured doses of tricaine to either remove the heart beat in order to ensure the embryos never experienced flow or only at a reduced rate might show a reduction in phenotype (despite the presence of high levels of VEGF and KDR(L)).

## 3.5 Discussion and Future Work

### 3.5.1 The Hypotheses

The first hypothesis to test, the first observation to make, was to assess the effect of the loss of *fih* on both wild type embryos and on *vhl* null embryos. Previous analysis of the *vhl-/-* zebrafish revealed that the embryos exhibit several phenotypes most likely as a result of activation of HIF signaling; including enlargement of the heart, increased buccal movement, hyperventilation, polycythemia, and an increase in vascular complexity (van Rooijen et al., 2010, van Rooijen et al., 2009). The loss of *vhl* in this case appears to suggest that a level of HIF regulation was removed and these observed phenotypes correlate with those that would be seen under hypoxia in order to respond to decreases in atmospheric oxygen. Given the roles of *fih* and *vhl* are independent of each other in regulating HIF function (FIH regulating HIF function, while VHL regulates HIF turnover), the hypothesis in this case would be that the loss of *fih* alone may not show dramatic phenotypes, however in the context of the loss of *vhl* it may alter or exacerbate phenotypes observed in the organisms where *vhl* was lost.

There have also been studies predicting the necessity for VHL acting as a bridge between FIH and HIF for efficient binding (Lee et al., 2003) suggesting a loss of *vhl* would disrupt the hydroxylation of HIF-α by *fih* as well. The hypothesis in this case would therefore be that the loss of *fih* as well, in an individual that had lost *vhl* function, would result in no alteration in the phenotypes observed.

### 3.5.2 HIF Regulation

These hypotheses could be tested when the *fih217/217* and *fih;vhl* double heterozygous carriers were generated. For instance, *fih217/217;vhl-/-* embryos were found to show further increases in the size of the heart/heart cavity compared to *vhl-/-* embryos along with increased complexity of the vascular patterning. Prolyl hydroxylase domain protein hydroxylation of HIF-α initiates the formation of a ubiquitination complex involving VHL protein and the degradation of HIF-α. The absence of VHL therefore leads to ectopic accumulation of HIF-α and downstream gene expression changes, of which *phd3* is one. The increase in vascular complexity, correlated with increased expression changes of the hypoxic target *phd3.* In contrast the expression of *phd3* in the *fih217/217* embryos did not differ from wild type embryos. These preliminary findings supported the first hypothesis.

The second hypothesis, that the FIH, VHL and HIF-α form a complex, with individual components being necessary to bridge between and act as chaperones for the others (Lee et al., 2003, Li et al., 2011b), see **Figure 14 in Introduction**. The findings from this study, that the loss of either *fih* or *vhl* have distinct effects on the down-stream signaling of HIF in the zebrafish suggest that more investigation is needed into the possible interactions between these proteins *in vivo.* Due to the different phenotypes observed in each of the single mutants compared with the double mutant, if either *fih* or *vhl* were needed to form the FIH-VHL-HIF-α complex, these phenotypes might be hypothesised to be more similar, which they are not.

Since *fih* has been shown to bind to and hydroxylate multiple ankyrin repeat domain proteins (ARDs) and affect the function of many of these (Cockman et al., 2006, Cockman et al., 2009, Coleman et al., 2007), it is conceivable that its loss is affecting other pathways besides HIF. However, our data suggest that these functions are not essential for early patterning of the embryo and are instead more involved in fine tuning the role of signaling, which conforms with findings in mice where *Fih* knockouts are viable and fertile (Zhang et al., 2010).

### 3.5.3 VEGF and angiogenesis

Overall, vascular patterning of the *fih217/217* embryos appeared, from these assays, to match that seen in wild type siblings, with no observable excess branching. The loss of *fih* in the *vhl-/-* embryos however did result in a further increase of vascular branching, with a concurrent increase in endothelial cell number, which might be more profound in time (not yet assessed). This correlated with the increase in *vegfaa* shown by *in situ* hybridisation in these double mutants. These findings were in support of the first hypothesis.

### 3.5.4 VEGF and vasculature permeability

Vascular endothelial growth factor (*vegf)* is also known as vascular permeability factor (*vpf*), and was originally identified as a tumour-secreted protein (Dvorak et al., 1995). Here it plays a role in increasing permeability and promoting extravasation of plasma proteins from the vessels (Dvorak et al., 1995). The increase in *vegf* expression along with the characterised vascular abnormalities (increased branching) in the *vhl-/-* embryos, led to further investigation of the vasculature in the *fih217/217;vhl-/-* embryos, based on the role of *vegf* in vascular permeability (Nagy et al., 2002). The zebrafish provides a model for observing alterations in vascular permeability, the embryos size and transparency makes imaging of fluid dynamics both within and without the vessels possible in real time (Arbiser, 2012). This has been shown in the *vhl-/-* embryos at 6-7dpf where dye was observed outside of the enclosing retinal vessel in the *vhl-/-* embryos and not in the wild type siblings several days post injection (van Rooijen et al., 2010).

Several distinct factors have been shown to regulate endothelial differentiation, growth and function. Multiple roles of VEGF have been described, in physiological angiogenesis, postnatal vessel remodeling and in tumour angiogenesis (Dvorak et al., 1995). It has been shown to increase microvascular permeability through enhancing functional activity of so called vesicular-vacuolar organelles (VVOs) involved in extravasation of circulating macromolecules from microvasculature (Dvorak et al., 1995). Increased *vegf-a* expression is reported to lead to an increase in vascular permeability (Nagy et al., 2012, Weis and Cheresh, 2005, Keck et al., 1989) and a development of a weakened vascular network with immature vessels that remain that way (Lu et al., 2011, Koukourakis et al., 2004). If these factors lead to the maintenance of a weaker/more immature vascular network in the *fih217/217;vhl-/-* embryos it is conceivable to that this could be a reason for this not being a viable assay in these mutants, however the levels of *vegf* expression in these *fih217/217;vhl-/-* embryos at early stages does suggest that the vascular integrity is compromised and would illustrate vascular permeability if the embryos matured past 4.5dpf. In order to clarify these details, the investigation of larger dyes and smaller time frames between injection and imaging could be utilised. Also the investigation of other factors known to affect vascular permeability in the zebrafish, such as VE-Cadherin (*cdh5),* which when knocked-down weakens cell-cell junctions, affecting vasculogenesis and sprouting of the vasculature could be attempted (Mitchell et al., 2010, Larson et al., 2004, Montero-Balaguer et al., 2009).

### 3.5.5 Conclusions

The observations using the *Tg(fli1;eGFP)* transgene to visualise the vasculature, in conjunction with the angiogram technique to reveal functional vessels, revealed that the loss of *fih* in a *vhl-/-* background did not in fact exacerbate all the observed phenotypes. Looping of the dorsal longitudinal vessel above the pigment line in the *vhl-/-* embryos showed instead a resolution to a more wild type phenotype in the *fih217/217;vhl-/-* embryos. In these embryos at the stages where this was observed (4-5dpf), a slowing of the blood flow was observed in the *fih217/217;vhl-/-* embryos and this reduction in shear stress could be hypothesised to be responsible for the resolution of this phenotype, following investigation by Dr. Watson. Further

investigation into the effects of flow on vascular patterning and remodeling are ongoing in the *vhl-/-* embryos.

Overall, these data support the hypothesis that the loss of *fih* does not result in a significant increase in hypoxic signaling, *vhl* being present to maintain HIF-α levels at normoxic levels. However, its loss in *vhl* mutants does have quantifiable effects on characterised phenotypes of these embryos, which indicate that these *vhl-/-* embryos don't exhibit full activation of hypoxic signaling in normoxia and that *fih* control is necessary for maintaining this homeostasis *in vivo.*

At this stage only structural characteristics had been tested, rather than the levels of hypoxic signaling in its entirety. One finding however was that while not generating phenotypes as distinct to wild type as seen when *vhl* is lost, the loss of *fih* was having an effect. The hypothesis and basis for further investigation was that the loss of *fih* was not significant enough to cause a phenotype, however it did sensitise embryos to the loss of *vhl* and therefore it does make a difference.

# 4 Transcriptome Analysis of Fih Function

## 4.1 Introduction

FIH is a hydroxylase with a wide variety of targets in addition to HIF, including Notch and NFκB (Cockman et al., 2009), with effects also in regulating metabolism as seen in the *Fih* knockout mouse study (Zhang et al., 2010). Although no morphological phenotype was noted, more subtle changes to the transcriptome may occur. In addition, not all defects need to have a morphological consequence and there may be sensory or genetic alterations that are not visible, their hearing or reflexes for example. As the *in vivo* function of the *fih* gene is not well characterised, it is well possible that the main function of *fih* lies outside the hypoxic signaling pathway. This is also consistent with the surprising phenotype of the mouse knockout. In order to characterise the effect of *fih* mutation further, a microarray experiment might provide novel candidate genes or pathways that are controlled by FIH. Furthermore by comparing changes to the transcriptome in *fih* mutants with changes in *vhl* mutants it might be possible to distinguish between those phenotypes caused by uncontrolled HIF signaling and those mechanisms that *fih* might control independently of HIF, e.g. Notch signaling.

Previous studies have been performed to assess the genes that could be designated as *vhl* targets, the majority of these were shown to be regulated by oxygen, but a number were not, indicating that at least some of the influences on gene expression were independent of HIF (Wykoff et al., 2000). To assess these possibilities *in vivo* along with assessing the possible influences of FIH in these mechanisms, a comparison of *vhl-/-* to *fih217/217;vhl-/-* embryos would allow us to confirm that *fih* acts by further enhancing the expression of HIF target genes.

For our purposes an Agilent two-colour microarray was performed, with each of the different mutants compared back to wild type and also *fih217/217;vhl-/-* compared to *vhl-/-* embryos. The microarray was performed at 3dpf, which is the time when the phenotypes of the *vhl-/-* and *fih217/217;vhl-/-* mutants begin to be strong enough to

sort the embryos from their siblings, but avoiding secondary changes due to, for example, reduced circulation in the *fih217/217;vhl-/-* embryos as much as possible.

## 4.2 Performing the microarray

The process of sample collection, preparation and labeling are described in the materials and methods section of this thesis along with the protocols used for the performance of the microarray, all performed in sequence. Embryos were collected in batches, multiple pairs were mated with embryos collected from each pair and grown until 3dpf, the time at which the distinguishing phenotypes of the *vhl* mutant and *fih;vhl* double mutant embryos could be identified by eye. This stage was also selected as it was believed to be prior to adaptations of the mutations or potential developmental delay causing significant alterations to the transcriptome. Since the collection of double mutants was rate limiting, multiple pairings, over multiple weeks had to be set up in order to collect sufficient embryos for each microarray sample. The embryos were sorted and then their identity confirmed by a second observer, individual embryos also being genotyped from each batch. The embryos were processed and labeled in batches in order to maintain consistency. The lengthy process of collection and optimisation produced a large amount of resulting microarray data, which was analysed using Genespring software.

## 4.3 Expression profiles revealed that *Fih* functions mainly through *Hif*

The Genespring software allows the data to be assessed in a number of different formats, which can be used to assess the fit of the data across the triplicates for each comparison to look for outliers (scatter plots), to look for clusters of genes where expression is being altered in one mutant group and not others (scatter plots and venn diagrams) or to compare the expression of individual genes across the different groups (heat maps).

Venn diagrams revealed the clusters of genes where expression was altered, to greater than log 2 fold compared to wild type, by the loss of *fih*, *vhl* or both genes (not shown). The venn diagrams suggested that the majority of those genes with altered expression

in the *fih217/217* embryos showed altered expression in the other two mutant groups and supported the indication that FIH function is largely through HIF activity. To assess this, along with other trends in the gene expression profiles, the microarray data sets were analysed in comparison with each other it was possible to look for correlations between the genes that were regulated in each mutant group **(Figure 52)**.

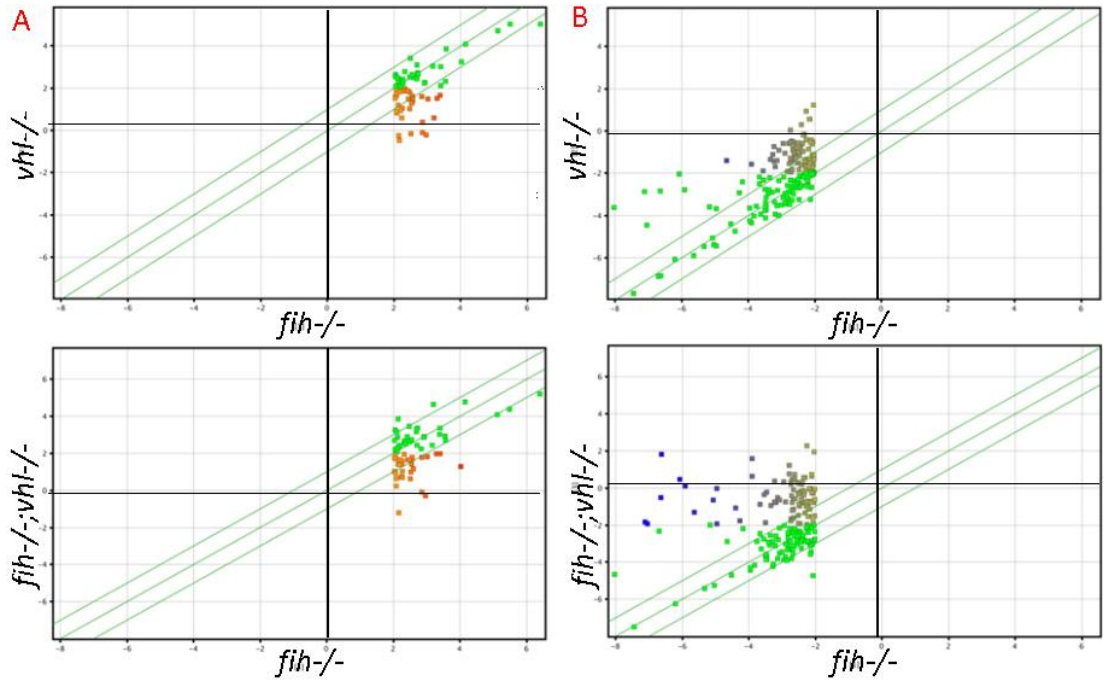


**Figure 52 Scatter plots were used to assess independent regulation of gene expression by *fih***

*Illustrates the correlations between both up and down regulated genes altered up or down by more than log 2 fold. The bold lines on each graph highlight the 0 fold change line. In each case the green highlighted genes indicate those that are log 2 fold up (or down) regulated in the both genotypes on each graph, the orange highlighted genes indicate those that were less than log 2 fold up regulated in either the vhl-/- or fih217/217;vhl-/- embryos, while the grey/blue highlighted genes are those less than 2 fold down regulated in either the vhl-/- or fih217/217;vhl-/- embryos. In each case, the majority of the genes highlighted are in green.* ***A)*** *Illustrates that almost all genes up-regulated significantly in fih mutants (>2 fold) are on or above the "no change" level in vhl mutants (above) and fih;vhl mutants (below)* ***B)*** *shows the equivalent effect for genes down-regulated in fih mutants.*

The scatter diagrams indicated that greater proportion of genes that were up (or down) regulated by log 2 fold in the *fih217/217* embryos were also up (or down)

regulated by the same degree, in either the *vhl-/-* or *fih217/217;vhl-/-* embryos, this indicated that FIH functions largely through HIF-α.

Individual entity lists could be generated from the scatter plots or venn diagrams, essentially highlighting individual clusters of genes and asking the software to isolate only the fold changes of those genes across the mutant groups.

## 4.4 Validation

### 4.4.1 Cluster/GO terms

Cluster analysis and the assessment of Gene Ontology (GO) terms within entity lists (formed using Genespring software during analysis of particular criteria from the datasets) would normally provide information connecting genes within a particular set in terms of their function or connected pathways. The Agilent Zebrafish version II microarray probe set, which was used for all of these microarrays, was not annotated with sufficient detail, making this type of analysis difficult (data not shown). Other tools are being developed for analysing GO terms in zebrafish microarray data sets, including GeneTools (eGOn v2.0) a web based ontology software, and Database for Annotation, Visualisation and Integrated Discovery (DAVID). A tool was also developed by Stockhammer et al to connect the better GO annotation of the human genome with data from zebrafish UniGene lists (Stockhammer et al., 2009). Tools such as these might be used to increase the GO analysis of this data-set.

### 4.4.2 Identifying Hits

Certain entity lists, such as those indicated to be selectively up or down-regulated in individual mutants or in particular segments of scatter diagrams (**Figure 52**), were used to identify particular hits for follow up. For example, two hits were identified as being selectively regulated in the *fih217/217* embryos by assessing the 63 genes identified by the venn diagram in **Figure 52** and the heat maps as being down-regulated specifically in these embryos, for further details of the follow up of these targets.

The need to annotate the microarray data sets for individual entity lists in order to make connections and identify potential hits required a level of selective identification

of hits. Websites such as www.iHOP-net.org (Information Hyperlinked Over Proteins) proved to be useful tools in searching for the genes coded by specific zgc numbers and this was used to annotate whole entity lists in the search for potential hits. However, this was laborious and while this work continued in the background certain pathways were targeted for wider investigation in the dataset based on hypotheses concerning the function of *fih* and the observed phenotypes in the embryos, such as vascular patterning, blood markers, and the notch pathway. For the identification of these targets the whole dataset was analysed in its entirety and individual components known to be involved in either the phenotype or pathway were searched for by hand. The fold changes observed for these individual components were then compiled into an excel spreadsheet for assessing the trends within the group of genes in each individual mutant group, see **Figure 53**.

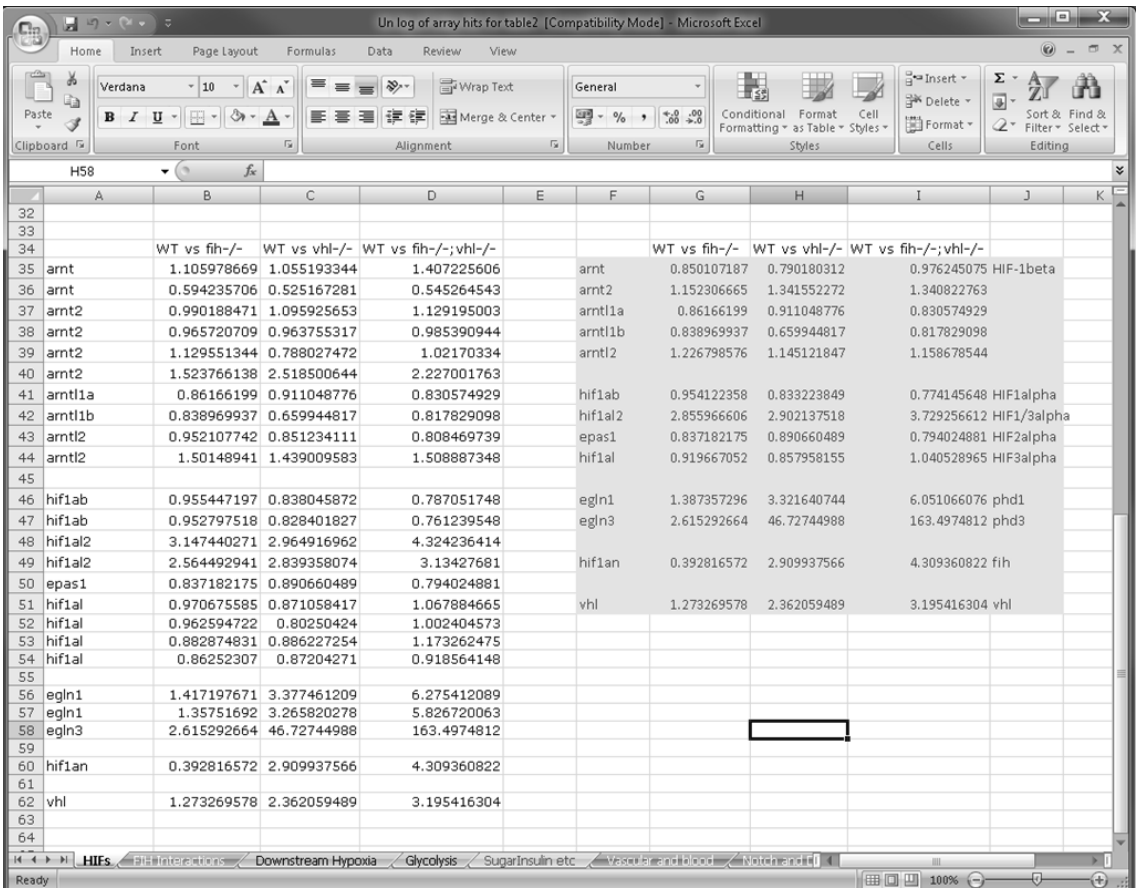


| | A | B | C | D | E | F | G | H | I | J |
|---|---|---|---|---|---|---|---|---|---|---|
| 34 | | WT vs fih-/- | WT vs vhl-/- | WT vs fih-/-;vhl-/- | | | WT vs fih-/- | WT vs vhl-/- | WT vs fih-/-;vhl-/- | |
| 35 | arnt | 1.105978669 | 1.055193344 | 1.407225606 | | arnt | 0.850107187 | 0.790180312 | 0.976245075 | HIF-1beta |
| 36 | arnt | 0.594235706 | 0.525167281 | 0.545264543 | | arnt2 | 1.152306665 | 1.341552272 | 1.340822763 | |
| 37 | arnt2 | 0.990188471 | 1.095925653 | 1.129195003 | | arntl1a | 0.86166199 | 0.911048776 | 0.830574929 | |
| 38 | arnt2 | 0.965720709 | 0.963755317 | 0.985390944 | | arntl1b | 0.838969937 | 0.659944817 | 0.817829098 | |
| 39 | arnt2 | 1.129551344 | 0.788027472 | 1.02170334 | | arntl2 | 1.226798576 | 1.145121847 | 1.158678544 | |
| 40 | arnt2 | 1.523766138 | 2.518500644 | 2.227001763 | | | | | | |
| 41 | arntl1a | 0.86166199 | 0.911048776 | 0.830574929 | | hif1ab | 0.954122358 | 0.833223849 | 0.774145648 | HIF1alpha |
| 42 | arntl1b | 0.838969937 | 0.659944817 | 0.817829098 | | hif1al2 | 2.855966606 | 2.902137518 | 3.729256612 | HIF1/3alpha |
| 43 | arntl2 | 0.952107742 | 0.851234111 | 0.808469739 | | epas1 | 0.837182175 | 0.890660489 | 0.794024881 | HIF2alpha |
| 44 | arntl2 | 1.50148941 | 1.439009583 | 1.508887348 | | hif1al | 0.919667052 | 0.857958155 | 1.040528965 | HIF3alpha |
| 45 | | | | | | | | | | |
| 46 | hif1ab | 0.955447197 | 0.838045872 | 0.787051748 | | egln1 | 1.387357296 | 3.321640744 | 6.051066076 | phd1 |
| 47 | hif1ab | 0.952797518 | 0.828401827 | 0.761239548 | | egln3 | 2.615292664 | 46.72744988 | 163.4974812 | phd3 |
| 48 | hif1al2 | 3.147440271 | 2.964916962 | 4.324236414 | | | | | | |
| 49 | hif1al2 | 2.564492941 | 2.839358074 | 3.13427681 | | hif1an | 0.392816572 | 2.909937566 | 4.309360822 | fih |
| 50 | epas1 | 0.837182175 | 0.890660489 | 0.794024881 | | | | | | |
| 51 | hif1al | 0.970675585 | 0.871058417 | 1.067884665 | | vhl | 1.273269578 | 2.362059489 | 3.195416304 | vhl |
| 52 | hif1al | 0.962594722 | 0.80250424 | 1.002404573 | | | | | | |
| 53 | hif1al | 0.882874831 | 0.886227254 | 1.173262475 | | | | | | |
| 54 | hif1al | 0.86252307 | 0.87204271 | 0.918564148 | | | | | | |
| 55 | | | | | | | | | | |
| 56 | egln1 | 1.417197671 | 3.377461209 | 6.275412089 | | | | | | |
| 57 | egln1 | 1.35751692 | 3.265820278 | 5.826720063 | | | | | | |
| 58 | egln3 | 2.615292664 | 46.72744988 | 163.4974812 | | | | | | |
| 59 | | | | | | | | | | |
| 60 | hif1an | 0.392816572 | 2.909937566 | 4.309360822 | | | | | | |
| 61 | | | | | | | | | | |
| 62 | vhl | 1.273269578 | 2.362059489 | 3.195416304 | | | | | | |
| 63 | | | | | | | | | | |
| 64 | | | | | | | | | | |

**Figure 53 One method of data collation was to cherry pick through the data and collect individual fold change numbers into a new Excel spreadsheet**

*Screen shot of excel sheet used to collate individual components of individual pathways and genes thought to contribute to individual phenotypes.*

The expression levels of these families of genes were then displayed in graphs in order to observe patterns and changes within the family of genes or between the different mutant groups, see data through the rest of this chapter.

| Group | Gene | Microarray Derived Fold Change | | | qRT-PCR | *in situ* hybridisation |
|---|---|---|---|---|---|---|
| | | WT vs Fih217/217 | WT vs Vhl-/- | WT vs Fih217/217;Vhl-/- | | |
| RAAS | Angiotensinogen (Agt) | 0.22 | 1.50 | 0.98 | | |
| | Angiotensin converting enzyme 1 (Ace1) | 0.88 | 0.94 | 0.87 | | |
| | Angiotensin converting enzyme 2 (Ace2) | 0.24 | 0.72 | 0.93 | | |
| | Renin | 1.38 | 1.02 | 1.27 | | |
| | Cyp11b2 (Aldosterone) | 0.39 | 0.40 | 0.67 | | |
| | Angiotensin II receptor Type 1 (Agt1ar) | 0.69 | 1.04 | 1.26 | | |
| | Apelin (Apln) | 0.63 | 0.86 | 0.91 | | |
| | Apelin receptor a (Agtrl1a/Aplnra/Msr) | | | | | |
| | Apelin receptor b (Agtrl1b/Aplnrb) | 1.42 | 1.49 | 1.86 | | |
| Hypoxia Pathway | Hypoxia-inducible factor1 a like (Hif1 al) | 0.92 | 0.86 | 1.04 | | |
| | Hypoxia-inducible factor1 a like 2 (Hif1 al2) | 2.86 | 2.90 | 3.73 | | |
| | Hypoxia-inducible factor1 ab (Hif1 ab) | 0.95 | 0.83 | 0.77 | | |
| | Aryl hydrocarbon receptor nuclear translocator (Hif1 b) | 1.11 | 1.06 | 1.41 | | |
| | Aryl hydrocarbon receptor nuclear translocators 2 (Hif1b2) | 1.29 | 1.46 | 1.47 | | |
| | Hif1an (Factor inhibiting hif (Fih)) | 0.39 | 2.91 | 4.31 | | |
| | Von Hippel lindau (Vhl) | 1.27 | 2.36 | 3.20 | | |
| | Prolyl hydroxylase domain containing protein 1 (Phd1) | 1.39 | 3.32 | 6.05 | | |
| | Prolyl hydroxylase domain containing protein 3 (Phd3) | 2.62 | 46.73 | 163.50 | | |
| Vegf Ligands | Vascular endothelial growth factor aa (Vegfaa) | 1.03 | 2.31 | 4.45 | | |
| | Vascular endothelial growth factor ab (Vegfab) | 1.10 | 2.63 | 9.83 | | |
| | Vascular endothelial growth factor c (Vegfc) | 0.95 | 1.01 | 1.16 | | |
| | c-fos induced growth factor (Vegfd) | 0.99 | 1.00 | 1.13 | | |
| Vegf Receptors | Vascular endothelial growth factor Receptor 1 (Flt1) | 0.84 | 2.12 | 2.21 | | |
| | Vascular endothelial growth factor Receptor 2 (Kdr/Flk1) | 1.40 | 1.90 | 2.78 | | |
| | Vascular endothelial growth factor Receptor 3 (Flt4) | 1.11 | 1.31 | 1.32 | | |
| Vascular Markers | EphrinB2a | 1.15 | 1.15 | 1.41 | | |
| | Friend Leukemia Integration 1 Transcription Factor 1a (Fli1a) | 0.97 | 1.00 | 1.09 | | |
| | Friend Leukemia Integration 1 Transcription Factor 1b (Fli1b) | 1.06 | 1.24 | 1.47 | | |
| Pancreatic Metabolism | Amylase 2a (Amy2a) | 0.17 | 0.53 | 0.82 | | |
| | Chymotrypsinogen | 0.26 | 0.65 | 0.94 | | |
| Glycolysis Enzymes | Hexokinase 1 (Hex) | 1.20 | 1.99 | 2.90 | | |
| | Phosphoglucose isomerase (Gpib) | 1.04 | 1.37 | 1.27 | | |
| | Phosphofructokinase, muscle b (Pfkm-b) | 1.08 | 2.39 | 4.01 | | |
| | Triosephosphate isomerase 1a (Tpi1a) | 1.25 | 1.21 | 0.99 | | |

| | | | | | | |
|---|---|---|---|---|---|---|
| | Triosephosphate isomerase 1b (Tpi1b) | 0.97 | 1.72 | 1.90 | | |
| | Phosphoglycerate kinase 1 (Pgk1) | 0.93 | 1.72 | 2.06 | | |
| | Phosphoglycerate mutase 1a (Pgam1a) | 1.00 | 3.81 | 5.54 | | |
| | Phosphoglycerate mutase 1b (Pgam1b) | 0.64 | 0.67 | 0.49 | | |
| | Enolase1 (Eno1) | 0.92 | 2.00 | 3.98 | | |
| | Pyruvate kinase, muscle a (Pkm2a) | 0.83 | 1.60 | 2.25 | | |
| | Pyruvate kinase, muscle b (Pkm2b) | 1.08 | 1.13 | 1.08 | | |
| | Lactate Dehydrogenase (Ldha/LdhA4) | 0.98 | 2.25 | 3.49 | | |
| Gluconeogenesis | Preproinsulin | 0.78 | 1.08 | 1.63 | | |
| | Insulin growth factor binding protein 1a | 0.96 | 2.96 | 11.53 | | |
| | Phosphoenolpyruvate carboxykinase (Pepck) | 1.22 | 3.00 | 11.17 | | |
| Glucose and fatty acid Regulation | Glucose transporter 1 (Glut1) | 0.88 | 1.15 | 1.03 | | |
| | Peroxisome proliferators-activated receptor γ (PPARγ) | 1.01 | 1.30 | 1.51 | | |
| | PPARγ-coactivator 1α (PGC1α) | 0.84 | 0.77 | 0.76 | | |
| | Uncoupling protein 1 | 0.94 | 0.76 | 0.72 | | |
| | Uncoupling protein 4 | 0.85 | 1.68 | 1.94 | | |
| | Uncoupling protein 5 | 1.21 | 1.05 | 0.78 | | |
| | Adiponectin-like (Adipoql) | 0.75 | 0.71 | 0.55 | | |
| | Adiponectin like 2 (adipol2) | 0.83 | 0.75 | 0.53 | | |
| | Adiponectin receptor 1a (adipor1a) | 0.92 | 0.92 | 0.81 | | |
| | Adiponectin receptor 1b (adipor1b) | 0.87 | 0.86 | 0.77 | | |
| | Adiponectin receptor 2 (adipor2) | 0.69 | 0.67 | 0.75 | | |
| | Fatty acid binding protein 1a (Fabp1a) | 7.48 | 4.78 | 7.38 | | |
| Blood Markers | Erythropoietin (Epo) | 1.38 | 3.37 | 14.24 | | |
| | Erythropoietin Receptor (EpoR) | 0.89 | 1.12 | 1.51 | | |
| | GATA transcription factor 1 (GATA1) | 1.58 | 2.06 | 2.68 | | |
| | Delta-aminolevulinate synthase 2 (Alas2) | 3.32 | 7.52 | 11.59 | | |
| | Hemopexin (Hpx) | 3.36 | 4.39 | 12.99 | | |
| Coagulation Cascade | Factor I - Fibrinogen alpha chain (Fga) | 1.02 | 1.11 | 1.29 | | |
| | Factor I - (Fibrinogen beta (Fgb) | 1.10 | 1.16 | 1.28 | | |
| | Factor I - Fibrinogen gamma (Fgg) | 1.31 | 1.35 | 1.41 | | |
| | Factor II - Thrombin (FII) | 1.15 | 1.33 | 1.30 | | |
| | Factor X (F10) | 2.26 | 2.24 | 2.29 | | |
| | von Willebrand factor 5B1 | 1.28 | 2.05 | 2.39 | | |
| | von Willebrand factor 5B2 | 1.29 | 1.20 | 0.79 | | |
| | Kininogen (Kng1) | 1.17 | 1.59 | 1.71 | | |

| | | | | | | |
|---|---|---|---|---|---|---|
| | Fibronectin 1a (Fn1) | 0.98 | 1.00 | 1.06 | | |
| | Fibronectin 1b (Fn1b) | 0.74 | 1.03 | 1.24 | | |
| | Heparin cofactor 1 (serpind1) | 1.01 | 1.22 | 1.30 | | |
| | Plasminogen (plg) | 1.35 | 1.47 | 1.74 | | |
| | Plasminogen activator inhibitor 1 (PAI1/serpine1) | 1.33 | 1.11 | 1.20 | | |
| | Plasminogen activator inhibitor 2 (serpine2) | 1.15 | 2.12 | 2.94 | | |
| Notch Pathway | Notch1a | 1.40 | 1.29 | 1.76 | | |
| | Notch1b | 0.49 | 0.45 | 0.58 | | |
| | Notch2 | 0.90 | 0.92 | 0.89 | | |
| | Notch3 (Notch5) | 0.77 | 0.90 | 1.26 | | |
| | Jagged1b (Jag1) | 1.06 | 0.93 | 0.97 | | |
| | Jagged2 (Jag2) | 1.75 | 1.51 | 1.85 | | |
| | Delta A | 1.33 | 1.27 | 1.45 | | |
| | Delta B | 0.98 | 0.83 | 0.96 | | |
| | Delta C | 0.95 | 1.07 | 1.35 | | |
| | Delta D | 1.12 | 1.26 | 1.61 | | |
| | Delta-like ligand 4 (Dll4) | 0.95 | 1.19 | 2.90 | | |
| Notch Targets | Hairy related protein-Epidermal growth factor receptor (Her1) | 1.40 | 1.18 | 1.44 | | |
| | Hairy related protein (Her8a) | 1.31 | 1.68 | 2.41 | | |
| | Hairy related protein (Her12) | 0.08 | 0.06 | 0.07 | | |
| | Hairy/enhancer-of-split related with YRPW motif (Hey2) | 1.45 | 1.61 | 1.55 | | |
| Notch Inhibition | Notch-regulated ankyrin repeat-containing protein (Nrarpa) | 1.22 | 1.34 | 1.84 | | |
| | Notch-regulated ankyrin repeat-containing protein (Nrarpb) | 1.10 | 1.18 | 1.23 | | |
| Vessel Chemokine | C-X-C chemokine receptor type 4a (Cxcr4a) | 1.01 | 1.47 | 5.26 | | |
| Apoptosis | Induced myeloid leukemia cell differentiation protein (Mcl1b) | 1.56 | 3.04 | 5.70 | | |
| | BCL2/adenovirus E1B 19 kDa protein-interacting protein 3-like (Bnip3l) | 1.06 | 2.30 | 3.76 | | |
| | Caspase C | 0.73 | 1.43 | 2.35 | | |
| Hypoxic Target | Troponin T1 (Tnnt1) | 2.38 | 2.07 | 5.87 | | |
| | Nitric oxide synthase 2a (Nos2a) | 1.27 | 1.34 | 2.15 | | |
| | Parathyroid hormone 1a (Pth1a) | 2.99 | 4.70 | 5.10 | | |

**Table 15** *Key genes of interest selected as hits from the larger microarray data set. Those indicated in green are the genes that were used for qRT-PCR validation of the microarray data set. Patterns of altered gene expression from each mutant in the microarray data set were confirmed by qRT-PCR and also in situ hybridisation. Data for PEPCK only from qRT-PCR as this was not annotated in the array*

### 4.4.3 qRT-PCR Validation

Once selected genes had been identified for validation qRT-PCR primers were designed to each one in turn, according to criteria dictated in the materials and methods chapter of this thesis. Once each primer pair was optimised biological triplicate samples for each mutant (initially from cDNA generated from the RNA used for the microarray), with technical triplicates of each sample were then run, in order to calculate the ΔΔct for each gene of interest compared to β-actin, which was used as a reference gene throughout. For information on the method development and validation of qRT-PCR, see Materials and Methods chapter.

As independent correlation of the microarray and qRT-PCR data the fold changes derived from 10 genes were plotted on one graph, see **Figure 54**.

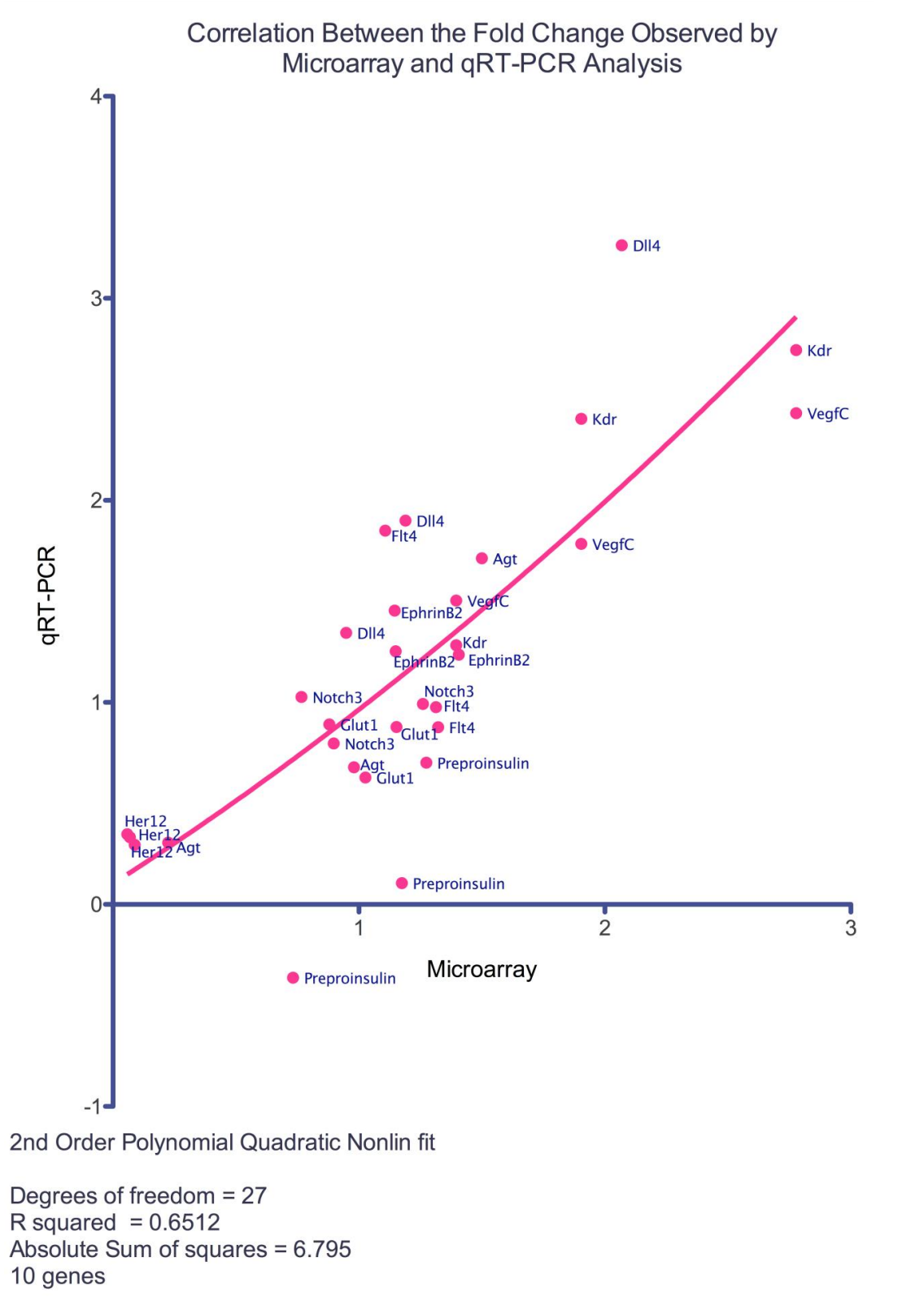


**Figure 54 Correlation between microarray and qRT-PCR data was used to interpret the validity of the microarray data.**

*Using 10 genes as examples the fold change derived from the microarray was plotted against the fold change derived from qRT-PCR and a linear regression analysis was performed in order to assess the correlation between the two assays, specific to each of the three mutants.*

The correlation between the fold change derived from the microarray and that derived from the qRT-PCR shows that the microarray data-set is independently validated. This confidence has been used to further interpret the microarray derived fold changes of certain genes that have not been independently validated by qRT-PCR throughout the rest of this study.

| Group | Gene | qRT-PCR Derived Fold Change | | |
|---|---|---|---|---|
| | | WT vs Fih217/217 | WT vs Vhl-/- | WT vs Fih217/217;Vhl-/- |
| RAAS | Angiotensinogen (Agt) | 0.31 | 3.15 | 0.68 |
| | Angiotensin converting enzyme 1 (Ace1) | 0.81 | 0.90 | 0.78 |
| | Angiotensin converting enzyme 2 (Ace2) | 0.33 | 1.07 | 0.50 |
| | Renin | 1.92 | 3.09 | 3.20 |
| | Cyp11b2 (Aldosterone) | 0.39 | 0.40 | 0.67 |
| | Prolyl hydroxylase domain containing protein 3 (Phd3) | 2.24 | 232.7 | 251.7 |
| Vegf Ligands | Vascular endothelial growth factor aa (Vegfaa) | 1.56 | 7.08 | 6.61 |
| | Vascular endothelial growth factor c (Vegfc) | 1.50 | 1.79 | 2.43 |
| | Vascular endothelial growth factor Receptor 2 (Kdr/Flk1) | 1.69 | 2.86 | 3.11 |
| | Vascular endothelial growth factor Receptor 3 (Flt4) | 1.85 | 0.98 | 0.88 |
| Vascular Markers | EphrinB2a | 1.25 | 1.54 | 1.17 |
| Pancreatic Metabolism | Amylase 2a (Amy2a) | 1.32 | 10.32 | 4.70 |
| | Chymotrypsinogen | 0.35 | 1.82 | 1.04 |
| Glycolysis Enzymes | Hexokinase 1 (Hex) | 1.43 | 2.04 | 1.97 |
| Gluconeogenesis | Preproinsulin | 0.73 | 1.18 | 1.27 |
| | Phosphoenolpyruvate carboxykinase (Pepck) | 1.22 | 3.00 | 11.17 |
| Glucose and fatty acid Regulation | Glucose transporter 1 (Glut1) | 0.94 | 1.02 | 0.64 |
| Blood Marker | Delta-aminolevulinate synthase 2 (Alas2) | 2.86 | 8.15 | 9.48 |
| Notch Pathway | Notch3 (Notch5) | 0.98 | 1.32 | 1.00 |
| | Delta-like ligand 4 (Dll4) | 1.47 | 2.31 | 2.73 |
| Notch Target | Hairy related protein (Her12) | 0.29 | 0.35 | 0.33 |
| Notch Inhibition | Notch-regulated ankyrin repeat-containing protein (Nrarpa) | 1.35 | 1.48 | 1.36 |
| Vessel Chemokine | C-X-C chemokine receptor type 4a (Cxcr4a) | 1.25 | 2.42 | 3.47 |

**Table 16** *Compiled list of qRT-PCR data*

## 4.5 Hypoxic Signaling

### 4.5.1 Loss of *fih* does not affect *hifα* or *hifβ* expression levels

To assess alterations in the HIF pathway caused by the loss of *fih* and/or *vhl*, microarray data was scanned for expression levels of various components of the pathway, see **Table 15.**

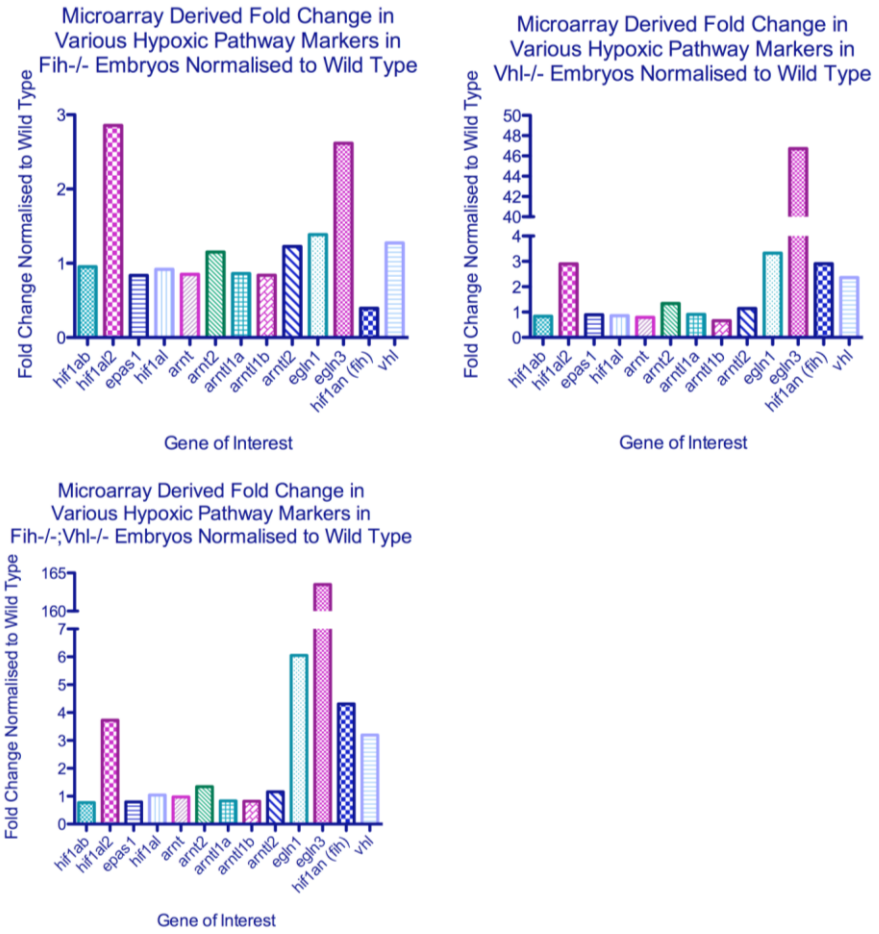


**Figure 55 Fold change in hypoxic pathway genes**

*The top left graph indicates the expression of the hypoxic pathway component genes in the fih217/217 embryos, the top right graph indicates the same for the vhl-/- embryos and the bottom left graph indicates the same for the fih217/217;vhl-/- embryos.* ***Abbreviations:-*** *Using ensembl genome browser to match the zebrafish genes annotated in the microarray with the human homologues, (in brackets): - hif-1αb (HIF-1α), hif-1aL2 (HIF-2αa/HIF-2αb), epas-1 (HIF-2αa/HIF-2αb), hif-1aL (HIF-3α), arnt (HIF-β), egln1 (PHD1), egln3 (PHD3), hif1an (FIH), vhl (VHL). The probe sequence for epas-1 was missing from current list and checking exact homologue is ongoing.*

The lack of significant alterations in gene expression of the HIF genes in response to the loss of *fih* and/or *vhl* is not necessarily probative given that HIF protein is mainly regulated by protein degradation. The fold changes observed indicated that *hif-α-like* and *hif-αb* genes, along with the two *hif-1β/arnt* genes, are not being differentially regulated in any of the three mutants, whereas *hif-1α-like2,* is up-regulated in all three mutants. This suggested that this isoform is individually affected by the loss of *fih* and *vhl* and then expression was increased further by the combined loss of both *fih* and *vhl*. This isoform has been described as a possible ortholog to both human *HIF-1α* and *HIF-3α* on Ensembl. Expression trends in *fih* (*hif1an*) show down-regulation in the *fih217/217* embryos, then up-regulation in the *vhl-/-* embryos. The up-regulation of *fih* in *fih217/217;vhl-/-* embryos indicates nonsense mediated decay.

#### 4.5.2 Loss of *fih* increases expression of HIF target genes compared to *vhl-/-* embryos

The trends in gene expression for *vhl* and *phd3* genes demonstrate a pattern that was seen in several of the targets that were assessed:- a slight alteration in expression in the *fih217/217* embryos, an increased level of altered expression in the *vhl-/-* embryos and a further increase in altered expression in the *fih217/217;vhl-/-* embryos, and these could be alterations either up or down compared with wild-type. Over-expression of HIF targets has been shown in response to increasing expression of HIF, along with functional inactivation of VHL gene (Wiesener et al., 2001). This further trend in increased expression in *fih217/217;vhl-/-* embryos follows the hypothesis, already described that both FIH and VHL regulate HIF-*α* function.

In **Figure 55**, using expression of *phd3* as an example, as it has been shown to be a sensitive readout of HIF function, it was possible to see that expression is up-regulated by a factor of 2 in *fih217/217* embryos versus up-regulated by a factor of 200 in *vhl-/-* embryos indicating that FIH is responsible for 1% HIF function, although this remains an assumption pending further testing.

qRT-PCR validation of the microarray was performed using cDNA from the three biological replicate samples that were used in the microarray. These findings were then confirmed with an independent sample of each of the mutant embryos at the same stage, in order to be sure that the qRT-PCR faithfully validated the microarray

findings; and that the findings were not specific to those three samples but were consistent with the mutants, see **Figure 56**.

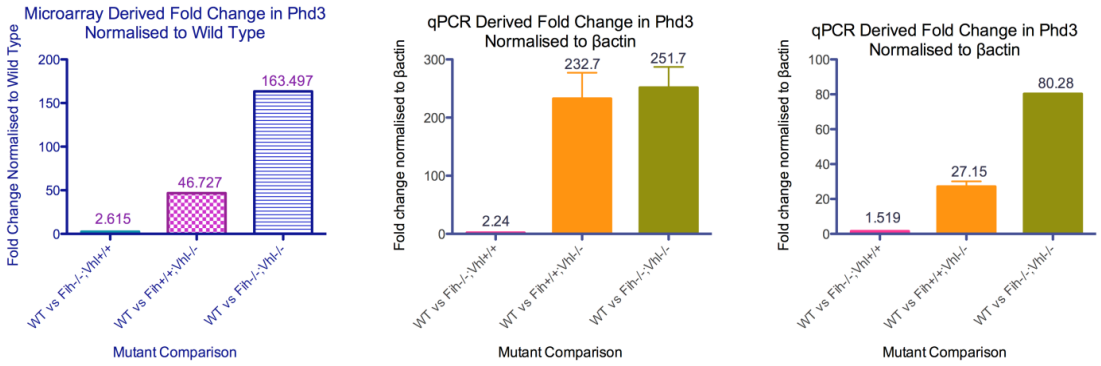


**Figure 56 Fold change in *phd3* used for microarray validation**

***Left)*** *The fold change derived from the microarray.* ***Centre)*** *The fold change derived from qRT-PCR using cDNA from samples that were used in the microarray.* ***Right)*** *The fold change in phd3 derived from independent biological samples of each of the mutants.*

The trend changes in expression correlate throughout the three graphs in **Figure 56**, which indicated that the findings were indeed consistent for the mutants and not simply the three samples that had been used to perform the microarray.

## 4.6 Blood

### 4.6.1 Loss of *fih* enhances expression of genes involved in blood-cell development

Where *fih* is lost in conjunction with *vhl*, as in the *fih217/217;vhl-/-* embryos, pooling of blood in the ventral tail region and a cessation of circulation at between 4.5 and 5dpf can be seen, the latter can be as observed in image deletion angiograms, see **Figure 57**.

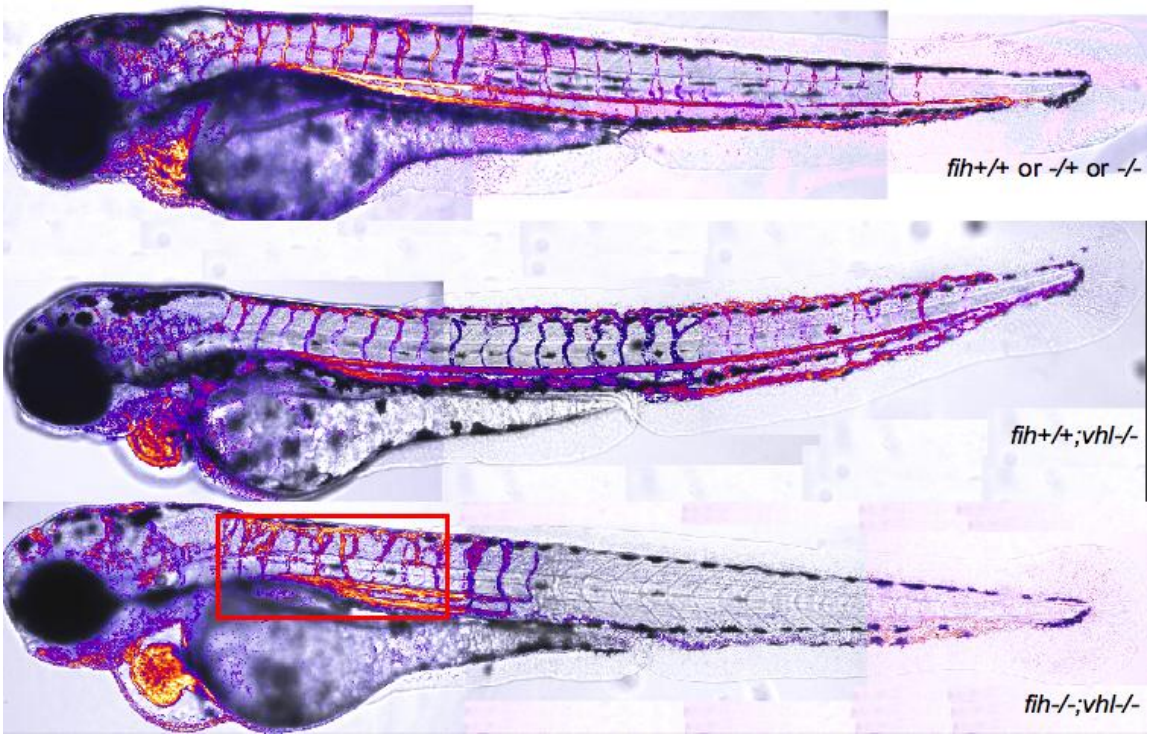


**Figure 57 Image deletion angiograms of embryos at 5dpf**

*Illustrate the continued circulation in WT, and vhl-/- embryos throughout the embryo (the top embryo is representative of the phenotype observed in wild type, as well as fih -/+ and -/- embryos). The lack of visible circulation in the posterior trunk and tail of the fih217/217;vhl-/- embryos at this stage was present in all embryos observed at this stage. N=3.*

These observations could be the result of enhanced polycythemia in these embryos (a phenotype that is known to be present in the *vhl-/-* embryos), enhanced coagulation, or the result of altered vascular function. The loss of *fih* as well as *vhl* in these embryos has the effect of releasing *Hif* from all normoxic inhibitory regulation. In order to further investigate this, the expression levels of various genes involved in blood-cell development were assessed in these embryos using the microarray data-set.

The expression of *epo* mRNA was assessed by *in situ* hybridisation in order to validate the microarray findings, see **Table 13** and **Figure 58**.

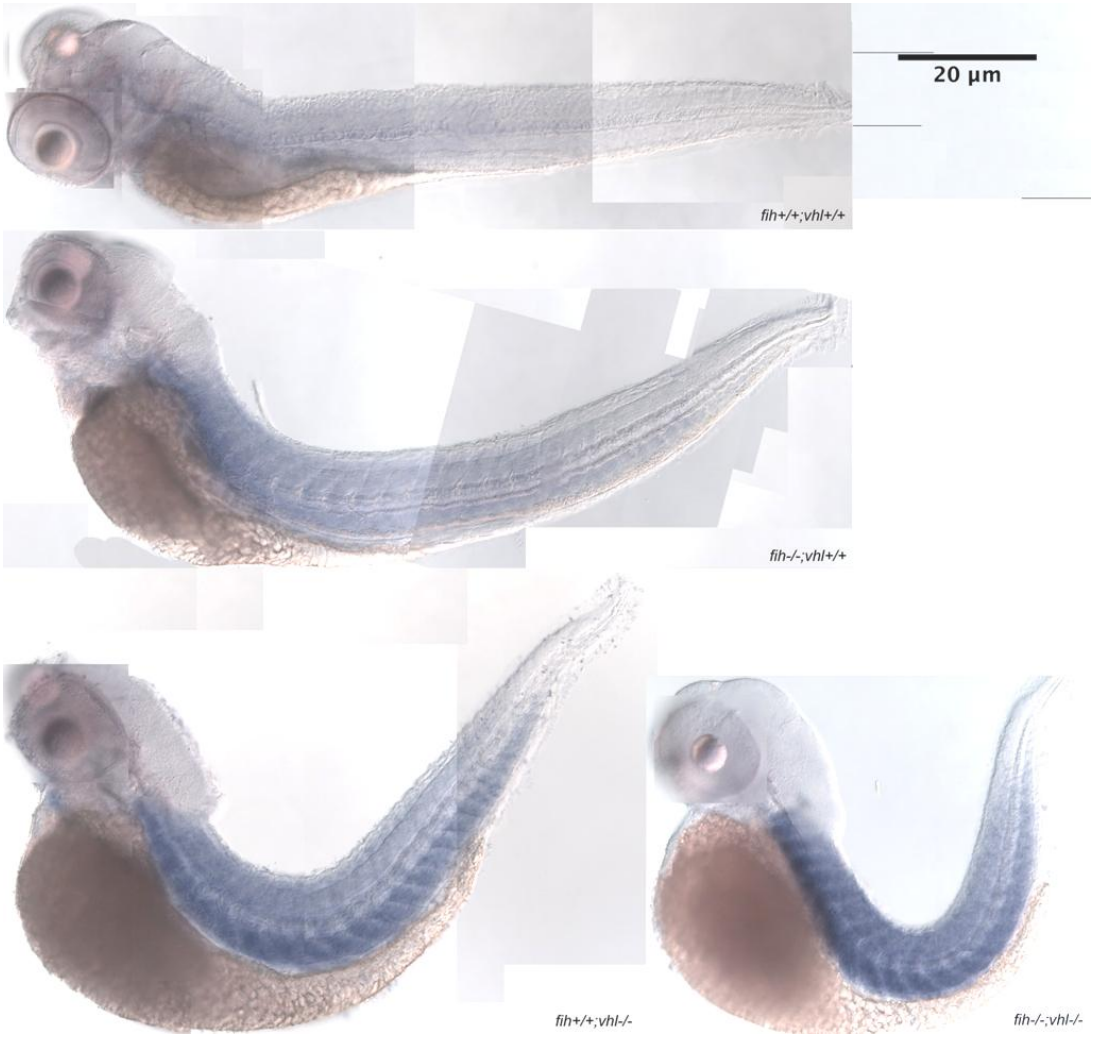


**Figure 58 Illustrates *in situ* hybridisation of *epo* at 4dpf**

*mRNA expression of epo was assessed by in situ hybridisation in 4dpf zebrafish embryos. These images are composite images taken on multiple focal planes.*

The expression of *epo* appeared elevated in the *fih217/217* embryos compared to the wild type sibling, further elevated in the *vhl-/-* embryos and further elevated again in the *fih217/217;vhl-/-* embryos. This was quantified using the microarray data-set, along with several other key regulators of erythropoiesis and heme scavenging; see **Table 15** and **Table 16**. These genes are involved in various processes from erythropoiesis (*epo*) and erythroid development/differentiation (*gata1*), to heme biosynthesis (*alas2*) and the binding of free heme (*hpx*).

Literature surrounding expression of erythrocyte density and genes involved in this, Alas2, hexokinase and others, see **Table 13,** lead the investigation to an attempt to

assess the erythrocyte density and other parameters of the blood cells, through high speed imaging techniques, see **Figure 59.**

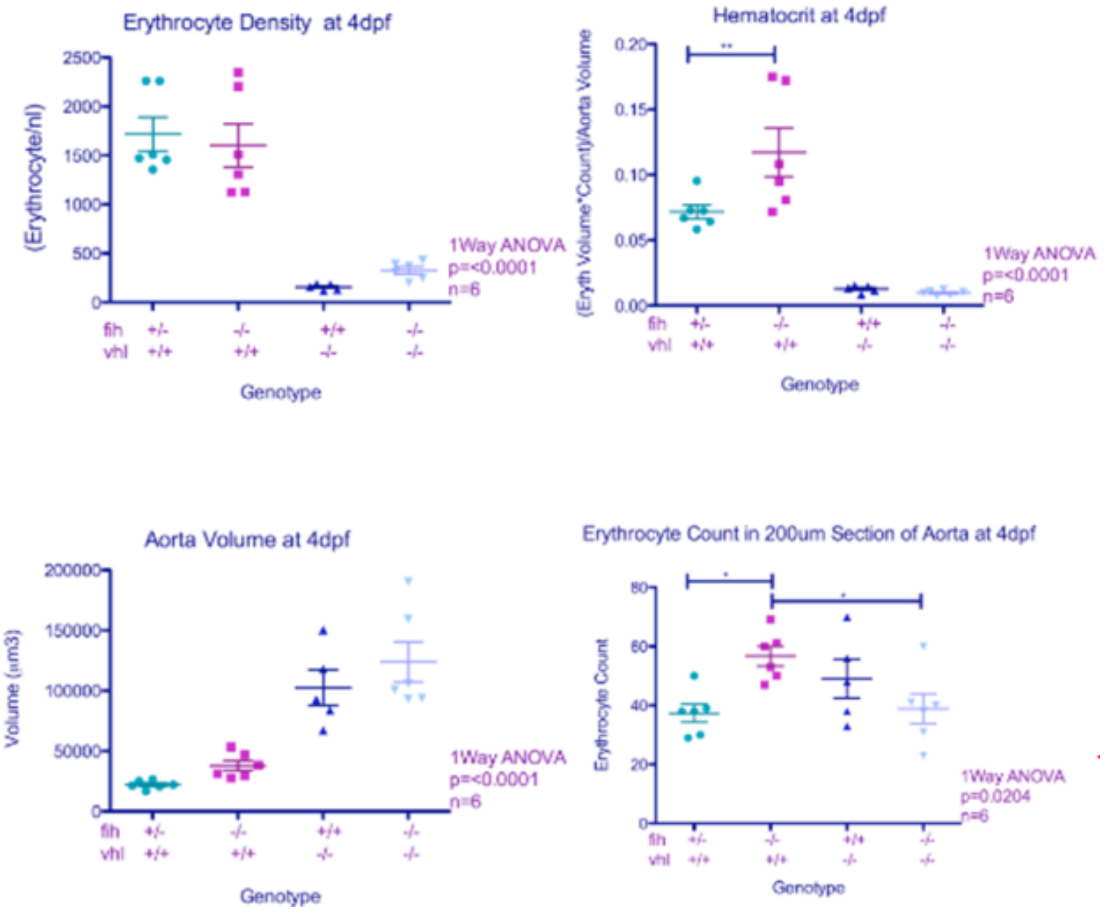


**Figure 59 Quantification of erythrocyte density, erythrocyte count and erythrocyte volume**

*Using high speed imaging and ImageJ software (protocol in Materials and Methods). Hemoatocrit is the volume percentage of red blood cells in a given volume of blood.*

The data revealed that while a slightly elevated erythroid count, aortic diameter, and hemoatocrit, could be observed in the *fih217/217* embryos compared with wild type, the same could not be said of either the *vhl-/-* embryos or the *fih217/217;vhl-/-* embryos. The erythropoetic markers that were assessed do however demonstrate that the loss of *fih* in *vhl-/-* embryos leads to an increase in erythrocyte markers and an inferred increase in erythrocyte numbers in these double mutants compared with *vhl-/-* embryos.

## 4.7 Vascular Branching

Several features of the vasculature of the *fih217/217, vhl-/-* and *fih217/217;vhl-/-* embryos were characterised in **Chapter 3**, and searches through the microarray data for indications of mechanisms for some of these were possible, including the assessment of genes known to be involved in tip-cell migration and differentiation.

### 4.7.1 Tip cell guidance by *cxcr4a*

The extra branching of the blood vessels in the *vhl-/-* embryos and the *fih217/217;vhl-/-* embryos led to the assessment of chemokines cxcr4 and sdf-1 in the microarray data set, **see Table 13 and Figure 60**.

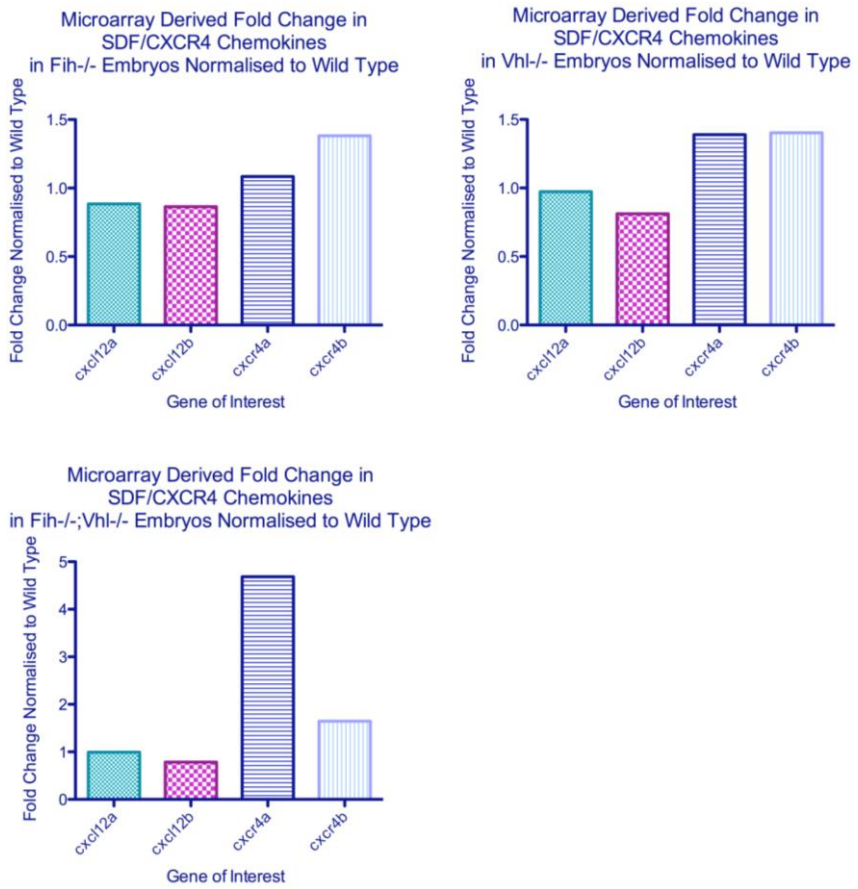


**Figure 60 Microarray derived fold change in chemokine expression**

*The top left graph indicates the expression of chemokines in the fih217/217 embryos, the top right graph indicates the same for the vhl-/- embryos and the bottom left graph indicates the same for the fih217/217;vhl-/- embryos. Abbreviations:- chemokine (C-X-C) motif ligand (cxcl12 or sdf-1), chemokine (C-X-C) motif receptor (cxcr4)*

The microarray data indicated that the expression levels of both isoforms of *sdf-1/cxcl12* was not altered in any of the three mutant groups, and that the second isoform of *cxcr4* was also not significantly altered by the loss of either Fih or Vhl, although it was elevated significantly in double mutants, this was further quantified by qRT-PCR techniques **(Figure 60)** and *in situ* hybridisation **(**Figure 61**)**.

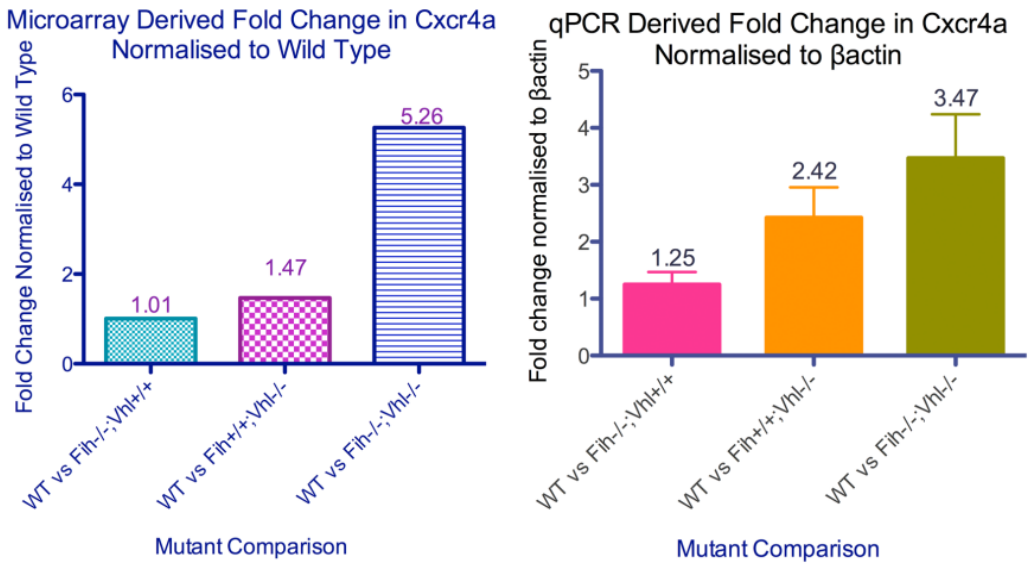


**Figure 61 Microarray and qPCR-validation of *cxcr4a* expression**

*Quantification of cxcr4a expression by microarray and qRT-PCR techniques at 3dpf. The expression pattern showed an increase in expression in the fih217/217 embryos and no change in expression in the vhl-/- embryos or the fih217/217;vhl-/- embryos, all compared to wild type.*

The expression of *cxcr4a* demonstrated the expression pattern that had been seen for other hypoxic targets, such as *phd3* and *vegf,* an *in situ* hybridisation was performed for *cxcr4a* in order to assess the locations as well as levels of expression within the embryos, see **Figure 62.**

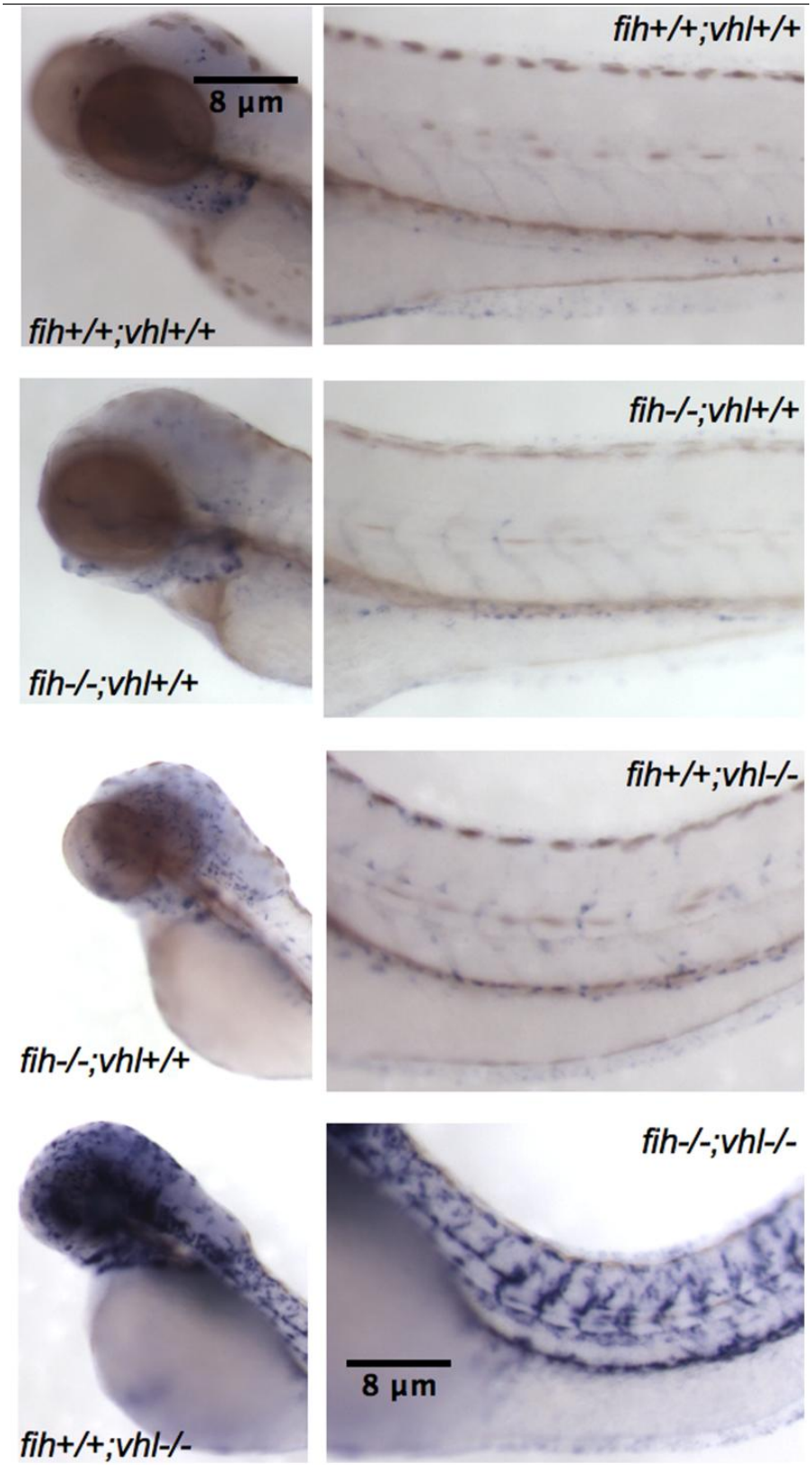


**Figure 62** ***in situ*** **hybridisation pattern of** ***cxcr4*** **expression**

*Cxcr4a expression patterns in the fih and vhl mutant embryos at 4dpf revealing increasing levels of expression in the fih only mutant embryos through to the fih217/217;vhl-/- double mutant embryos.*

The strikingly increased expression of *cxcr4a* in the *fih217/217;vhl-/-* embryos is in agreement with the increased level of branching in the vasculature observed in these embryos and a pattern of tip-cell enrichment.

### 4.7.2 Expression of Notch signaling components and downstream targets

As previously described, the Notch signaling pathway, in combination with vegf signaling, has been shown to be involved in both the distinction between tip and stalk cell fates, and also in vascular remodeling, see **Table 13**. Observations in the *vhl-/-* and *fih217/217;vhl-/-* embryos using both angiogram and *Tg(fli1;eGFP)* imaging revealed increased vascular branching over time in these embryos **(Chapter 3)**. Before assessing the expression of Notch target genes we assessed whether the loss of *fih* or *vhl* had significant effects on the genes of the pathway itself (data not shown), see **Table 13** for background. The majority of the genes that were annotated in the microarray were not differentially expressed in the *fih217/217* embryos, there were slight overall elevations in expression in the *vhl-/-* embryos and this was then further elevated in the *fih217/217;vhl-/-* embryos.

Expression of *deltaC* (*dllc*) has been shown throughout early development of the zebrafish embryo, see **Table 13**. On the basis that this might be a vascular specific ligand, the levels of *deltaC* were assessed by *in situ* hybridisation and in the microarray data set in the *fih217/217* and *vhl-/-* embryos, see **Figure 63.**

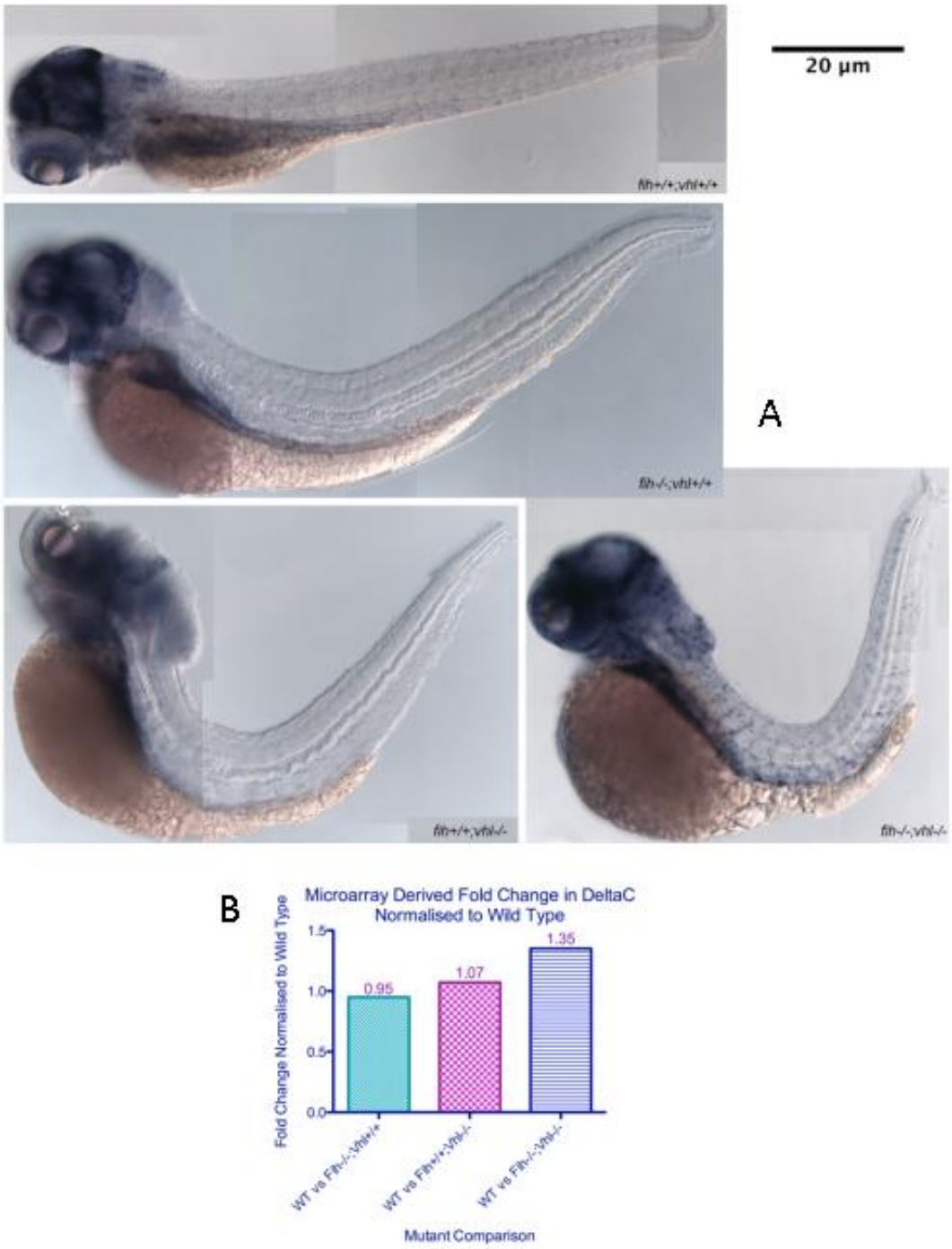


**Figure 63 Expression level of *deltaC* by *in situ* hybridisation and microarray**

**A)** *Expression of DeltaC, pattern by in situ (4dpf) and* ***B)*** *quantified by microarray (3dpf). These images are composite images taken on multiple focal planes.*

*DeltaC* expression in the different mutants showed that it was up-regulated in the *fih217/217;vhl-/-* embryos by *in situ* hybridisation, and quantified as such by microarray analysis. The *in situ* revealed its expression at 5dpf is concentrated around the head vasculature and the region of the pronephric ducts; in the wild type,

*fih217/217* only and *vhl-/-* only embryos. However in the *fih217/217;vhl-/-* embryos the expression is expanded throughout the embryos in a pattern consistent with ISVs and slightly stronger expression in the region of the pronephric ducts. Increased expression of *deltaC* was observed in the *in situ* hybridisation, however the changes, as quantified by the microarray data, were not large. These findings indicated the need for further investigation of other Notch ligands and receptors, which were assessed by microarray and qRT-PCR.

Alterations in *notch3* expression have also been shown to be involved in vascular tone and blood flow, see **Table 13 and Figure 64.**

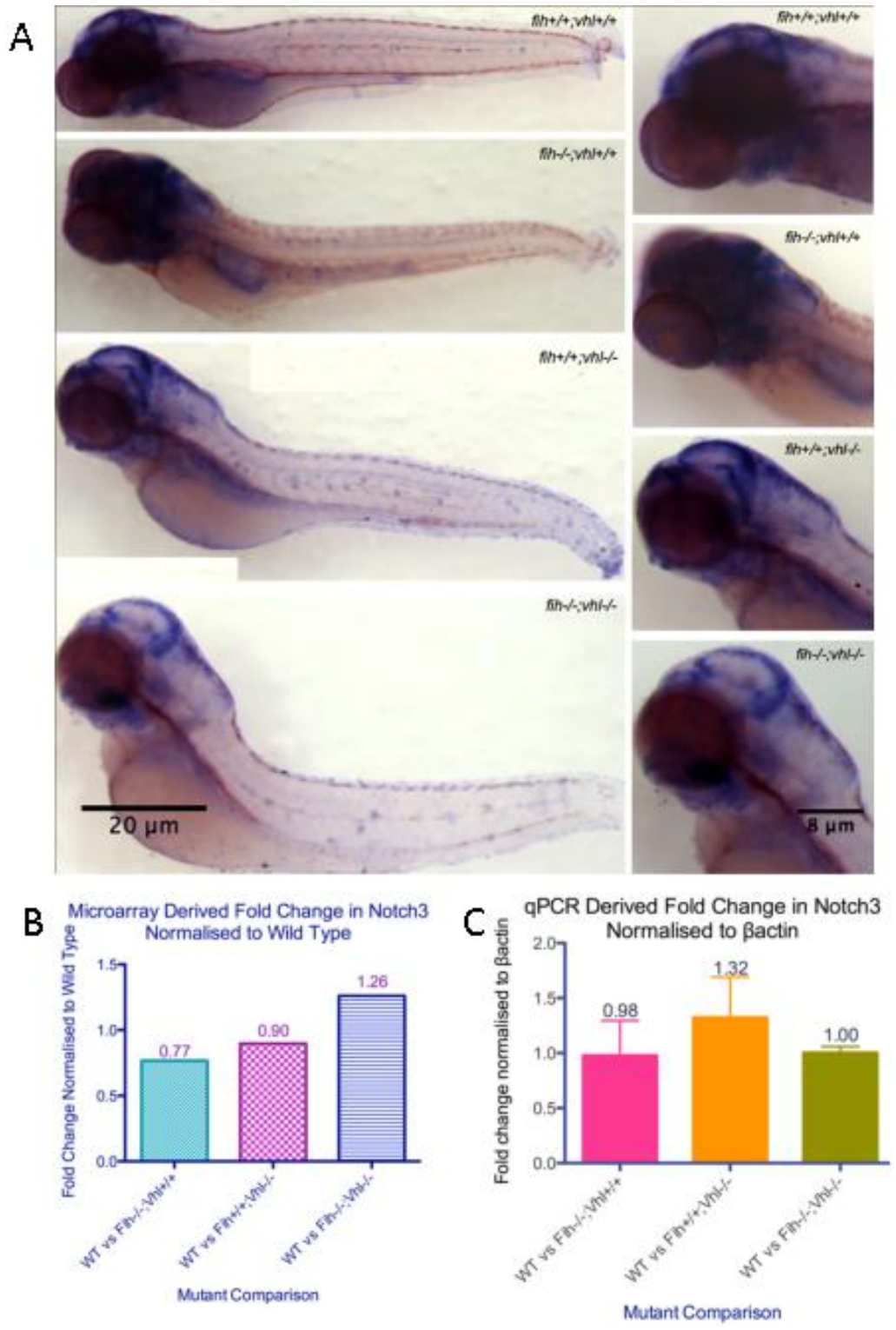


**Figure 64 Expression of *notch3* by *in situ* hybridisation, microarray and qRT-PCR**

**A)** *Expression pattern of notch3 in the mutants by in situ hybridisation at 4dpf. These images are composite images taken over multiple focal planes. Expression of notch3 at 3dpf was also quantified by both microarray* ***(B)*** *and qRT-PCR techniques* ***(C).***

The expression profile of *notch3* in the different mutants indicates that its expression is not altered in the *fih217/217* only embryos, that It has slightly up-regulated in the *vhl-/-* only embryos, and then not altered in the *fih217/217;vhl-/-* embryos, compared back to wild type, as shown by the qRT-PCR and the *in situ* hybridisation. The lack of dramatic changes to *notch3* or *deltaC* expression suggests that while their role in aortic specification is present in each of the groups of embryos It has not responsible for differential phenotypes.

### 4.7.3 Notch Inhibition (Chemical and Intrinsic)

Initial observations and the known effect the need for lateral inhibition, set up by differential Notch receptor and ligand on neighbouring cells in the vasculature indicated an opportunity to assess the effect of the inhibition of Notch signaling on the vasculature of these embryos. This would aid the investigation as to whether this was the causative signaling pathway being affected to generate the increased branching in the double mutants. Treatment with N-[N-(3,5-difluorophenacetyl)-L-alanyl]-S-phenylglycine-*t*-butyl ester (DAPT), a γ-secretase inhibitor, was used to assess the effect of global inhibition of Notch-signaling on the branching pattern of the vasculature, see **Figure 65**.

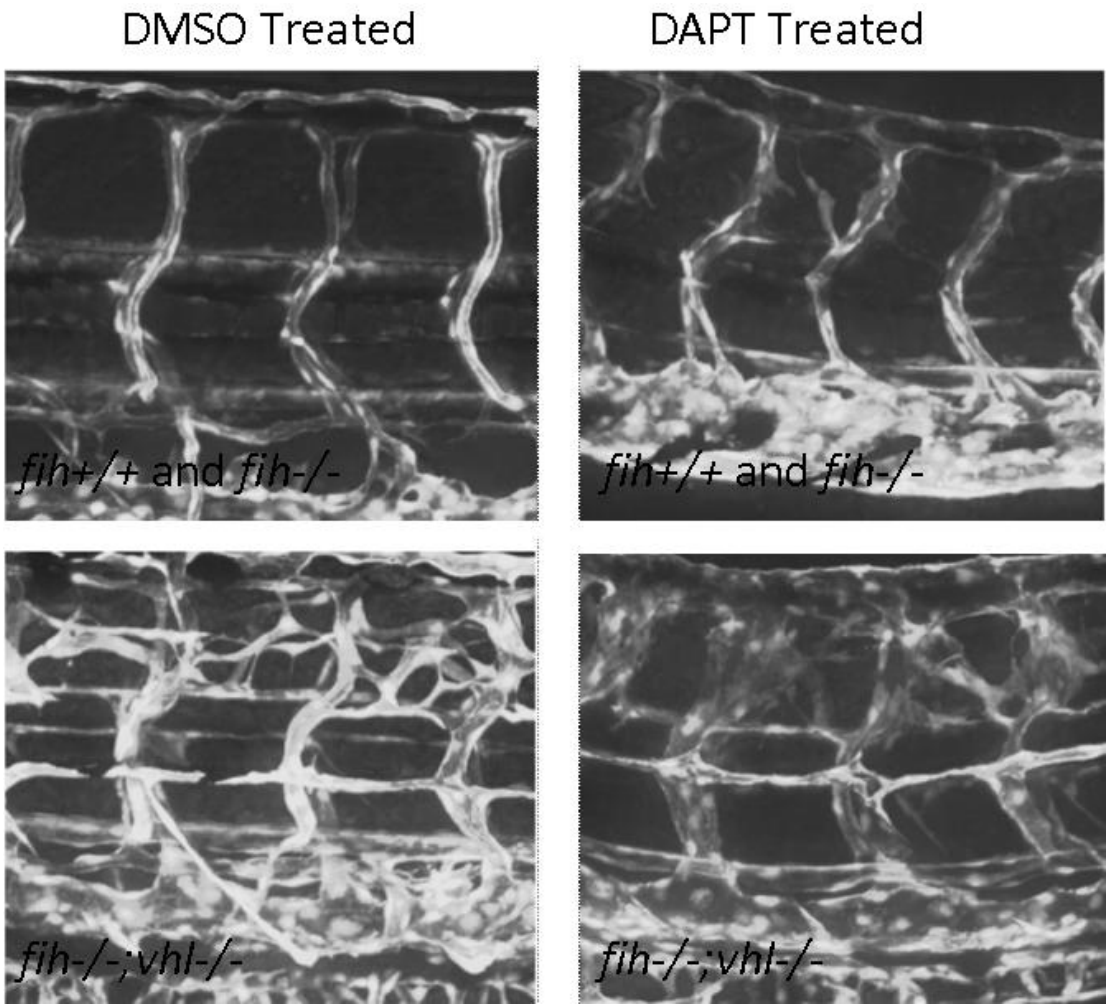


**Figure 65 The effect of DAPT treatment (Notch signaling inhibition) on vascular branching, revealing the increased branching and sprouting of the blood vessels**

*The left panel indicates DMSO control treated embryos while the right panel indicates DAPT treated embryos. The top panel indicates the common phenotype observed in both wild type (fih+/+) embryos and in fih217/217 embryos. The bottom panel indicates the phenotype observed in the fih217/217;vhl-/- embryos. The vhl-/- embryos weren't represented. N=1 cross with multiple embryos.*

The data from the DAPT treatment can only be used as an indicator of the effect of inhibiting the notch signaling pathway on the vascular branching due to the low number of embryos imaged. What can be indicated is that upon treatment of both wild-type and *fih217/217* embryos with DAPT there was an observable increase in branching of the ISVs.

Overall expression of Notch expression were also assessed using the *fih;vhl;Tg(csl-venus)qmc61* zebrafish line (Gerring, M. pers. Comm.), see **Figure 66**.

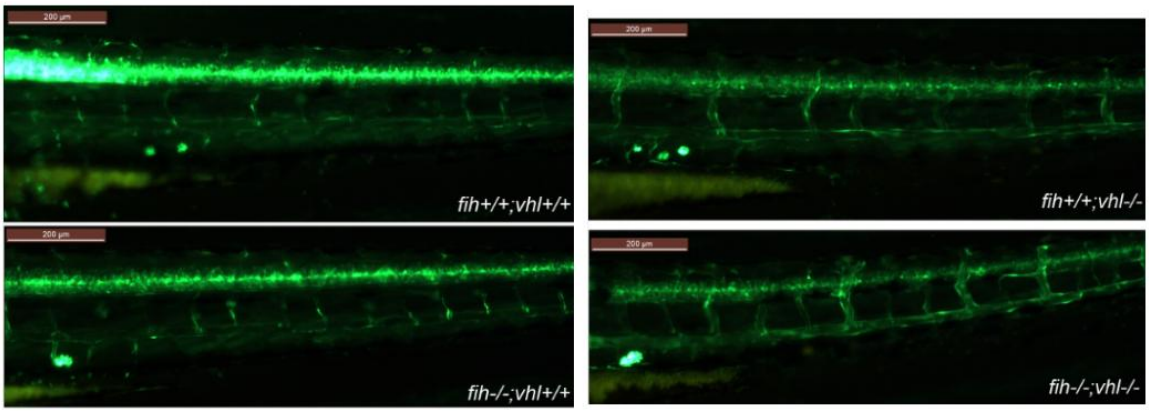


**Figure 66 The overall expression of Notch signaling**

*Levels of Notch signaling using the fih;vhl;Tg(csl-venus)qmc61 zebrafish line (Gerring, M. pers. Comm.),*

The vascular expression of the *Tg(csl-venus)qmc61* expression correlated with the Notch pathway's known roles in vascular development, as well as with the increased expression observed in the microarray and qRT-PCR.

The expression patterns of other components of the pathway with roles in negative regulation, notch regulated ankyrin repeat domain protein (NRARP) and the notch intracellular domain (NICD), were assessed using microarray and qRT-PCR techniques, see **Table 15 and Table 16.**

The discrepancy in the expression of *nrarpa* in the *fih217/217;vhl-/-* embryos between the microarray data and the qRT-PCR is slight but makes drawing conclusions on the role of *nrarpa* in the increased branching and tip cell formation observed in these embryos difficult and further tests would need to be conducted. However, NRARP is also a target of Notch signaling so the slight elevation of expression could also indicate slight activation of the pathway so care must be taken using it as an indication of the pathway's activation.

More importantly, we checked the microarray for indications of increased levels of Notch signaling by analysing target/effector genes such as the *her* and *hey* genes, where there were differences in expression levels, most notably in *her12* expression, were annotated in the microarray data and collated, see **Table 15 and Table 16.**

*Her12* showed the strongest down-regulation (12-18 fold) and was confirmed by qRT-PCR, albeit at a somewhat less impressive level, it is expressed in several places where Notch signaling is known to be active and was also found to be expressed in the endothelial cells. The finding that *her12* is down-regulated is not consistent with the idea that Notch signaling can be enhanced by HIF or by the loss of FIH. Nevertheless some *her* and *hey* genes showed a weak up-regulation, thus a small effect in particular tissues cannot be excluded.

## 4.8 Discussion and Future Work

### 4.8.1 Performing the Microarray

The microarray was performed in order to assess candidate genes or pathways that are being controlled by Fih and to compare changes to the transcriptome in *fih* mutants with changes in *vhl* it might be possible to distinguish between those phenotypes caused by uncontrolled HIF signaling and those mechanisms that *fih* might control independently of HIF; e.g. Notch signaling. Samples were carefully collected, prepared and analysed to ensure as much consistency between triplicate samples and the highest quality possible. Venn diagrams, scatter plots and heat maps provided entity lists of potential hits, which was only made laborious by the need to systematically and individually annotate genes from codes. Looking at the trends rather than the specifics however it was possible to see that high proportions of genes that could be seen to be up- or down-regulated in the *fih217/217* embryos were also up- or down-regulated in the *vhl-/-* embryos, this indicated that FIH was acting predominantly through HIF.

The microarray revealed few genes with expression patterns that were drastically different in the *fih217/217* embryos compared with the wild type embryos. When looking at the genes that were most strongly up-regulated there were few that were immediately annotated, and even once probe sequences had been used to annotate the list there were few genes with increased expression that were easily connected to the phenotypes observed and several mapped to regions that were not transcribed according to Ensembl it is tempting to speculate that many of these could be false positives from the microarray. Nevertheless the tight correlation between up-

regulated genes between *fih* and *vhl* mutants suggests that there is a true effect of *fih* on the transcriptome detectable.

### 4.8.2 Microarray Validation

The physiological follow up to all of the potential hits has not been completed, although the microarray was validated for 20 genes by qRT-PCR and so a certain level of interpretation has been made. However conclusions drawn from the data rely, for these interpretations, on the connection between phenotypes and gene expression and remain speculation until such time as they can be assessed.

Processing the data took on multiple approaches in order to both search for trends based on the relationship between expression in the different groups, and also selectively sorting through the data-set to identify hits. The need to move to a more targeted search process didn't prevent the identification of several genes selectively regulated by the loss of *fih,* to be described.

Once the hits were identified and qRT-PCR primers were optimised it was also possible to begin assessing the microarray as a validated data-set and begin pooling together the expression levels of families of genes either surrounding the validated hits or based around previously observed phenotypes.

One experiment used to assess the validity of the microarray data was to obtain a new sample from each of the different genotypes of embryos, and compare the qRT-PCR results from these with those obtained by performing qRT-PCR on the same samples as the microarray. The data showed the same trend in gene expression of *phd3,* although at different magnitude. While acknowledging that both these techniques (microarray and qRT-PCR) exhibit their own levels of bias and specificity, the correlation between the profiles in these three graphs suggests that the microarray data can be used to draw preliminary conclusions on gene expression changes in these embryos.

### 4.8.3 HIF Family Genes

The first family of genes to select was the *hif* family members that were annotated in the array, along with the *phds, fih* and *vhl* themselves. It was clear that expression in

*fih217/217* embryos was almost entirely unchanged, with two exceptions *hif-1al2 (*a *HIF-1/HIF-3* homologue) and *phd3*, whereas in *vhl-/-* and *fih217/217;vhl-/-* embryos expression of *phd3* rose to 46 fold and 163 fold respectively compared to wild type. Expression of *phd3* was validated by qRT-PCR and demonstrated that Fih was contributing to 1% of Hif function in altering the expression of *phd3.* The increased expression of *hif-1al2* may not be significant in itself since Hif activity and function is known to be regulated at the protein level. The increased expression of *fih* in *fih217/217;vhl-/-* embryos could be due to *fih* being a HIF target gene, which is unlike what has been published on *fih* and would need to be investigated further.

The microarray revealed expression patterns that correlated with the hypothesis proposed in **Figure 6 of the Introduction**, that the roles of Fih and Vhl in regulating Hif levels and activity are distinct. The loss of *fih* alone leaves Vhl to function, responding to Phd3 hydroxylation of Hif to induce its breakdown, ensuring continued regulation of Hif function, suggesting that down-stream expression of target genes could be kept to close to wild type levels. In the *vhl-/-* embryos, this breakdown of Hif fails to occur and regulation of Hif function is left to Fih hydroxylation at the active site of Hif co-activators, allowing an increase in down-stream target gene expression. The double mutants have neither of these mechanisms in place and expression of down-stream targets therefore resembles that during hypoxia, when Fih, Phds and therefore Vhl are naturally inhibited.

#### 4.8.4 HIF Targets

The expression of the haematopoiesis inducing hormone *epo,* the first gene in which an HRE was identified, along with *vegf* demonstrated the same expression profile as *phd3* across the three mutant groups. Since two known phenotypes of the *vhl-/-* embryos are polycythemia and hyper-branching of the vascular network, the elevated expression of these genes correlated and further validated the microarray findings, especially in combination with observations in the *fih-/-;vhl-/-* embryos of these phenotypes being enhanced compared to *vhl-/-* only embryos and observing the further up-regulation of these genes. Also a point of note and worthy of further investigation, given that polycythemia that has been characterised in the *vhl-/-* embryos, is the observation of elevated *vegf-ab* in these embryos and its role in

haematopoiesis (Bahary et al., 2007). The further up-regulation of *vegf-ab* in the *fih217/217;vhl-/-* could therefore be indicative of an increase in blood cells in these embryos too, which is yet to be definitively characterised.

Given the interactions between the different Vegf ligands and receptors and the alterations in expression of *vegf-aa* in the embryos, the other members of the Vegf family along with other vascular markers that could contribute to the visible differences in the vasculature were investigated, see **Table 15 and Table 16**. The increase in VEGF receptor expression is less pronounced than the increase in ligand expression. The ligand binding with particular receptors indicates that the increase in expression of *vegf-aa* and *-ab,* along with the increased expression of *flt-1* and *kdr/flk-1* are the receptors that these ligands have been shown to bind to. These ligands and receptors are known to bind to each other, the correlation in their changes in expression patterns are therefore connected.

The slight increase in expression of *vegf-c* is not correlated with an increase in *flt-4* (the ligand), which would have been indicative of simultaneous increases in both blood vessel proliferation as well as lymphangiogenesis. The up-regulation of *flt-1* and *kdr* is to the same degree in the *vhl-/-* embryos and the *fih217/217;vhl-/-* embryos, which suggests that the loss of *fih* is not a major factor in the regulation of these receptor genes. The microarray results indicate that the loss of *fih* only has an impact on *vegf-aa* and *vegf-ab* in the context of the *vhl-/-* embryos. Taken together, the *fih217/217* embryos exhibit slight elevation in *kdr* expression, the *vhl-/-* and *fih217/217;vhl-/-* embryos have increased expression in both *vegf-aa* and *vegf-ab* along with increased expression of both *flt-1* and *kdr-l/flk-1.* The further increase seen in these double mutants indicates that VEGF signaling is further increased. The striking effect of *vegf-ab* expression is interesting and merits further investigation and suggests a more important role of *vegf-ab* than was currently assumed. The *vegf-a* locus is duplicated in the zebrafish, isoforms *vegf-aa* and *vegf-ab,* and these have been shown to have distinct expression patterns by *in situ* hybridisation (Bahary et al., 2007). *vegf-ab* morphants have been shown to develop normal vasculature and haematopoiesis until 2dpf, whereas *vegf-aa* morphants lack the major intersegmental vessels and show reduced haematopoiesis, indicating distinct roles for the two genes (Bahary et al., 2007). Although both *vegf-aa* and *vegf-ab* are increased, from the current

experiments, it is not clear what the relative expression of *vegf-aa* is to *vegf-ab*, if *vegf-aa* is normally 100 fold higher expressed than *vegf-ab*, the 9 fold increase of *vegf-ab* is still a minor contribution to the total VEGF signal. It would be interesting to block the function of *vegf-ab* by morpholinos or mutation and see whether it could modulate the double mutant phenotype. Similarly morpholinos against *vegf-aa* or even chemical could be used to (partially) block VEGF function to determine whether the phenotypic alterations in *fih;vhl* double mutants are the result of increased VEGF signaling (Bahary et al., 2007, Liang et al., 2001, Nasevicius et al., 2000).

Overall the expression of these genes was not significantly altered in the *fih217/217* embryos, with the exception of a slight elevation in *kdr/flk1*. In the *vhl-/-* embryos the expression of *vegf-a, vegf-ab, flt1 and kdr/flk1* can be seen to be elevated, and these same genes are elevated, albeit further elevated, in the *fih217/217;vhl-/-* embryos. The expression levels demonstrated in the microarray were assessed by qRT-PCR for validation, see **Table 16**. This supports the hypothesis made whereby the differing effects of Fih and Vhl regulation of Hif.

The expression patterns of many of these genes has been described on the Zfin.org website, *Vegf-aa* has been shown in the blood vessels, the caudal vein plexus, the dorsal aorta, the ISVs and the new sprouting vessels, whereas *Vegf-ab* shown in ISVs, nucleate erythrocytes and the sub-intestinal vein, indicating more restriction of the expression of this gene in the zebrafish. The microarray data showed that *vegf-ab* was the highest regulated gene in the *fih217/217;vhl-/-* embryos but all these ligands demonstrated the trend in expression of slight increased expression in the *fih217/217* embryos, an increase in the *vhl-/-* embryos and a further increase in expression in the *fih217/217;vhl-/-*embryos. VEGF-AB was not validated at this time, by qRT-PCR, however primers were ordered.

The microarray data suggested little to no alteration in expression of either *vegf-c* or *vegf-d,* both of which have been connected mainly with lymph-angiogenesis rather than vascular-angiogenesis (Vlahakis et al., 2005), new data is blurring this slightly, suggesting that the lymphatic system is not being differentially organised in these embryos.

The previously described trend in expression was present except for all three of the Vegf receptors that were annotated. There was a discrepancy between the microarray data and the qRT-PCR profiles for *flt4*, where the microarray suggested that there were no changes observed in expression between the different mutants and the qRT-PCR showed an increase in expression in the *fih217/217* embryos and no change in expression in the *vhl-/-* embryos or the *fih217/217;vhl-/-* embryos, all compared to wild type, see Table 15 and Table 16. This discrepancy could be due to the increased sensitivity of the qRT-PCR assay in comparison with the microarray (Dallas et al., 2005), ensuring continued caution in interpreting the data.

In the zebrafish, the two *kdr* genes have been shown to have strikingly different effects with *kdr-l* having been shown to be functionally necessary for artery development (Covassin et al., 2009), the qRT-PCR for this gene is ongoing to confirm the microarray findings, since they indicate *kdr* is differentially expressed rather than *kdr-l*.

The alterations in both vegf ligands and receptors could well be responsible for, or a contributing factor, to the altered vascular phenotypes that were observed in the *Tg(Fli1:eGFP)* background. In early zebrafish embryos, arterial fates are induced by VEGF signaling from the somites, as well as via Notch signaling (Adams et al., 1999, Herbert et al., 2009, Iso et al., 2006), and *ephrinB2/ephB4* expression. *EphrinB2* (arterial) and *ephB4* (venous) have been shown to be differentially expressed in the primary vascular plexus in the early chick embryo prior to the onset of circulation (Moyon et al., 2001, Othman-Hassan et al., 2001, Kume, 2010). Since shear stress has also been shown to increase the expression of *ephrinB2* via VEGF-Notch signaling pathways *in vitro* (Masumura et al., 2009, Obi et al., 2009) and *in vivo* (Suzuki et al., 2012) the expression of this marker was also analysed.

In this case of ephrin B2 (see Table 15 and Table 16) the expression of *ephrinB2a* didn't alter across the three different mutants at 3dpf, at this stage its expression is restricted to the dorsal aorta as shown by Zfin.org. Murine embryonic stem (ES) cells expressing *kdr/flk1* that are then exposed to shear stress exhibit *ephrinB2* expression whereas *ephB4* mRNA (associated with venous cells) decreased (Masumura et al., 2009). This has been shown, in mouse ES cells, to be regulated by Notch signaling, where abolition of notch intracellular domain (NICD) translocation blocked stress-induced up-

regulation of *ephrinB2* expression, and forced NICD expression induces mRNA expression of *ephrinB2* (Masumura et al., 2009, Iso et al., 2006). More specifically, Dll4-Notch stimulation and not Jagged1-Notch markedly induced *ephrinB2* expression (Iso et al., 2006). Observations in *ephrinB2-/-* and *ephB4-/-* mice have revealed deficiencies in primary capillary remodeling into the mature vascular network, with no clear boundaries between the arterial and venous vessels (Wang et al., 1998). The expression of this gene is therefore important for the establishing of arterial-venous interactions, not necessarily in the initial endothelial specification (Wang et al., 1998, Kume, 2010). The absence of an effect of *vhl* and/or *fih* loss on *ephrinB2* expression suggests that it does not play a distinct role in the different vascular phenotypes that were observed in the *fih217/217* and *vhl-/-* embryos at 3-4dpf. In the absence of further data on earlier embryos however, effects during the initial arteriovenous specification cannot be excluded.

Observations of alterations in heart function in the *vhl-/-* and *fih217/217;vhl-/-* embryos compared to wild type siblings (described in more detail in Chapter 5 as well as (van Rooijen et al., 2010) lead to the assessment of troponin T2 heart marker in the microarray data set, see Table 15. The expression of *tnnt2c* is up-regulated to roughly the same degree in both the *fih217/217* embryos and the *vhl-/-* embryos, and then that expression is doubled in the *fih217/217;vhl-/-* embryos, indicating that *tnnt2c* was influenced equally by the loss of either *fih* or *vhl* and then further by the loss of both genes, indicating perhaps an independent effect. Phenotypes observed in the heart size and function of these embryos can therefore be thought to be caused by alternate factors, which need to be investigated.

#### 4.8.5 Inflammation

Having described the positive effect of FIH hydroxylation on NFκ-B1 and Iκ-Bα activity in Section 6.6.3, the expression levels of these and other inflammatory markers were assessed in the microarray data set. Since the effect of FIH has been shown to be post-translation, with hydroxylation events at designated Asn residues affecting the stability of the proteins, it was not surprising that the levels gene expression were not significantly altered in any of the three mutants being studied compared with wild type. However, since FIH has been shown to bind to many proteins besides these and

in order to assess the role of *fih in vivo* a preliminary search for the expression of NF-κB target genes was made in the microarray dataset. No alterations were observed in the expression of TNFa or TNFb (known to also be involved in activation of NF-κB), or in target genes such as interleukin 6 (IL-6), signal transducer and activator of transcription 3 (STAT3), or bcl-xl (data in supplementary excel file) in the *fih217/217* embryos at 3dpf, see **Table 13** for references. Further investigation of the microarray dataset could be performed, however the data suggests that *fih* is not directly influencing *nfκb* expression or activity *in* vivo. The observation of little or no changes in expression of NFκB or IκB family members remains just that, since the role of FIH interaction with these has been shown to be post-translational. Of course it cannot be excluded that *fih* has an effect on NFκB in a particular cell type. For instance, hypoxia has been shown to affect the behaviour and function of neutrophils with hypoxia able to increase NF-κB protein expression and activity and mediate neutrophil survival (Walmsley et al., 2005). The direct effect of *fih* on neutrophil and/or macrophage behaviour would also be possible with the crossing of the *fih217/217* fish with GFP-transgenics available at the university which label these cell types.

#### 4.8.6 HIF and Circulatory System

One observation in the *vhl-/-* embryos which elicited a specific search through the microarray data was that of the enlarged heart and increased cardiac output compared to wild type siblings. This along with observations described in **Chapter 3**, of the further enlargement of the heart and associated oedema in the *fih217/217;vhl-/-* embryos lead to the assessment of the troponin family of genes known to be integral to skeletal and cardiac muscle contraction along with association of the sarcomeres. In the zebrafish the assembly of sarcomeres and the role of thin filaments has been linked to *Tnnt2*, the *silent heart* locus (Ferrante et al., 2011, Sehnert et al., 2002). Since the loss of the Tnnt family has been linked to the failure of sarcomeres to form, the increased expression of one of these genes correlates with the enlarged hearts that are observed in the *vhl-/-* embryos and particularly the *fih217/217;vhl-/-* embryos compared to both the wild type and *fih217/217* siblings and with the increased amount of work that is required in these mutants, although this requires further investigation. *Tnnt2c* expression showed a similar level of up-regulation in either *fih* or

*vhl* single mutant, with a further up-regulation in *fih217/217;vhl-/-* embryos, indicating that it may contribute to extra work needed in these embryos. Here *tnnt2* over-expression may indicate a sign of cardiac stress (indicated in humans (Gomes et al., 2002, Linnemann et al., 2012)) and may in turn correspond with an observation in the *fih/-* embryos that the hearts may be pumping harder against normal vessels, whereas *vhl-/-* has less problems at 3dpf and *fih217/217;vhl-/-* embryos a more

#### 4.8.7 Blood and Circulation

Data from the initial analysis attempted to count RBCs along the aorta was difficult to interpret since the *vhl-/-* embryos have been previously shown to exhibit polycythemia (van Rooijen et al., 2009). This data was generated from counts and measurements made from images taken during high-speed imaging, and to ensure the aorta was at precisely the same angle for each fish in order to measure the inner wall of the vessel made the accurate mounting of the embryos essential and difficult to compare. There was consistency between the different parameters that were assessed when they were compared with the other data from the same group, however the lack of corroboration of previously reported findings in the *vhl-/-* embryos does raise concerns about drawing conclusions based on these data in isolation.

Utilising the microarray data to test hypotheses became another avenue of investigation. Following observations in the *fih217/217;vhl-/-* embryos that circulation in the tail and trunk ceased to flow from 4.5dpf. The attempted assay that was used to assess erythrocyte volume, number and haematocrit (erythrocyte number per unit volume) was difficult to assess through inherent difficulty in consistency of mounting embryos for imaging and in built human error in measuring. Data did suggest differences but did not confirm results known for *vhl-/-* embryos, albeit at a different developmental stage. Assays such as taking blood smears and using *o*-dinanisidine and May-Grunwald Giemsa stains have been used to quantify and characterise blood cells, along with confocal imaging at high magnification and would aid in characterising blood phenotype in these double mutants (van Rooijen et al., 2009). One possible hypothesis to explain the sluggish circulation in double mutants was the possibility of increased clotting. To this end all the clotting factors in the intrinsic as well as extrinsic coagulation cascades that were annotated in the array were isolated to reveal that

several were up-regulated in the *fih217/217;vhl-/-* embryos, although not dramatically and it is not clear from their RNA level whether these influence the actual clotting process *in vivo*. The increased expression of *vegf* that has also been reported in the *fih217/217;vhl-/-* embryos could also be a contributing factor in the sluggish circulation, releasing fluid from the vessels leaving the RBCs to clump.

Epo is an essential hormone involved in red blood cell production and also plays roles in breathing rates and tidal volumes (Semenza and Wang, 1992, Yalcin et al., 2007). Since it plays other roles besides those in haematopoiesis, other genes were also assessed including runt-related transcription factor (*runx*) and t-cell acute lymphocytic leukemia (*scl/tal1*) although these were not differentially regulated.

Up-regulation of several genes involved in erythrocyte proliferation and heme scavenging in response to HIF signaling is consistent with published data. However *angpt1* and *epo-r,* which have previously been demonstrated to be elevated in the *vhl-/-* embryos at 7.5dpf (van Rooijen et al., 2009) are not significantly different from wild type at 3dpf, suggesting that further investigation of later time-points might be necessary to infer conclusions from this data. Gata1 mRNA and protein levels have been shown to be increased under hypoxic conditions (Zhang et al., 2011) and the up-regulation of *gata1*, along with *epo,* in the *fih217/217;vhl-/-* embryos is a strong indication that haematopoietic proliferation and erythroid differentiation is being initiated in these embryos despite their normoxic environment.

Assays such as taking blood smears and using *o*-dinanisidine and May-Grunwald Giemsa stains to quantify and characterise blood cells, along with confocal imaging at high magnification would aid in characterising the potential polycythemia in these double mutants (van Rooijen et al., 2009).

#### 4.8.8 Blood flow and blood clotting

Blood flow analysis by high speed video-microscopy of the *fih217/217;vhl-/-* embryos was assessed in **Chapter 3** and revealed that blood flow in the *fih217/217;vhl-/-* embryos became sluggish and then ceased around 4.5dpf. This reduced flow infers a reduction in LSS and therefore supports the connection between LSS and *cxcr4* expression proposed by Melchionna and Packham (Melchionna et al., 2005, Packham

et al., 2009). The *in situ* hybridisation images shown by Packham et al for *cxcr4* expression in *tnnt2* morphants (where flow is never initiated), compared to control morphants, do reveal an up-regulation of *cxcr4* (Packham et al., 2009), however not to the same extent as observed in the *fih217/217;vhl-/-* embryos. Further investigations into the stage at which the *cxcr4* expression becomes elevated, would aid the investigation of how this expression correlates with observations of the slowing of circulation in the *fih217/217;vhl-/-* embryos. Also, if blood flow were to be slowed, potentially using titrated doses of tricaine, it would be possible to assess to what extent flow was able to influence *cxcr4* expression, in conjunction with *fih* and/or *vhl* function.

Since only *fih217/217;vhl-/-* embryos show circulation defects, clotting factors was thought to play a role in this, increased expression of Factor 10 (F10 or FX) was observed in each of the mutant groups. This suggested the possibility that if proliferation of the erythrocytes was not entirely responsible for the sluggish circulation then another candidate could be coagulation. However only minor changes (<2 fold) were observed, with no clear correlation with *fih;vhl* double mutant phenotype (since changes were also observed in the single mutants).

Analysis of clotting has been tested in adult zebrafish by analysing the bleeding times (Jagadeeswaran and Sheehan, 1999), although the small volumes of plasma make assessing total coagulation activity (TCA) difficult (Jagadeeswaran et al., 2000). This being the case in the adult fish along with the fact that the *fih217/217;vhl-/-* embryos do not survive to adulthood makes the direct assessment of clotting in these fish more difficult. An assay has been developed using a nitrogen laser to create a vascular lesion in order to observe dynamic wound healing response and assessing the role of thrombocytes in clot formation (Gregory et al., 2002, Thattaliyath et al., 2005, Lang et al., 2010), this technique could be used to assess wound healing and clotting in the embryos. These assays could be tested in order to assess the contribution of clotting factors in the circulation defect in the *fih217/217;vhl-/-* embryos.

### 4.8.9 Vascular Development

*Cxcr4a* over-expression causes a directed migration of somitic cells to the aortic region in a manner similar to that seen in Notch induced migration in the chick embryo (Ohata et al., 2009). Hypoxia can induce expression of *cxcr4* through *Hif-1* activation in human monocytes, macrophages, endothelial cells and cancer cells (Zagzag et al., 2005). The regulation of *cxcr4* levels in endothelial cells may occur transcriptionally or post-transcriptionally (Melchionna et al., 2005). Increasing laminar shear stress (LSS) has been shown to result in down-regulation of *cxcr4a* in endothelial cells (Melchionna et al., 2005) and mediates collateral vessel formation in zebrafish embryos (Packham et al., 2009). Blood flow rates and perturbations, such as arterial occlusions, are detected by the endothelial lining of the vasculature, and this results in alterations in gene expression and further regulation of blood flow and EC function (Melchionna et al., 2005, Packham et al., 2009). The hypothesis was that LSS maintained *cxcr4* expression on the endothelium at lower levels than in ECs either subjected to low LSS or kept in static conditions. High levels of *cxcr4* expression have been found in ECs from human carotid artery atherosclerotic lesions, while found at low levels in minimally diseased carotid artery endothelium (Melchionna et al., 2005). Since this was not an avenue of investigation, assessing the vascular phenotypes, as well as observations of the migration of endothelial cells (using the *Tg(fli1;eGFP)* line) in response to chemical inhibitors such as AMD3100, a specific cxcr4 inhibitor, could answer some of these questions as to post-translational role of cxcr4 in the vascular patterning of the *fih;vhl* embryos.

Investigation of other tip-cell enriched genes such as nidogen-1 (*nid1)*, uPAR, apelin (*apln*), and angiopoetin 2 (*angpt2),* each identified as being tip-cell enriched by assessment of endothelial cells from *dll4+/-* compared to wild type retina in the mouse (del Toro et al., 2010) would be needed to further investigate these phenotypes.

### 4.8.10 Notch signaling and its role in vascular development

Connections between notch signaling and blood vessel development and arrangement has been studied widely in different models, see **Table 13**, and connections between these data sets have been seen in the fih217/217;vhl-/- embryos, see **Figure 67**.

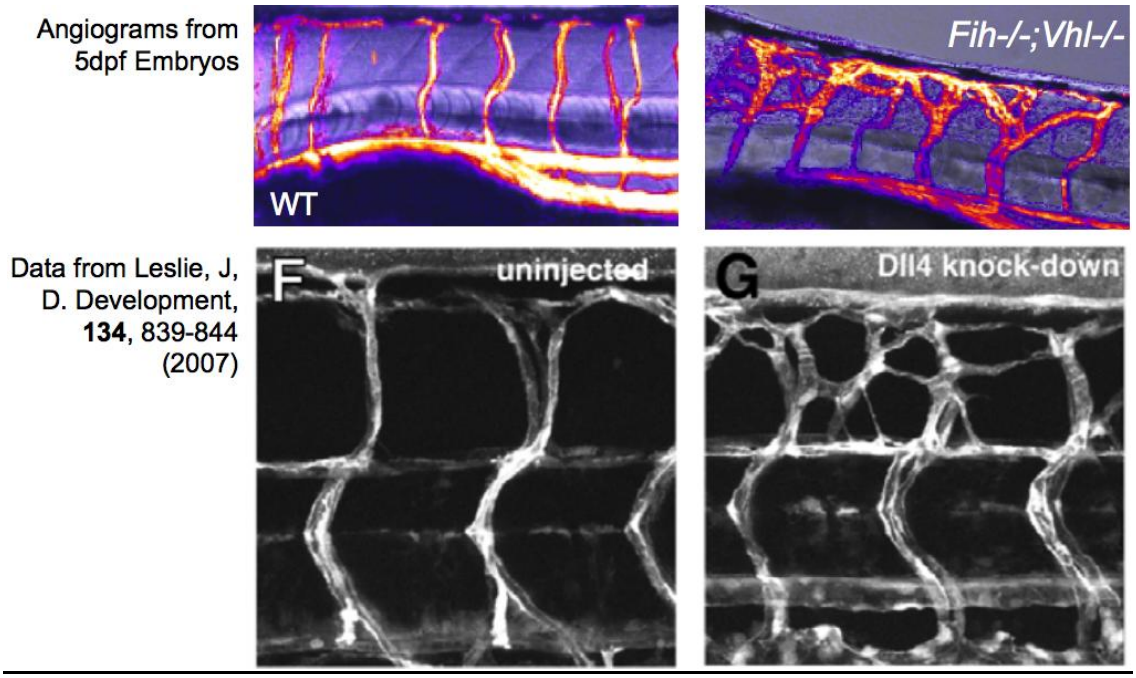


**Figure 67 Correlation between phenotypes of Dll4 MO knockdown and vascular branching of fih217/217;vhl-/- embryos**

*Literature derived correlation between the phenotype of a Dll4 MO knockdown and the subsequent increase in branching of the vessels with the increase in vascular branching observed in the fih217/217vhl-/- embryos.*

In order for the hypothesis to be tested, the levels of *dll4* expression in the fih217/217;vhl-/- embryos were assessed and the indication from the morpholino experiments would need for *dll4* to be down-regulated for the hypothesis to be supported, see **Table 15 and Table 16**.

Since *dll4* is a Notch activator expressed in the tip-cells and involved in the lateral inhibition to prevent neighbouring stalk-cells taking on tip-cell identity the loss of *dll4* has been shown to result in the increased branching of the vasculature through an increase in tip-cell identity. This led to the hypothesis that increased branching of the vessels in the *vhl-/-* and *fih217/217;vhl-/-* embryos could be induced by a decrease in *dll4* expression. When this was tested, an increase in *dll4* was found to be highest in double mutants. On the other hand, since *vegf* has been shown to induce the expression of *dll4,* in itself potentially increasing the number of tip-cells and inducing the branching phenotype, it is possible that the increased level of *dll4* expression

observed by microarray and qRT-PCR could simply be a read-out of the increased number of tip-cells.

High levels of *dll4* have also been shown to result in decreased expression of identifiable markers immature pericytes, suggesting that there is an interaction between *Dll4* and pericytes. This was proposed to be important for pericyte coverage, but that this coverage wasn't essential for vessel maturation in tumour vasculature (Li et al., 2007b). These connections to hypoxia driven *dll4* expression in tumour vasculature and pericyte coverage suggest that these roles might be more critical in these embryos than its direct effect on tip-cell differentiation in the *fih217/217;vhl-/-* embryos.

Activation of *dll4* and *hey2* has been shown to be induced by *vegf* in conjunction with *foxc1* and *foxc2* (Hayashi and Kume, 2008). Foxc transcription factors have been shown to activate the Hey2 promoter in ECs, potentially through direct interaction with Su(H) (Hayashi and Kume, 2008), implicating these transcription factors in the arterial program. *Foxc1a* expression is lowest and *foxc1b* is only slightly elevated in the *fih217/217;vhl-/-* embryos, while *dll4* expression is slightly elevated in the *fih217/217* embryos and more strongly elevated in the *fih217/217;vhl-/-* embryos. Expression of *hey2* is slightly elevated, to around the same level in each of the zebrafish embryo groups indicating that if *dll4* is involved in its regulation there are other factors contributing to the differential regulation of *dll4,* which is where *vegf* becomes a possible candidate. Down-regulation of *dll4* is not the cause of the increased branching, but there is increased expression of *deltaC* as well as *notch1b,* which could be contributing factors.

The expression of *dll4* in the zebrafish is indicated to be specific to the vasculature and the primitive pronephric duct, when assessed on Zfin.org, however alternative expression domains could be possible. The possibility that *dll4* is expressed elsewhere makes drawing definitive conclusions on the role of *dll4* in the vascular branching phenotype in these embryos difficult. However, overall levels of Notch signaling have been observed, using the *Tg(csl-venus)qmc61* line (Gering, M. pers. Comm..) indicating a strong increase in overall Notch signaling in the *fih217/217;vhl-/-* embryos, which could indicate that the *dll4* expression was more likely to reflect, simply, an increase in

tip-cell number. The *Tg(csl-venus)qmc61* line provides a tool, as yet, not completely utilised for assessing the *fih217/217* zebrafish response to alterations in Notch expression and the role of Notch in the vascular patterning defects in the *fih217/217;vhl-/-* embryos.

The connection between FIH and Notch has been shown to be in post-translational modification, and in the sequestering of FIH away from HIF modification due to enhanced binding capacity to Notch (Zheng et al., 2008). As such the lack of immediate and significant alterations in the expression of the ligands and receptors themselves are not sufficient to rule out the interaction in this model.

The mechanism of Notch signaling in the lateral inhibition of tip-cells having been shown, the inhibition of Notch could still be involved in the increased branching of the vessels, so the next thing to investigate was to assess other methods of Notch inhibition. The *fih217/217;vhl-/-* embryos when treated with DAPT didn't exhibit the same drastic increase in branching, potentially due to the increased number of branches that already exist in these embryos. Altogether this is consistent with the previously published data that inhibition of Notch signaling is capable of increasing vascular branching in the zebrafish embryos. The increase of branching in the wild type and *fih217/217* embryos in response to DAPT treatment does indicate that a decreased activation of Notch could be responsible for the vascular patterning in the *vhl-/-* and *fih217/217;vhl-/-* embryos.

# 5 Evaluation of Mouse versus Zebrafish Data on the effects of the loss of FIH

A report in 2010 demonstrated that finding that loss of *Fih*, in a mouse knockout model, surprisingly resulted in a "wide-ranging derangement of physiological response and causes a hypermetabolic phenotype, but result[ed] in few of the classical effects of HIF activation *in vivo*" such as increased vascularisation or high levels of erythropoiesis (Zhang et al., 2010). The mice exhibited lower body weight despite increased food and water intake and were protected from high-fat-diet weight gain. The mice had increased $O_2$ consumption and increased evolution of $CO_2$. They also had an increased heart rate with no alteration in breathing frequency but with an increased tidal volume. The mice had decreased EPO expression following hypoxia. Mice were administered with insulin in hypoxia, and this resulted in a decrease in AMPK, leading to an alteration to fasting glucose and fed insulin levels as well as reduced lipogenesis. They also had an increase in ATP generation and increased heat production (Zhang et al. 2010). The findings from the study by Zhang et al were able to put the data from this study in context.

## 5.1 Comparing Two Data-sets

A study has been published describing findings in a mouse model of *Fih* knockout (Zhang et al., 2010), and this study also included a microarray study, using mouse embryonic fibroblasts (MEFs) as sample cells. Scatter diagrams were generated following an average being made across the two replicates for each sample (WT, *fih-/-, vhl-/-* and *fih-/-;vhl-/-)* by comparing the *fih-/-* data set against the *vhl-/-* data set it was possible to isolate genes that were down-regulated in one data set and not the other, see Figure 52. Venn diagrams also provided information on genes that were up or down regulated in individual mutant MEFs and not the others. Looking at the 478 genes that were isolated by this method as being down-regulated in the *Fih-/-* MEFs and not in either the *Vhl-/-* MEFs or the *Fih-/-;Vhl-/-* MEFs, it was possible to see that genes including angiopoeitin like 1 (angptl1), ephrin receptor A3 and A5

(epha3/epha5), C-X-C receptor 1 (CXCR1), friend leukemia factor 1 (Fli1), uncoupling protein 2 (ucp2), and carbonic anhydrase 3 (car3) were all represented. Several of these genes provide commonalities between the mouse MEF expression profiles and those found in the whole zebrafish embryo data set. Another commonality between the two data sets was that when looking at the up-regulated genes in the *Fih-/-* MEFs that weren't up-regulated in the other groups there were only 8 genes isolated, indicating that the loss of Fih, either in MEFs or in the zebrafish embryo, does not lead to significant induction of gene expression, and is more likely to lead to down-regulation of expression.

Some of the genes listed in **Table 17** were not annotated in the zebrafish microarray, such as *adm*, *fabp4* or *kdm3a* although other family member genes were annotated, or in the case of Li202b do not have fish homologues. Key differences in the source material (MEFs versus whole organism) as well as different microarray platforms (Affymetrix versus Agilent) between the two studies make it difficult to draw direct correlations between the data-sets. However, with this in mind it is possible to see that in general, where there are homologues to be found in both studies the trend in expression (increased or decreased) in response to the loss of *fih* or *vhl* or both was consistent between the two studies. **Table 17** also shows that the fold changes observed in the MEFs are documented as being stronger than those seen in the zebrafish embryos, for the most part, with the exception of the change in expression of *egln3* in response to the loss of either *vhl* or both *fih* and *vhl.* *W*here deviations are present it could be due to tissue/organism specific alterations in the expression or other factors introduced by the different studies. The list did provide several directions to search within the present study, including hypoxic targets (*egln3*), metabolic indicators (*ca9, fabp4*), and endothelial markers (*end2, adm/adm2*) and several of these will be discussed in more detail through this chapter.

A list of genes that were deemed hits from this previous study into the effect of the loss of *Fih*, was provided in the supplementary data and has been reproduced here, see **Table 17**.

| Symbol | WT vs Fih217/217 | WT vs Vhl-/- | WT vs Fih217/217;Vhl-/- | Fih217/217;Vhl-/- vs Vhl-/- |
|---|---|---|---|---|
| **Car9** | 1.01 | 4.45 | 236.25 | 52.91 |
| **Cahz** | 1.51 | 2.24 | 3.75 | 1.39 |
| **Edn2** | 2.34 | 3.72 | 103.62 | 27.84 |
| **Edn2** | 1.37 | 2.26 | 4.31 | 1.77 |
| **Ankrd37** | 1.45 | 6.93 | 75.75 | 10.92 |
| **Angkrd37** | 1.31 | 5.08 | 16.41 | 1.73 |
| **Cox7a1** | 0.93 | 3.43 | 19.51 | 5.86 |
| **No homolog** | | | | |
| **Pygl** | 1.54 | 14.04 | 74.49 | 5.31 |
| **Pygl** | 0.72 | 1.35 | 1.02 | 0.64 |
| **Egln3** | 1.81 | 8.75 | 36.34 | 4.15 |
| **Egln3** | 2.61 | 46.73 | 163.5 | 1.29 |
| **Adm** | 1.04 | 4.55 | 18.83 | 4.14 |
| **Multiple homologes** | | | | |
| **Cdkn1a** | 0.93 | 1.33 | 4.61 | 3.46 |
| **No sig change** | | | | |
| **Adm2** | 1.33 | 10.96 | 37.18 | 3.38 |
| **Adm2** | 1.20 | 2.75 | 4.16 | 1.29 |
| **Fabp4** | 1.15 | 1.70 | 5.19 | 3.05 |
| **No homolog** | | | | |
| **Li202b** | 0.90 | 2.64 | 7.25 | 2.75 |
| **No homolog** | | | | |
| **Ddit4** | 1.43 | 1.96 | 4.87 | 2.49 |
| **Ddit4** | 1.03 | 3.56 | 3.90 | 0.13 |
| **Adam8** | 1.29 | 2.69 | 6.32 | 2.35 |
| **Adam8** | 0.84 | 1.12 | 0.95 | 0.90 |
| **Papass2** | 1.26 | 1.70 | 3.50 | 2.06 |
| **Papass2** | 1.15 | 1.04 | 0.93 | 1.00 |
| **Galr2** | 0.88 | 4.74 | 9.56 | 2.02 |
| **Galr2** | 1.19 | 1.13 | 1.45 | 1.20 |
| **Kdm3a** | 1.26 | 2.00 | 3.99 | 2.00 |
| **No homolog** | | | | |
| --- | --- | --- | --- | --- |
| **GCK** | 1.17 | 1.16 | 1.42 | 1.22 |
| **G6Pase** | 1.70 | 1.26 | 0.85 | 0.73 |

**Table 17 Describes expression fold change of genes in *Fih-/-* mouse (top line of each row) vs *fih217/217* zebrafish (bottom line of each row)**

*Taken from Supplementary Data Table S1 (Zhang et al., 2010) and adapted for this study. Describes the expression fold change of genes that were selected from Zhang microarray with expression validated by qRT-PCR (black text) and the comparable expression in the zebrafish microarray (red text).*

***Abbreviations:*** *Carbonic anhydrase 9 (CA9), Endothelin 2 (edn2), ankyrin repeat domain protein 37 (ankrd37), cytochrome c oxidase subunit VIIa 1 (cox7a1), liver glycogen phosphorylase (pygl), EGL nine homolog 3 (egln3), adrenomedullin (adm), cyclin-dependant kinase inhibitor 1A (cdkn1a), adrenomedullin 2 (adm2), fatty acid binding protein 4, adipocyte (fabp4), interferon activated gene 202B (li202b), DNA-damage-inducible transcript 4 (Ddit4), a disintegrin and metallopeptidase domain 8 (Adam8), 3'-phosphoadenosine 5'-phosphosulfate synthase 2 (Papass2), galactin receptor 2 (Galr2), lysine (K)-specific demethylase 3A (Kdm3a), (GCK), (G6Pase)*

The first element of note from this table of genes **(Table 17)** is that it does not indicate a single gene where the loss of *Fih* in the MEFs caused a significant alteration in gene expression compared to wild type, which exceeded the gene expression change caused by the loss of either *Vhl* or both *Fih;Vhl.* The relevance of this could be that this was not a factor that was being assessed in this study or that no such genes were identified in this study. The data set is available through the GEO database and was imported into Genespring software in order to assess this and allow for further comparison between the two data sets. There are multiple ways of importing the data, allowing for the use of all the data or control samples to be used in both normalisation and baseline transformation, and the information on how this was done in the original analysis wasn't available and therefore replicating the analysis was difficult. However, trends that matched with data described in **Table 17** allowed for some interpretation to be made of the data.

## 5.2 The loss of *fih* causes hyperactivity in zebrafish larvae

Observations in the *Fih-/-* mice revealed that these nocturnal animals exhibited a surprising hypo-activity during dark cycles, breaking fewer photo-beams than their wild type littermates, despite an increase in food and water consumption and increased metabolic rate (Zhang et al., 2010). To examine whether analogous effects could be observed in zebrafish *fih* mutants, a Viewpoint imaging system was used to track embryo movements at different stages of development, a system that has been used in multiple studies (Delcourt et al., 2009, Steenbergen et al., 2011, Ellis et al., 2012). After optimising the parameters of the imaging protocols for background optics and tracking abilities various assays were performed. Embryos at 4 and 5dpf were observed both in the light and in the dark, to quantify the levels of movement they exhibit under each condition. Initial experiments observing the activity levels of the zebrafish embryos aimed to assess the embryos response to light and dark cycles, every 15 minutes, see **Figure 68**.

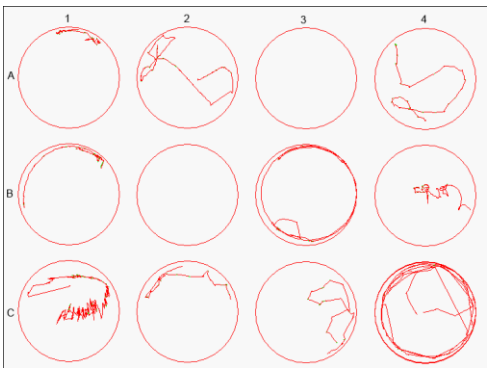


**Figure 68 Plate layout used for viewpoint tracking experiments**

*Using the Viewpoint software for tracking individual embryos the traces are collected over the course of the protocol and can be displayed over the well plate to look at patterns, which the software then uses to provide quantitative data. Plate layout for this example included wild type embryos in wells A1-B2 and fih217/217 embryos in wells B3-C4.*

The parameters of the tests can be grouped to classify particular rates of movement, from low speed, standard and burst movement. The quantified data can then be plotted on a graph to identify the trends in movement over the course of the protocol, in terms of a % of time spent in burst movement, see **Figure 69**.

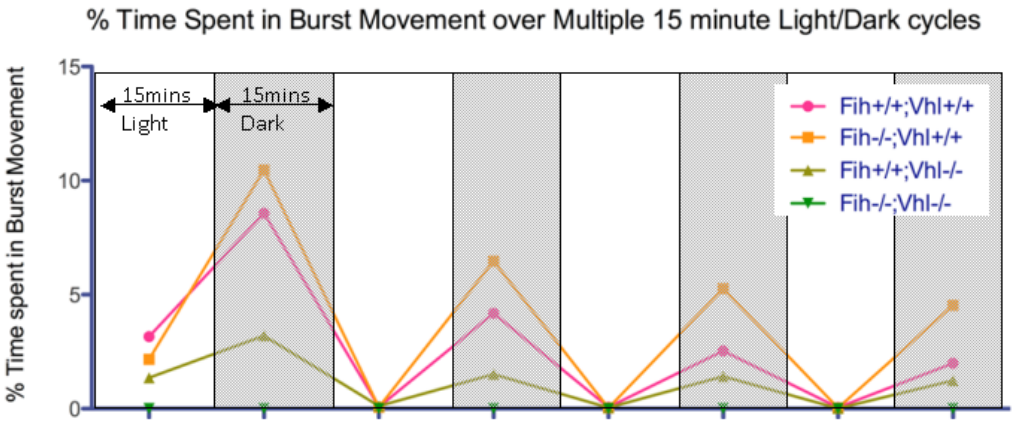


**Figure 69 Graph illustrates startle response to dark**

*% time spent in burst movement increases immediately after the light is switched off and returns to baseline when the lights are switched on. The strongest extent of this pattern was exhibited by fih217/217 embryos.*

The observed activity levels were highest in the dark, with a peak of activity just as the lights were switched off. This was reminiscent of a startle response to a predator being overhead, suggesting that the *fih217/217* embryos had a stronger startle response compared to WT embryos. Studies such as these have been used to assess zebrafish responses to light and their ability to adapt to changing light levels as well as responses to a dark stripe in a circular tank (Li and Dowling, 1997, Fleisch and Neuhauss, 2006). If the pattern of light-dark cycles were repeated and maintained at the same intervals it was observed that in all the groups, the startle response to the lights going off reduced steadily as the fish became habituated to the cycle, a response that has also been previously characterised in the zebrafish (Wong et al., 2010). Overall, the *fih217/217* embryos spent a greater proportion of time in burst movement in the dark cycles compared with the light and also moved more overall than the other genotypes being imaged. The *fih217/217* embryos had a greater startle response to the light being switched off compared with the other embryos.

In order to assess the embryos responses to more physiological light cycles the experiments were repeated recording movement over 24hours between 4 and 5dpf with the lights on the same light cycle as is used in the aquaria, light-dark for 14hours and 10hours respectively, see **Figure 70**.

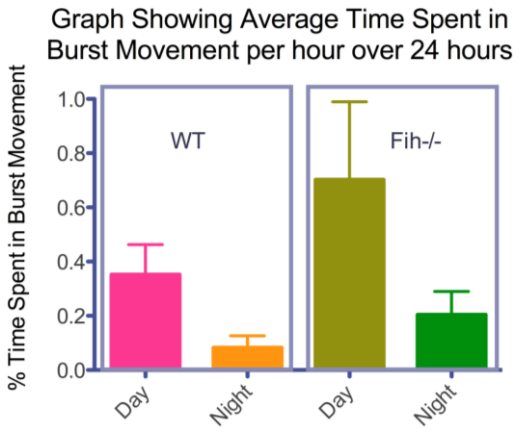


**Figure 70 Graph illustrates average time in burst movement over 24 hours**

*The % time spent in burst movement in light (Day) and dark (Night) cycles over 24 hours. The fih217/217 embryos spend more time in burst movement overall and that is stronger in the light.*

The *fih217/217* embryos spent more time in burst movement compared to WT siblings in the light. Embryos at this age spend the majority of their time in quiescence, and so the proportion of the time the embryos are spending in burst movement only amounts to an average around 1% of the time measured (de Esch et al., 2012, MacPhail et al., 2009). The trend increase in movement supports the data that was observed in the pilot test of 15minute cycles, that the *fih217/217* embryos exhibit a hyperactive phenotype compared with wild type siblings.

As the levels of activity are quite low in young larvae, the next test was to observe the embryos at 10dpf, when movement has become more consistent, and this test confirmed that the *fih217/217* embryos spent more time in motion compared to WT siblings, see **Figure 71** (Lange et al., 2012, Norton and Bally-Cuif, 2010). The protocol involved tracking the embryos more directly, and was able to provide data on total distance swum instead of % time in movement.

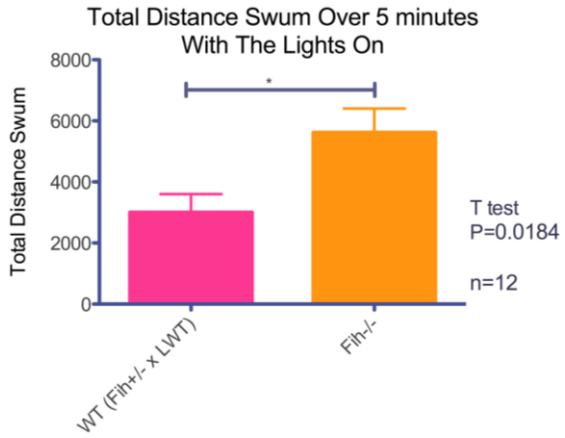


**Figure 71 Graph Illustrates total distance swum over 5 minutes**

*The total distance swum over a five minute period, demonstrates that the fih217/217 embryos swim further than wt siblings. Units of distance are in µM.*

Overall, the *fih217/217* zebrafish exhibited an increased activity level compared to wild type embryos and this did not correlate with the findings in the *Fih-/-* mouse, leading to the need for further interpretation.

Studies by the Bally-Cuif lab into the attention-deficit hyperactivity disorder (ADHD)-susceptibility gene lphn3.1 used knockdown studies to demonstrate hyperactivity in

the zebrafish, connecting this gene with phenotypes that are connected with ADHD. They have also demonstrated that treatment of these morphants with methylphenidate and atomoxetine (drugs used in the treatment of ADHD) rescues the hyperactivity phenotype. Given that fetal hypoxia has been connected with the incidence of ADHD (Toft, 1999, Juarez et al., 2008), MPH (Ritalin) was administered to these embryos and their % change in activity comparing 5 minutes of activity after treatment with 5 minutes of activity before treatment was assessed to investigate the effect of the drug on the hyperactivity phenotype. Over the range of concentrations of Ritalin that were tested and a treatment time of one hour (that used by the Bally-Cuif lab to test their Lphn MO zebrafish) there was no dose at which the activity levels of the *fih217/217* embryos decreased, suggesting either the need for further investigation or that a different mechanism is involved in the hyperactivity in these *fih217/217* embryos, although the data is not shown.

## 5.3 Loss of Fih causes alterations in metabolic factors compared to wild type

Following on from the connection between activity and metabolism that were assessed by Zhang et al in their characterisation of *Fih-/-* mice and leading on from the observations of metabolic gene expression previously described in from the microarray data, several assays were attempted to assess metabolic parameters in the zebrafish.

Increased presence of ATP and reductions in AMPK were observed in the *Fih-/-* mouse embryos, and a fluorescent plate reader assay called ATPLite, was tested in the zebrafish to assess total levels of ATP in the embryos, normalised to total DNA as a surrogate measure of cell number, see **Figure 72**.

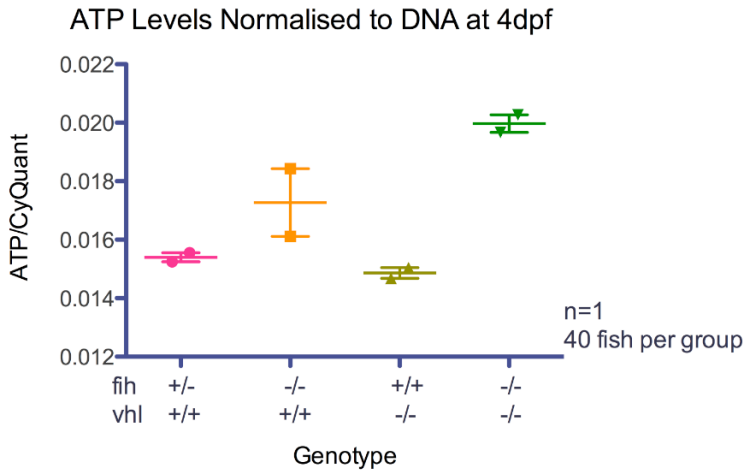


**Figure 72 Graph illustrates ATP levels in wt, *fih217/217, vhl-/-* and *fih217/217;vhl-/-* embryos**

*Graph illustrates the results of a pilot attempt to assess total ATP levels in zebrafish embryos. Replicate samples of 40 embryos were utilised within the assay in order to provide an average.*

The *vhl-/-* embryos did not display an increase in total ATP compared to wild type embryos, however both the *fih217/217* embryos and the *fih217/217;vhl-/-* embryos did and this could suggest a correlation between a high level of activity and the hyper-metabolic phenotype in these embryos, while simultaneously correlating with findings from the *Fih-/-* mouse data. Due to time constraints this assay has only been done once so further repeats are required.

Another pilot test was attempted to assess total levels of cholesterol, as another feature of metabolism which was assessed in the investigation of the *Fih-/-* mouse. This utilised an enzymatic, colourimetric assay developed by Roche and used to assess cholesterol in blood samples. The limitations of the assay include a statement that recovery is possible within ± 10% of initial values at a cholesterol concentration of 5.2 mmol/L (200 mg/dL). This meant that the assay required optimisation on sample preparation and number of embryos because the assay had been largely untested in zebrafish. Large numbers of whole embryos (80+), homogenised in PBS, were required in order to provide a reading on this assay, see **Figure 73**.

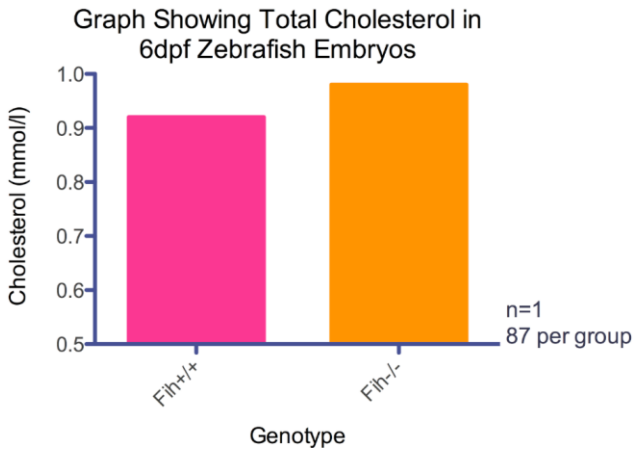


**Figure 73 Graph illustrates total cholesterol level in wt and *fih217/217* embryos**

*Roche Cobas enzymatic assay to quantify cholesterol concentrations in whole zebrafish embryos. The units are provided by the assay, and indicate total cholesterol in mmol per litre of sample.*

Since the assays in the mouse and fish studies have used such different tissue samples It has impossible to compare the results directly, however, to put even this preliminary data into context the study of *Fih-/-* mice by Zhang et al was consulted and here a decrease in total cholesterol was observed, compared with wild type mice. This remained true even when the mice were fed on a high fat diet (HFD) (Supplementary Table 3 (Zhang et al., 2010)). In the mouse study, this was attributed to the *Fih* knockout mice exhibiting improved lipid homeostasis. In this assay, an increase in cholesterol was observed in *fih217/217* embryos at 5dpf. The increase in cholesterol does correlate with the observation that there was an increase expression of *fabp1a* and *fabp1b* in the *fih217/217* embryos. The literature indicates a correlation between increased circulating levels of *fabps* and increased levels of cholesterol/triglycerides/LDL (Xu et al., 2007). The difference in the findings between the two studies could be due to a difference in response to *fabps* or diet between the two animal models, see **Table 17**. It would also be beneficial to investigate potential assays for assessing the differences in levels of TG, FFA, HDL, and LDL/VLDL, in order to interpret information regarding a more accurate profile of lipid homeostasis in the zebrafish, as well as look into the possibility of larger tissue samples using adult zebrafish or even adult serum.

Zhang et al proposed that FIH was involved in the regulation of respiration, energy balance and lipid metabolism in what they suggested might be a HIF independent way (Zhang et al., 2010). The microarray that was performed in this study was utilised to assess the metabolic features of the transcriptome in the zebrafish embryos. However, simultaneous to these targeted searches, more general searches to look for any roles that Fih may play that were independent of Hif, involved the generation of heat maps to create a list of genes where expression was increased in the *fih217/217* embryos but not in the other mutants.

Following the full annotation of this list, using the probe sequences and the Ensembl genome browser BLAST function, revealed that of the 26 genes that were isolated several were connected with membrane/matrix interactions. These genes included integrin α2, glycoprotein A33 (transmembrane), phophatidylinositol glycan anchor biosynthesis, and SWI/SNF, matrix associated, actin dependent regulator of chromatin subfamily d member 1 (*smarcd1*). The finding of increased expression of *smarcd1* led to a targeted search through the microarray for other family members and identified a second probe to the same gene. When the fold change was averaged across both probes the difference in expression between the different mutant groups was obscured, showing it to be two fold up-regulated in all three groups compared to wild type. The SWI/SNF family has been connected with Fih function with ISWI expression resulting in repression of HIF target gene expression (Bnip3 and CA9). It was also possible to assess other family members and identify the expression pattern of expression for *smara5,* which has been shown to be a homologue of the human ISWI. The expression of *smara5* was not altered in any of the three mutant groups, however the expression of both *bnip3* and *cahz* (the active zebrafish CA) is highest in *fih217/217;vhl-/-* embryos. This can not rule out a connection between *fih* and *smara5* regulation of *ca9* and *bnip3*, however this would require further investigation. Aside from this connection this list yielded few potential targets that might indicate genes that might be causative for the phenotypes that had been observed up to this point.

Following this, the same heat map was generated for those genes that were down-regulated in the *fih217/217* embryos and were un changed in the *vhl-/-* and *fih217/217;vhl-/-* embryos, see **Figure 74**.

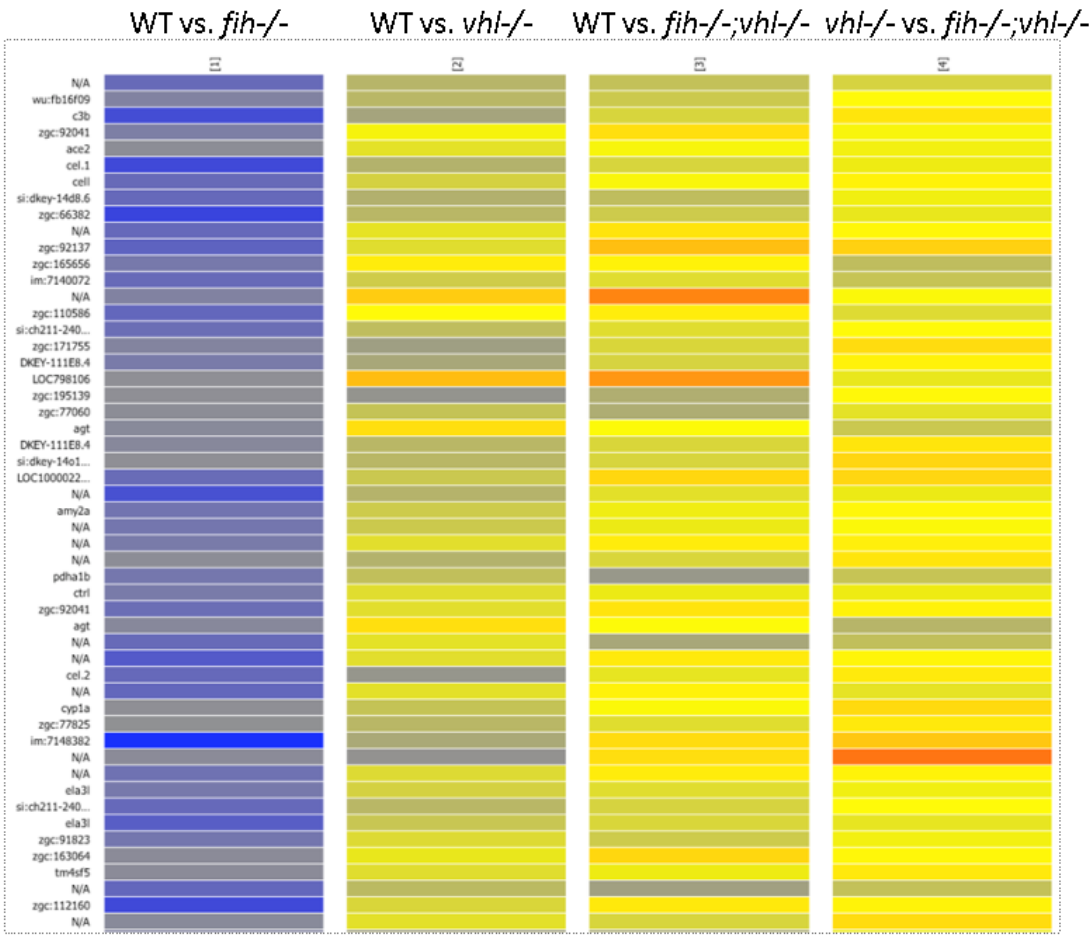


**Figure 74 Heat map illustrates genes down-regulated in *fih217/217* embryos only**

*Heat map illustrates the genes isolated by the venn diagram of up-regulated genes as being up-regulated specifically in the fih217/217 embryos and not the other mutant lines. The list was annotated in excel since the annotation was low for this entity list.*

Many genes were not annotated, but of those that were immediately annotated, two pancreatic enzymes, amylase 2a (*amy2a*) and chymotrypsinogen (*chymo*) both appeared to be down-regulated in *fih217/217* embryos and these genes appear not to be regulated in the other mutants. For confirmation of these trends, qRT-PCR was used to validate the findings and further quantify the changes in expression in the different mutant embryos, see **Figure 75**.

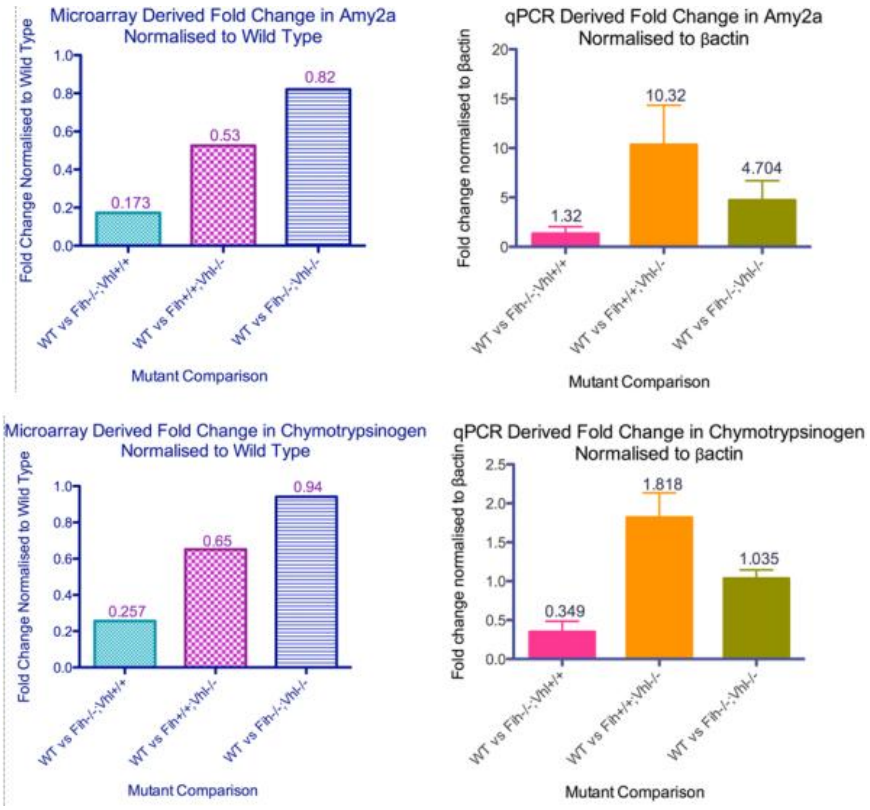


**Figure 75 Graphs demonstrate fold change in *amy2a* and *chymo***

*The quantification of the fold changes of both amy2a and chymo was validated by qRT-PCR. Both assays confirm that these genes are down regulated in the fih217/217 embryos and either up-regulated (in vhl-/- embryos) or unchanged (in fih217/217;vhl-/-).*

The qRT-PCR results for these two genes did not correlate with the microarray data, as had been the case for all previous genes tested. This will need further repeats and the assessment of other genes in this entity list in order to confirm these data.

A further assessment of the genes in the heat-map in **Figure 74**, using the probe sequences to search for the genes that were being assessed, revealed that 25% of genes were known to play roles in fat, sugar/carbohydrate or protein digestion and while these were not all validated by qRT-PCR, the trends have been shown in **Figure 76**Figure 76.

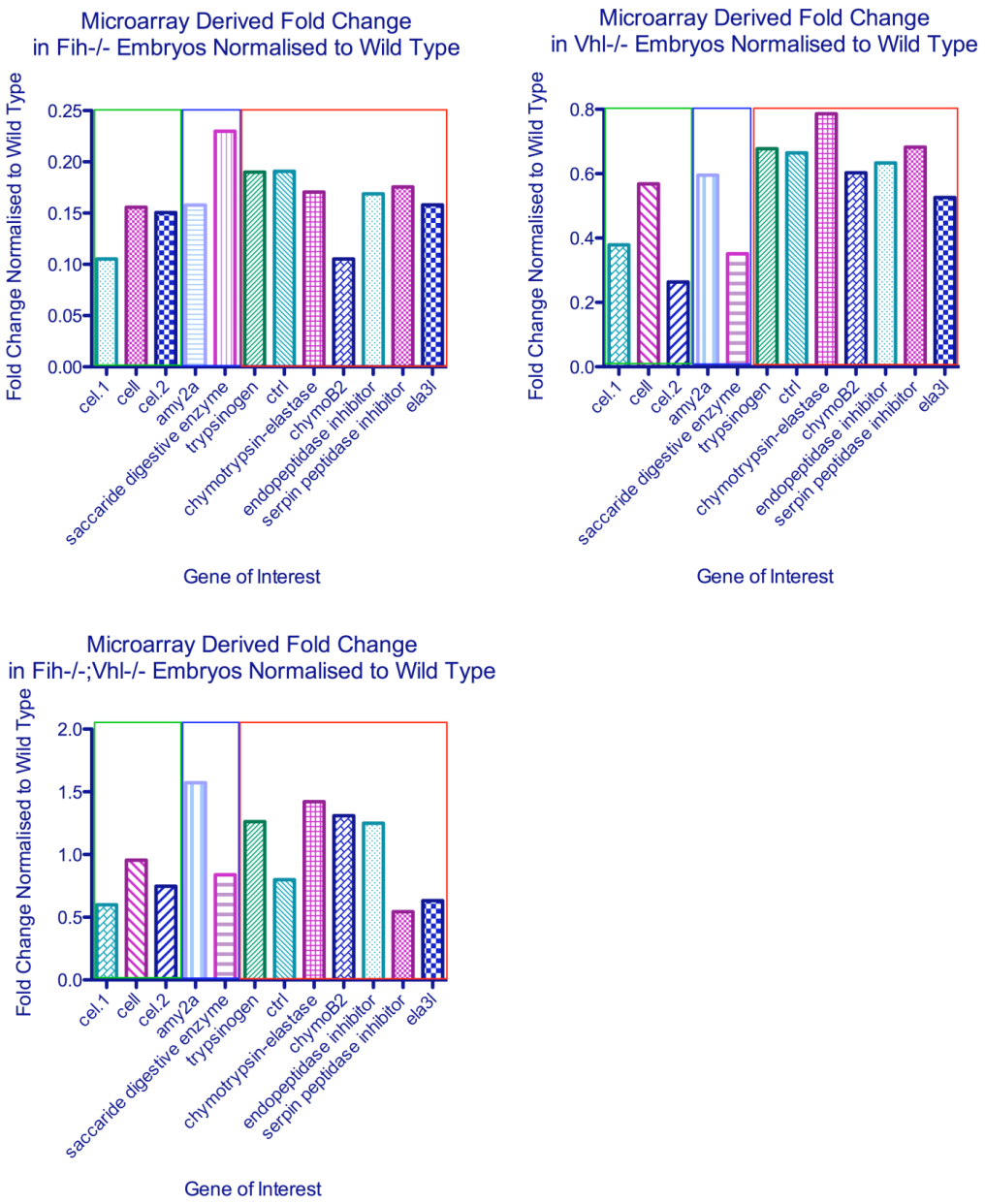


**Figure 76 Graphs indicate fold change in genes involved in metabolism**

*The top left graph indicates the expression of genes involved in digestion, in the fih217/217 embryos, the top right graph indicates the same for the vhl-/- embryos and the bottom left graph indicates the same for the fih217/217;vhl-/- embryos. The left box highlights genes involved in fat digestion, the centre box highlights genes involved in sugar/carbohydrate digestion, and the right box highlights genes involved in protein digestion.* ***Abbreviations:-*** *carboxyl ester lipase 1/2 (cel.1/2), carboxyl ester lipase like (cell), amylase2a (amy2a), chymotrypsin (ctrl), chymotrypsinogen B2 (chymoB2), elasetase-like (ela3l)*

Overall *fih* mutants appear to down-regulate several genes involved in fat, protein and carbohydrate digestion and to a greater extent than in the *vhl* mutants or the *fih;vhl* double mutants.

The investigation of the enzymes in the glycolytic pathway revealed few genes where the expression was significantly different in the *fih217/217* embryos compared with wild type embryos. However, following the annotation of the heat-map of genes that were down-regulated in the *fih217/217* embryos, pyruvate dehydrogenase (lipoamide) alpha 1b (pdha1b) was significantly down-regulated. Investigations of other family members showed that several other members of the family were also down-regulated in the *fih217/217* embryos, see **Figure 77**. Further investigation would be needed to ascertain whether these factors would influence cholesterol synthesis or simply its accumulation.

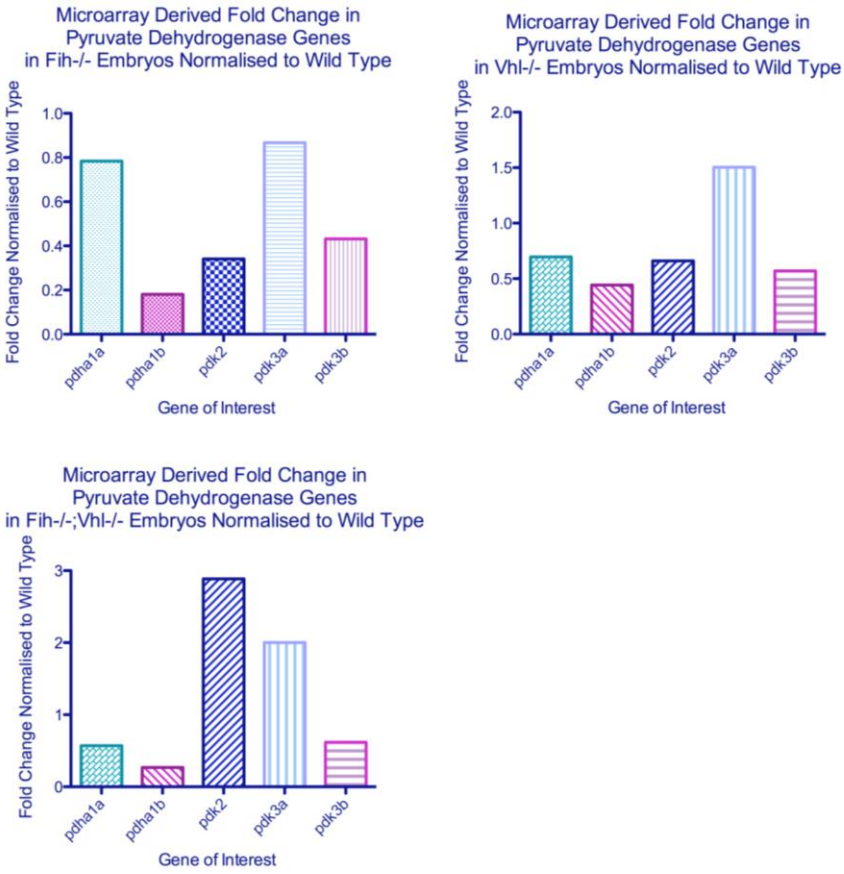


**Figure 77 Graphs indicate fold change in pyruvate dehydrogenase family genes**

*The top left graph indicates the expression of pyruvate dehydrogenase genes, in the fih217/217 embryos, the top right graph indicates the same for the vhl-/- embryos and the bottom left graph indicates the same for the fih217/217;vhl-/- embryos.* ***Abbreviations:-*** *pyruvate dehydrogenase (lipoamide) alpha 1a/b (pdh1a/b), pyruvate dehydrogenase kinase, isoenzyme 2/3/3b (pdk2/3/3b)*

Pyruvate dehydrogenase is a key component enzyme in the pyruvate dehydrogenase complex involved in converting pyruvate into acetyl-CoA. The significant decrease in pyruvate dehydrogenase indicates a decrease in pyruvate to acetyl-CoA conversion, and this might potentially drive the conversion of pyruvate to lactate

## 5.4 Investigation into expression of genes involved in glycolytic metabolism

Entry of glucose into the glycolytic pathway is regulated by 6-phosphofructo-2-kinase/fructose-2,6-biphosphatase 3 (pfkfb3), see **Table 13** and **Figure 78**.

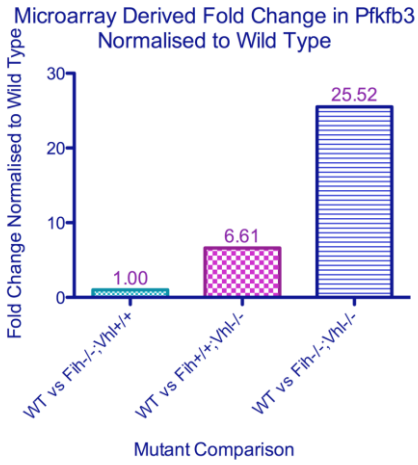


**Figure 78 Fold change in Pfkfb3**

*mRNA levels of expression* 6-phosphofructo-2-kinase/fructose-2,6-biphosphatase 3 (pfkfb3) *were measured by microarray and also validated by qRT-PCR at 3dpf in zebrafish embryos.*

Expression of Pfkfb3 followed the trend seen in *phd3* expression, highest in the double mutant.

Hexokinase1 (hk1) is another glucose sensor (**Table 13**) and its expression levels were assessed in the microarray and one of the genes used for qRT-PCR validation, see **Table 15 and Table 16.**

Flux, or energy transfer, through the glycolytic pathway refers to the adjustment needed to respond to conditions inside and outside the cell, involving the rate of ATP

production and the levels of sugar in the blood, see **Table 13**. Levels of LDH were assessed in the microarray to quantify the change in expression along with *in situ* hybridisation, see **Figure 79.**

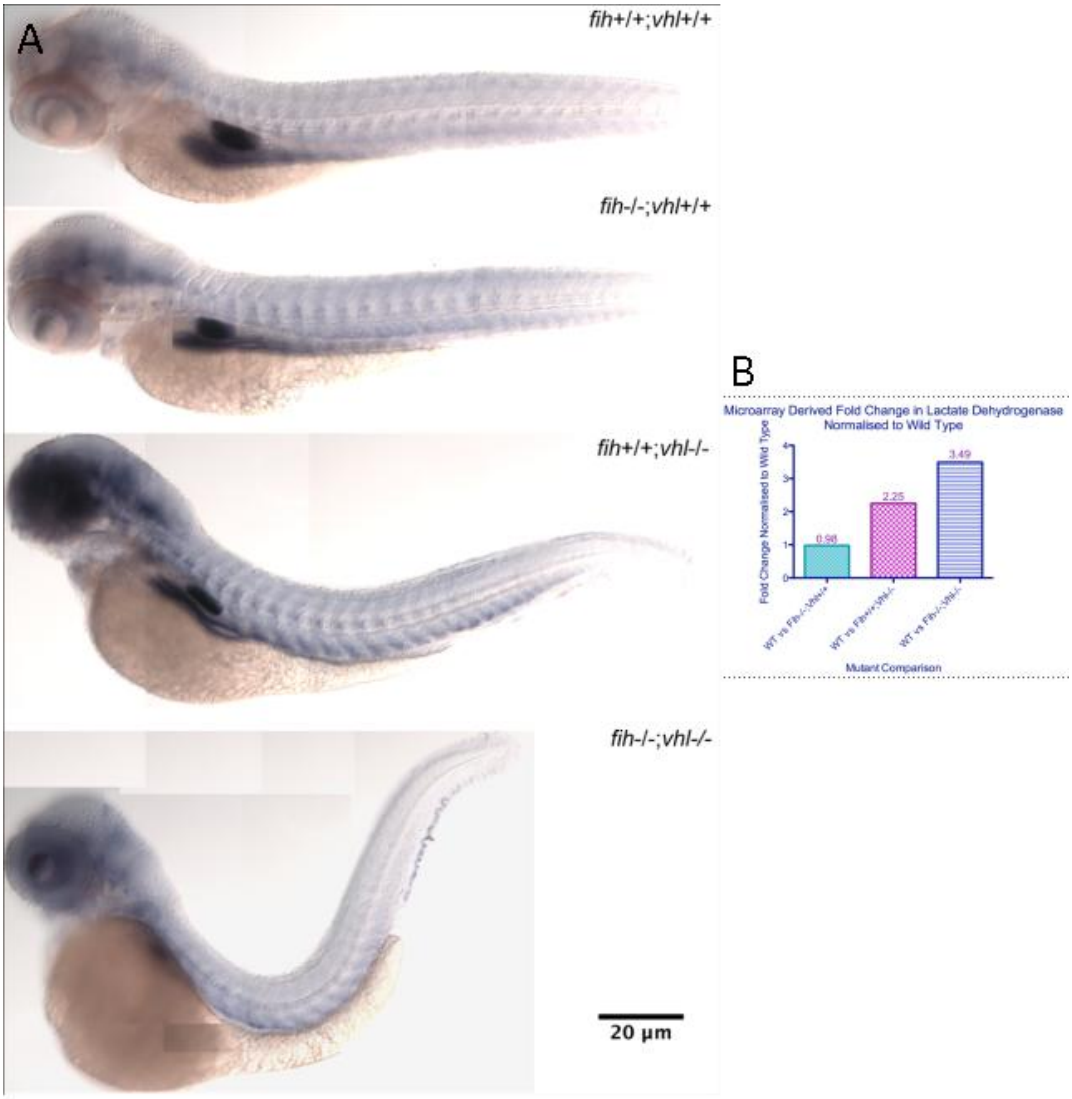


**Figure 79 *in situ* hybridisation of LDH with microarray quantification of expression**

***A)*** *in situ hybridisation techniques (4dpf) were used to assess LDH expression patterns, Expression is visible in the liver, kidneys and head of the zebrafish embryos. These images are composite images stitched together*. **B)** m*RNA derived fold changes in LDH quantified by microarray analysis (3dpf) in zebrafish embryos.*

The *in situ* indicated that there was little alteration in the level and location of LDH expression in the *fih217/217* embryos compared to wild type embryos, the *vhl-/-* embryos do indicate an increase in expression and an expansion of the expression in

the brains of the embryos. Levels of LDH are unchanged in *fih217/217* embryos, but were increased in *vhl-/-* and further increased in the *fih217/217;vhl-/-* embryos in the microarray, these findings correlate in the *fih217/217* embryos by *in situ* hybridisation and also the *vhl-/-* embryos, but not the *fih217/217;vhl-/-* embryos where the *in situ* hybridisation (4dpf) indicated a slight down-regulation.

## 5.5 Investigating effect of loss of *fih* on genes involved in insulin homeostasis

Components of the insulin and the gluconeogenesis pathway (the reverse process to glycolysis, the conversion of lactate to glucose) that were annotated in the microarray data-set, were assessed for expression in the *fih217/217, vhl-/-* and *fih217/217;vhl-/-* embryos, see **Table 13** for references. These data show that again *fih* results only in minor changes in expression of these genes, whereas *gcga* shows increasing expression going from *vhl* mutant to *fih;vhl* doubles, suggesting this gene is regulated via HIF. The expression of *pepck,* a lyase enzyme in the gluconeogenesis pathway, providing the reverse step from pyruvate kinase (the 7th step in the conversion of glucose to pyruvate) was assessed by qRT-PCR, see **Table 13** and **Figure 80**.

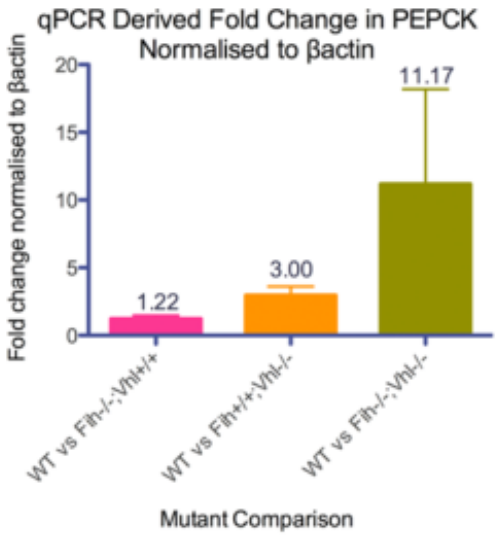


**Figure 80 mRNA levels of PEPCK were assessed by qRT-PCR at 3dpf in zebrafish embryos.**

Expression levels of *pepck (*see **Table 13**) were elevated in the *fih217/217* zebrafish to the same degree as had been found in the *Fih-/-* mice. Preproinsulin levels, see **Table 15 and Table 16**, were essentially unchanged or conceivably slightly decreased in the *fih217/217* embryos, and increased only slightly in both the *vhl-/-* and *fih217/217;vhl-/-* embryos.

Glucose transport was assessed in the zebrafish embryos by looking at levels of glucose transporter 1 (*glut-1/slc2a*), see **Figure 81.**

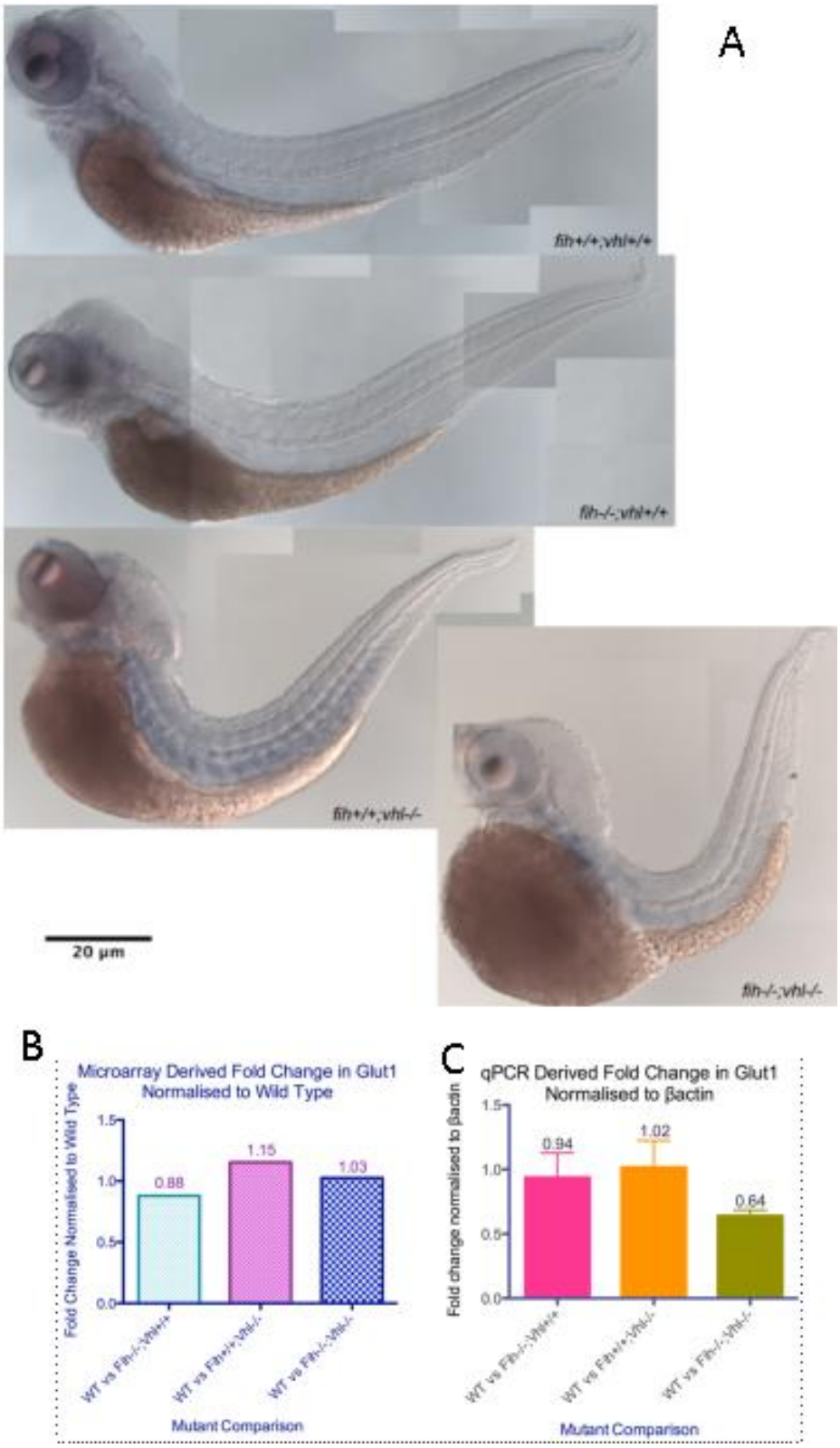


**Figure 81 *in situ* hybridisation of Glut1 with microarray and qRT-PCR quantification of expression**

**A)** *Demonstrates the in situ expression pattern of Glut1 mRNA in the different mutant embryos at 4dpf. These images are composite images stitched together.* ***B)*** *mRNA expression levels of Glut1 were quantified by microarray* ***C)*** *validated by qRT-PCR in 3dpf old zebrafish embryos*

The expression of Glut1 in the zebrafish at 3dpf by *in situ* did not show dramatic differences between the *fih217/217* embryos and the *fih217/217;vhl-/-* embryos, and this lack of significant difference was quantified by the microarray and qRT-PCR data**.** Levels of *glut1* can be confirmed as not to be significantly different across all three mutants, indicating that despite hypoxic regulation of the gene, its expression is not dramatically induced by the loss of either *fih* or *vhl,* or indeed by the loss of both. While there was no significant change in its expression at 3dpf these might become clearer over time, see **Table 13**. When assessing genes involved in glucose homeostasis and insulin regulation one of the other genes where expression was elevated was *fabp1a.*

In the *fih217/217* embryos, only fatty acid binding protein (*fabp1a)* was up-regulated, to a significant degree and more of these genes were up-regulated in the *vhl-/-* and *fih217/217;vhl-/-* embryos. Since *fabp1a* was elevated in all three of the *fih217/217, vhl-/-* and *fih217/217;vhl-/-* embryos, so further investigation was made into the expression of other members of the *fabp* gene family by searching through the microarray data set for other family members, see **Table 13** for references.

## 5.6 Investigating effect of loss of *fih* on genes involved in $O_2$ consumption and $CO_2$ evolution

The link to mitochondrial roles in metabolism led to the assessment of some of these genes in the *fih217/217* and *vhl-/-* zebrafish. Increased $O_2$ consumption can be caused by changes in uncoupled mitochondrial respiration and expression of mitochondrial uncoupling genes has been used as a surrogate for assessing this by Zhang et al (Zhang et al., 2010). Here they found increased expression of *Ucp1* and *Ucp3* in the brown adipose tissue (BAT) of the *Fih-/-* mice. The only uncoupling protein that was directly annotated in the zebrafish array was labeled *ucp4*. Using Ensembl genome browser and the sequence of the probe on the microarray it was possible to see that this was mis-labeled in the microarray annotation and actually mapped to the zebrafish *ucp1* gene an orthologue of the human *UCP1*. A further search found the *slc25a27* gene,

using Ensembl it was possible to show that this was the zebrafish *ucp4* gene. See **Table 15** for the gene regulation of three of these *ucp* genes in the zebrafish embryos.

Another gene that has been used both as a surrogate and in the direct assessment of $CO_2$:$O_2$ ratios and usage is carbonic anhydrase (CA), see **Table 13** and **Figure 82.**

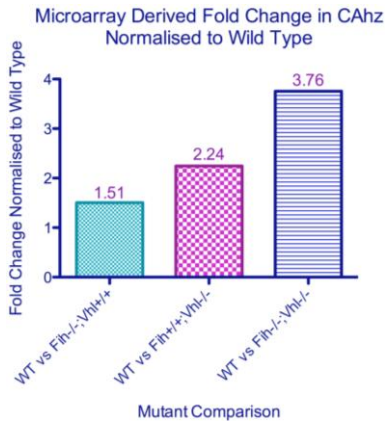


**Figure 82** *Microarray derived Cahz expression in the fih217/217, vhl-/- and fih217/217;vhl-/- embryos at 3dpf.*

## 5.7 Relationship between apoptosis and hypoxia

The connection between hypoxia and apoptosis has been a source of research and certain levels of uncertainty, **Table 13**. In the analysis of *Fih-/-* mice the expression of *BNIP3, a* pro apoptotic/autophagic gene, was unaltered in the brains of these mice. The microarray in this study having been performed on whole zebrafish embryos provided an opportunity to assess the apoptotic pathway in a more global sense and in the whole organism, see **Figure 83** for the findings.

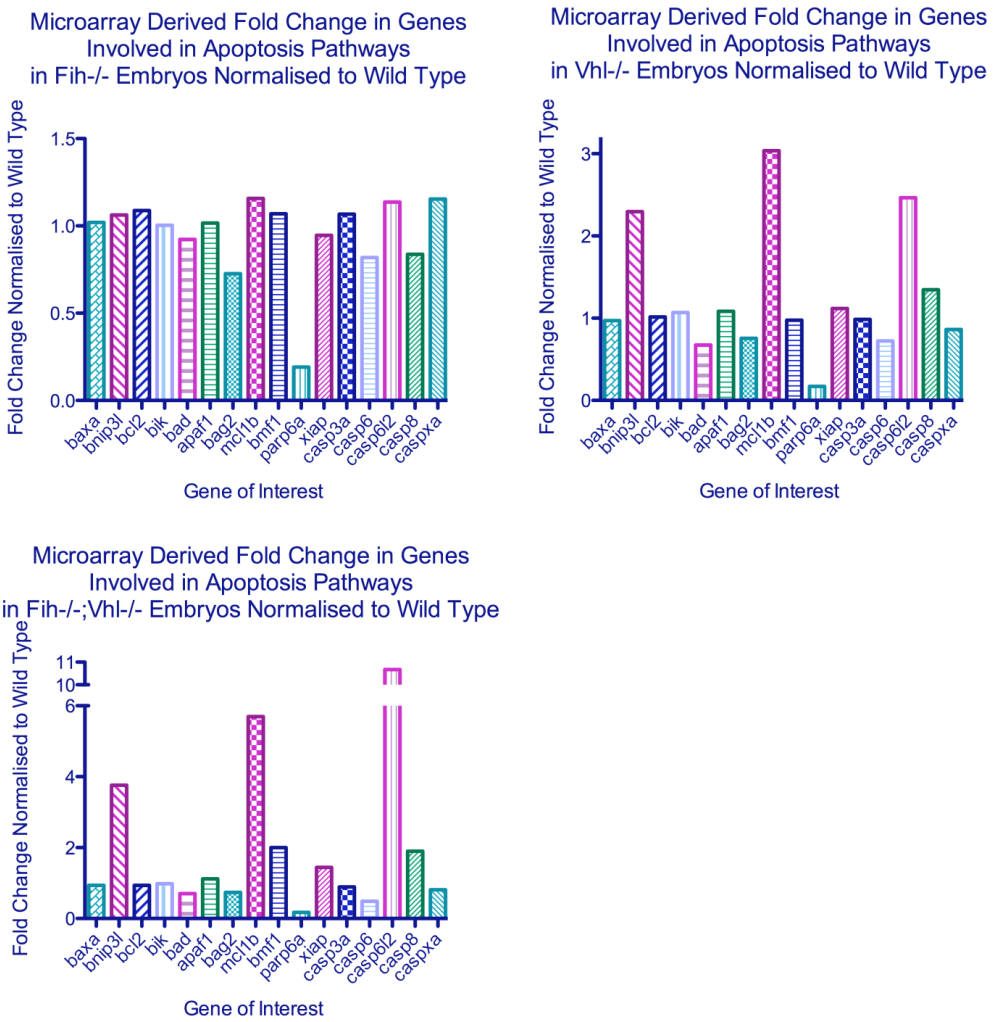


**Figure 83 Fold change of genes involved in apoptosis**

*The top left graph indicates the expression of genes involved in apoptosis in the fih217/217 embryos, the top right graph indicates the same for the vhl-/- embryos and the bottom left graph indicates the same for the fih217/217;vhl-/- embryos.* ***Abbreviations****:- bcl-2 associated X protein (baxa/b), bcl2/adenovirus E1B interacting protein 3-like (bnip3l), B-cell leukemia/lymphoma 2 (bcl-2), bcl-2-interacting killer (bik), bcl-2 antagonist of cell death (bad), apoptotic protease activating factor (apaf1), bcl2 associated athanogene (bag2), myeloid cell leukemia sequence (mcl1), bcl2 modifying factor 1 (bmf1), poly (ADP-ribose) polymerase family (parp), X-linked inhibitor of apoptosis (xiap), caspase (casp)*

In the zebrafish, there were changes in gene expression in several apoptotic genes investigated, both up-regulated (Bnip3l) and down-regulated (parp6a).

## 5.8 Discussion

Furthermore we obtained data consistent with a metabolic phenotype as was proposed by Zhang et al for the *Fih-/-* mice. To put the data linking the loss of FIH in both the mouse model published by (Zhang et al., 2010) and in the current study a summary table of the findings was collated, see **Figure 15**.

| | **Fih-/- mice** | **Fih217/217 zebrafish** |
|---|---|---|
| | (Zhang et al., 2010) | Current study (Unpublished data) |
| **ATP** | Increased | Increased (tentative) |
| **$0_2$ consumption and $CO_2$ evolution** | Increased | |
| **Heart Rate** | Increased | Increased |
| **Tidal Volume** | Increased | |
| **Water and Food Intake** | Increased | |
| **Activity Levels** | Decreased | Increased |
| **Heat production** | Increased | |
| **UCP genes** | Increased (1 and 3) | No change UCP1, 4 or 5 |
| **PGC1a level** | Increased | No change |
| **Insulin sensitivity** | Increased | |
| **RER** | No change | |
| **AMPK** | Decreased | |
| **Plasma EPO after hypoxia** | Decreased | No change in RNA by *in situ* |
| **Mass/body weight** | Decreased | |
| **Adipocyte size and lipid droplet number** | Decreased | |
| **Cholesterol and triglyceride** | Decreased | Increased (tentative) |
| **Fed Insulin levels** | Decreased | |
| **Weight gain on HFD** | Decreased | |
| **Breathing Frequency** | No change | |
| **Heart Size** | | No change |
| **Aortic Diameter** | | Increased |
| **Blood glucose** | No change | No change in preproinsulin – surrogate marker as response to insulin stimulus |

**Table 18** *Table describes the correlation of findings between the current study and that of (Zhang et al., 2010) in the Fih-/- mouse.*

Further investigation is needed before correlation between these two studies can be confirmed although **Table 18** indicates common investigation directions from the two

studies and shows that similar phenotypes are observed in the two different models, mouse and zebrafish. For example, since the *fih217/217* embryos survive to adulthood, assessments could be made regarding body mass and indeed potentially into weight gain on a high fat diet, provided that clutches of embryos were raised at the same density under the same conditions. Breathing frequency has not been checked in the *fih217/217* zebrafish embryos, and this could be done. Also new platforms are being developed for the observation of $O_2$ consumption and $CO_2$ evolution in the zebrafish embryo (Stackley et al., 2011, Pei et al., 2010, Barrionuevo and Burggren, 1999, Makky et al., 2008). Oil-Red-O and other stains can be used on frozen sections of zebrafish to assess lipid droplet size. These would provide further connections between the findings in the different models and may elucidate differences that aid in species or indeed tissue specific findings.

### 5.8.1 Metabolism

Following the publication of the findings of Zhang et al on the characterisation of the *Fih-/-* mouse model displaying features consistent with altered metabolism, genes involved in regulating metabolism were assessed in the microarray. This revealed that all of the enzymes involved in the conversion of glucose to lactate, which were annotated in the microarray, increasing numbers tended to be up-regulated to a greater extent in the *fih217/217;vhl-/-* embryos compared with *fih217/217* embryos alone. The expression levels of two enzymes at the extreme ends of the pathway, hexokinase and lactate dehydrogenase, were validated by qRT-PCR and *in situ* hybridisation, confirming the findings from the microarray. This trend suggested that the loss of *fih* in the *vhl-/-* embryos played a part in increasing the activity within the glycolytic pathway; however this remains to be tested and confirmed.

Since levels of pyruvate kinase, a rate limiting enzyme in the glycolysis pathway has also been shown to be influenced in obesity (Stolz and Martin, 1982), the level of expression of many of these enzymes was assessed using the raw microarray data. Levels of pyruvate kinase and other enzymes were not dramatically altered by the loss of *fih*, but many demonstrated elevated expression in the *vhl-/-* and *fih217/217;vhl-/-* embryos. This suggests that these genes are regulated by HIF dependent signaling and that the loss of *fih* alone was not sufficient to induce their transcription, while the loss

of *vhl* or the dual loss of both *fih* and *vhl* was. This correlated with published literature which has shown that glycogen storage and the induction of genes involved in glycolysis has been shown to be regulated by both HIF-1 and HIF-2 (Pelletier et al., 2012) and the up-regulation of glycolysis enzymes in the *fih217/217;vhl-/-* embryos correlates with strong induction of glycolysis in these embryos. Overall our data show only very mild effects on glycolytic enzymes in *fih* mutants and they are responsible metabolic phenotype in zebrafish *fih* mutants it is most likely the result of a very mild HIF activation rather than a unique HIF independent effect of *fih.* The assessment of metabolism and its regulation in Chuvash mice/Chuvash patients could provide some indications of whether alterations in metabolism are HIF-dependent, if for example glycolytic enzymes were differentially regulated in response to the loss of *vhl* only as in these models.

Similar results were obtained while assessing genes involved in glucose and fatty acid regulation in the microarray data-set *igfbp-1* and *fabp1a* stood out in these sets and were shown to be unchanged or up-regulated in the *fih217/217* embryos, further up-regulated in the *vhl-/-* embryos and further up-regulated in the *fih217/217;vhl-/-* embryos, with the same expression pattern seen for several other family members of each gene. Insulin growth factor binding proteins (IGFbps) perform regulatory roles on the IGFs mediating their functions. IGFbp-1 has been shown to be increased in fetuses exposed to hypoxia and intrauterine growth restriction (Tazuke et al., 1998) and is an established HIF target (Kajimura et al., 2005, Tazuke et al., 1998).

While assessing the connection between mitochondria and metabolism, as well as investigations concurrent with those in *Fih-/-* mice, the levels of mitochondrial uncoupling proteins (ucp) were investigated in the microarray. Expression of *ucp1* showed the expression profile over the mutants that had been seen for other hypoxic targets, lowest/unchanged in *fih217/217* embryos and highest in *fih217/217;vhl-/-* embryos. The expression of *UCP1* was shown to be significantly up-regulated in brown adipose tissue (BAT) in FIH nullizygous mice, along with levels of *PGC-1α,* while levels of *UCP2* and *UCP3* were similar between genotypes, along with *PGC-1α* in white adipose tissue (WAT). Since BAT has not been characterised in the zebrafish and the microarray was performed on whole organisms rather than tissue specific sections, direct comparisons were not possible. However it is possible to see that of the three

*ucp* genes that were annotated in the microarray (1, 4 and 5) none were up-regulated in the *fih217/217* embryos, although *ucp1* expression was up-regulated in the *fih217/217;vhl-/-* embryos.

In order to investigate the regulation of the glycolytic pathway in the zebrafish mutants, the microarray data was searched for the enzymes known to be involved in the conversion of glucose to lactate. All but a few (hexose diphosphate, fructose biphosphate aldose, phosphoenolpyruvate carboxykinase (pepck)) of the enzymes involved in the glycolytic pathway were annotated in the microarray and their expression was assessed in all three mutant groups. Of all these glycolytic enzymes, the majority were not differentially regulated in the *fih217/217* embryos but were strongly up-regulated in the *fih217/217;vhl-/-* embryos.

The up-regulation of *hk1* fits the trend in expression observed in other genes such as *phd3*, with a slight up-regulation in the *fih217/217* embryos, a further up-regulation in the *vhl-/-* embryos and a further up-regulation in the *fih217/217;vhl-/-* embryos. This correlates with the established connection between HIF-signaling and the glycolytic pathway and could be correlated with HIF target gene expression induced by the loss of FIH and/or VHL regulation. The expression does not give a strong indication for a HIF independent role for fih in *hk* expression.

Overall, these data do not give evidence that glycolytic enzymes are regulated by FIH rather than directly by HIF, which correlates with suggestions made by Zhang et al that while the *Fih* null mice exhibited an increased metabolic rate there was no observation of alterations in glucose homeostasis in these animals.

The microarray was performed at 3dpf and the *in situ* needs to be repeated, at the same stage as the microarray and the qRT-PCR assays (3dpf) in order to assess the discrepancy that was seen in the results. It may be due to possible proteasomal changes or via an impact on VHL/HIF interactions, see **Table 13**, this needs to be investigated further.

### 5.8.2 Insulin Homeostasis

Expression of *pepck* was increased dramatically in the *fih217/217;vhl-/-,* not demonstrated in the Zhang paper, suggesting an attempt to reverse glycolysis and convert pyruvate back to glucose in these embryos. The expression of *pepck* has also been shown, however, to be induced by the release of glucagons in cultured rat hepatocytes (Christ et al., 1997), and the expression levels of glucagons (data not shown) follows the same expression trend in these zebrafish embryos as that seen in **Figure 80** for *pepck.* The correlation of these findings leads to the suggestion that analysis of glucagon-pepck interactions might be an avenue of investigation worth pursuing.

Conditional inactivation of von Hippel-Lindau-like (*vhlh)* in β-cells promoted diversion of glucose away from mitochondria into lactate production, inducing increased glycolytically derived ATP and the secretion of elevated levels of insulin at lower glucose concentration (Zehetner et al., 2008). A targeted deletion of *Vhlh* pancreatic islet cells of mice allowed the assessment of responses to glucose, these mice exhibit diminished glucose stimulated changes in cytoplasmic $Ca^{2+}$, electrical activity and insulin secretion, indicating impaired systemic glucose tolerance, which can be rescued in *vhl-/-;hif-1α-/-* mice (Zehetner et al., 2008). The activation of preproinsulin in the *fih217/217;vhl-/-* embryos indicates that this process is being induced in these embryos and the slight activation seen at 3dpf could indicate that further increases might be seen at later stages. The minor alterations in *pepck* and *preproinsulin* expression observed in the *fih217/217* zebrafish indicate that control of glucose response is unlikely to be specifically regulated by FIH.

Circulating levels of *fabp* can be shown to correlate with metabolic risk factors including central adiposity, dyslipidemia (increased serum triglycerides and decreased high-density lipoprotein (HDL) cholesterol), fasting glucose, insulin resistance and blood pressure (Xu et al., 2007). These correlate with findings of increased expression of *fabps,* as well as with observed metabolic phenotypes in the *Fih217/217* mice and suggests that similar characteristics may be present in the *fih217/217* fish. However the mice demonstrated a decrease in serum triglycerides and cholesterol even when fed on HFD (Zhang et al., 2010), indicating a discrepancy that will be discussed in **Chapter 5**.

One member of the FABP family to show consistent down-regulation, contrary to the others, in all three zebrafish lines in this study was *fabp6* (data not shown). Ileal-type *fabp6,* also known as gastrotropin or bile-acid binding protein (*babp1)*, is dramatically down-regulated in all three zebrafish mutants being examined in this study. Its over-expression has been connected with cancer types as well as type2 diabetes (Fisher et al., 2009, Ohmachi et al., 2006). Its expression in the zebrafish has been shown in the liver, heart, intestine, ovary and kidney of adult fish by qRT-PCR and *in situ* hybridisation (Alves-Costa et al., 2008). The ligands of FABP6 are thought to be bile salts, indicating the involvement of FABP6 in their uptake from the ileal epithelium, and it has also been implicated in steroid metabolism (Alves-Costa et al., 2008). its down-regulation in all three of the zebrafish mutants being studied in this project indicates a potential increase in the levels of free bile salts, the synthesis of which is a major route of cholesterol metabolism in most species besides humans (Hofmann and Borgstroem, 1964). About 90% of excreted bile acids are reabsorbed by active transport in the ileum, potentially via *fabp6,* and recycled, moving them from the intestine to the liver and gallbladder (Hofmann and Borgstroem, 1964). In a mouse model of cholangiocyte bile salt transporters, the functional state of FABP6, the expression of which was shown to be decreased by feeding a lithogenic diet (0.5% cholic acid, 1% cholesterol and 15% dairy fat) was thought to influence the uptake of bile salts (Liu et al., 2008). The relationship between these findings and cholesterol production and metabolism could therefore be worthy of further investigation in the zebrafish.

The data also indicated decreased expression in adiponectin, which is an insulin-sensitising adipokine (biologically active molecule involved in maintaining cardiovascular homeostasis) with wide ranging implications in anti-diabetic, anti-atherogenic, anti-inflammatory and cardio-protective mechanisms (Wang et al., 2008, Xu and Vanhoutte, 2012). Expression of both *adipo-like, adipo-like2* and *adipoR1a/b/2* is, if anything, down-regulated in the *fih217/217* zebrafish as well as the *vhl-/-* embryos, and further down-regulated in the *fih217/217;vhl-/-* embryos. In *Fih-/-* mice, adipocyte area and size has been shown to be decreased compared with wild type siblings (Zhang et al., 2010), which could correlate with the decreased expression of adiponectin seen in the *fih217/217, vhl-/-* and *fih217/217;vhl-/-* zebrafish.

### 5.8.3 O2 consumption and CO2 evolution

The minor down-regulation of *ucp1* in the *fih217/217* embryos indicates is inconsistent with a predicted increase in expression, as was seen for *ucp1* and 3 in the *Fih-/-* mouse brown adipose tissue (BAT) and skeletal muscle (SM) although *ucp2* is slightly down-regulated in the *Fih-/-* mouse BAT and slightly up-regulated in the *Fih-/-* SM (Zhang et al., 2010). *Ucp1* was up-regulated in *vhl-/-* and *fih217/217;vhl-/-* embryos, which does correlate with expected alterations in expression and could be used as a surrogate to infer increased energy expenditure in these embryos. *Ucp4 (slc25a27)* and *ucp5 (slc25a14)* are not differentially regulated in the *fih217/217* embryos but could be considered to be slightly down-regulated in the *vhl-/-* and *fih217/217;vhl-/-* embryos. The zebrafish is an ectothermic species, i.e. they do not raise their body temperature above ambient by producing heat, so the presence of *ucp* homologues suggested that their role in the teleosts was not related to thermogenesis, as seen in mammals (Stuart et al., 1999). Expression of *UCP1* has been shown to be continuously expressed during differentiation and reduced total lipid accumulation, decreased glycerol and lactate output and increased glucose uptake (Si et al., 2007). Up-regulation of *ucp1* was proposed to reflect a down-regulation of fat synthesis, rather than an up-regulation of fatty acid oxidation, *in vitro* (Si et al., 2007), which ties this data in with altered expression seen for *fabp* family members as well as *adiponectin*. Further investigation would need to be performed in order to draw conclusions as to the interaction between these gene expression changes and oxygen consumption and/or fatty acid metabolism.

The elevated expression pattern, highest in the double *fih217/217;vhl-/-* embryos correlates with findings for *Car9* expression in the study of *Fih-/-* mice performed by Zhang et al, which was used to propose their hypothesis that there are a selection of genes that are highly dependent on FIH derived control of HIF when VHL is absent (Zhang et al., 2010). However we only found a very modest enhancement of expression suggesting differences in regulation at 3dpf, so further investigation of alternative stages, along with alternative assays to investigate $O_2$ consumption and $CO_2$ evolution would be necessary to draw further conclusions. It would be informative to be able to assess respiratory acidosis, as had been performed in the

mouse, however the investigation of a method for how to achieve this in the zebrafish is ongoing.

### 5.8.4 Apoptosis

Of the biomarkers of apoptosis that were annotated in the microarray several exhibited the expression profile seen for other hypoxic targets, most were lowest or unaltered in *fih217/217* embryos, which conforms with the mouse data, up-regulated in the *vhl-/-* embryos and further up-regulated in the *fih217/217;vhl-/-* embryos. This included the Bcl2/adenovirus E1b 19kDa interacting protein 3a (Bnip3l), a hypoxia induced gene which has been shown to contain an HRE in its promoter region (Bruick, 2000, Zhang et al., 2007). Over-expression of *BNIP3* reduces membrane potential of mitochondria, leading to dysfunction and the resulting caspase-independent apoptosis (autophagy) (Zhang et al., 2007). It has been shown that the ablation of an autophagy mediator *Beclin1,* enhances cell death under hypoxic conditions and that the ablation of *Bnip3* and/or *Bnip3l* also triggers cell death, implicating them in hypoxia-induced autophagy (Bellot et al., 2009).

Expression of *casp6l2* exhibited the same trend in expression in each of the three mutants as *bnip3*. Caspase-6-like 2, was identified for its role in cleavage of nuclear lamins, as well as caspase-2, 3 and 8 and deemed an executioner caspase.

In conjunction with the already established up-regulation of both pro- apoptotic markers by hypoxia based on the conditions, one of the other genes that showed the same expression pattern as *bnip3* in the three mutants was *mcl1. Mcl1* is one of several anti-apoptotic *bcl-2* family member genes (Glaser et al., 2012). The induction of both pro- and anti-apoptotic genes indicates the overall effect will be difficult to predict.

# 6 Regulation of Cardiovascular Development and Function

The difference in the roles of both FIH and VHL with respect to regulation of HIF (see **Figure 6)** could be hypothesised to result in different effects on the transcription of HIF target genes. The expression of HIF target genes, as assessed using microarray data, indicate that Fih exerts its effects on the transcriptome mainly through HIF as indicated in **Figure 6**. The majority of the data from both physiological assays and the microarray at this point had indicated that the loss of *fih* in the zebrafish while affecting the phenotypes of the *vhl-/-* embryos, created no quantifiable physiological phenotypes compared to wild type siblings.

## 6.1 Effect of *fih* on aorta and blood circulation

### 6.1.1 Loss of *fih* causes an increase in aortic diameter compared to WT siblings

Imaging studies of the vasculature in *fih217/217, vhl-/-* and *fih217/217;vhl-/-* zebrafish embryos compared with wild type siblings, described in **Chapter 3**, showed few measurable physiological differences between wild type and *fih217/217* embryos. The heart of the *fih217/217* embryos was not measurably different compared with wild type embryos. There were no changes in the number of ISVs or in the branching profile of the vessels in the *fih217/217* embryos compared with wild type embryos. This was also true of the *Fih-/-* mice, where vascular branching phenotypes were assessed by imaging of the ears and no significant differences were observed.

Closer inspection of images of the blood vessels from image deletion angiograms were analysed for vessel diameter and showed that the *fih217/217* embryos had a small but significant difference in aortic diameter compared with WT siblings, see **Figure 84.**

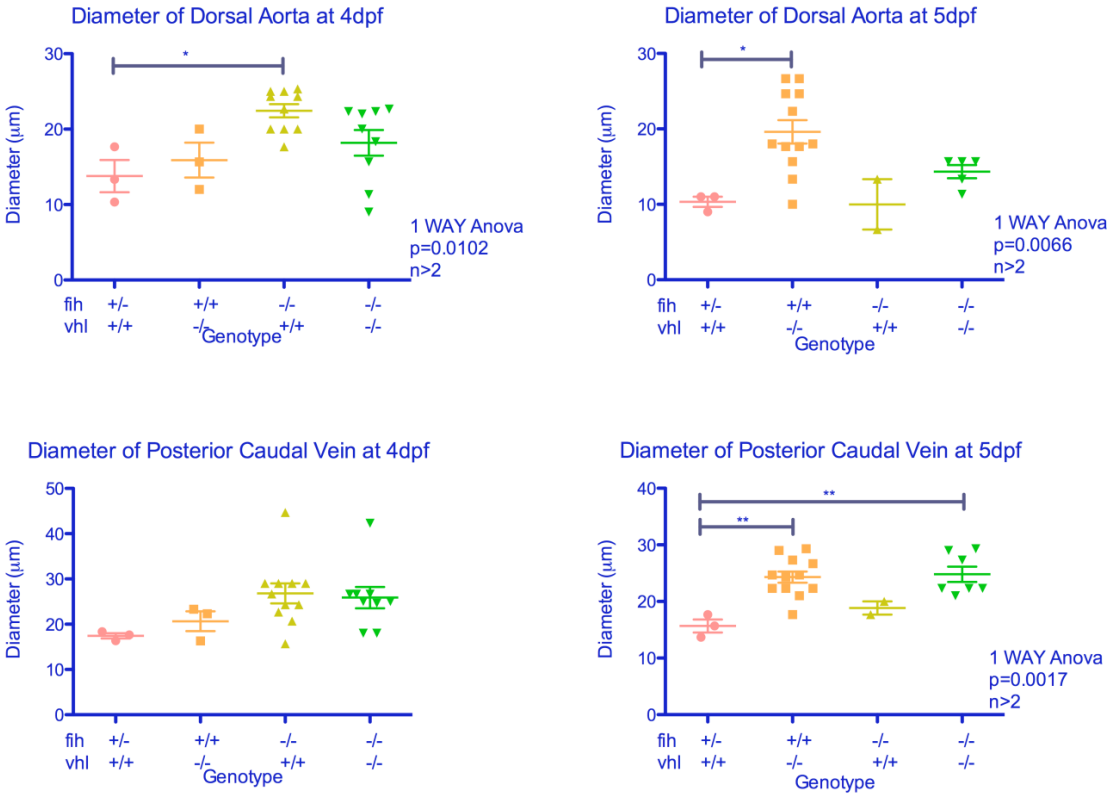


**Figure 84 Quantification of Diameter of Dorsal Aorta and Posterior Caudal Vein**

*ImageJ was use to measure the internal diameter of the two major vessels, the dorsal aorta and the posterior caudal vein, of embryos imaged for Image-deletion-angiograms.*

The level of change in the vessel diameter in these embryos remained small and because the angiogram data set required post-imaging genotyping, the number of embryos of each genotype was skewed. Assessing the diameter of the dorsal aorta over time showed that the diameter of the aorta in *fih217/217* embryos and WT siblings stayed constant between 2-5dpf. The *vhl-/-* embryos had a significantly wider aortic diameter compared with *fih217/217* embryos and WT siblings. The further loss of *fih* in the *vhl-/-* embryos resulted in a slightly wider aortic diameter compared with *vhl-/-* embryos up to 4dpf, see **Figure 85**Figure 85.

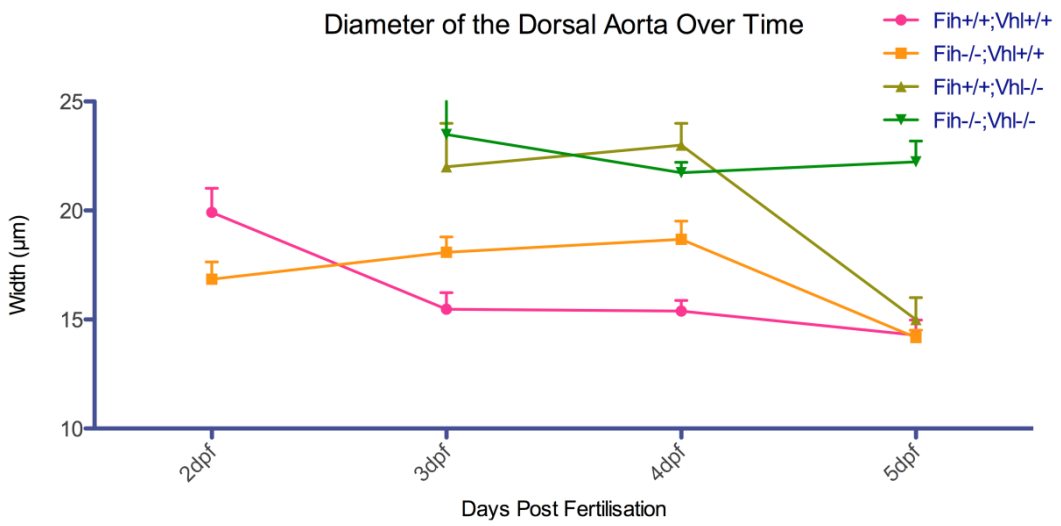


**Figure 85 Assessment of diameter of dorsal aorta over time.**

*Each point represents the average diameter from 3-12 embryos and the error bars indicate standard deviation.*

Since the *fih217/217* zebrafish develop to adult hood, null animals can be isolated in tanks and in-crossed, allowing for increased numbers of embryos to be analysed without the need for post-analysis genotyping. For this experiment careful staging was done to prevent age differences, wild-types were obtained from related individuals (LWT adults x *fih+/-* adults provide a clutch of *fih+/+* and *fih+/-* embryos - see Materials and Methods). The difference in the diameter of the dorsal aorta between the wild type and *fih217/217* embryos, however, revealed the first measurable phenotype that distinguished the *fih217/217* embryos from their wild type siblings, independent of the loss of *vhl*.

### 6.1.2 *fih217/217* embryos have increased blood velocity compared to WT siblings

In the *fih217/217;vhl-/-* embryos blood flow along the aorta was observed to slow over time until it ceased between 4 and 5dpf. The angiograms, in **Figure 57**, also demonstrate the loss of circulation in the tail. High speed imaging of blood flow along the aorta was compressed into kymographs, in order to quantify the observed slowing of the blood flow in the *fih217/217;vhl-/-* embryos, see **Figure 86**. Initially a software program called Correlator was used in order to convert the kymographs into traces,

however the software appeared to pick up movement of pixels even in images taken where circulation had ceased.

Vibrations in the air and the table on which the microscope was mounted were hypothesised to cause the software to detect pixel movements where none were present in the embryo, making it impossible to use the software to quantify the slowing/cessation of circulation. This lead to manual assessment of the kymographs, using ImageJ to draw and measure rate of movement over three traces per kymograph to achieve an average for each embryo. Each trace within the kymograph tracks the progress of an individual pixel moving along the aorta within a rectangle with a 1 pixel width. When the traces are stacked on top of each other they demonstrate time on the y-axis and distance traveled on the x-axis, depicted in Materials and Methods. A level of subjectivity is present in placing the boxes around the heart beats, so the genotype of embryos within particular experiments would be blinded to prevent bias. ImageJ Software was used to measure the height and width of three rectangles, such as those imaged in **Figure 33,** for every kymograph and the speed of the blood flow was calculated for each embryo, the numbers were then collated and used to ascertain patterns in blood flow rates over time, see **Figure 86**Figure 86.

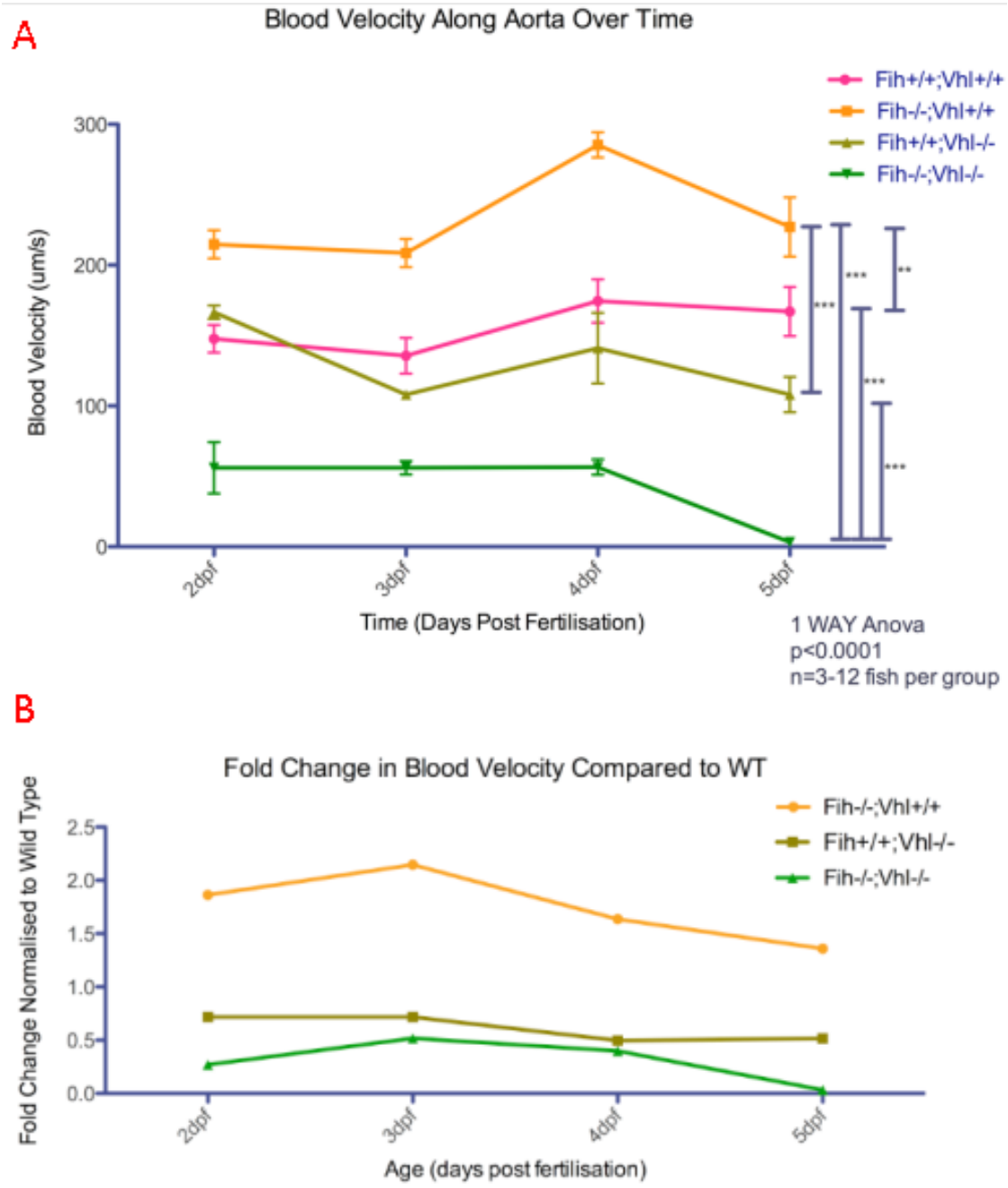


**Figure 86 Graph showing quantification of blood velocity**

**A)** *Illustrates blood velocity along the aorta over time. Each point represents the average diameter from 3-12 embryos and the error bars indicate standard deviation.* ***B)*** *Indicates the fold change in blood velocity compared to wild type embryos*

Observation of the green line of the graph in **Figure 86A** confirmed and quantified the observation that had been made that by 5dpf the flow of blood along the aorta in the *fih217/217;vhl-/-* embryos had ceased, while the heart continued to beat. What had not been directly observed before quantification was that there was an increase in

velocity in the *fih217/217* embryos compared to wild type siblings, and that this was present throughout the first 5 days of development and that it was higher than that recorded for any of the other mutants. Since vascular resistance to flow is related to path length and, inversely, to the fourth power of diameter (Wakhloo et al., 2005) the assessment of blood flow was assessed in the context of vessel diameter. The data from measuring the diameter of the aorta, along with the blood velocity along the aorta were compiled and collated in order to lend statistical significance to the increased velocity and increased aortic diameter observed in these embryos, see **Figure 87**.

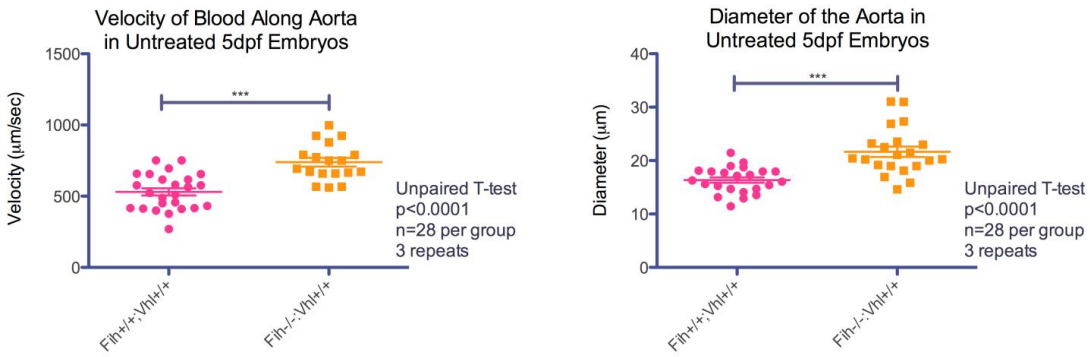


**Figure 87 Velocity along the aorta and aortic diameter compiled over multiple assays.**

In order to further ascertain the role of *fih* in the increase in blood velocity, two different novel compounds that were designed to be specific *Fih* inhibitors (C. Schofield, pers. Comm..) were administered to wild type embryos from the 1 cell stage through to 5dpf. Kymographs were generated and the blood velocity and aortic diameter were assessed, in comparison with untreated wild type and *fih217/217* embryos at the same stage. A range of concentrations of both of the two compounds were assessed, and the effects of the compound were measured using the high-speed imaging technique and assessing blood velocity as a way of assessing whether or not the compound was capable of phenocopying the *fih217/217* embryo phenotype, see **Figure 88**.

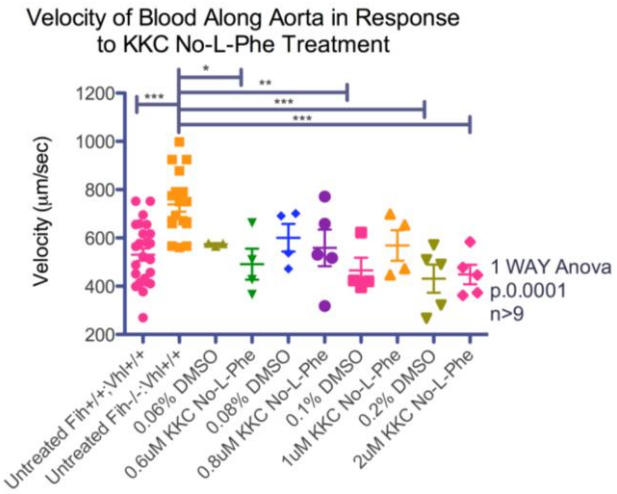


**Figure 88 Graph illustrating blood velocity in response to KKC-No-L-Phe Treatement**

*Treatments with KKC-No-L-Phe at the doses tested did not result in increases in blood velocity compared with untreated wild type embryos.*

None of the concentrations of KKC-No-L-Phe that were assessed resulted in an increase in blood velocity to phenocopy that seen in the *fih217/217* embryos. However, after optimising the dosage of the second compound (KKC396), beginning with the same range of concentrations used to test KKC No-L-Phe, it was possible to demonstrate that 1µM KKC396 treatment resulted in increased blood velocity and increased aortic diameter compared to untreated and DMSO controls (see **Figure 89**).

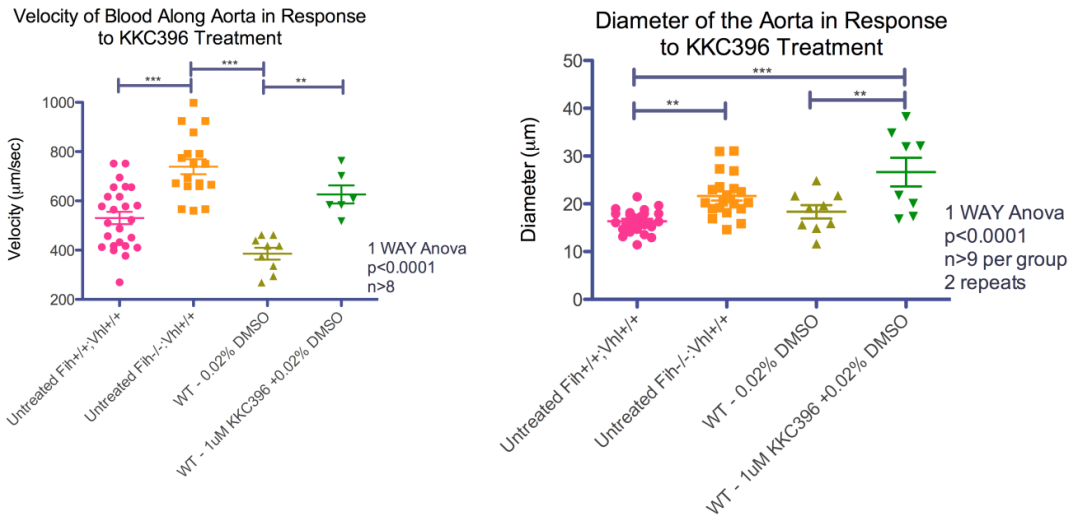


**Figure 89 Graphs illustrate blood velocity and aortic diameter in response to KKC396 treatment**

*Graphs demonstrate increased blood velocity observed in fih217/217 embryos compared with wt siblings and the increase in velocity following KKC396 treatment in wt embryos. The same trend is observed in the aortic diameter.*

This compound had been designed to be a hydroxylase inhibitor that has specificity for *Fih* and, that being so It has possible to infer that observing the same alteration in velocity using this compound as that observed in the genetic null suggests that *Fih* plays a direct role in controlling the phenotype. The increase in velocity did not reach the level of that observed in untreated *fih217/217* embryos compared to untreated wild type embryos, which can be interpreted as the difference in penetrance of a genetic null and a chemical inhibitor of protein function. The trend increase was significant and this indicated that the increase in blood velocity was dependent on a lack of *Fih*. Further investigation into the effects of alternative doses and treatment times will need to be completed since increasing the concentration could demonstrate the relative specificity of the compound by potentially showing effects on other enzymes.

## 6.2 Effect of *fih* on cardiac function

### 6.2.1 *fih217/217* embryos have increased heart rate compared to WT siblings

Hypoxia has been shown to induce multiple cardiovascular phenotypes, many of which can be investigated in the zebrafish, including cardiac output, stroke volume and end diastolic volume, along with increased ISV vascularisation index, see **Table 13.** The increase in blood velocity along the aorta in the *fih217/217* embryos compared with wild type siblings is almost certainly the result of altered cardiac function.

High speed imaging of the heart of embryos at various stages was used to measure the heart rate of the various mutants. The heart rate of the WT siblings was the lowest increasing steadily over time, the *fih217/217* and *vhl-/-* embryos showed a higher heart rate compared to wt at 2dpf and remained higher until apparently stabilising at 5dpf. The *fih217/217;vhl-/-* embryos had a less clearly defined pattern, although higher than all other groups at 4dpf, see **Figure 90**.

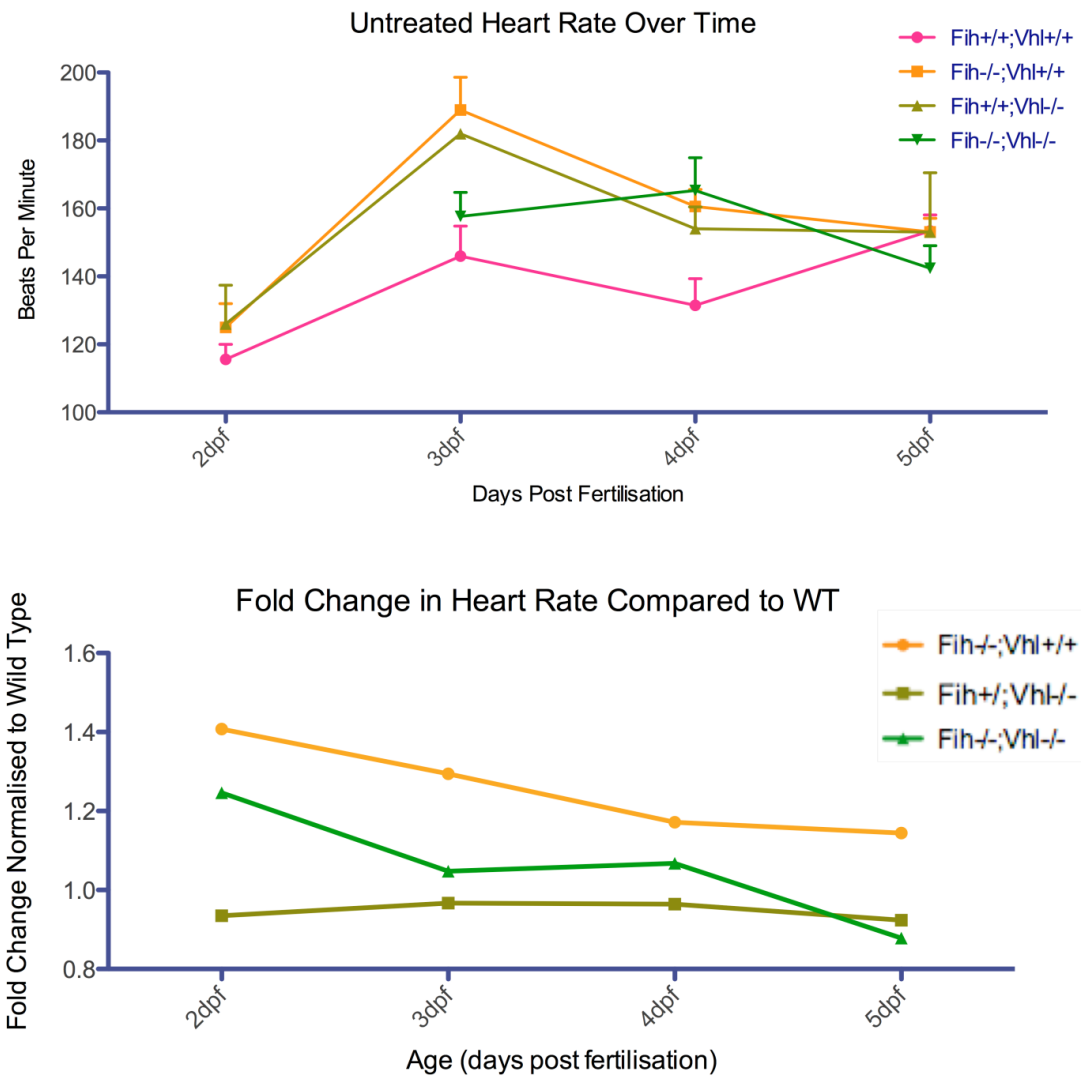


**Figure 90 Graphs illustrate heart rate over time**

***A)*** *Graph demonstrates average heart rate over time where each point represents the average diameter from 10+ embryos and the error bars indicate standard deviation.* ***B)*** *Indicates the fold change in heart rate compared to wild type embryos over time.*

The correlation between the increase in velocity of blood along the aorta and the increase in the diameter of the dorsal aorta in the *fih217/217* embryos compared with wild type embryos is possible only if there is a simultaneous increase in cardiac output.

### 6.2.2 Loss of *fih* causes an increase in cardiac output compared to *vhl-/-* embryos

Using the same images as had been used to count the heart rate of these embryos, an attempt was made to assess the cardiac output of the embryos, using ImageJ to draw around the inner wall of the ventricle and use the 'Fit-to-ellipse' algorithm in the

software to calculate the volume of the chamber at the beginning and end of the heart beat, see

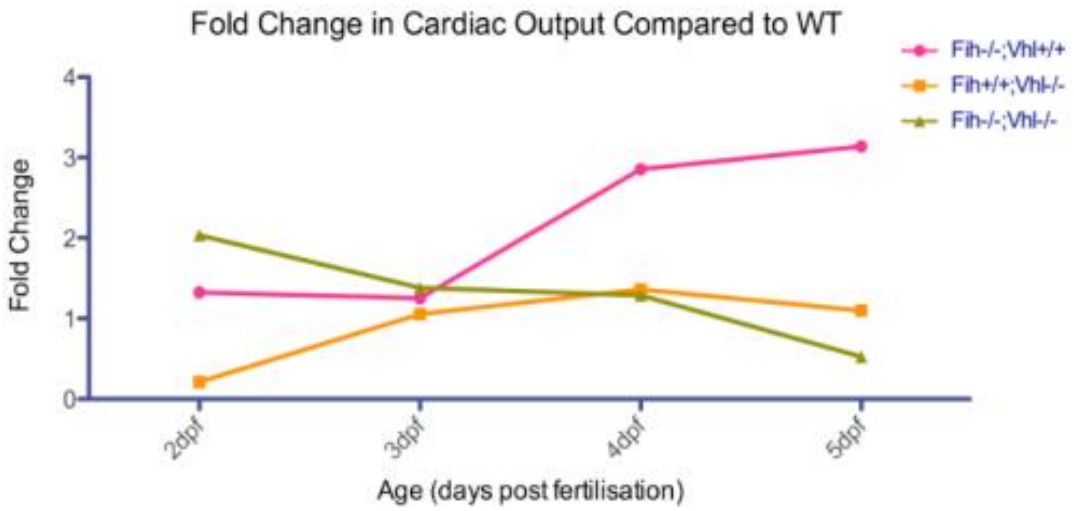


**Figure 91**.

Fold Change in Cardiac Output Compared to WT
Fih-/-;Vhl+/+
Fih+/+;Vhl-/-
Fih-/-;Vhl-/-
Fold Change
0
1
2
3
4
2dpf
3dpf
4dpf
5dpf
Age (days post fertilisation)

**Figure 91 Graphs indicates fold change in cardiac output measured at different points through development.**

The greatest fold change in cardiac output compared to wild type was seen in the *fih* null embryos at 4 and 5dpf.

## 6.3 Renin-Angiotensin-Aldosterone System

### 6.3.1 Expression

The *fih217/217* embryos phenotype has aspects that appear to be HIF independent, or at least much more strongly regulated by *fih* than by *vhl.* From the microarray data, two genes that were immediately annotated as being down-regulated in the *fih217/217* embryos independent of the other mutants were Angiotensinogen (Agt) and Angiotensin converting enzyme 2 (Ace2). These are two components of the Renin-Angiotensin-Aldosterone System (RAAS), a hormone system that is set up to homeostatically regulate blood pressure and water (fluid) balance, see **Figure 92** for schematic representation of the pathway.

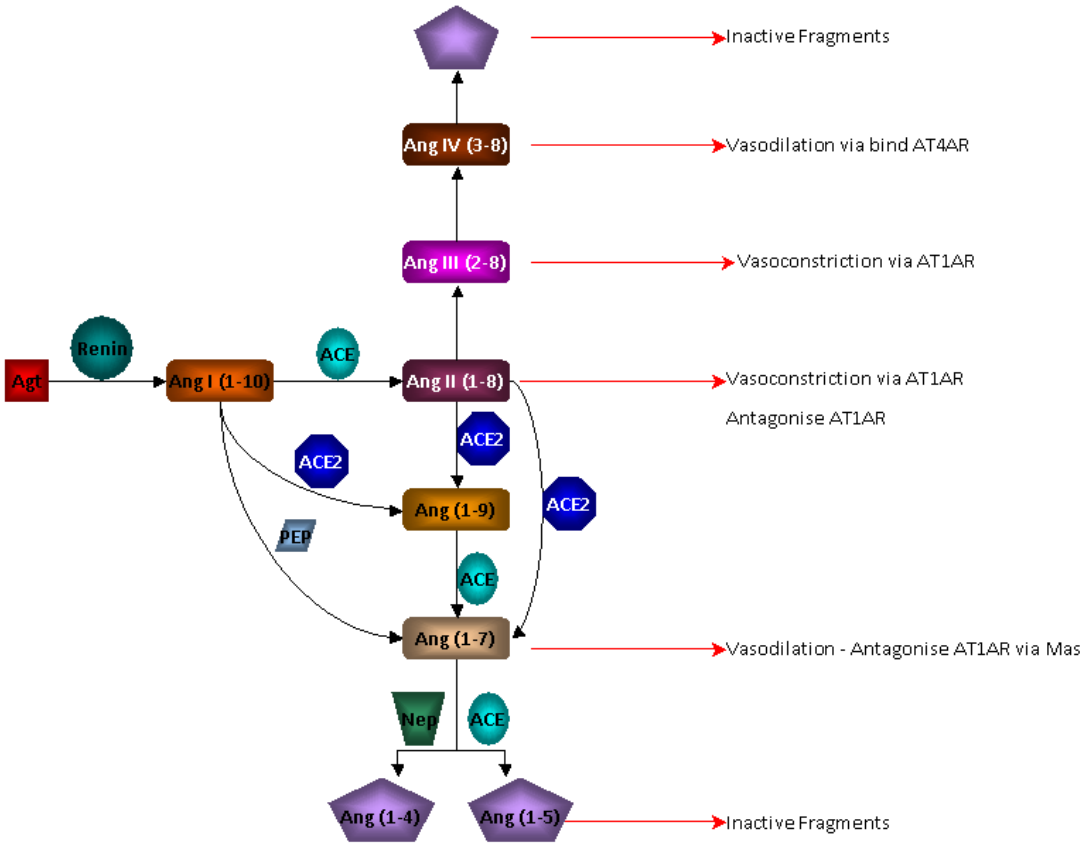


**Figure 92 The RAAS pathway**

*The RAAS pathway is initiated by the production of angiotensinogen (agt) in the liver, which is cleaved by renin (produced in the kidney) to form angiotensin I (AngI). AngI is further cleaved by angiotensin converting enzymes (Ace1 and 2) to angiotensin II (AngII) and other breakdown products to initiate sympathetic activity, $Na^+$, $Cl^-$ reabsorption along with $K^+$ excretion, this along with aldosterone secretion from the*

*kidney initiates $H_20$ retention. Arteriolar vasoconstriction results in increased blood pressure. The system is in place to initiate water and salt retention, effective circulating volume increases along with perfusion of the juxtaglomerular apparatus, which in turn acts as a negative feedback on renin excretion from the kidney to turn off the process. More abbreviations:- Sodium (Na+), Chloride ($Cl^-$), potassium ($K^+$), water ($H_20$), Prolyl-endopeptidase (Pep), neprilysin (Nep), angiotensin receptors (AT1AR, AT4AR).*

Having highlighted two genes from this pathway as significantly down-regulated in the *fih217/217* embryos, the expression levels of various other genes involved in the RAAS pathway were assessed in the microarray data-set, see **Figure 93**.

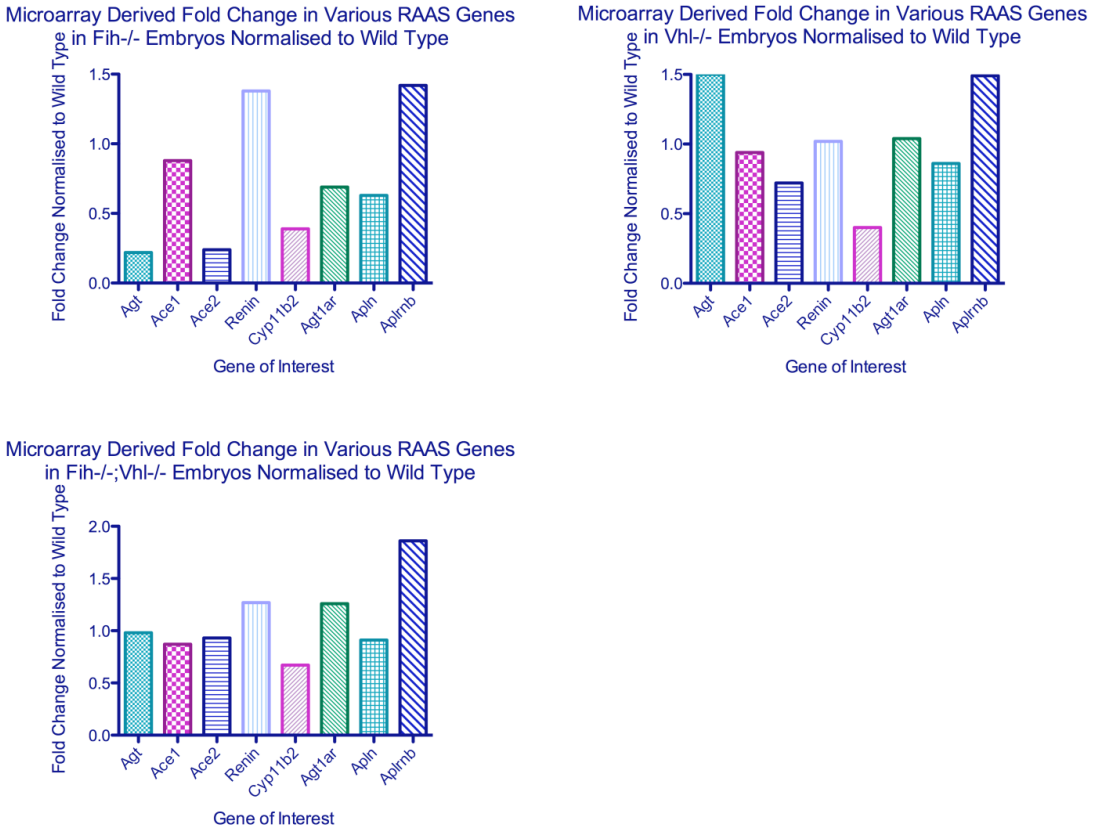


**Figure 93 Graphs indicate expression of RAAS component genes**

*The top left graph indicates the expression of the RAAS component genes in the fih217/217 embryos, the top right graph indicates the same for the vhl-/- embryos and the bottom left graph indicates the same for the fih217/217;vhl-/- embryos.* ***Abbreviations:-*** *angiotensinogen (agt), angiotensin converting enzyme (ace) angiotensin converting enzyme 2 (ace2), aldosterone synthase (cyp11b2), angiotensin receptor 1 (at1ar), apelin (apln), apelinrb (aplnrb).*

When the expression of the different components of the RAAS pathway are depicted alongside each other for the different mutants, it is clear that *agt*, *ace2, at1ar* and *apln* are independently down-regulated in the *fih217/217* embryos and not either the *vhl-/-* embryos or the *fih217/217;vhl-/-* embryos. An exception would be aldosterone synthase (cyp11b2), the gene involved in synthesising aldosterone, which is a downstream effector of the RAAS and is down-regulated across all three mutant groups. In order to confirm the findings from the microarray and assess other components of the RAAS, qRT-PCR was used, see **Table 15 and Table 16**.

The qRT-PCR data confirmed the microarray data for *agt and ace2,* lowest in the *fih217/217* embryos, not altered in or even up-regulated in the *vhl-/-* embryos and then down-regulated to a lesser extent in the *fih217/217;vhl-/-* embryos. The expression of *ace1* was used as a control, having not shown altered expression in the microarray in any of the three mutants, and the qRT-PCR confirmed this too. Agt is an α-2-globulin that is produced constitutively, with plasma levels increased in response to AngII. It is down-regulated in the *fih217/217* embryos, and not in the *vhl-/-* embryos, but where the qRT-PCR results differ from the microarray was that it is down-regulated, to a certain degree in the *fih217/217;vhl-/-* embryos. This trend was also true of the Ace2 gene, confirming the microarray findings. In order to assess other components and isolate these two genes, *ace1*, *renin*, aldosterone synthase (*cyp11b2*) and Angiotensin type 1 receptor (*at1ar*) were also assessed, see **Table 15 and Table 16.**

*Ace1* showed no differential regulation in any of the mutants, and the microarray suggested that the same was true of Renin, however qRT-PCR showed that Renin was up-regulated and to a greater extent in both the *vhl-/-* and *fih217/217;vhl-/-* embryos compared with the *fih217/217*. Slight discrepancies in the qRT-PCR confirmation of the microarray data for renin has made it difficult to confirm the microarray inference that renin expression was not altered in the *fih217/217* embryos compared with wild type embryos. The induction of the RAAS in the model therefore needs to be assessed using an alternative gene and/or alternative assays. Aldosterone synthase, downstream effector of the RAAS was down-regulated in all the embryos, to a greater extent in the *fih217/217* and *vhl-/-* embryos, inferring a decrease in activation of the pathway as the decreased expression of renin. The Angiotensin receptor is down-

regulated in the *fih217/217* embryos and not the other two mutants, and this might connect with the down-regulation of *agt*/*ace2*.

### 6.3.2 The effect of altering the RAAS by addition of chemical inhibitors

In order to blockade different components of the renin-angiotensin pathway, two different RAAS inhibitors were used; Telmisartan (an angiotensin II receptor type I antagonist ($AT_1AR$)) and Captopril (an ACE inhibitor). Embryos were treated from 0dpf through to 4dpf at which point the blood flow rate along the aorta was analysed by high speed imaging. Once the concentration of compound was optimised, the results were pooled in order to assess the trend, see **Figure 94**.

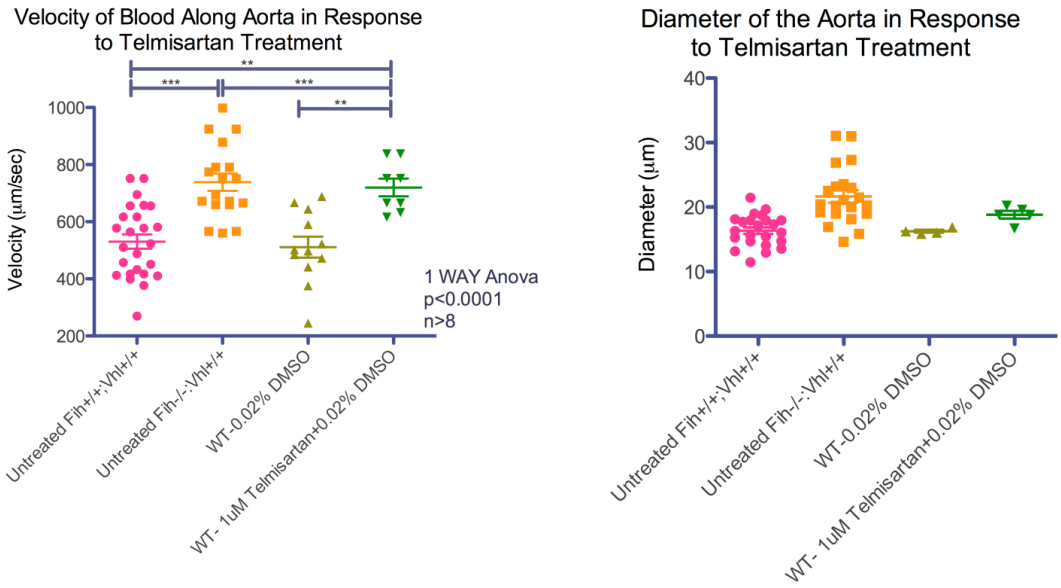


**Figure 94 Graphs illustrate blood velocity and aortic diameter in response to telmisartan treatment**

*Results of treatment of wild type embryos with Telmisartan ($AT_1AR$ receptor antagonist) mimic the findings in fih217/217 embryos, embryos exhibit elevated blood velocity along the aorta, with a slight but not significant increase in the diameter of the aorta.*

Increases in velocity observed following treatment with telmisartan phenocopy the increase in blood velocity observed in the *fih217/217* embryos. This could be suggested to support the hypothesis that $AT_1AR$ is a significant receptor in the RAAS

and is also suggestive of this being causative in the development of the phenotype. An increase in blood velocity, as shown, would most likely be caused by increased heart rate, it therefore follows that if phenocopies are parallel telmisartan also increases heart rate, and this would not be expected from a drug used to treat hypertension.

Captopril is an ace inhibitor known not to directly influence *ace2* **(Table 13)** and this was used to compare the results with those observed following treatment with telmisartan, see **Figure 95**.

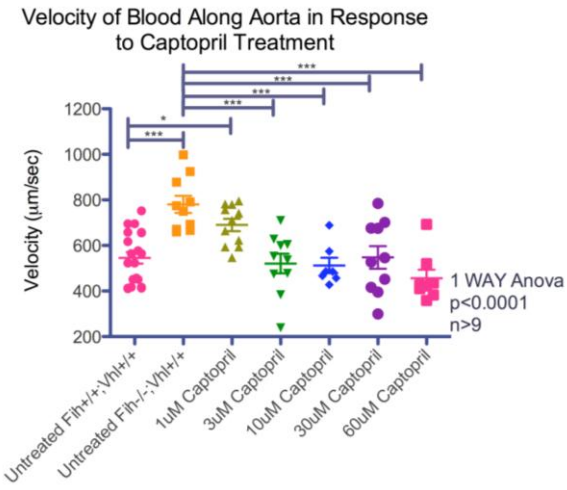


**Figure 95 Graphs illustrate blood velocity in response to Captopril treatment**

*Treatment of wild type embryos with the ace inhibitor, Captopril, demonstrated only minor effects on blood velocity at the lowest concentration used, to mimic the findings of the fih217/217 embryos.*

The data from this assay showed that over a range of concentrations none but the lowest were capable of inducing an increase in blood velocity along the aorta. Given that the two different drugs have different mechanisms of action in inhibiting the RAAS, and that the data from each of the tests does not provide a coherent conclusion. The investigation was in to whether or not chemically inhibiting the RAAS has the same effect as that seen in the *fih217/217* embryos, and without further experiments it is currently difficult to draw conclusions on the involvement of the RAAS system in the *fih* phenotype.

The Kallikrein-Kinin system (KKS) has also been connected with glucose homeostasis, with bradykinin stimulation shown in isolated muscle or fat cells shown to improve insulin action and glucose uptake by promoting glut4 translocation to plasma

membrane . Increased gluconeogenesis has been shown to be connected with increased expression of pepck and glucose-6-phosphatase (G6pase), and bradykinin has been shown to decrease hepatic mRNA expression of pepck. The expression of *pepck* (**Figure 70**) and glucose-6-phosphate (**Table 15**) have been shown by qRT-PCR and the microarray data not to be dramatically altered in the *fih217/217* embryos but in the *fih217/217;vhl-/-* embryos *pepck* expression is dramatically increased while *g6pase* is down-regulated. Assessing the levels of bradykinin expression itself, along with the expression of *pepck* and *g6pase* in response to bradykinin administration in the zebrafish could aid in the assessment of the role of bradykinin in gluconeogenesis in this model.

## 6.4 Discussion and Future Work

### 6.4.1 Phenotype

Gross morphological analysis**,** showed no phenotypes that distinguished *fih217/217* embryos from wild type siblings, and this is consistent with the fact that they are fully viable and fertile.

### 6.4.2 Vascular Phenotypes and Function

On the other hand *fih* mutants showed distinct phenotypes when in a *vhl-/-* background. However, upon quantifying the features of the vessels in the image deletion angiograms, used to illustrate the branching phenotype of the vasculature in the *vhl-/-* embryos as well as the slowing of circulation in the *fih217/217;vhl-/-* embryos, an increase in aortic diameter was observed between the *fih217/217* embryos and wild type siblings. In addition a surprising increase in the rate of blood flow along the aorta was observed in the *fih217/217* embryos compared to wild type siblings, which could conceivably due to either a slight activation of HIF or a HIF independent effect of FIH. The use of several novel compounds designed to act as specific *fih* inhibitors demonstrated that the same phenotype was observed with KKC396 treatment of wild type embryos as that seen in *fih217/217* embryos, indicating a direct link between the loss of *fih* and the phenotype. Since an increase in blood velocity could be related to an altered heart rate, this phenotype was also assessed in the embryos, and found to be elevated. Our calculations from velocity and aortic diameter suggest cardiac output was elevated in the *fih217/217* embryos, however a

direct measurement did not give reliable results as it failed to corroborate previous findings in the *vhl-/-* embryos and alternative methods will need to be investigated in order to confirm this. A possible control for the specificity of the compounds would be to treat *fih* MZ mutants with compound, if they are totally specific for fih this should not result in any further increase as these embryos don't have any *fih* anymore.

Throughout the imaging for measuring the aortic diameter, blood velocity, heart rate and cardiac output of the embryos, the embryos were immobilised in 0.7% agarose made up in E3 embryo medium, with low dose tricaine. This was necessary because the high speed imaging for the blood velocity required that the embryos be entirely immobile and not twitching throughout the imaging, even though this was only seconds in duration. Tricaine is an anesthetic which is known to affect heart rate under long term exposure, slowing it down (Denvir et al., 2008). For this reason the embryos were mounted in agarose in small batches and imaged immediately, ensuring that the effect of the tricaine was minimised and standardised across all of the embryos that were imaged. This was an attempt to ensure that any differences that were observed between the measurements made in wild type embryos compared to *fih217/217* embryos were affected to the same degree by the using of the anesthetic. Alternative assays which would allow for the quantification of these phenotypes without the use of the anesthetic would be worth investigating, such as those discussed by Chan et al (Chan et al., 2009).

The cardiac output assay came across similar difficulties as when attempting to assess erythrocyte density, with the same caveats in the data. The imaging required the mild and brief sedation of the embryos and mounting them on coverslips in low-melt point agarose. If the mounting was slightly less than identical for each embryo this resulted in slight alterations in the angles at which the embryos were lying and slight changes in the focus around the ventricle of the heart as it was being imaged, resulting in built-in error, which over multiple embryos resulted in the data indicating changes in cardiac output that didn't confirm data previously published for the *vhl-/-* embryos (van Rooijen et al., 2009). Time scale for these assays only overlaps at 4 and 5dpf, however an fold increase in cardiac output is still indicated by Rooijen et al, which is not seen in the data from this study. Alternative assays, such as laser scanning velocimetry (Malone et al., 2007) or the high-speed imaging technique optimised by Schwerte et al

(Schwerte et al., 2006), would be needed in order to further investigate the difference in cardiac output in these embryos. Anesthetic immobilisation of the embryos, which is known to affect cardiac function and blood flow rates (Denvir et al., 2008), was still necessary for each of these assays, and would need to be taken into account to ensure consistency of the results.

### 6.4.3 Lipid Metabolism

Carboxyl ester lipase is a key regulator of lipid nutrient absorption. Mice with null mutations in both carboxyl ester lipase and pancreatic triglycerate lipase gained a significant amount less weight on a high fat diet compared with wild type mice (Gilham et al., 2007). This lack of weight gain was proposed to be due to their absorption of few calories from the high fat diet (HFD) resulting in less fat mass accumulation (Gilham et al., 2007). The investigation of other genes involved in lipid and fatty acid regulation/transport, showed that adiponectin family genes were only slightly down-regulated in the *fih217/217* embryos, while *fabp* family genes were up-regulated in all the embryos (*fih217/217, vhl-/-* and *fih217/217;vhl-/-* embryos). The significant down-regulation of carboxyl ester lipase and the connection between the null-mutation in the mouse and HFD weight gain protection is suggestive of this gene playing a role in the HFD weight gain protection observed in *Fih-/-* mice, and could be worth further investigation. Since the *fih217/217* animals reach maturity, it would be possible to raise zebrafish, ensuring the same raising density and sex ratio, on normal and high fat diet and assess for such things as weight gain and lipid distribution using Oil-Red-O staining techniques, in conjunction with qRT-PCR to assess gene expression changes.

### 6.4.4 Activity

One of the phenotypes observed in the *Fih-/-* mice was a hypoactive phenotype during the dark cycles, when mice are characteristically more active. The acquisition of the Zebralab system for observing and tracking zebrafish larvae movement allowed for this phenotype to be assessed in the *fih217/217* fish, and several phenotypes were observed. Surprisingly the activity levels of the *fih217/217* embryos were higher than that in the wild type embryos. Such short light:dark cycles during a normal “fish daytime” could be perceived as a predator shadows (Fleisch and Neuhauss, 2006, Li and Dowling, 1997), to assess the zebrafish larval behaviour in normal day:night cycle

the lights were adapted to simulate those in the aquarium 14hour light and 10 hour dark. Instead of the decrease in activity seen in the *Fih-/-* mice, an increase both in duration of swimming and distance swum was seen in the zebrafish embryos, both in the light and dark compared with wild type embryos. Given the proposal that the loss of *Fih* induces a hypermetabolic phenotype in the mouse (Zhang et al., 2010) the increase in activity profile is in keeping with the hypothesis, both in terms of total activity and the increase in activity in response to the light being switched off. However, the mouse study exhibited a hypoactive phenotype in their assay, lending discrepancies between the two models. The preliminary assays to measure ATP and cholesterol also indicate corroboration for the hypermetabolic phenotype of *fih217/217* zebrafish embryos; however both of these assays will need to be repeated to confirm the results. As a potential explanation for the discrepancy in the mouse and fish activity data, the *Fih* null mice, assuming that they are hypermetabolic might not necessarily be in a position to use the excess energy as they've been shown to release more heat than their wild type siblings (Zhang et al., 2010), potentially explaining their not having an increased activity level. The zebrafish being ectothermic means that excess energy produced isn't released as heat and this could mean that their activity levels are more likely to correlate with excess energy than those seen in the mouse.

### 6.4.5 Metabolism

The connection between hyperactivity and metabolism has been made in the literature in multiple contexts and models, including a model of *Pgc-1α-/-* mice. These mice exhibit constitutively active gluconeogenic enzyme activation and are paradoxically lean and resistant to diet induced obesity due to hyperactivity (Lin et al., 2004). These phenotypes are consistent with those that were observed in the *Fih-/-* mice, although no changes were observed in *Pgc-1α* in these animals (Zhang et al., 2010).

### 6.4.6 Blood Flow Rates

An elevated blood flow velocity phenotype was identified, in *fih* mutants, with altered expression of RAAS genes *agt* and *ace2.* In adult physiology the RAAS plays critical roles in cardiovascular control and therefore in cardiovascular disease pathogenesis (Basso and Terragno, 2001, Bader, 2010, Jacoby and Rader, 2003). Angiotensinogen is produced in the liver and released and cleaved into active Angiotensin I by Renin,

which is produced in the kidneys (Bader, 2010), making renin the initial rate limiting enzyme in the pathway. Angiotensin I is further cleaved by Ace enzymes 1 and 2 to release Angiotensin II and other breakdown products. These bind to Angiotensin Receptors in various tissues in order to exert various effects, such as the kidney (sodium retention, fibrosis), adrenal gland (aldosterone release), heart (inotropy, chronotropy, hypertrophy, fibrosis), vessels (constriction, hypertrophy) and brain (thirst, salt appetite, sympathetic activation, vasopressin release) (Bader, 2010). In adult humans decreasing the activity of the RAAS results in decreasing tension of blood vessels and blood volume and an overall reduction in blood pressure as a result, a result that is achieved pharmaceutically with ACE inhibitors in the treatment of hypertension (Aronow, 2012). Since fish embryonic circulation may be regulated quite differently (for instance there are no vascular smooth muscle cells around the vessels at 4dpf (Santoro et al., 2009)) wild type embryos were treated with various ace inhibitors in order to explore the connection between the down-regulation of *agt* and *ace2* and the blood velocity phenotype in the *fih217/217* embryos.

Further investigation using both of these drugs (Telmisartan and Captopril) in combination with other drugs used in the regulation of the RAAS could provide further confirmation of the interactions between the loss of *fih* and the down-regulation of *agt* and *ace2* in the zebrafish. There is also the possibility of using these drugs and following up on other phenotypes that have been observed, such as the influence on activity levels. The possibility of attempting to rescue the phenotypes by administering *ace2* to *fih217/217* embryos, or identifying a method for measuring the concentration of Ang(1-7) in the *fih217/217* embryos, would also be worth pursuing. Two classes of drugs were tested, an ace inhibitor and an ace receptor antagonist. Other drugs within these classes, as well as other drugs known to influence the pathway, need to be tested to further investigate these effects.

Observation of the RAAS pathway diagram indicates that in the absence of Ace2 to convert AngI to Ang(1-9), AngI will instead be converted into AngII, due to the presence of Ace1. However, the hypothesis that the aortic vasodilation that was seen in the *fih217/217* embryos compared to wild type could be regulated by this pathway, would indicate that AngII (known to induce vasoconstriction through interactions with Agt1AR) is not being over-produced. The pathway was assessed again and the alternative arm of the

pathway, for the conversion of AngI to Ang(1-7) (which induces vasodilation through interaction with Mas receptor) was assessed. In the absence of Ace2, Pep is present to convert AngI to Ang(1-7) and that this breakdown product has been shown to signal through the Mas receptor and induce vasodilation, antagonising the $AT_1AR$ leading to increased NO production and an increase in blood flow. This is the phenotype that is seen in the embryos, and so this correlates with the findings. However, the increases in diameter and heart rate that have been shown in this study between the wild type and *fih217/217* embryos is small and while increased NO has been shown to cause vasodilation in the zebrafish it has over time been shown to be stronger in *vhl-/-* embryos compared to *fih217/217* embryos, indicating an alternative method of regulation (Rooijen E,. pers comm.). In this case, it could be suggested that in *vhl* mutants, vessel diameter increases more strongly than *fih* mutants, while heart size remains similar. The down-regulation of *ace2* and *agt* together in the *fih* mutants could be affecting the conversion of angiotensin to Ang(1-7) more strongly than to AngII and might thus provide net vasoconstrictive effect in *vhl* mutants (albeit still vasodilated relative to wild type and explaining the vasodilation in the *fih* mutants). Sequencing studies have shown that the zebrafish do not have a Mas receptor homologue (Alenina et al., 2008), indicating that if Ang(1-7) is produced in the zebrafish it is likely to be signaling through a different receptor in order to induce these phenotypes, if indeed there is a connection. The literature was assessed for studies of the effect of down-regulation or loss of these and other members of the RAAS. The data from several of these studies has been summarised in Table 19**.**

| | **Agt-/- mice** | **AT2AR-/- mice** | **AT2AR-/- mice** |
|---|---|---|---|
| **Author** | (Kim et al., 2002) | (Yvan-Charvet et al., 2005) | (Kouyama et al., 2005) |
| $0_2$ consumption and $CO_2$ evolution | | Decreased light | Increased |
| Water and Food Intake | Increased | No change | |
| Total energy expenditure | | Increased | |
| Activity Levels | Increased | | Increased on HFD |
| Lipid oxidation | | Decreased | |
| Heat production | | | No change |
| UCP genes | Increased | Increased | |
| Glucose clearance | | Increased | Increased |
| Insulin sensitivity | No change | Increased | Increased |

| | | | |
|---|---|---|---|
| RER | | | Increased |
| RQ | | Decreased | Decreased |
| Mass/body weight | Decreased | No change | No change |
| Fat mass | Decreased | | |
| Adipocyte size and lipid droplet number | Decreased | Decreased | No change on NFD but Decreased on HFD |
| Adipose tissue mass | | | Decreased |
| Cholesterol and triglyceride | Decreased | | |
| FAS activity | Decreased | Decreased | |
| Fed Insulin levels | | Decreased | |
| Blood pressure | | | Decreased |
| Weight gain on HFD | Decreased | Decreased | Decreased |
| Blood glucose | No change | No change | No change |

**Table 19** *Table describes a summary of findings from several studies of the individual knock-out of angiotensinogen (agt) and angiotensin type2 receptor ($AT_2AR$) in mouse.*

Mouse knockout models of renin (Takahashi et al., 2007), ace (Jayasooriya et al., 2008) and ace2 (Niu et al., 2008) have also been investigated. These studies, while investigating many of the same features as those indicated in **Table 3**, didn't assess any of the same features as had been assessed in the *fih217/217* zebrafish model, making interpretations between these difficult. The increased activity level observed in the *Agt-/-* mouse does, however, correlate with observations in the *fih217/217* zebrafish where *agt* is down-regulated. This provides preliminary support for a hypothesis that the decrease in *agt* expression observed in the *fih217/217* embryos was correlated with the phenotypes that have been characterised to differentiate the wild type embryos from the *fih217/217* embryos, while leaving scope for further investigation into how this is achieved.

Different axes of the RAAS have been shown to affect different outcomes and the Ang(1-7) breakdown product of angiotensin has been shown to signal through the Mas receptor. Mas receptor knockout mice have been assessed for some of the same phenotypes as those from *renin, at2r, ace* and *ace2* knockout mice. The findings from two such *Mas-/-* mouse papers has been summarised in Table 20.

| | **Mas-/- mice** | **Mas-/- mice** |
|---|---|---|
| | (Santos et al., 2006) | (Lemos et al., 2005) |
| Heart Rate | | Decreased |
| Activity Levels | | Increased (anxiety) |
| Glucose clearance | Decreased | |
| Insulin sensitivity | Decreased | |
| Mass/body weight | No change | |
| Fat mass | Increased | |
| Adipocyte size and lipid droplet number | No change | |
| Cholesterol and triglyceride | Increased | |
| Blood pressure | | Decreased (male)<br>Increased (female) |
| Fasting glucose or insulin | Increased | |

**Table 20** *Table describes a summary of findings from several studies of the individual knock-out of mas receptor in mouse.*

Again the observations in these studies were into the same phenotypes as had been assessed in the Agt-/- mice, however the Mas-/- mice exhibits a decreased heart rate, the opposite to that seen in the *fih217/217* zebrafish and making the hypothesis that this alternative RAAS axis was being utilised difficult to corroborate. The increased cholesterol as well as increased activity levels does correlate, however, suggesting that further investigation, into targeted inhibition of the pathway might aid in further characterising the phenotypes directly connected with this. After the Mas receptor was not found in the microarray and, using Ensembl genome database it was possible to investigate this and the Mas receptor does not have a zebrafish homologue (Alenina et al., 2008). In this case, if Ang(1-7) was being produced following the loss of *ace2,* rather than producing increased levels of AngII due to the continued presence of *ace1* then the Ang(1-7) in the zebrafish could be seen to be interacting with an alternative receptor. Investigation into selective knock-down of the different receptors of the RAAS, might elucidate the exact interactions, and which arm of the pathway, if any, is responsible for inducing the increased heart rate observed in the *fih217/217* zebrafish. There are reports in the literature which connect the use of ACE inhibitors in hypertension and heart failure with increased levels of Ang(1-7) through bradykinin-dependent mechanisms (Tom et al., 2003). The direct mechanism of Ang(1-7)-bradykinin induced vasodilation has been proposed to be that Ang(1-7) acts as a

localised synergistic modulator of kinin-induced vasodilation by inhibiting ACE and releasing NO (Li et al., 1997, Tom et al., 2001, Oliveira et al., 1999). Further investigation specifically inhibiting individual components of the Kinin-Bradykinin pathways (using morpholinos, for example) would allow for the investigation of which receptor might be regulating downstream effects such as vasodilation and blood velocity.

Angiotensin II (AngII) is the major effector of RAAS, and is a powerful vasoactive mediator associated with hypertension and renal failure. The role of Vegf on the permeability changes in the vasculature have been described in **Chapter 9**, AngII has also been implicated in the permeability of the vasculature (Bodor et al., 2012). AngII can stimulate the release of other vasoactive and pro-inflammatory cytokines, increased leukocyte rolling, adhesion and migration in rat mesenteric post-capillary venules (Bodor et al., 2012). VEGF induces fenestrate formation *in vivo* and *in vitro* and increase in plasmalemmal vesicle-1 (PV-1), which has been shown to be correlated with disruption of blood-brain barrier in the ischemic brain and with micro-vascular leakage in diabetic retinopathy (Bodor et al., 2012). Cell surface openings have been shown to increase in parallel with permeability and the development of fused vesiculo-vacuolar structures or vaeolae or both. AngII plays a role in regulating these cell surface openings through $AT_1AR$ and PV-1 protein synthesis in a p38 MAP kinase-dependent manner (Bodor et al., 2012). The connection between the RAAS and VEGF in regulating micro-vascular leakage indicates another avenue of investigation into the vessel competence in the *fih217/217;vhl-/-* embryos and suggests that vascular competence might be worthy of testing in the *fih217/217* embryos. If AngII is indeed being over-produced due to the loss of *ace2* in the *fih217/217* embryos and this does result in increased cell surface openings, then the injection of fluorescent dyes into the circulation may reveal this upon observation of the leakage of the dye from the vessels, an experiment which has not been performed at late states, to date.

The ACE2 gene was identified from 5' sequencing of a cDNA library of human heart failure patients. It was shown to have a single matrix metalloproteinase (MMP) active site (with 42% homology with ACE) and a transmembrane domain, with more restricted expression than ACE (Donoghue et al., 2000). As well as hydrolysing carboxyl terminal leucine from AngI to generate Ang(1-9), ACE2 also cleaves des-Arg

Bradykinin and neurotensin, but not bradykinin or several other vasoactive and hormonal peptides. These findings along with those connecting the beneficial effects of ACE inhibitors with both a decrease in ACE and subsequent decrease in AngII with an increase in kinin levels and the levels of both B1 and B2 type bradykinin receptors (Erdos et al., 2010). ACE inhibitors have been shown to potentiate bradykinin and ACE-resistant bradykinin analogues through enhancing interactions on the cell surface and lead to elevated arachidonic acid and NO release *in vitro* (Erdos et al., 2010). The connection between ACE and Bradykinin family regulation lead to the assessment of these family member genes in the microarray data set. The literature indicates that a decrease in ACE leads to a subsequent increase in both kinin and both types of bradykinin receptor. The microarray data however, indicate that any alterations in expression of bradykinin family members were small and seem unlikely to be relevant to phenotypes seen in this study.

The data from this study supports several of the findings that were reported in the study by Zhang et al of the *Fih-/-* mouse. They add information on the effect on blood velocity and vessel diameter, along with putting forward a possible mechanism for initiating these phenotypes (the RAAS).

# 7 Discussion

The initial hypothesis was that the loss of *fih* alone would have no effect on the phenotype of the embryos compared with wild type, rather its loss in combination with *vhl would* further sensitise the system and enhanced features of the *vhl* null mutants. This hypothesis was provided with support when features such as vascular branching and heart rate were exacerbated in the *fih;vhl* double mutants, compared with the *vhl* only mutants, where the *fih* null mutants showed no distinguishing features compared with wild type.

The hypothesis, suggested by Lee et al, (Lee et al., 2003), that VHL is necessary in the formation of the complex between VHL, HIF and FIH, implied that the loss of *fih* in an individual that had lost *vhl* function, would result in no alteration in the phenotypes observed. This hypothesis is not supported by the data from this thesis.

FIH is an asparaginyl hydroxylase, characterised for its interaction with HIF and subsequently shown to have many more substrates. The identification of the *fih*$^{i217}$ zebrafish mutant provided a tool for assessing the role of *fih* in HIF signaling, and also enabled the function of *fih* in other related pathways to be investigated.

Preliminary hypotheses that the loss of *fih* and the loss of *vhl* would have distinct downstream effects on overall levels of HIF-signaling due to their different roles in Hif-α regulation (inhibition of activity versus targeting for breakdown)(Lancaster et al., 2004), were supported by the data from this study. The homozygous loss of *vhl* in the zebrafish results in embryonic lethality before 15dpf, indicating that Vhl protein is essential to ensure HIF-α breakdown. In the zebrafish embryo, the loss of *vhl* induces expression of HIF-signaling targets along with downstream effects such as increased buccal movement, cardiac output and heart rate as well as angiogenesis, and erythropoiesis (van Rooijen et al., 2010, van Rooijen et al., 2009). However, homozygous *fih* null zebrafish are fully viable and fertile, confirming that the functional inhibition of Hif-α by *fih* provides a secondary mechanism of control that is most necessary only in the absence of *vhl.*

The direct interaction between HIF-α, FIH and VHL during HIF-α regulation has generated multiple modelling opportunities *in vitro* and these have agreed that it is at least possible, if not necessary, for the three proteins to interact. In 2003 Lee et al proposed that a complex formed in hypoxia between the FIH dimer, VHL and HIF-α, with FIH acting as a bridge bringing together the association between VHL and HIF-α (Lee et al., 2003). Later, in 2011, a secondary bridging model was proposed with HIF-α acting as a chaperone for FIH-VHL interactions, which in turn were proposed to allow FIH-HIF-α binding (Li et al., 2011b). The proposal here is that in hypoxia the FIH-VHL complex disassembles, following stabilisation of HIF-α by VHL binding to the ODDD, decreasing FIH-TAD-C binding (Li et al., 2011b). The *fih* and *vhl* mutant zebrafish provide a model for assessing the downstream HIF-signaling following the loss of either or both of these genes. The loss of *fih* alone caused little increase in the expression of HIF target genes compared to wild type, the loss of *vhl* alone caused an increase in target gene expression, while the loss of both caused a further increase in expression. If, as has been proposed by (Lee et al., 2003), FIH was a necessary chaperone for the interaction between VHL and HIF-ODDD, then its loss in the zebrafish could be thought to mimic that seen in the absence of *vhl* itself, which was not seen. The model in Li et al (Li et al., 2011b) provides an alternative, suggesting an interaction that correlates more with the model in Lancaster et al (Lancaster et al., 2004) that VHL provides the predominant control over HIF function, inhibiting FIH interaction with HIF-α (Li et al., 2011b). The step-wise increase in HIF target gene expression in response to the loss of first *fih* then *vhl* then both makes it difficult to see how a model that would necessitate all three proteins interacting in order to inhibit HIF-α enough to induce signaling difficult to interpret, these data would rather suggest that *fih* and *vhl* are simply two levels of regulation.

In the investigation of *fih* independent effects and through the early stages of the investigation there were no measurable differences between *fih217/217* embryos and their wild type siblings, their overall shape, vascular patterning, endothelial cell number, and expression of classical HIF target genes were all consistent. These features were altered, where *fih* was lost in a *vhl* background, and this would indicate that *fih* is acting predominantly on HIF and that other substrates are secondary. One situation where the loss of *fih* did not exacerbate a previously observed phenotype of

the *vhl-/-* embryos was in the vascular patterning in the tail. Instead, the loss of *fih* caused large extra loops of ISVs up and over the DLV to resolve to appear more like wild type. The hypothesis that this might be regulated by flow rates in the vessels determining their arrangement and remodeling constitutes a separate and worthy area of study (Oliver. Watson. pers. Comm.).

It has been shown that FIH has many more substrates besides HIF-α (Cockman et al., 2009, Coleman et al., 2007). There have been several studies to investigate the interactions of FIH, within and between the different pathways that these hydroxylation events potentially connect. Models have been proposed to indicate that the multiple hydroxylation partners of FIH (including Notch (Zheng et al., 2008) and IκB (Shin et al., 2009)), have higher binding efficiencies, in comparison with FIH-HIF binding, and are therefore capable of sequestering FIH away from HIF. The preferential binding of FIH to proteins other than HIF-α has been proposed as a mechanism of relieving FIH inhibition on HIF-α through the sequestering away to other proteins such as Notch/NICD. The prevalence of FIH-binding partners, however, makes these models difficult to pin to one specific interaction *in vivo.* There was no effect of the loss of either *fih* or *vhl* or both on the expression of IκB, NFκB or indeed those down-stream target genes that could be identified (which might have been supposed to increase in expression), to indicate a response. However the effect of *fih* is suggested to be post-translational and therefore further investigation could elucidate interactions between the proteins *in vivo.*

The proposed interaction between FIH and Notch/NICD provided an avenue of investigation since the Notch signaling pathway has been implicated in arterio-venous fate choice in the developing vasculature, as well as in the determination and maintenance of tip-cell/stalk-cell balance in the remodeling vasculature. In the zebrafish, it had been shown that following inhibition of notch using chemical inhibitors such as DAPT, or morpholinos specific to *dll4,* the vasculature took on a hyper-branched appearance through the loss of lateral inhibition of tip-cells which is normally provided by *dll4* (Leslie et al., 2007). FIH hydroxylation of Notch is proposed to enhance signaling and so its loss should result in a decrease in efficiency and might therefore be expected to simulate, to some extent, the increased branching of the vasculature seen by Leslie et al. This was not the case in the *fih217/217* embryos,

however in the *fih217/217;vhl-/-* embryos the vasculature exhibited an increase in branching compared with *vhl-/-* embryos, indicating an effect of the loss of *fih* on these embryos. This effect cannot be confirmed as being regulated by *fih* independent of alterations in Notch signaling as there is a concurrent increase in *vegf* family gene expression, and this will require further investigation to identify the independent roles.

The release of the study describing the metabolic phenotypes of the *Fih* mutant mouse, published after the start of this current PhD project, provided an alternative avenue of investigation, and some surprising results (Zhang et al., 2010). It was possible to assess several of the same features as those assessed in the mouse model, and find the correlations between the two data sets. The role of *Fih* in regulating metabolic rather than HIF-regulated phenotypes had not been reported, and the investigation of heart rate and activity were within the scope of the zebrafish study. Following the investigation of the heart rate, vessel diameter and cardiac output in the zebrafish embryos, which followed that done in the *vhl-/-* embryos, the observation was made that the *fih217/217* embryos exhibited an elevated heart rate and vessel diameter compared to wild type siblings. This was found to be specific to the loss of *fih* by the use of a hydroxylase inhibitor which had been designed to be specific to *fih*. A tool that would provide alternative controls for this experiment along with others is the *fih;pcs2+* construct. This was not mentioned through the text as time constraints meant that it was not used during this project. It provides opportunities in the future for using it as an expression construct, for re-introducing *fih* into *fih* null embryos and observing the rescue of phenotypes, however, and this work will be ongoing. The elevated heart rate, increased aortic diameter and hyperactivity provided observations that distinguished the *fih217/217* embryos from wild type siblings, and a connection with the mouse study. Zhang et al. suggest that Fih could provide a unique mechanism for regulating metabolism, which they imply could be independent of HIF signaling.

The whole embryo microarray performed in the *fih217/217* mutant zebrafish yielded two candidate downstream genes (*agt* and *ace2*), which were not identified in the mouse study. The two genes were down-regulated only in the *fih217/217* zebrafish and not the *vhl-/-* embryos or the *fih217/217;vhl-/-* embryos (at least not to the same extent as the single). These genes provided a connection to one pathway, the renin-angiotensin-aldosterone system, which plays roles in fluid homeostasis and as such

affects vascular tone (dilation/relaxation) as well as circulating fluid volumes. While investigations into the exact connection between these genes being down-regulated and the increased vessel diameter and heart rate that have been seen in these embryos are preliminary it does suggest that the connection may be relevant and that one *fih* independent role is in regulating the RAAS.

# Bibliography


ADAMS, R. H., WILKINSON, G. A., WEISS, C., DIELLA, F., GALE, N. W., DEUTSCH, U., RISAU, W. & KLEIN, R. 1999. Roles of ephrinB ligands and EphB receptors in cardiovascular development: demarcation of arterial/venous domains, vascular morphogenesis, and sprouting angiogenesis. *Genes Dev,* 13**,** 295-306.

AGILENT. *Agilent Two-Colour Microarray-Based Exon Analysis* [Online]. Available: http://www.chem.agilent.com/library/usermanuals/public/g4140-90052_two-color_exon_1.0.pdf.

ALARCON, C., SERNA, J., PEREZ-VILLAMIL, B. & DE PABLO, F. 1998. Synthesis and differentially regulated processing of proinsulin in developing chick pancreas, liver and neuroretina. *FEBS Lett,* 436**,** 361-6.

ALENINA, N., XU, P., RENTZSCH, B., PATKIN, E. L. & BADER, M. 2008. Genetically altered animal models for Mas and angiotensin-(1-7). *Exp Physiol,* 93**,** 528-37.

ALIDOOSTI, M., GHAEDI, M., SOLEIMANI, A., BAKHTIYARI, S., REZVANFARD, M., GOLKHU, S. & MOHAMMADTAGHVAEI, N. 2011. Study on the role of environmental parameters and HIF-1A gene polymorphism in coronary collateral formation among patients with ischemic heart disease. *Clin Biochem,* 44**,** 1421-4.

ALVES-COSTA, F. A., DENOVAN-WRIGHT, E. M., THISSE, C., THISSE, B. & WRIGHT, J. M. 2008. Spatio-temporal distribution of fatty acid-binding protein 6 (fabp6) gene transcripts in the developing and adult zebrafish (Danio rerio). *FEBS J,* 275**,** 3325-34.

APPELHOFF, R. J., TIAN, Y. M., RAVAL, R. R., TURLEY, H., HARRIS, A. L., PUGH, C. W., RATCLIFFE, P. J. & GLEADLE, J. M. 2004. Differential function of the prolyl hydroxylases PHD1, PHD2, and PHD3 in the regulation of hypoxia-inducible factor. *J Biol Chem,* 279**,** 38458-65.

ARBISER, J. L. 2012. Zebrafish lead the way in control of vascular permeability. *Blood,* 120**,** 2162-4.

ARONOW, W. S. 2012. Treatment of systemic hypertension. *Am J Cardiovasc Dis,* 2**,** 160-70.

ARTAVANIS-TSAKONAS, S., MUSKAVITCH, M. A. & YEDVOBNICK, B. 1983. Molecular cloning of Notch, a locus affecting neurogenesis in Drosophila melanogaster. *Proc Natl Acad Sci U S A,* 80**,** 1977-81.

BADER, M. 2010. Tissue renin-angiotensin-aldosterone systems: Targets for pharmacological therapy. *Annu Rev Pharmacol Toxicol,* 50**,** 439-65.

BAHARY, N., GOISHI, K., STUCKENHOLZ, C., WEBER, G., LEBLANC, J., SCHAFER, C. A., BERMAN, S. S., KLAGSBRUN, M. & ZON, L. I. 2007. Duplicate VegfA genes and orthologues of the KDR receptor tyrosine kinase family mediate vascular development in the zebrafish. *Blood,* 110**,** 3627-36.

BARRIONUEVO, W. R. & BURGGREN, W. W. 1999. O2 consumption and heart rate in developing zebrafish (Danio rerio): influence of temperature and ambient O2. *Am J Physiol,* 276**,** R505-13.

BARROS, C. C., HARO, A., JAQUELINE RUSSO, F., SCHADOCK, I., SOARES ALMEIDA, S., CASTELLANI REIS, F., ROCHA MORAES, M., HAIDAR, A., EMIKO HIRATA, A., MORI, M., BACURAU, R. F., WURTELE, M., BADER, M., BOSCO PESQUERO, J. & CARVALHO ARAUJO, R. 2012. Bradykinin inhibits hepatic gluconeogenesis in obese mice. *Lab Invest*.

BASSO, N. & TERRAGNO, N. A. 2001. History about the discovery of the renin-angiotensin system. *Hypertension,* 38**,** 1246-9.

BATES, D. O. 2010. An interstitial hypothesis for breast cancer related lymphoedema. *Pathophysiology,* 17**,** 289-94.

BEDOGNI, B., WARNEKE, J. A., NICKOLOFF, B. J., GIACCIA, A. J. & POWELL, M. B. 2008. Notch1 is an effector of Akt and hypoxia in melanoma development. *J Clin Invest,* 118**,** 3660-70.

BELLOT, G., GARCIA-MEDINA, R., GOUNON, P., CHICHE, J., ROUX, D., POUYSSEGUR, J. & MAZURE, N. M. 2009. Hypoxia-induced autophagy is mediated through hypoxia-inducible factor induction of BNIP3 and BNIP3L via their BH3 domains. *Mol Cell Biol,* 29**,** 2570-81.

BENTLEY, K., MARIGGI, G., GERHARDT, H. & BATES, P. A. 2009. Tipping the balance: robustness of tip cell selection, migration and fusion in angiogenesis. *PLoS Comput Biol,* 5**,** e1000549.

BERRA, E., BENIZRI, E., GINOUVES, A., VOLMAT, V., ROUX, D. & POUYSSEGUR, J. 2003. HIF prolyl-hydroxylase 2 is the key oxygen sensor setting low steady-state levels of HIF-1alpha in normoxia. *EMBO J,* 22**,** 4082-90.

BHF, B. H. F. 2010. *Heartstats (http://www.bhf.org.uk/research/heart-statistics.aspx)* [Online]. Available: http://www.bhf.org.uk/research/heart-statistics.aspx.

BLANCO-VIVES, B. & SANCHEZ-VAZQUEZ, F. J. 2009. Synchronisation to light and feeding time of circadian rhythms of spawning and locomotor activity in zebrafish. *Physiol Behav,* 98**,** 268-75.

BLUM, Y., BELTING, H. G., ELLERTSDOTTIR, E., HERWIG, L., LUDERS, F. & AFFOLTER, M. 2008. Complex cell rearrangements during intersegmental vessel sprouting and vessel fusion in the zebrafish embryo. *Dev Biol,* 316**,** 312-22.

BODOR, C., NAGY, J. P., VEGH, B., NEMETH, A., JENEI, A., MIRZAHOSSEINI, S., SEBE, A. & ROSIVALL, L. 2012. Angiotensin II increases the permeability and PV-1 expression of endothelial cells. *Am J Physiol Cell Physiol,* 302**,** C267-76.

BOULOS, N., HELLE, F., DUSSAULE, J. C., PLACIER, S., MILLIEZ, P., DJUDJAJ, S., GUERROT, D., JOUTEL, A., RONCO, P., BOFFA, J. J. & CHATZIANTONIOU, C. 2011. Notch3 is essential for regulation of the renal vascular tone. *Hypertension,* 57**,** 1176-82.

BROU, C., LOGEAT, F., GUPTA, N., BESSIA, C., LEBAIL, O., DOEDENS, J. R., CUMANO, A., ROUX, P., BLACK, R. A. & ISRAEL, A. 2000. A novel proteolytic cleavage involved in Notch signaling: the role of the disintegrin-metalloprotease TACE. *Mol Cell,* 5**,** 207-16.

BRUICK, R. K. 2000. Expression of the gene encoding the proapoptotic Nip3 protein is induced by hypoxia. *Proc Natl Acad Sci U S A,* 97**,** 9082-7.

BRUICK, R. K. & MCKNIGHT, S. L. 2001. A conserved family of prolyl-4-hydroxylases that modify HIF. *Science,* 294**,** 1337-40.

BUNN, H. F. & POYTON, R. O. 1996. Oxygen sensing and molecular adaptation to hypoxia. *Physiol Rev,* 76**,** 839-85.

BURRI, P. H., HLUSHCHUK, R. & DJONOV, V. 2004. Intussusceptive angiogenesis: its emergence, its characteristics, and its significance. *Dev Dyn,* 231**,** 474-88.

BUSKE, C. & GERLAI, R. 2011. Shoaling develops with age in Zebrafish (Danio rerio). *Prog Neuropsychopharmacol Biol Psychiatry,* 35**,** 1409-15.

BUSSMANN, J., LAWSON, N., ZON, L. & SCHULTE-MERKER, S. 2008. Zebrafish VEGF receptors: a guideline to nomenclature. *PLoS Genet,* 4**,** e1000064.

CALVO, M. N., BARTRONS, R., CASTANO, E., PERALES, J. C., NAVARRO-SABATE, A. & MANZANO, A. 2006. PFKFB3 gene silencing decreases glycolysis, induces cell-cycle delay and inhibits anchorage-independent growth in HeLa cells. *FEBS Lett,* 580**,** 3308-14.

CAO, R., JENSEN, L. D., SOLL, I., HAUPTMANN, G. & CAO, Y. 2008. Hypoxia-induced retinal angiogenesis in zebrafish as a model to study retinopathy. *PLoS One,* 3**,** e2748.

CAOLO, V., MOLIN, D. G. & POST, M. J. 2012. Notch regulation of hematopoiesis, endothelial precursor cells, and blood vessel formation: orchestrating the vasculature. *Stem Cells Int,* 2012**,** 805602.

CARMELIET, P. 2003. Angiogenesis in health and disease. *Nat Med,* 9**,** 653-60.

CHA, Y. R. & WEINSTEIN, B. M. 2007. Visualization and experimental analysis of blood vessel formation using transgenic zebrafish. *Birth Defects Res C Embryo Today,* 81**,** 286-96.

CHAN, D. A., SUTPHIN, P. D., DENKO, N. C. & GIACCIA, A. J. 2002. Role of prolyl hydroxylation in oncogenically stabilized hypoxia-inducible factor-1alpha. *J Biol Chem,* 277**,** 40112-7.

CHAN, P. K., LIN, C. C. & CHENG, S. H. 2009. Noninvasive technique for measurement of heartbeat regularity in zebrafish (Danio rerio) embryos. *BMC Biotechnol,* 9**,** 11.

CHICO, T. J., INGHAM, P. W. & CROSSMAN, D. C. 2008. Modeling cardiovascular disease in the zebrafish. *Trends Cardiovasc Med,* 18**,** 150-5.

CHIN, B. S., BLANN, A. D., GIBBS, C. R., CHUNG, N. A., CONWAY, D. G. & LIP, G. Y. 2003. Prognostic value of interleukin-6, plasma viscosity, fibrinogen, von Willebrand factor, tissue factor and vascular endothelial growth factor levels in congestive heart failure. *Eur J Clin Invest,* 33**,** 941-8.

CHO, Y. H., YOO, S. D. & SHEEN, J. 2006. Regulatory functions of nuclear hexokinase1 complex in glucose signaling. *Cell,* 127**,** 579-89.

CHOI, Y. K., KIM, C. K., LEE, H., JEOUNG, D., HA, K. S., KWON, Y. G., KIM, K. W. & KIM, Y. M. 2010. Carbon monoxide promotes VEGF expression by increasing HIF-1alpha protein level via two distinct mechanisms, translational activation and stabilization of HIF-1alpha protein. *J Biol Chem,* 285**,** 32116-25.

CHRIST, B., NATH, A. & JUNGERMANN, K. 1997. Mechanism of the impairment of the glucagon-stimulated phosphoenolpyruvate carboxykinase gene expression by interleukin-6 in rat hepatocytes: inhibition of the increase in cyclic 3',5' adenosine monophosphate and the downstream cyclic 3',5' adenosine monophosphate action. *Hepatology,* 26**,** 73-80.

CHUNG, A. S., LEE, J. & FERRARA, N. 2010. Targeting the tumour vasculature: insights from physiological angiogenesis. *Nat Rev Cancer,* 10**,** 505-14.

CLISSOLD, P. M. & PONTING, C. P. 2001. JmjC: cupin metalloenzyme-like domains in jumonji, hairless and phospholipase A2beta. *Trends Biochem Sci,* 26**,** 7-9.

COCKMAN, M. E., LANCASTER, D. E., STOLZE, I. P., HEWITSON, K. S., MCDONOUGH, M. A., COLEMAN, M. L., COLES, C. H., YU, X., HAY, R. T., LEY, S. C., PUGH, C. W., OLDHAM, N. J., MASSON, N., SCHOFIELD, C. J. & RATCLIFFE, P. J. 2006. Posttranslational hydroxylation of ankyrin repeats in IkappaB proteins by the hypoxia-inducible factor (HIF) asparaginyl hydroxylase, factor inhibiting HIF (FIH). *Proc Natl Acad Sci U S A,* 103**,** 14767-72.

COCKMAN, M. E., WEBB, J. D., KRAMER, H. B., KESSLER, B. M. & RATCLIFFE, P. J. 2009. Proteomics-based identification of novel factor inhibiting hypoxia-inducible factor (FIH) substrates indicates widespread asparaginyl hydroxylation of ankyrin repeat domain-containing proteins. *Mol Cell Proteomics,* 8**,** 535-46.

COLEMAN, M. L., MCDONOUGH, M. A., HEWITSON, K. S., COLES, C., MECINOVIC, J., EDELMANN, M., COOK, K. M., COCKMAN, M. E., LANCASTER, D. E., KESSLER, B. M., OLDHAM, N. J., RATCLIFFE, P. J. & SCHOFIELD, C. J. 2007. Asparaginyl hydroxylation of the Notch ankyrin repeat domain by factor inhibiting hypoxia-inducible factor. *J Biol Chem,* 282**,** 24027-38.

CONDE, E., ALEGRE, L., BLANCO-SANCHEZ, I., SAENZ-MORALES, D., AGUADO-FRAILE, E., PONTE, B., RAMOS, E., SAIZ, A., JIMENEZ, C., ORDONEZ, A., LOPEZ-CABRERA, M., DEL PESO, L., DE LANDAZURI, M. O., LIANO, F., SELGAS, R., SANCHEZ-TOMERO, J. A. & GARCIA-BERMEJO, M. L. 2012. Hypoxia inducible factor 1-alpha (HIF-1 alpha) is induced during reperfusion after renal ischemia and is critical for proximal tubule cell survival. *PLoS One,* 7**,** e33258.

COUFFINHAL, T., SILVER, M., ZHENG, L. P., KEARNEY, M., WITZENBICHLER, B. & ISNER, J. M. 1998. Mouse model of angiogenesis. *Am J Pathol,* 152**,** 1667-79.

COVASSIN, L. D., SIEKMANN, A. F., KACERGIS, M. C., LAVER, E., MOORE, J. C., VILLEFRANC, J. A., WEINSTEIN, B. M. & LAWSON, N. D. 2009. A genetic screen for vascular mutants in zebrafish reveals dynamic roles for Vegf/Plcg1 signaling during artery development. *Dev Biol,* 329**,** 212-26.

COVASSIN, L. D., VILLEFRANC, J. A., KACERGIS, M. C., WEINSTEIN, B. M. & LAWSON, N. D. 2006. Distinct genetic interactions between multiple Vegf receptors are required for

development of different blood vessel types in zebrafish. *Proc Natl Acad Sci U S A,* 103**,** 6554-9.

CRUK, U. C. R. 2011. *Cancer Statistics UK* [Online]. Available: http://info.cancerresearchuk.org/prod_consump/groups/cr_common/@nre/@sta/documents/generalcontent/018070.pdf.

CUMMINS, E. P., BERRA, E., COMERFORD, K. M., GINOUVES, A., FITZGERALD, K. T., SEEBALLUCK, F., GODSON, C., NIELSEN, J. E., MOYNAGH, P., POUYSSEGUR, J. & TAYLOR, C. T. 2006. Prolyl hydroxylase-1 negatively regulates IkappaB kinase-beta, giving insight into hypoxia-induced NFkappaB activity. *Proc Natl Acad Sci U S A,* 103**,** 18154-9.

D'ANGELO, G., DUPLAN, E., BOYER, N., VIGNE, P. & FRELIN, C. 2003. Hypoxia up-regulates prolyl hydroxylase activity: a feedback mechanism that limits HIF-1 responses during reoxygenation. *J Biol Chem,* 278**,** 38183-7.

DALLAS, P. B., GOTTARDO, N. G., FIRTH, M. J., BEESLEY, A. H., HOFFMANN, K., TERRY, P. A., FREITAS, J. R., BOAG, J. M., CUMMINGS, A. J. & KEES, U. R. 2005. Gene expression levels assessed by oligonucleotide microarray analysis and quantitative real-time RT-PCR -- how well do they correlate? *BMC Genomics,* 6**,** 59.

DANIORERIO.COM 2012. DanioRerio.com.

DANN, C. E., 3RD, BRUICK, R. K. & DEISENHOFER, J. 2002. Structure of factor-inhibiting hypoxia-inducible factor 1: An asparaginyl hydroxylase involved in the hypoxic response pathway. *Proc Natl Acad Sci U S A,* 99**,** 15351-6.

DE ESCH, C., VAN DER LINDE, H., SLIEKER, R., WILLEMSEN, R., WOLTERBEEK, A., WOUTERSEN, R. & DE GROOT, D. 2012. Locomotor activity assay in zebrafish larvae: Influence of age, strain and ethanol. *Neurotoxicol Teratol,* 34**,** 425-33.

DE VAL, S. & BLACK, B. L. 2009. Transcriptional control of endothelial cell development. *Dev Cell,* 16**,** 180-95.

DEL TORO, R., PRAHST, C., MATHIVET, T., SIEGFRIED, G., KAMINKER, J. S., LARRIVEE, B., BREANT, C., DUARTE, A., TAKAKURA, N., FUKAMIZU, A., PENNINGER, J. & EICHMANN, A. 2010. Identification and functional analysis of endothelial tip cell-enriched genes. *Blood,* 116**,** 4025-33.

DELCOURT, J., BECCO, C., VANDEWALLE, N. & PONCIN, P. 2009. A video multitracking system for quantification of individual behavior in a large fish shoal: advantages and limits. *Behav Res Methods,* 41**,** 228-35.

DENVIR, M. A., TUCKER, C. S. & MULLINS, J. J. 2008. Systolic and diastolic ventricular function in zebrafish embryos: influence of norepenephrine, MS-222 and temperature. *BMC Biotechnol,* 8**,** 21.

DEVRIES, I. L., HAMPTON-SMITH, R. J., MULVIHILL, M. M., ALVERDI, V., PEET, D. J. & KOMIVES, E. A. 2010. Consequences of IkappaB alpha hydroxylation by the factor inhibiting HIF (FIH). *FEBS Lett,* 584**,** 4725-30.

DODD, A., CURTIS, P. M., WILLIAMS, L. C. & LOVE, D. R. 2000. Zebrafish: bridging the gap between development and disease. *Hum Mol Genet,* 9**,** 2443-9.

DOMENE, C. & ILLINGWORTH, C. J. 2012. Effects of point mutations in pVHL on the binding of HIF-1alpha. *Proteins,* 80**,** 733-46.

DONOGHUE, M., HSIEH, F., BARONAS, E., GODBOUT, K., GOSSELIN, M., STAGLIANO, N., DONOVAN, M., WOOLF, B., ROBISON, K., JEYASEELAN, R., BREITBART, R. E. & ACTON, S. 2000. A novel angiotensin-converting enzyme-related carboxypeptidase (ACE2) converts angiotensin I to angiotensin 1-9. *Circ Res,* 87**,** E1-9.

DRAKE, C. J. & FLEMING, P. A. 2000. Vasculogenesis in the day 6.5 to 9.5 mouse embryo. *Blood,* 95**,** 1671-9.

DUMONT, D. J., FONG, G. H., PURI, M. C., GRADWOHL, G., ALITALO, K. & BREITMAN, M. L. 1995. Vascularization of the mouse embryo: a study of flk-1, tek, tie, and vascular endothelial growth factor expression during development. *Dev Dyn,* 203**,** 80-92.

DVORAK, H. F., BROWN, L. F., DETMAR, M. & DVORAK, A. M. 1995. Vascular permeability factor/vascular endothelial growth factor, microvascular hyperpermeability, and angiogenesis. *Am J Pathol,* 146**,** 1029-39.

EDVINSSON, L. I. & POVLSEN, G. K. 2011. Vascular plasticity in cerebrovascular disorders. *J Cereb Blood Flow Metab,* 31**,** 1554-71.

EHEBAUER, M. T., CHIRGADZE, D. Y., HAYWARD, P., MARTINEZ ARIAS, A. & BLUNDELL, T. L. 2005. High-resolution crystal structure of the human Notch 1 ankyrin domain. *Biochem J,* 392**,** 13-20.

ELKINS, J. M., HEWITSON, K. S., MCNEILL, L. A., SEIBEL, J. F., SCHLEMMINGER, I., PUGH, C. W., RATCLIFFE, P. J. & SCHOFIELD, C. J. 2003. Structure of factor-inhibiting hypoxia-inducible factor (HIF) reveals mechanism of oxidative modification of HIF-1 alpha. *J Biol Chem,* 278**,** 1802-6.

ELKS, P. M., VAN EEDEN, F. J., DIXON, G., WANG, X., REYES-ALDASORO, C. C., INGHAM, P. W., WHYTE, M. K., WALMSLEY, S. R. & RENSHAW, S. A. 2011. Activation of hypoxia-inducible factor-1alpha (Hif-1alpha) delays inflammation resolution by reducing neutrophil apoptosis and reverse migration in a zebrafish inflammation model. *Blood,* 118**,** 712-22.

ELLIS, L., CLAUSER, E., MORGAN, D. O., EDERY, M., ROTH, R. A. & RUTTER, W. J. 1986. Replacement of insulin receptor tyrosine residues 1162 and 1163 compromises insulin-stimulated kinase activity and uptake of 2-deoxyglucose. *Cell,* 45**,** 721-32.

ELLIS, L. D., SEIBERT, J. & SOANES, K. H. 2012. Distinct models of induced hyperactivity in zebrafish larvae. *Brain Res,* 1449**,** 46-59.

ELO, B., VILLANO, C. M., GOVORKO, D. & WHITE, L. A. 2007. Larval zebrafish as a model for glucose metabolism: expression of phosphoenolpyruvate carboxykinase as a marker for exposure to anti-diabetic compounds. *J Mol Endocrinol,* 38**,** 433-40.

ENSEMBL. 2012. *Ensembl Genome Browser* [Online]. Available: http://www.ensembl.org/index.html.

EPSTEIN, A. C., GLEADLE, J. M., MCNEILL, L. A., HEWITSON, K. S., O'ROURKE, J., MOLE, D. R., MUKHERJI, M., METZEN, E., WILSON, M. I., DHANDA, A., TIAN, Y. M., MASSON, N., HAMILTON, D. L., JAAKKOLA, P., BARSTEAD, R., HODGKIN, J., MAXWELL, P. H., PUGH, C. W., SCHOFIELD, C. J. & RATCLIFFE, P. J. 2001. C. elegans EGL-9 and mammalian homologs define a family of dioxygenases that regulate HIF by prolyl hydroxylation. *Cell,* 107**,** 43-54.

ERDOS, E. G., TAN, F. & SKIDGEL, R. A. 2010. Angiotensin I-converting enzyme inhibitors are allosteric enhancers of kinin B1 and B2 receptor function. *Hypertension,* 55**,** 214-20.

EREZ, N., MILYAVSKY, M., EILAM, R., SHATS, I., GOLDFINGER, N. & ROTTER, V. 2003. Expression of prolyl-hydroxylase-1 (PHD1/EGLN2) suppresses hypoxia inducible factor-1alpha activation and inhibits tumor growth. *Cancer Res,* 63**,** 8777-83.

ESTEBAN, M. A., HARTEN, S. K., TRAN, M. G. & MAXWELL, P. H. 2006. Formation of primary cilia in the renal epithelium is regulated by the von Hippel-Lindau tumor suppressor protein. *J Am Soc Nephrol,* 17**,** 1801-6.

EVANS, C. E., BRANCO-PRICE, C. & JOHNSON, R. S. 2012. HIF-mediated endothelial response during cancer progression. *Int J Hematol,* 95**,** 471-7.

FAHLING, M. & PERSSON, P. B. 2012. Oxygen sensing, uptake, delivery, consumption and related disorders. *Acta Physiol (Oxf),* 205**,** 191-3.

FERRANTE, M. I., KIFF, R. M., GOULDING, D. A. & STEMPLE, D. L. 2011. Troponin T is essential for sarcomere assembly in zebrafish skeletal muscle. *J Cell Sci,* 124**,** 565-77.

FFS, F. F. S. 2011. *Fish For Science* [Online]. Available: http://fishforscience.com/model-organisms/why-zebrafish.

FIRTH, J. D., EBERT, B. L. & RATCLIFFE, P. J. 1995. Hypoxic regulation of lactate dehydrogenase A. Interaction between hypoxia-inducible factor 1 and cAMP response elements. *J Biol Chem,* 270**,** 21021-7.

FISCHER, A., KLAMT, B., SCHUMACHER, N., GLAESER, C., HANSMANN, I., FENGE, H. & GESSLER, M. 2004a. Phenotypic variability in Hey2 -/- mice and absence of HEY2 mutations in patients with congenital heart defects or Alagille syndrome. *Mamm Genome,* 15**,** 711-6.

FISCHER, A., SCHUMACHER, N., MAIER, M., SENDTNER, M. & GESSLER, M. 2004b. The Notch target genes Hey1 and Hey2 are required for embryonic vascular development. *Genes Dev,* 18**,** 901-11.

FISHER, E., GRALLERT, H., KLAPPER, M., PFAFFLIN, A., SCHREZENMEIR, J., ILLIG, T., BOEING, H. & DORING, F. 2009. Evidence for the Thr79Met polymorphism of the ileal fatty acid binding protein (FABP6) to be associated with type 2 diabetes in obese individuals. *Mol Genet Metab,* 98**,** 400-5.

FLAMME, I., FROLICH, T. & RISAU, W. 1997. Molecular mechanisms of vasculogenesis and embryonic angiogenesis. *J Cell Physiol,* 173**,** 206-10.

FLEISCH, V. C. & NEUHAUSS, S. C. 2006. Visual behavior in zebrafish. *Zebrafish,* 3**,** 191-201.

FLEMING, A. 2007. Zebrafish as an alternative model organism for modelling and drug discovery: implications for the 3Rs.

FOLKMAN, J. 1985. Tumor angiogenesis. *Adv Cancer Res,* 43**,** 175-203.

FONG, G. H. 2008. Mechanisms of adaptive angiogenesis to tissue hypoxia. *Angiogenesis,* 11**,** 121-40.

FONG, G. H. 2009. Regulation of angiogenesis by oxygen sensing mechanisms. *J Mol Med (Berl),* 87**,** 549-60.

FONG, G. H. & TAKEDA, K. 2008. Role and regulation of prolyl hydroxylase domain proteins. *Cell Death Differ,* 15**,** 635-41.

FORMENTI, F., BEER, P. A., CROFT, Q. P., DORRINGTON, K. L., GALE, D. P., LAPPIN, T. R., LUCAS, G. S., MAHER, E. R., MAXWELL, P. H., MCMULLIN, M. F., O'CONNOR, D. F., PERCY, M. J., PUGH, C. W., RATCLIFFE, P. J., SMITH, T. G., TALBOT, N. P. & ROBBINS, P. A. 2011. Cardiopulmonary function in two human disorders of the hypoxia-inducible factor (HIF) pathway: von Hippel-Lindau disease and HIF-2alpha gain-of-function mutation. *FASEB J,* 25**,** 2001-11.

FORSYTHE, J. A., JIANG, B. H., IYER, N. V., AGANI, F., LEUNG, S. W., KOOS, R. D. & SEMENZA, G. L. 1996. Activation of vascular endothelial growth factor gene transcription by hypoxia-inducible factor 1. *Mol Cell Biol,* 16**,** 4604-13.

FORTINI, M. E. & ARTAVANIS-TSAKONAS, S. 1994. The suppressor of hairless protein participates in notch receptor signaling. *Cell,* 79**,** 273-82.

FOSKETT, A. M., EZEKIEL, U. R., TRZECIAKOWSKI, J. P., ZAWIEJA, D. C. & MUTHUCHAMY, M. 2011. Hypoxia and extracellular matrix proteins influence angiogenesis and lymphangiogenesis in mouse embryoid bodies. *Front Physiol,* 2**,** 103.

FOUQUET, B., WEINSTEIN, B. M., SERLUCA, F. C. & FISHMAN, M. C. 1997. Vessel patterning in the embryo of the zebrafish: guidance by notochord. *Dev Biol,* 183**,** 37-48.

FREI, C. & EDGAR, B. A. 2004. Drosophila cyclin D/Cdk4 requires Hif-1 prolyl hydroxylase to drive cell growth. *Dev Cell,* 6**,** 241-51.

FREW, I. J. & KREK, W. 2007. Multitasking by pVHL in tumour suppression. *Curr Opin Cell Biol,* 19**,** 685-90.

GENG, H., HARVEY, C. T., PITTSENBARGER, J., LIU, Q., BEER, T. M., XUE, C. & QIAN, D. Z. 2011. HDAC4 protein regulates HIF1alpha protein lysine acetylation and cancer cell response to hypoxia. *J Biol Chem,* 286**,** 38095-102.

GERETY, S. S., WANG, H. U., CHEN, Z. F. & ANDERSON, D. J. 1999. Symmetrical mutant phenotypes of the receptor EphB4 and its specific transmembrane ligand ephrin-B2 in cardiovascular development. *Mol Cell,* 4**,** 403-14.

GERHARDT, H., GOLDING, M., FRUTTIGER, M., RUHRBERG, C., LUNDKVIST, A., ABRAMSSON, A., JELTSCH, M., MITCHELL, C., ALITALO, K., SHIMA, D. & BETSHOLTZ, C. 2003. VEGF guides angiogenic sprouting utilizing endothelial tip cell filopodia. *J Cell Biol,* 161**,** 1163-77.

GERING, M., RODAWAY, A. R., GOTTGENS, B., PATIENT, R. K. & GREEN, A. R. 1998. The SCL gene specifies haemangioblast development from early mesoderm. *EMBO J,* 17**,** 4029-45.

GEUDENS, I. & GERHARDT, H. 2011. Coordinating cell behaviour during blood vessel formation. *Development,* 138**,** 4569-83.

GHOSH, S., PAEZ-CORTEZ, J. R., BOPPIDI, K., VASCONCELOS, M., ROY, M., CARDOSO, W., AI, X. & FINE, A. 2011. Activation dynamics and signaling properties of Notch3 receptor in the developing pulmonary artery. *J Biol Chem,* 286**,** 22678-87.

GILHAM, D., LABONTE, E. D., ROJAS, J. C., JANDACEK, R. J., HOWLES, P. N. & HUI, D. Y. 2007. Carboxyl ester lipase deficiency exacerbates dietary lipid absorption abnormalities and resistance to diet-induced obesity in pancreatic triglyceride lipase knockout mice. *J Biol Chem,* 282**,** 24642-9.

GILMOUR, K. M., DESFORGES, P. R. & PERRY, S. F. 2004. Buffering limits plasma HCO3- dehydration when red blood cell anion exchange is inhibited. *Respir Physiol Neurobiol,* 140**,** 173-87.

GILMOUR, K. M., THOMAS, K., ESBAUGH, A. J. & PERRY, S. F. 2009. Carbonic anhydrase expression and CO2 excretion during early development in zebrafish Danio rerio. *J Exp Biol,* 212**,** 3837-45.

GLASER, S. P., LEE, E. F., TROUNSON, E., BOUILLET, P., WEI, A., FAIRLIE, W. D., IZON, D. J., ZUBER, J., RAPPAPORT, A. R., HEROLD, M. J., ALEXANDER, W. S., LOWE, S. W., ROBB, L. & STRASSER, A. 2012. Anti-apoptotic Mcl-1 is essential for the development and sustained growth of acute myeloid leukemia. *Genes Dev,* 26**,** 120-5.

GNARRA, J. R., LERMAN, M. I., ZBAR, B. & LINEHAN, W. M. 1995. Genetics of renal-cell carcinoma and evidence for a critical role for von Hippel-Lindau in renal tumorigenesis. *Semin Oncol,* 22**,** 3-8.

GNARRA, J. R., WARD, J. M., PORTER, F. D., WAGNER, J. R., DEVOR, D. E., GRINBERG, A., EMMERT-BUCK, M. R., WESTPHAL, H., KLAUSNER, R. D. & LINEHAN, W. M. 1997. Defective placental vasculogenesis causes embryonic lethality in VHL-deficient mice. *Proc Natl Acad Sci U S A,* 94**,** 9102-7.

GOMES, A. V., GUZMAN, G., ZHAO, J. & POTTER, J. D. 2002. Cardiac troponin T isoforms affect the Ca2+ sensitivity and inhibition of force development. Insights into the role of troponin T isoforms in the heart. *J Biol Chem,* 277**,** 35341-9.

GORDEUK, V. R., SERGUEEVA, A. I., MIASNIKOVA, G. Y., OKHOTIN, D., VOLOSHIN, Y., CHOYKE, P. L., BUTMAN, J. A., JEDLICKOVA, K., PRCHAL, J. T. & POLYAKOVA, L. A. 2004. Congenital disorder of oxygen sensing: association of the homozygous Chuvash polycythemia VHL mutation with thrombosis and vascular abnormalities but not tumors. *Blood,* 103**,** 3924-32.

GRADIN, K., TAKASAKI, C., FUJII-KURIYAMA, Y. & SOGAWA, K. 2002. The transcriptional activation function of the HIF-like factor requires phosphorylation at a conserved threonine. *J Biol Chem,* 277**,** 23508-14.

GRANATO, M. & NUSSLEIN-VOLHARD, C. 1996. Fishing for genes controlling development. *Curr Opin Genet Dev,* 6**,** 461-8.

GRAY, C., PACKHAM, I. M., WURMSER, F., EASTLEY, N. C., HELLEWELL, P. G., INGHAM, P. W., CROSSMAN, D. C. & CHICO, T. J. 2007. Ischemia is not required for arteriogenesis in zebrafish embryos. *Arterioscler Thromb Vasc Biol,* 27**,** 2135-41.

GREGORY, M., HANUMANTHAIAH, R. & JAGADEESWARAN, P. 2002. Genetic analysis of hemostasis and thrombosis using vascular occlusion. *Blood Cells Mol Dis,* 29**,** 286-95.

GREIJER, A. E. & VAN DER WALL, E. 2004. The role of hypoxia inducible factor 1 (HIF-1) in hypoxia induced apoptosis. *J Clin Pathol,* 57**,** 1009-14.

GROENMAN, F. A., RUTTER, M., WANG, J., CANIGGIA, I., TIBBOEL, D. & POST, M. 2007. Effect of chemical stabilizers of hypoxia-inducible factors on early lung development. *Am J Physiol Lung Cell Mol Physiol,* 293**,** L557-67.

GRUBER, M., HU, C. J., JOHNSON, R. S., BROWN, E. J., KEITH, B. & SIMON, M. C. 2007. Acute postnatal ablation of Hif-2alpha results in anemia. *Proc Natl Acad Sci U S A,* 104**,** 2301-6.

GUIDOLIN, D., REBUFFAT, P. & ALBERTIN, G. 2011. Cell-oriented modeling of angiogenesis. *ScientificWorldJournal,* 11**,** 1735-48.

GUSTAFSSON, M. V., ZHENG, X., PEREIRA, T., GRADIN, K., JIN, S., LUNDKVIST, J., RUAS, J. L., POELLINGER, L., LENDAHL, U. & BONDESSON, M. 2005. Hypoxia requires notch signaling to maintain the undifferentiated cell state. *Dev Cell,* 9**,** 617-28.

HABECK, H., ODENTHAL, J., WALDERICH, B., MAISCHEIN, H. & SCHULTE-MERKER, S. 2002. Analysis of a zebrafish VEGF receptor mutant reveals specific disruption of angiogenesis. *Curr Biol,* 12**,** 1405-12.

HAK, S., REITAN, N. K., HARALDSETH, O. & DE LANGE DAVIES, C. 2010. Intravital microscopy in window chambers: a unique tool to study tumor angiogenesis and delivery of nanoparticles. *Angiogenesis,* 13**,** 113-30.

HALIN, S., RUDOLFSSON, S. H., VAN ROOIJEN, N. & BERGH, A. 2009. Extratumoral macrophages promote tumor and vascular growth in an orthotopic rat prostate tumor model. *Neoplasia,* 11**,** 177-86.

HANSON, E. S., RAWLINS, M. L. & LEIBOLD, E. A. 2003. Oxygen and iron regulation of iron regulatory protein 2. *J Biol Chem,* 278**,** 40337-42.

HARA, T., MIMURA, K., ABE, T., SHIOI, G., SEIKI, M. & SAKAMOTO, T. 2011. Deletion of the Mint3/Apba3 gene in mice abrogates macrophage functions and increases resistance to lipopolysaccharide-induced septic shock. *J Biol Chem,* 286**,** 32542-51.

HARDY, A. P., PROKES, I., KELLY, L., CAMPBELL, I. D. & SCHOFIELD, C. J. 2009. Asparaginyl beta-hydroxylation of proteins containing ankyrin repeat domains influences their stability and function. *J Mol Biol,* 392**,** 994-1006.

HAYASHI, H. & KUME, T. 2008. Foxc transcription factors directly regulate Dll4 and Hey2 expression by interacting with the VEGF-Notch signaling pathways in endothelial cells. *PLoS One,* 3**,** e2401.

HEIKKILA, M., PASANEN, A., KIVIRIKKO, K. I. & MYLLYHARJU, J. 2011. Roles of the human hypoxia-inducible factor (HIF)-3alpha variants in the hypoxia response. *Cell Mol Life Sci,* 68**,** 3885-901.

HEINKE, J., PATTERSON, C. & MOSER, M. 2012. Life is a pattern: vascular assembly within the embryo. *Front Biosci (Elite Ed),* 4**,** 2269-88.

HELFRICH, I. & SCHADENDORF, D. 2011. Blood vessel maturation, vascular phenotype and angiogenic potential in malignant melanoma: one step forward for overcoming anti-angiogenic drug resistance? *Mol Oncol,* 5**,** 137-49.

HELLSTROM, M., PHNG, L. K., HOFMANN, J. J., WALLGARD, E., COULTAS, L., LINDBLOM, P., ALVA, J., NILSSON, A. K., KARLSSON, L., GAIANO, N., YOON, K., ROSSANT, J., IRUELA-ARISPE, M. L., KALEN, M., GERHARDT, H. & BETSHOLTZ, C. 2007. Dll4 signalling through Notch1 regulates formation of tip cells during angiogenesis. *Nature,* 445**,** 776-80.

HER, G. M., CHIANG, C. C., CHEN, W. Y. & WU, J. L. 2003. In vivo studies of liver-type fatty acid binding protein (L-FABP) gene expression in liver of transgenic zebrafish (Danio rerio). *FEBS Lett,* 538**,** 125-33.

HERBERT, S. P., HUISKEN, J., KIM, T. N., FELDMAN, M. E., HOUSEMAN, B. T., WANG, R. A., SHOKAT, K. M. & STAINIER, D. Y. 2009. Arterial-venous segregation by selective cell sprouting: an alternative mode of blood vessel formation. *Science,* 326**,** 294-8.

HEWITSON, K. S., MCNEILL, L. A., RIORDAN, M. V., TIAN, Y. M., BULLOCK, A. N., WELFORD, R. W., ELKINS, J. M., OLDHAM, N. J., BHATTACHARYA, S., GLEADLE, J. M., RATCLIFFE, P. J., PUGH, C. W. & SCHOFIELD, C. J. 2002. Hypoxia-inducible factor (HIF) asparagine hydroxylase is identical to factor inhibiting HIF (FIH) and is related to the cupin structural family. *J Biol Chem,* 277**,** 26351-5.

HICKEY, M. M., LAM, J. C., BEZMAN, N. A., RATHMELL, W. K. & SIMON, M. C. 2007. von Hippel-Lindau mutation in mice recapitulates Chuvash polycythemia via hypoxia-inducible factor-2alpha signaling and splenic erythropoiesis. *J Clin Invest,* 117**,** 3879-89.

HICKEY, M. M., RICHARDSON, T., WANG, T., MOSQUEIRA, M., ARGUIRI, E., YU, H., YU, Q. C., SOLOMIDES, C. C., MORRISEY, E. E., KHURANA, T. S., CHRISTOFIDOU-SOLOMIDOU, M. & SIMON, M. C. 2010. The von Hippel-Lindau Chuvash mutation promotes pulmonary hypertension and fibrosis in mice. *J Clin Invest,* 120**,** 827-39.

HIRSILA, M., KOIVUNEN, P., XU, L., SEELEY, T., KIVIRIKKO, K. I. & MYLLYHARJU, J. 2005. Effect of desferrioxamine and metals on the hydroxylases in the oxygen sensing pathway. *FASEB J,* 19**,** 1308-10.

HO, T. K., SHIWEN, X., ABRAHAM, D., TSUI, J. & BAKER, D. 2012. Stromal-Cell-Derived Factor-1 (SDF-1)/CXCL12 as Potential Target of Therapeutic Angiogenesis in Critical Leg Ischaemia. *Cardiol Res Pract,* 2012**,** 143209.

HOFER, T., WENGER, R. H., KRAMER, M. F., FERREIRA, G. C. & GASSMANN, M. 2003. Hypoxic up-regulation of erythroid 5-aminolevulinate synthase. *Blood,* 101**,** 348-50.

HOFMANN, A. F. & BORGSTROEM, B. 1964. The Intraluminal Phase of Fat Digestion in Man: The Lipid Content of the Micellar and Oil Phases of Intestinal Content Obtained during Fat Digestion and Absorption. *J Clin Invest,* 43**,** 247-57.

HOLSCHER, M., SCHAFER, K., KRULL, S., FARHAT, K., HESSE, A., SILTER, M., LIN, Y., PICHLER, B. J., THISTLETHWAITE, P., EL-ARMOUCHE, A., MAIER, L. S., KATSCHINSKI, D. M. & ZIESENISS, A. 2012. Unfavourable consequences of chronic cardiac HIF-1alpha stabilization. *Cardiovasc Res,* 94**,** 77-86.

HUANG, L. E., ARANY, Z., LIVINGSTON, D. M. & BUNN, H. F. 1996. Activation of hypoxia-inducible transcription factor depends primarily upon redox-sensitive stabilization of its alpha subunit. *J Biol Chem,* 271**,** 32253-9.

ICHIOKA, S., SHIBATA, M., KOSAKI, K., SATO, Y., HARII, K. & KAMIYA, A. 1997. Effects of shear stress on wound-healing angiogenesis in the rabbit ear chamber. *J Surg Res,* 72**,** 29-35.

ILIOPOULOS, O., LEVY, A. P., JIANG, C., KAELIN, W. G., JR. & GOLDBERG, M. A. 1996. Negative regulation of hypoxia-inducible genes by the von Hippel-Lindau protein. *Proc Natl Acad Sci U S A,* 93**,** 10595-9.

ILIOPOULOS, O., OHH, M. & KAELIN, W. G., JR. 1998. pVHL19 is a biologically active product of the von Hippel-Lindau gene arising from internal translation initiation. *Proc Natl Acad Sci U S A,* 95**,** 11661-6.

ISO, T., MAENO, T., OIKE, Y., YAMAZAKI, M., DOI, H., ARAI, M. & KURABAYASHI, M. 2006. Dll4-selective Notch signaling induces ephrinB2 gene expression in endothelial cells. *Biochem Biophys Res Commun,* 341**,** 708-14.

ISOBE, T., AOYAGI, K., KOUFUJI, K., SHIROUZU, K., KAWAHARA, A., TAIRA, T. & KAGE, M. 2012. Clinicopathological significance of hypoxia-inducible factor-1 alpha (HIF-1alpha) expression in gastric cancer. *Int J Clin Oncol*.

ISOGAI, S., HORIGUCHI, M. & WEINSTEIN, B. M. 2001. The vascular anatomy of the developing zebrafish: an atlas of embryonic and early larval development. *Dev Biol,* 230**,** 278-301.

IWAI, K., DRAKE, S. K., WEHR, N. B., WEISSMAN, A. M., LAVAUTE, T., MINATO, N., KLAUSNER, R. D., LEVINE, R. L. & ROUAULT, T. A. 1998. Iron-dependent oxidation, ubiquitination, and degradation of iron regulatory protein 2: implications for degradation of oxidized proteins. *Proc Natl Acad Sci U S A,* 95**,** 4924-8.

IWAI, K., YAMANAKA, K., KAMURA, T., MINATO, N., CONAWAY, R. C., CONAWAY, J. W., KLAUSNER, R. D. & PAUSE, A. 1999. Identification of the von Hippel-lindau tumor-suppressor protein as part of an active E3 ubiquitin ligase complex. *Proc Natl Acad Sci U S A,* 96**,** 12436-41.

IYER, N. V., KOTCH, L. E., AGANI, F., LEUNG, S. W., LAUGHNER, E., WENGER, R. H., GASSMANN, M., GEARHART, J. D., LAWLER, A. M., YU, A. Y. & SEMENZA, G. L. 1998. Cellular and developmental control of O2 homeostasis by hypoxia-inducible factor 1 alpha. *Genes Dev,* 12**,** 149-62.

JAAKKOLA, P., MOLE, D. R., TIAN, Y. M., WILSON, M. I., GIELBERT, J., GASKELL, S. J., KRIEGSHEIM, A., HEBESTREIT, H. F., MUKHERJI, M., SCHOFIELD, C. J., MAXWELL, P. H., PUGH, C. W. & RATCLIFFE, P. J. 2001. Targeting of HIF-alpha to the von Hippel-Lindau ubiquitylation complex by O2-regulated prolyl hydroxylation. *Science,* 292**,** 468-72.

JACOBY, D. S. & RADER, D. J. 2003. Renin-angiotensin system and atherothrombotic disease: from genes to treatment. *Arch Intern Med,* 163**,** 1155-64.

JAGADEESWARAN, P., GREGORY, M., JOHNSON, S. & THANKAVEL, B. 2000. Haemostatic screening and identification of zebrafish mutants with coagulation pathway defects: an approach to identifying novel haemostatic genes in man. *Br J Haematol,* 110**,** 946-56.

JAGADEESWARAN, P. & SHEEHAN, J. P. 1999. Analysis of blood coagulation in the zebrafish. *Blood Cells Mol Dis,* 25**,** 239-49.

JAKOBSSON, L., FRANCO, C. A., BENTLEY, K., COLLINS, R. T., PONSIOEN, B., ASPALTER, I. M., ROSEWELL, I., BUSSE, M., THURSTON, G., MEDVINSKY, A., SCHULTE-MERKER, S. & GERHARDT, H. 2010. Endothelial cells dynamically compete for the tip cell position during angiogenic sprouting. *Nat Cell Biol,* 12**,** 943-53.

JAYASOORIYA, A. P., MATHAI, M. L., WALKER, L. L., BEGG, D. P., DENTON, D. A., CAMERON-SMITH, D., EGAN, G. F., MCKINLEY, M. J., RODGER, P. D., SINCLAIR, A. J., WARK, J. D., WEISINGER, H. S., JOIS, M. & WEISINGER, R. S. 2008. Mice lacking angiotensin-converting enzyme have increased energy expenditure, with reduced fat mass and improved glucose clearance. *Proc Natl Acad Sci U S A,* 105**,** 6531-6.

JELKMANN, W. 1992. Erythropoietin: structure, control of production, and function. *Physiol Rev,* 72**,** 449-89.

JUAREZ, I., GRATTON, A. & FLORES, G. 2008. Ontogeny of altered dendritic morphology in the rat prefrontal cortex, hippocampus, and nucleus accumbens following Cesarean delivery and birth anoxia. *J Comp Neurol,* 507**,** 1734-47.

KAELIN, W. G., JR. 2002. Molecular basis of the VHL hereditary cancer syndrome. *Nat Rev Cancer,* 2**,** 673-82.

KAJIMURA, S., AIDA, K. & DUAN, C. 2005. Insulin-like growth factor-binding protein-1 (IGFBP-1) mediates hypoxia-induced embryonic growth and developmental retardation. *Proc Natl Acad Sci U S A,* 102**,** 1240-5.

KALUZ, S., KALUZOVA, M. & STANBRIDGE, E. J. 2008. Regulation of gene expression by hypoxia: integration of the HIF-transduced hypoxic signal at the hypoxia-responsive element. *Clin Chim Acta,* 395**,** 6-13.

KAMURA, T., KOEPP, D. M., CONRAD, M. N., SKOWYRA, D., MORELAND, R. J., ILIOPOULOS, O., LANE, W. S., KAELIN, W. G., JR., ELLEDGE, S. J., CONAWAY, R. C., HARPER, J. W. & CONAWAY, J. W. 1999. Rbx1, a component of the VHL tumor suppressor complex and SCF ubiquitin ligase. *Science,* 284**,** 657-61.

KATO, H., INOUE, T., ASANOMA, K., NISHIMURA, C., MATSUDA, T. & WAKE, N. 2006. Induction of human endometrial cancer cell senescence through modulation of HIF-1alpha activity by EGLN1. *Int J Cancer,* 118**,** 1144-53.

KATO, H., SAKAI, T., TAMURA, K., MINOGUCHI, S., SHIRAYOSHI, Y., HAMADA, Y., TSUJIMOTO, Y. & HONJO, T. 1996. Functional conservation of mouse Notch receptor family members. *FEBS Lett,* 395**,** 221-4.

KATOH, M. 2007. Integrative genomic analyses on HES/HEY family: Notch-independent HES1, HES3 transcription in undifferentiated ES cells, and Notch-dependent HES1, HES5, HEY1, HEY2, HEYL transcription in fetal tissues, adult tissues, or cancer. *Int J Oncol,* 31**,** 461-6.

KECK, P. J., HAUSER, S. D., KRIVI, G., SANZO, K., WARREN, T., FEDER, J. & CONNOLLY, D. T. 1989. Vascular permeability factor, an endothelial cell mitogen related to PDGF. *Science,* 246**,** 1309-12.

KEITH, B., JOHNSON, R. S. & SIMON, M. C. 2012. HIF1alpha and HIF2alpha: sibling rivalry in hypoxic tumour growth and progression. *Nat Rev Cancer,* 12**,** 9-22.

KELLY, L., MCDONOUGH, M. A., COLEMAN, M. L., RATCLIFFE, P. J. & SCHOFIELD, C. J. 2009. Asparagine beta-hydroxylation stabilizes the ankyrin repeat domain fold. *Mol Biosyst,* 5**,** 52-8.

KERTSCHO, H., LAUSCHER, P., RAAB, L., ZACHAROWSKI, K. & MEIER, J. 2012. Effects of hyperoxic ventilation on 6-h survival at the critical haemoglobin concentration aggravated by experimentally induced tachycardia in anaesthetized pigs. *Acta Physiol (Oxf),* 204**,** 582-91.

KIBEL, A., ILIOPOULOS, O., DECAPRIO, J. A. & KAELIN, W. G., JR. 1995. Binding of the von Hippel-Lindau tumor suppressor protein to Elongin B and C. *Science,* 269**,** 1444-6.

KIDD, S., KELLEY, M. R. & YOUNG, M. W. 1986. Sequence of the notch locus of Drosophila melanogaster: relationship of the encoded protein to mammalian clotting and growth factors. *Mol Cell Biol,* 6**,** 3094-108.

KIM, S., URS, S., MASSIERA, F., WORTMANN, P., JOSHI, R., HEO, Y. R., ANDERSEN, B., KOBAYASHI, H., TEBOUL, M., AILHAUD, G., QUIGNARD-BOULANGE, A., FUKAMIZU, A., JONES, B. H., KIM, J. H. & MOUSTAID-MOUSSA, N. 2002. Effects of high-fat diet, angiotensinogen (agt) gene inactivation, and targeted expression to adipose tissue on lipid metabolism and renal gene expression. *Horm Metab Res,* 34**,** 721-5.

KIMMEL, C. B., BALLARD, W. W., KIMMEL, S. R., ULLMANN, B. & SCHILLING, T. F. 1995. Stages of embryonic development of the zebrafish. *Dev Dyn,* 203**,** 253-310.

KIMURA, H., WEISZ, A., OGURA, T., HITOMI, Y., KURASHIMA, Y., HASHIMOTO, K., D'ACQUISTO, F., MAKUUCHI, M. & ESUMI, H. 2001. Identification of hypoxia-inducible factor 1 ancillary sequence and its function in vascular endothelial growth factor gene induction by hypoxia and nitric oxide. *J Biol Chem,* 276**,** 2292-8.

KINOSHITA, K., GORYO, K., TAKADA, M., TOMOKUNI, Y., ASO, T., OKUDA, H., SHUIN, T., FUKUMURA, H. & SOGAWA, K. 2007. Ternary complex formation of pVHL, elongin B and elongin C visualized in living cells by a fluorescence resonance energy transfer-fluorescence lifetime imaging microscopy technique. *FEBS J,* 274**,** 5567-75.

KOTH, C. M., BOTUYAN, M. V., MORELAND, R. J., JANSMA, D. B., CONAWAY, J. W., CONAWAY, R. C., CHAZIN, W. J., FRIESEN, J. D., ARROWSMITH, C. H. & EDWARDS, A. M. 2000. Elongin from Saccharomyces cerevisiae. *J Biol Chem,* 275**,** 11174-80.

KOUKOURAKIS, M. I., GIATROMANOLAKI, A., SIVRIDIS, E., PASTOREK, J., KARAPANTZOS, I., GATTER, K. C. & HARRIS, A. L. 2004. Hypoxia-activated tumor pathways of angiogenesis and pH regulation independent of anemia in head-and-neck cancer. *Int J Radiat Oncol Biol Phys,* 59**,** 67-71.

KOUYAMA, R., SUGANAMI, T., NISHIDA, J., TANAKA, M., TOYODA, T., KISO, M., CHIWATA, T., MIYAMOTO, Y., YOSHIMASA, Y., FUKAMIZU, A., HORIUCHI, M., HIRATA, Y. & OGAWA, Y. 2005. Attenuation of diet-induced weight gain and adiposity through increased energy expenditure in mice lacking angiotensin II type 1a receptor. *Endocrinology,* 146**,** 3481-9.

KRANTZ, S. B. 1991. Erythropoietin. *Blood,* 77**,** 419-34.

KRIEG, M., HAAS, R., BRAUCH, H., ACKER, T., FLAMME, I. & PLATE, K. H. 2000. Up-regulation of hypoxia-inducible factors HIF-1alpha and HIF-2alpha under normoxic conditions in renal carcinoma cells by von Hippel-Lindau tumor suppressor gene loss of function. *Oncogene,* 19**,** 5435-43.

KRIKKEN, J. A., VAN REE, R. M., KLOOSTER, A., SEELEN, M. A., BORGHUIS, T., LEMS, S. P., SCHOUTEN, J. P., BAKKER, W. W., GANS, R. O., NAVIS, G. & BAKKER, S. J. 2010. High plasma hemopexin activity is an independent risk factor for late graft failure in renal transplant recipients. *Transpl Int,* 23**,** 805-12.

KUCEJOVA, B., SUNNY, N. E., NGUYEN, A. D., HALLAC, R., FU, X., PENA-LLOPIS, S., MASON, R. P., DEBERARDINIS, R. J., XIE, X. J., DEBOSE-BOYD, R., KODIBAGKAR, V. D., BURGESS, S. C. & BRUGAROLAS, J. 2011. Uncoupling hypoxia signaling from oxygen sensing in the liver results in hypoketotic hypoglycemic death. *Oncogene,* 30**,** 2147-60.

KUME, T. 2010. Specification of arterial, venous, and lymphatic endothelial cells during embryonic development. *Histol Histopathol,* 25**,** 637-46.

LAI, E. C. 2004. Notch signaling: control of cell communication and cell fate. *Development,* 131**,** 965-73.

LAI, Y., SONG, M., HAKALA, K., WEINTRAUB, S. T. & SHIIO, Y. 2011. Proteomic dissection of the von Hippel-Lindau (VHL) interactome. *J Proteome Res,* 10**,** 5175-82.

LAMAR, E., DEBLANDRE, G., WETTSTEIN, D., GAWANTKA, V., POLLET, N., NIEHRS, C. & KINTNER, C. 2001. Nrarp is a novel intracellular component of the Notch signaling pathway. *Genes Dev,* 15**,** 1885-99.

LAMMERT, E. & AXNICK, J. 2012. Vascular lumen formation. *Cold Spring Harb Perspect Med,* 2**,** a006619.

LANCASTER, D. E., MCNEILL, L. A., MCDONOUGH, M. A., APLIN, R. T., HEWITSON, K. S., PUGH, C. W., RATCLIFFE, P. J. & SCHOFIELD, C. J. 2004. Disruption of dimerization and substrate phosphorylation inhibit factor inhibiting hypoxia-inducible factor (FIH) activity. *Biochem J,* 383**,** 429-37.

LANDO, D., PEET, D. J., GORMAN, J. J., WHELAN, D. A., WHITELAW, M. L. & BRUICK, R. K. 2002a. FIH-1 is an asparaginyl hydroxylase enzyme that regulates the transcriptional activity of hypoxia-inducible factor. *Genes Dev,* 16**,** 1466-71.

LANDO, D., PEET, D. J., WHELAN, D. A., GORMAN, J. J. & WHITELAW, M. L. 2002b. Asparagine hydroxylation of the HIF transactivation domain a hypoxic switch. *Science,* 295**,** 858-61.

LANG, M. R., GIHR, G., GAWAZ, M. P. & MULLER, II 2010. Hemostasis in Danio rerio: is the zebrafish a useful model for platelet research? *J Thromb Haemost,* 8**,** 1159-69.

LANGE, M., NORTON, W., COOLEN, M., CHAMINADE, M., MERKER, S., PROFT, F., SCHMITT, A., VERNIER, P., LESCH, K. P. & BALLY-CUIF, L. 2012. The ADHD-susceptibility gene lphn3.1 modulates dopaminergic neuron formation and locomotor activity during zebrafish development. *Mol Psychiatry*.

LARSON, J. D., WADMAN, S. A., CHEN, E., KERLEY, L., CLARK, K. J., EIDE, M., LIPPERT, S., NASEVICIUS, A., EKKER, S. C., HACKETT, P. B. & ESSNER, J. J. 2004. Expression of VE-cadherin in zebrafish embryos: a new tool to evaluate vascular development. *Dev Dyn,* 231**,** 204-13.

LATIF, F., TORY, K., GNARRA, J., YAO, M., DUH, F. M., ORCUTT, M. L., STACKHOUSE, T., KUZMIN, I., MODI, W., GEIL, L. & ET AL. 1993. Identification of the von Hippel-Lindau disease tumor suppressor gene. *Science,* 260**,** 1317-20.

LAWSON, N. D., VOGEL, A. M. & WEINSTEIN, B. M. 2002. sonic hedgehog and vascular endothelial growth factor act upstream of the Notch pathway during arterial endothelial differentiation. *Dev Cell,* 3**,** 127-36.

LAWSON, N. D. & WEINSTEIN, B. M. 2002a. Arteries and veins: making a difference with zebrafish. *Nat Rev Genet,* 3**,** 674-82.

LAWSON, N. D. & WEINSTEIN, B. M. 2002b. In vivo imaging of embryonic vascular development using transgenic zebrafish. *Dev Biol,* 248**,** 307-18.

LAWTON, M., TONG, M., GUNDOGAN, F., WANDS, J. R. & DE LA MONTE, S. M. 2010. Aspartyl-(asparaginyl) beta-hydroxylase, hypoxia-inducible factor-alpha and Notch cross-talk in regulating neuronal motility. *Oxid Med Cell Longev,* 3**,** 347-56.

LEE, C., KIM, S. J., JEONG, D. G., LEE, S. M. & RYU, S. E. 2003. Structure of human FIH-1 reveals a unique active site pocket and interaction sites for HIF-1 and von Hippel-Lindau. *J Biol Chem,* 278**,** 7558-63.

LEE, J. W., BAE, S. H., JEONG, J. W., KIM, S. H. & KIM, K. W. 2004. Hypoxia-inducible factor (HIF-1)alpha: its protein stability and biological functions. *Exp Mol Med,* 36**,** 1-12.

LEMOS, V. S., SILVA, D. M., WALTHER, T., ALENINA, N., BADER, M. & SANTOS, R. A. 2005. The endothelium-dependent vasodilator effect of the nonpeptide Ang(1-7) mimic AVE 0991 is abolished in the aorta of mas-knockout mice. *J Cardiovasc Pharmacol,* 46**,** 274-9.

LESLIE, J. D., ARIZA-MCNAUGHTON, L., BERMANGE, A. L., MCADOW, R., JOHNSON, S. L. & LEWIS, J. 2007. Endothelial signalling by the Notch ligand Delta-like 4 restricts angiogenesis. *Development,* 134**,** 839-44.

LI, H., KO, H. P. & WHITLOCK, J. P. 1996. Induction of phosphoglycerate kinase 1 gene expression by hypoxia. Roles of Arnt and HIF1alpha. *J Biol Chem,* 271**,** 21262-7.

LI, J., WANG, E., DUTTA, S., LAU, J. S., JIANG, S. W., DATTA, K. & MUKHOPADHYAY, D. 2007a. Protein kinase C-mediated modulation of FIH-1 expression by the homeodomain protein CDP/Cut/Cux. *Mol Cell Biol,* 27**,** 7345-53.

LI, J. L., SAINSON, R. C., SHI, W., LEEK, R., HARRINGTON, L. S., PREUSSER, M., BISWAS, S., TURLEY, H., HEIKAMP, E., HAINFELLNER, J. A. & HARRIS, A. L. 2007b. Delta-like 4 Notch ligand regulates tumor angiogenesis, improves tumor vascular function, and promotes tumor growth in vivo. *Cancer Res,* 67**,** 11244-53.

LI, L. & DOWLING, J. E. 1997. A dominant form of inherited retinal degeneration caused by a non-photoreceptor cell-specific mutation. *Proc Natl Acad Sci U S A,* 94**,** 11645-50.

LI, L., QU, Y., LI, J., XIONG, Y., MAO, M. & MU, D. 2007c. Relationship between HIF-1alpha expression and neuronal apoptosis in neonatal rats with hypoxia-ischemia brain injury. *Brain Res,* 1180**,** 133-9.

LI, M., LIU, C., BIN, J., WANG, Y., CHEN, J., XIU, J., PEI, J., LAI, Y., CHEN, D., FAN, C., XIE, J., TAO, Y. & WU, P. 2011a. Mutant hypoxia inducible factor-1alpha improves angiogenesis and tissue perfusion in ischemic rabbit skeletal muscle. *Microvasc Res,* 81**,** 26-33.

LI, P., CHAPPELL, M. C., FERRARIO, C. M. & BROSNIHAN, K. B. 1997. Angiotensin-(1-7) augments bradykinin-induced vasodilation by competing with ACE and releasing nitric oxide. *Hypertension,* 29**,** 394-400.

LI, S. H., CHUN, Y. S., LIM, J. H., HUANG, L. E. & PARK, J. W. 2011b. von Hippel-Lindau protein adjusts oxygen sensing of the FIH asparaginyl hydroxylase. *Int J Biochem Cell Biol,* 43**,** 795-804.

LIANG, D., CHANG, J. R., CHIN, A. J., SMITH, A., KELLY, C., WEINBERG, E. S. & GE, R. 2001. The role of vascular endothelial growth factor (VEGF) in vasculogenesis, angiogenesis, and hematopoiesis in zebrafish development. *Mech Dev,* 108**,** 29-43.

LIEN, C. L., HARRISON, M. R., TUAN, T. L. & STARNES, V. A. 2012. Heart repair and regeneration: Recent insights from zebrafish studies. *Wound Repair Regen*.

LIMAN, T. G. & ENDRES, M. 2012. New vessels after stroke: postischemic neovascularization and regeneration. *Cerebrovasc Dis,* 33**,** 492-9.

LIN, J., WU, P. H., TARR, P. T., LINDENBERG, K. S., ST-PIERRE, J., ZHANG, C. Y., MOOTHA, V. K., JAGER, S., VIANNA, C. R., REZNICK, R. M., CUI, L., MANIERI, M., DONOVAN, M. X., WU, Z., COOPER, M. P., FAN, M. C., ROHAS, L. M., ZAVACKI, A. M., CINTI, S., SHULMAN, G. I., LOWELL, B. B., KRAINC, D. & SPIEGELMAN, B. M. 2004. Defects in adaptive energy metabolism with CNS-linked hyperactivity in PGC-1alpha null mice. *Cell,* 119**,** 121-35.

LIN, T. Y., LIAO, B. K., HORNG, J. L., YAN, J. J., HSIAO, C. D. & HWANG, P. P. 2008. Carbonic anhydrase 2-like a and 15a are involved in acid-base regulation and Na+ uptake in zebrafish H+-ATPase-rich cells. *Am J Physiol Cell Physiol,* 294**,** C1250-60.

LINKE, S., STOJKOSKI, C., KEWLEY, R. J., BOOKER, G. W., WHITELAW, M. L. & PEET, D. J. 2004. Substrate requirements of the oxygen-sensing asparaginyl hydroxylase factor-inhibiting hypoxia-inducible factor. *J Biol Chem,* 279**,** 14391-7.

LINNEMANN, B., SUTTER, T., SIXT, S., RASTAN, A., SCHWARZWAELDER, U., NOORY, E., BUERGELIN, K., BESCHORNER, U. & ZELLER, T. 2012. Elevated cardiac troponin T contributes to prediction of worse in-hospital outcomes after endovascular therapy for acute limb ischemia. *J Vasc Surg,* 55**,** 721-9.

LISY, K. & PEET, D. J. 2008. Turn me on: regulating HIF transcriptional activity. *Cell Death Differ,* 15**,** 642-9.

LIU, J. J., GLICKMAN, J. N., MASYUK, A. I. & LARUSSO, N. F. 2008. Cholangiocyte bile salt transporters in cholesterol gallstone-susceptible and resistant inbred mouse strains. *J Gastroenterol Hepatol,* 23**,** 1596-602.

LIU, Z. J., SHIRAKAWA, T., LI, Y., SOMA, A., OKA, M., DOTTO, G. P., FAIRMAN, R. M., VELAZQUEZ, O. C. & HERLYN, M. 2003. Regulation of Notch1 and Dll4 by vascular endothelial growth factor in arterial endothelial cells: implications for modulating arteriogenesis and angiogenesis. *Mol Cell Biol,* 23**,** 14-25.

LOBODA, A., JOZKOWICZ, A. & DULAK, J. 2010. HIF-1 and HIF-2 transcription factors--similar but not identical. *Mol Cells,* 29**,** 435-42.

LONSER, R. R., GLENN, G. M., WALTHER, M., CHEW, E. Y., LIBUTTI, S. K., LINEHAN, W. M. & OLDFIELD, E. H. 2003. von Hippel-Lindau disease. *Lancet,* 361**,** 2059-67.

LU, J., ZHAO, J., MA, J., LIU, K., YANG, H., HUANG, Y., QIN, Z., BAI, R., LI, P., YAN, W., ZHAO, M. & DONG, Z. 2011. VEGF-A-induced immature DCs not mature DCs differentiation into endothelial-like cells through ERK1/2-dependent pathway. *Cell Biochem Funct,* 29**,** 294-302.

LUBMAN, O. Y., KOPAN, R., WAKSMAN, G. & KOROLEV, S. 2005. The crystal structure of a partial mouse Notch-1 ankyrin domain: repeats 4 through 7 preserve an ankyrin fold. *Protein Sci,* 14**,** 1274-81.

MACPHAIL, R. C., BROOKS, J., HUNTER, D. L., PADNOS, B., IRONS, T. D. & PADILLA, S. 2009. Locomotion in larval zebrafish: Influence of time of day, lighting and ethanol. *Neurotoxicology,* 30**,** 52-8.

MAEDA, H. 2001. The enhanced permeability and retention (EPR) effect in tumor vasculature: the key role of tumor-selective macromolecular drug targeting. *Adv Enzyme Regul,* 41**,** 189-207.

MAHER, E. R., NEUMANN, H. P. & RICHARD, S. 2011. von Hippel-Lindau disease: a clinical and scientific review. *Eur J Hum Genet,* 19**,** 617-23.

MAHON, P. C., HIROTA, K. & SEMENZA, G. L. 2001. FIH-1: a novel protein that interacts with HIF-1alpha and VHL to mediate repression of HIF-1 transcriptional activity. *Genes Dev,* 15**,** 2675-86.

MAKINO, Y., UENISHI, R., OKAMOTO, K., ISOE, T., HOSONO, O., TANAKA, H., KANOPKA, A., POELLINGER, L., HANEDA, M. & MORIMOTO, C. 2007. Transcriptional up-regulation of inhibitory PAS domain protein gene expression by hypoxia-inducible factor 1 (HIF-1): a negative feedback regulatory circuit in HIF-1-mediated signaling in hypoxic cells. *J Biol Chem,* 282**,** 14073-82.

MAKKY, K., DUVNJAK, P., PRAMANIK, K., RAMCHANDRAN, R. & MAYER, A. N. 2008. A whole-animal microplate assay for metabolic rate using zebrafish. *J Biomol Screen,* 13**,** 960-7.

MALONE, M. H., SCIAKY, N., STALHEIM, L., HAHN, K. M., LINNEY, E. & JOHNSON, G. L. 2007. Laser-scanning velocimetry: a confocal microscopy method for quantitative measurement of cardiovascular performance in zebrafish embryos and larvae. *BMC Biotechnol,* 7**,** 40.

MALTEPE, E., SCHMIDT, J. V., BAUNOCH, D., BRADFIELD, C. A. & SIMON, M. C. 1997. Abnormal angiogenesis and responses to glucose and oxygen deprivation in mice lacking the protein ARNT. *Nature,* 386**,** 403-7.

MANALO, D. J., ROWAN, A., LAVOIE, T., NATARAJAN, L., KELLY, B. D., YE, S. Q., GARCIA, J. G. & SEMENZA, G. L. 2005. Transcriptional regulation of vascular endothelial cell responses to hypoxia by HIF-1. *Blood,* 105**,** 659-69.

MARANCHIE, J. K., VASSELLI, J. R., RISS, J., BONIFACINO, J. S., LINEHAN, W. M. & KLAUSNER, R. D. 2002. The contribution of VHL substrate binding and HIF1-alpha to the phenotype of VHL loss in renal cell carcinoma. *Cancer Cell,* 1**,** 247-55.

MARTI, H. H. 2004. Erythropoietin and the hypoxic brain. *J Exp Biol,* 207**,** 3233-42.

MARXSEN, J. H., STENGEL, P., DOEGE, K., HEIKKINEN, P., JOKILEHTO, T., WAGNER, T., JELKMANN, W., JAAKKOLA, P. & METZEN, E. 2004. Hypoxia-inducible factor-1 (HIF-1) promotes its degradation by induction of HIF-alpha-prolyl-4-hydroxylases. *Biochem J,* 381**,** 761-7.

MASSON, N. & RATCLIFFE, P. J. 2003. HIF prolyl and asparaginyl hydroxylases in the biological response to intracellular O(2) levels. *J Cell Sci,* 116**,** 3041-9.

MASUMURA, T., YAMAMOTO, K., SHIMIZU, N., OBI, S. & ANDO, J. 2009. Shear stress increases expression of the arterial endothelial marker ephrinB2 in murine ES cells via the VEGF-Notch signaling pathways. *Arterioscler Thromb Vasc Biol,* 29**,** 2125-31.

MATSUMORI, R., SHIMADA, K., KIYANAGI, T., HIKI, M., FUKAO, K., HIROSE, K., OHSAKA, H., MIYAZAKI, T., KUME, A., YAMADA, A., TAKAGI, A., OHMURA, H., MIYAUCHI, K. & DAIDA, H. 2012. Clinical significance of the measurements of urinary liver-type fatty acid binding protein levels in patients with acute coronary syndrome. *J Cardiol*.

MAXWELL, P. H., WIESENER, M. S., CHANG, G. W., CLIFFORD, S. C., VAUX, E. C., COCKMAN, M. E., WYKOFF, C. C., PUGH, C. W., MAHER, E. R. & RATCLIFFE, P. J. 1999. The tumour suppressor protein VHL targets hypoxia-inducible factors for oxygen-dependent proteolysis. *Nature,* 399**,** 271-5.

MCNEILL, L. A., HEWITSON, K. S., CLARIDGE, T. D., SEIBEL, J. F., HORSFALL, L. E. & SCHOFIELD, C. J. 2002. Hypoxia-inducible factor asparaginyl hydroxylase (FIH-1) catalyses hydroxylation at the beta-carbon of asparagine-803. *Biochem J,* 367**,** 571-5.

MELCHIONNA, R., PORCELLI, D., MANGONI, A., CARLINI, D., LIUZZO, G., SPINETTI, G., ANTONINI, A., CAPOGROSSI, M. C. & NAPOLITANO, M. 2005. Laminar shear stress inhibits CXCR4 expression on endothelial cells: functional consequences for atherogenesis. *FASEB J,* 19**,** 629-31.

MELVIN, A., MUDIE, S. & ROCHA, S. 2011. The chromatin remodeler ISWI regulates the cellular response to hypoxia: role of FIH. *Mol Biol Cell,* 22**,** 4171-81.

MERRILL, M. J., EDWARDS, N. A. & LONSER, R. R. 2011. Notch receptor and effector expression in von Hippel-Lindau disease-associated central nervous system hemangioblastomas. *J Neurosurg,* 115**,** 512-7.

METZEN, E., BERCHNER-PFANNSCHMIDT, U., STENGEL, P., MARXSEN, J. H., STOLZE, I., KLINGER, M., HUANG, W. Q., WOTZLAW, C., HELLWIG-BURGEL, T., JELKMANN, W., ACKER, H. & FANDREY, J. 2003. Intracellular localisation of human HIF-1 alpha hydroxylases: implications for oxygen sensing. *J Cell Sci,* 116**,** 1319-26.

METZEN, E., STIEHL, D. P., DOEGE, K., MARXSEN, J. H., HELLWIG-BURGEL, T. & JELKMANN, W. 2005. Regulation of the prolyl hydroxylase domain protein 2 (phd2/egln-1) gene: identification of a functional hypoxia-responsive element. *Biochem J,* 387**,** 711-7.

MIELE, L. 2011. Transcription factor RBPJ/CSL: a genome-wide look at transcriptional regulation. *Proc Natl Acad Sci U S A,* 108**,** 14715-6.

MITCHELL, I. C., BROWN, T. S., TERADA, L. S., AMATRUDA, J. F. & NWARIAKU, F. E. 2010. Effect of vascular cadherin knockdown on zebrafish vasculature during development. *PLoS One,* 5**,** e8807.

MONTERO-BALAGUER, M., SWIRSDING, K., ORSENIGO, F., COTELLI, F., MIONE, M. & DEJANA, E. 2009. Stable vascular connections and remodeling require full expression of VE-cadherin in zebrafish embryos. *PLoS One,* 4**,** e5772.

MORRIS, M. R., MAINA, E., MORGAN, N. V., GENTLE, D., ASTUTI, D., MOCH, H., KISHIDA, T., YAO, M., SCHRAML, P., RICHARDS, F. M., LATIF, F. & MAHER, E. R. 2004. Molecular genetic analysis of FIH-1, FH, and SDHB candidate tumour suppressor genes in renal cell carcinoma. *J Clin Pathol,* 57**,** 706-11.

MOTOIKE, T., LOUGHNA, S., PERENS, E., ROMAN, B. L., LIAO, W., CHAU, T. C., RICHARDSON, C. D., KAWATE, T., KUNO, J., WEINSTEIN, B. M., STAINIER, D. Y. & SATO, T. N. 2000. Universal GFP reporter for the study of vascular development. *Genesis,* 28**,** 75-81.

MOYON, D., PARDANAUD, L., YUAN, L., BREANT, C. & EICHMANN, A. 2001. Plasticity of endothelial cells during arterial-venous differentiation in the avian embryo. *Development,* 128**,** 3359-70.

NAGY, J. A., CHANG, S. H., DVORAK, A. M. & DVORAK, H. F. 2009. Why are tumour blood vessels abnormal and why is it important to know? *Br J Cancer,* 100**,** 865-9.

NAGY, J. A., DVORAK, A. M. & DVORAK, H. F. 2012. Vascular hyperpermeability, angiogenesis, and stroma generation. *Cold Spring Harb Perspect Med,* 2**,** a006544.

NAGY, J. A., VASILE, E., FENG, D., SUNDBERG, C., BROWN, L. F., DETMAR, M. J., LAWITTS, J. A., BENJAMIN, L., TAN, X., MANSEAU, E. J., DVORAK, A. M. & DVORAK, H. F. 2002. Vascular permeability factor/vascular endothelial growth factor induces lymphangiogenesis as well as angiogenesis. *J Exp Med,* 196**,** 1497-506.

NANGAKU, M. & ECKARDT, K. U. 2007. Hypoxia and the HIF system in kidney disease. *J Mol Med (Berl),* 85**,** 1325-30.

NASEVICIUS, A., LARSON, J. & EKKER, S. C. 2000. Distinct requirements for zebrafish angiogenesis revealed by a VEGF-A morphant. *Yeast,* 17**,** 294-301.

NEUFELD, G., COHEN, T., GENGRINOVITCH, S. & POLTORAK, Z. 1999. Vascular endothelial growth factor (VEGF) and its receptors. *FASEB J,* 13**,** 9-22.

NICOLI, S., TOBIA, C., GUALANDI, L., DE SENA, G. & PRESTA, M. 2008. Calcitonin receptor-like receptor guides arterial differentiation in zebrafish. *Blood,* 111**,** 4965-72.

NIU, M. J., YANG, J. K., LIN, S. S., JI, X. J. & GUO, L. M. 2008. Loss of angiotensin-converting enzyme 2 leads to impaired glucose homeostasis in mice. *Endocrine,* 34**,** 56-61.

NOLAN, T., HANDS, R. E. & BUSTIN, S. A. 2006. Quantification of mRNA using real-time RT-PCR. *Nat Protoc,* 1**,** 1559-82.

NORRBY, K. 2006. In vivo models of angiogenesis. *J Cell Mol Med,* 10**,** 588-612.

NORTON, W. & BALLY-CUIF, L. 2010. Adult zebrafish as a model organism for behavioural genetics. *BMC Neurosci,* 11**,** 90.

NUNES, S. S., REKAPALLY, H., CHANG, C. C. & HOYING, J. B. 2011. Vessel arterial-venous plasticity in adult neovascularization. *PLoS One,* 6**,** e27332.

NUSSLEIN-VOLHARD, C. 2008. Coming to Life: How Genes Drive Development - Ref:Role of Genetic Information.

OBI, S., YAMAMOTO, K., SHIMIZU, N., KUMAGAYA, S., MASUMURA, T., SOKABE, T., ASAHARA, T. & ANDO, J. 2009. Fluid shear stress induces arterial differentiation of endothelial progenitor cells. *J Appl Physiol,* 106**,** 203-11.

OEHME, F., ELLINGHAUS, P., KOLKHOF, P., SMITH, T. J., RAMAKRISHNAN, S., HUTTER, J., SCHRAMM, M. & FLAMME, I. 2002. Overexpression of PH-4, a novel putative proline 4-hydroxylase, modulates activity of hypoxia-inducible transcription factors. *Biochem Biophys Res Commun,* 296**,** 343-9.

OHATA, E., TADOKORO, R., SATO, Y., SAITO, D. & TAKAHASHI, Y. 2009. Notch signal is sufficient to direct an endothelial conversion from non-endothelial somitic cells conveyed to the aortic region by CXCR4. *Dev Biol,* 335**,** 33-42.

OHH, M., PARK, C. W., IVAN, M., HOFFMAN, M. A., KIM, T. Y., HUANG, L. E., PAVLETICH, N., CHAU, V. & KAELIN, W. G. 2000. Ubiquitination of hypoxia-inducible factor requires direct binding to the beta-domain of the von Hippel-Lindau protein. *Nat Cell Biol,* 2**,** 423-7.

OHISHI, K., VARNUM-FINNEY, B., FLOWERS, D., ANASETTI, C., MYERSON, D. & BERNSTEIN, I. D. 2000. Monocytes express high amounts of Notch and undergo cytokine specific apoptosis following interaction with the Notch ligand, Delta-1. *Blood,* 95**,** 2847-54.

OHMACHI, T., INOUE, H., MIMORI, K., TANAKA, F., SASAKI, A., KANDA, T., FUJII, H., YANAGA, K. & MORI, M. 2006. Fatty acid binding protein 6 is overexpressed in colorectal cancer. *Clin Cancer Res,* 12**,** 5090-5.

OKA, C., NAKANO, T., WAKEHAM, A., DE LA POMPA, J. L., MORI, C., SAKAI, T., OKAZAKI, S., KAWAICHI, M., SHIOTA, K., MAK, T. W. & HONJO, T. 1995. Disruption of the mouse RBP-J kappa gene results in early embryonic death. *Development,* 121**,** 3291-301.

OLIVEIRA, M. A., FORTES, Z. B., SANTOS, R. A., KOSLA, M. C. & DE CARVALHO, M. H. 1999. Synergistic effect of angiotensin-(1-7) on bradykinin arteriolar dilation in vivo. *Peptides,* 20**,** 1195-201.

ONG, S. G. & HAUSENLOY, D. J. 2012. Hypoxia-inducible factor as a therapeutic target for cardioprotection. *Pharmacol Ther,* 136**,** 69-81.

OTHMAN-HASSAN, K., PATEL, K., PAPOUTSI, M., RODRIGUEZ-NIEDENFUHR, M., CHRIST, B. & WILTING, J. 2001. Arterial identity of endothelial cells is controlled by local cues. *Dev Biol,* 237**,** 398-409.

PACKHAM, I. M., GRAY, C., HEATH, P. R., HELLEWELL, P. G., INGHAM, P. W., CROSSMAN, D. C., MILO, M. & CHICO, T. J. 2009. Microarray profiling reveals CXCR4a is downregulated by blood flow in vivo and mediates collateral formation in zebrafish embryos. *Physiol Genomics,* 38**,** 319-27.

PAJUSOLA, K., KUNNAPUU, J., VUORIKOSKI, S., SORONEN, J., ANDRE, H., PEREIRA, T., KORPISALO, P., YLA-HERTTUALA, S., POELLINGER, L. & ALITALO, K. 2005. Stabilized HIF-1alpha is superior to VEGF for angiogenesis in skeletal muscle via adeno-associated virus gene transfer. *FASEB J,* 19**,** 1365-7.

PASTORE, Y. D., JELINEK, J., ANG, S., GUAN, Y., LIU, E., JEDLICKOVA, K., KRISHNAMURTI, L. & PRCHAL, J. T. 2003. Mutations in the VHL gene in sporadic apparently congenital polycythemia. *Blood,* 101**,** 1591-5.

PATEL-HETT, S. & D'AMORE, P. A. 2011. Signal transduction in vasculogenesis and developmental angiogenesis. *Int J Dev Biol,* 55**,** 353-63.

PATEL, N. S., LI, J. L., GENERALI, D., POULSOM, R., CRANSTON, D. W. & HARRIS, A. L. 2005a. Up-regulation of delta-like 4 ligand in human tumor vasculature and the role of basal expression in endothelial cell function. *Cancer Res,* 65**,** 8690-7.

PATEL, T. H., KIMURA, H., WEISS, C. R., SEMENZA, G. L. & HOFMANN, L. V. 2005b. Constitutively active HIF-1alpha improves perfusion and arterial remodeling in an endovascular model of limb ischemia. *Cardiovasc Res,* 68**,** 144-54.

PAUSE, A., LEE, S., WORRELL, R. A., CHEN, D. Y., BURGESS, W. H., LINEHAN, W. M. & KLAUSNER, R. D. 1997. The von Hippel-Lindau tumor-suppressor gene product forms a stable complex with human CUL-2, a member of the Cdc53 family of proteins. *Proc Natl Acad Sci U S A,* 94**,** 2156-61.

PEAR, W. S. & SIMON, M. C. 2005. Lasting longer without oxygen: The influence of hypoxia on Notch signaling. *Cancer Cell,* 8**,** 435-7.

PEI, W., KRATZ, L. E., BERNARDINI, I., SOOD, R., YOKOGAWA, T., DORWARD, H., CICCONE, C., KELLEY, R. I., ANIKSTER, Y., BURGESS, H. A., HUIZING, M. & FELDMAN, B. 2010. A model of Costeff Syndrome reveals metabolic and protective functions of mitochondrial OPA3. *Development,* 137**,** 2587-96.

PELLETIER, J., BELLOT, G., GOUNON, P., LACAS-GERVAIS, S., POUYSSEGUR, J. & MAZURE, N. M. 2012. Glycogen Synthesis is Induced in Hypoxia by the Hypoxia-Inducible Factor and Promotes Cancer Cell Survival. *Front Oncol,* 2**,** 18.

PELSTER, B. & BURGGREN, W. W. 1996. Disruption of hemoglobin oxygen transport does not impact oxygen-dependent physiological processes in developing embryos of zebra fish (Danio rerio). *Circ Res,* 79**,** 358-62.

PELSTER, B., SANGER, A. M., SIEGELE, M. & SCHWERTE, T. 2003. Influence of swim training on cardiac activity, tissue capillarization, and mitochondrial density in muscle tissue of zebrafish larvae. *Am J Physiol Regul Integr Comp Physiol,* 285**,** R339-47.

PENG, J., ZHANG, L., DRYSDALE, L. & FONG, G. H. 2000. The transcription factor EPAS-1/hypoxia-inducible factor 2alpha plays an important role in vascular remodeling. *Proc Natl Acad Sci U S A,* 97**,** 8386-91.

PERRY, S. F. & GILMOUR, K. M. 2006. Acid-base balance and CO2 excretion in fish: unanswered questions and emerging models. *Respir Physiol Neurobiol,* 154**,** 199-215.

PERSSON, A. B. & BUSCHMANN, I. R. 2011. Vascular growth in health and disease. *Front Mol Neurosci,* 4**,** 14.

PESCADOR, N., CUEVAS, Y., NARANJO, S., ALCAIDE, M., VILLAR, D., LANDAZURI, M. O. & DEL PESO, L. 2005. Identification of a functional hypoxia-responsive element that regulates the expression of the egl nine homologue 3 (egln3/phd3) gene. *Biochem J,* 390**,** 189-97.

PFAFFENROTH, E. C. & LINEHAN, W. M. 2008. Genetic basis for kidney cancer: opportunity for disease-specific approaches to therapy. *Expert Opin Biol Ther,* 8**,** 779-90.

PHNG, L. K. & GERHARDT, H. 2009. Angiogenesis: a team effort coordinated by notch. *Dev Cell,* 16**,** 196-208.

POSS, K. D., WILSON, L. G. & KEATING, M. T. 2002. Heart regeneration in zebrafish. *Science,* 298**,** 2188-90.

PRABHAKAR, N. R. 2000. Oxygen sensing by the carotid body chemoreceptors. *J Appl Physiol,* 88**,** 2287-95.

PRABHAKAR, N. R. & SEMENZA, G. L. 2012. Gaseous messengers in oxygen sensing. *J Mol Med (Berl),* 90**,** 265-72.

PURSGLOVE, S. E. & MACKAY, J. P. 2005. CSL: a notch above the rest. *Int J Biochem Cell Biol,* 37**,** 2472-7.

QI, H., GERVAIS, M. L., LI, W., DECAPRIO, J. A., CHALLIS, J. R. & OHH, M. 2004. Molecular cloning and characterization of the von Hippel-Lindau-like protein. *Mol Cancer Res,* 2**,** 43-52.

QUINN, T. P., PETERS, K. G., DE VRIES, C., FERRARA, N. & WILLIAMS, L. T. 1993. Fetal liver kinase 1 is a receptor for vascular endothelial growth factor and is selectively expressed in vascular endothelium. *Proc Natl Acad Sci U S A,* 90**,** 7533-7.

RANTANEN, K., PURSIHEIMO, J., HOGEL, H., HIMANEN, V., METZEN, E. & JAAKKOLA, P. M. 2008. Prolyl hydroxylase PHD3 activates oxygen-dependent protein aggregation. *Mol Biol Cell,* 19**,** 2231-40.

RAVAL, R. R., LAU, K. W., TRAN, M. G., SOWTER, H. M., MANDRIOTA, S. J., LI, J. L., PUGH, C. W., MAXWELL, P. H., HARRIS, A. L. & RATCLIFFE, P. J. 2005. Contrasting properties of hypoxia-inducible factor 1 (HIF-1) and HIF-2 in von Hippel-Lindau-associated renal cell carcinoma. *Mol Cell Biol,* 25**,** 5675-86.

RAYA, A., CONSIGLIO, A., KAWAKAMI, Y., RODRIGUEZ-ESTEBAN, C. & IZPISUA-BELMONTE, J. C. 2004. The zebrafish as a model of heart regeneration. *Cloning Stem Cells,* 6**,** 345-51.

RICHARD, D. E., BERRA, E., GOTHIE, E., ROUX, D. & POUYSSEGUR, J. 1999. p42/p44 mitogen-activated protein kinases phosphorylate hypoxia-inducible factor 1alpha (HIF-1alpha) and enhance the transcriptional activity of HIF-1. *J Biol Chem,* 274**,** 32631-7.

RIDER, M. H., BERTRAND, L., VERTOMMEN, D., MICHELS, P. A., ROUSSEAU, G. G. & HUE, L. 2004. 6-phosphofructo-2-kinase/fructose-2,6-bisphosphatase: head-to-head with a bifunctional enzyme that controls glycolysis. *Biochem J,* 381**,** 561-79.

RISAU, W. 1997. Mechanisms of angiogenesis. *Nature,* 386**,** 671-4.

ROBINSON, C. J. & STRINGER, S. E. 2001. The splice variants of vascular endothelial growth factor (VEGF) and their receptors. *J Cell Sci,* 114**,** 853-65.

ROCHER, A., OBESO, A., HERREROS, B. & GONZALEZ, C. 1988. Activation of the release of dopamine in the carotid body by veratridine. Evidence for the presence of voltage-dependent Na+ channels in type I cells. *Neurosci Lett,* 94**,** 274-8.

RUMMER, J. L. & BRAUNER, C. J. 2011. Plasma-accessible carbonic anhydrase at the tissue of a teleost fish may greatly enhance oxygen delivery: in vitro evidence in rainbow trout, Oncorhynchus mykiss. *J Exp Biol,* 214**,** 2319-28.

SABAN, E., CHEN, Y. H., HANGASKY, J. A., TAABAZUING, C. Y., HOLMES, B. E. & KNAPP, M. J. 2011a. The second coordination sphere of FIH controls hydroxylation. *Biochemistry,* 50**,** 4733-40.

SABAN, E., FLAGG, S. C. & KNAPP, M. J. 2011b. Uncoupled O2-activation in the human HIF-asparaginyl hydroxylase, FIH, does not produce reactive oxygen species. *J Inorg Biochem,* 105**,** 630-6.

SAINSON, R. C. & HARRIS, A. L. 2006. Hypoxia-regulated differentiation: let's step it up a Notch. *Trends Mol Med,* 12**,** 141-3.

SAKAMOTO, T., NIIYA, D. & SEIKI, M. 2011. Targeting the Warburg effect that arises in tumor cells expressing membrane type-1 matrix metalloproteinase. *J Biol Chem,* 286**,** 14691-704.

SAKAMOTO, T. & SEIKI, M. 2009. Mint3 enhances the activity of hypoxia-inducible factor-1 (HIF-1) in macrophages by suppressing the activity of factor inhibiting HIF-1. *J Biol Chem,* 284**,** 30350-9.

SAKAMOTO, T. & SEIKI, M. 2010. A membrane protease regulates energy production in macrophages by activating hypoxia-inducible factor-1 via a non-proteolytic mechanism. *J Biol Chem,* 285**,** 29951-64.

SANTHAKUMAR, K., JUDSON, E. C., ELKS, P. M., MCKEE, S., ELWORTHY, S., VAN ROOIJEN, E., WALMSLEY, S. S., RENSHAW, S., CROSS, S. S. & VAN EEDEN, F. J. 2012. A zebrafish model to study and therapeutically manipulate hypoxia signaling in tumorigenesis. *Cancer Res*.

SANTORO, M. M., PESCE, G. & STAINIER, D. Y. 2009. Characterization of vascular mural cells during zebrafish development. *Mech Dev,* 126**,** 638-49.

SANTOS, R. A., CASTRO, C. H., GAVA, E., PINHEIRO, S. V., ALMEIDA, A. P., PAULA, R. D., CRUZ, J. S., RAMOS, A. S., ROSA, K. T., IRIGOYEN, M. C., BADER, M., ALENINA, N., KITTEN, G. T. & FERREIRA, A. J. 2006. Impairment of in vitro and in vivo heart function in angiotensin-(1-7) receptor MAS knockout mice. *Hypertension,* 47**,** 996-1002.

SCHEER, N., RIEDL, I., WARREN, J. T., KUWADA, J. Y. & CAMPOS-ORTEGA, J. A. 2002. A quantitative analysis of the kinetics of Gal4 activator and effector gene expression in the zebrafish. *Mech Dev,* 112**,** 9-14.

SCHOENFELD, A., DAVIDOWITZ, E. J. & BURK, R. D. 1998. A second major native von Hippel-Lindau gene product, initiated from an internal translation start site, functions as a tumor suppressor. *Proc Natl Acad Sci U S A,* 95**,** 8817-22.

SCHWERTE, T., PREM, C., MAIROSL, A. & PELSTER, B. 2006. Development of the sympatho-vagal balance in the cardiovascular system in zebrafish (Danio rerio) characterized by power spectrum and classical signal analysis. *J Exp Biol,* 209**,** 1093-100.

SCHWERTE, T., UBERBACHER, D. & PELSTER, B. 2003. Non-invasive imaging of blood cell concentration and blood distribution in zebrafish Danio rerio incubated in hypoxic conditions in vivo. *J Exp Biol,* 206**,** 1299-307.

SCORTEGAGNA, M., DING, K., OKTAY, Y., GAUR, A., THURMOND, F., YAN, L. J., MARCK, B. T., MATSUMOTO, A. M., SHELTON, J. M., RICHARDSON, J. A., BENNETT, M. J. & GARCIA, J. A. 2003. Multiple organ pathology, metabolic abnormalities and impaired homeostasis of reactive oxygen species in Epas1-/- mice. *Nat Genet,* 35**,** 331-40.

SEHNERT, A. J., HUQ, A., WEINSTEIN, B. M., WALKER, C., FISHMAN, M. & STAINIER, D. Y. 2002. Cardiac troponin T is essential in sarcomere assembly and cardiac contractility. *Nat Genet,* 31**,** 106-10.

SEIZINGER, B. R., ROULEAU, G. A., OZELIUS, L. J., LANE, A. H., FARMER, G. E., LAMIELL, J. M., HAINES, J., YUEN, J. W., COLLINS, D., MAJOOR-KRAKAUER, D. & ET AL. 1988. Von Hippel-Lindau disease maps to the region of chromosome 3 associated with renal cell carcinoma. *Nature,* 332**,** 268-9.

SEMENZA, G. L. 2004. Hydroxylation of HIF-1: oxygen sensing at the molecular level. *Physiology (Bethesda),* 19**,** 176-82.

SEMENZA, G. L. 2010. Defining the role of hypoxia-inducible factor 1 in cancer biology and therapeutics. *Oncogene,* 29**,** 625-34.

SEMENZA, G. L., NEJFELT, M. K., CHI, S. M. & ANTONARAKIS, S. E. 1991. Hypoxia-inducible nuclear factors bind to an enhancer element located 3' to the human erythropoietin gene. *Proc Natl Acad Sci U S A,* 88**,** 5680-4.

SEMENZA, G. L. & WANG, G. L. 1992. A nuclear factor induced by hypoxia via de novo protein synthesis binds to the human erythropoietin gene enhancer at a site required for transcriptional activation. *Mol Cell Biol,* 12**,** 5447-54.

SHANKARAN, S. S., SIEGER, D., SCHROTER, C., CZEPE, C., PAULY, M. C., LAPLANTE, M. A., BECKER, T. S., OATES, A. C. & GAJEWSKI, M. 2007. Completing the set of h/E(spl) cyclic genes in zebrafish: her12 and her15 reveal novel modes of expression and contribute to the segmentation clock. *Dev Biol,* 304**,** 615-32.

SHEN, X., WAN, C., RAMASWAMY, G., MAVALLI, M., WANG, Y., DUVALL, C. L., DENG, L. F., GULDBERG, R. E., EBERHART, A., CLEMENS, T. L. & GILBERT, S. R. 2009. Prolyl hydroxylase inhibitors increase neoangiogenesis and callus formation following femur fracture in mice. *J Orthop Res,* 27**,** 1298-305.

SHIBUYA, M. 2006. Differential roles of vascular endothelial growth factor receptor-1 and receptor-2 in angiogenesis. *J Biochem Mol Biol,* 39**,** 469-78.

SHIN, D. H., LI, S. H., YANG, S. W., LEE, B. L., LEE, M. K. & PARK, J. W. 2009. Inhibitor of nuclear factor-kappaB alpha derepresses hypoxia-inducible factor-1 during moderate hypoxia by sequestering factor inhibiting hypoxia-inducible factor from hypoxia-inducible factor 1alpha. *FEBS J,* 276**,** 3470-80.

SI, Y., PALANI, S., JAYARAMAN, A. & LEE, K. 2007. Effects of forced uncoupling protein 1 expression in 3T3-L1 cells on mitochondrial function and lipid metabolism. *J Lipid Res,* 48**,** 826-36.

SIEKMANN, A. F., COVASSIN, L. & LAWSON, N. D. 2008. Modulation of VEGF signalling output by the Notch pathway. *Bioessays,* 30**,** 303-13.

SIEKMANN, A. F. & LAWSON, N. D. 2007. Notch signalling limits angiogenic cell behaviour in developing zebrafish arteries. *Nature,* 445**,** 781-4.

SJOLUND, J., JOHANSSON, M., MANNA, S., NORIN, C., PIETRAS, A., BECKMAN, S., NILSSON, E., LJUNGBERG, B. & AXELSON, H. 2008. Suppression of renal cell carcinoma growth by inhibition of Notch signaling in vitro and in vivo. *J Clin Invest,* 118**,** 217-28.

SMITH, T. G., BROOKS, J. T., BALANOS, G. M., LAPPIN, T. R., LAYTON, D. M., LEEDHAM, D. L., LIU, C., MAXWELL, P. H., MCMULLIN, M. F., MCNAMARA, C. J., PERCY, M. J., PUGH, C. W., RATCLIFFE, P. J., TALBOT, N. P., TREACY, M. & ROBBINS, P. A. 2006. Mutation of von Hippel-Lindau tumour suppressor and human cardiopulmonary physiology. *PLoS Med,* 3**,** e290.

SMITH, T. G., ROBBINS, P. A. & RATCLIFFE, P. J. 2008. The human side of hypoxia-inducible factor. *Br J Haematol,* 141**,** 325-34.

SMITHERS, L., HADDON, C., JIANG, Y. J. & LEWIS, J. 2000. Sequence and embryonic expression of deltaC in the zebrafish. *Mech Dev,* 90**,** 119-23.

SOILLEUX, E. J., TURLEY, H., TIAN, Y. M., PUGH, C. W., GATTER, K. C. & HARRIS, A. L. 2005. Use of novel monoclonal antibodies to determine the expression and distribution of the hypoxia regulatory factors PHD-1, PHD-2, PHD-3 and FIH in normal and neoplastic human tissues. *Histopathology,* 47**,** 602-10.

SOUILHOL, C., CORMIER, S., TANIGAKI, K., BABINET, C. & COHEN-TANNOUDJI, M. 2006. RBP-Jkappa-dependent notch signaling is dispensable for mouse early embryonic development. *Mol Cell Biol,* 26**,** 4769-74.

SPENCE, R., GERLACH, G., LAWRENCE, C. & SMITH, C. 2008. The behaviour and ecology of the zebrafish, Danio rerio. *Biol Rev Camb Philos Soc,* 83**,** 13-34.

STACKLEY, K. D., BEESON, C. C., RAHN, J. J. & CHAN, S. S. 2011. Bioenergetic profiling of zebrafish embryonic development. *PLoS One,* 6**,** e25652.

STEENBERGEN, P. J., RICHARDSON, M. K. & CHAMPAGNE, D. L. 2011. Patterns of avoidance behaviours in the light/dark preference test in young juvenile zebrafish: a pharmacological study. *Behav Brain Res,* 222**,** 15-25.

STOCKHAMMER, O. W., ZAKRZEWSKA, A., HEGEDUS, Z., SPAINK, H. P. & MEIJER, A. H. 2009. Transcriptome profiling and functional analyses of the zebrafish embryonic innate immune response to Salmonella infection. *J Immunol,* 182**,** 5641-53.

STOLZ, D. J. & MARTIN, R. J. 1982. Role of insulin in food intake, weight gain and lipid deposition in the Zucker obese rat. *J Nutr,* 112**,** 997-1002.

STOLZE, I. P., TIAN, Y. M., APPELHOFF, R. J., TURLEY, H., WYKOFF, C. C., GLEADLE, J. M. & RATCLIFFE, P. J. 2004. Genetic analysis of the role of the asparaginyl hydroxylase factor inhibiting hypoxia-inducible factor (FIH) in regulating hypoxia-inducible factor (HIF) transcriptional target genes [corrected]. *J Biol Chem,* 279**,** 42719-25.

STRASSER, G. A., KAMINKER, J. S. & TESSIER-LAVIGNE, M. 2010. Microarray analysis of retinal endothelial tip cells identifies CXCR4 as a mediator of tip cell morphology and branching. *Blood,* 115**,** 5102-10.

STUART, J. A., HARPER, J. A., BRINDLE, K. M. & BRAND, M. D. 1999. Uncoupling protein 2 from carp and zebrafish, ectothermic vertebrates. *Biochim Biophys Acta,* 1413**,** 50-4.

SUGIMACHI, K., TANAKA, S., TERASHI, T., TAGUCHI, K. & RIKIMARU, T. 2002. The mechanisms of angiogenesis in hepatocellular carcinoma: angiogenic switch during tumor progression. *Surgery,* 131**,** S135-41.

SUNG, K. C., KIM, K. S. & LEE, S. 2005. Hypoxic regulation of VEGF, HIF-1(alpha) in coronary collaterals development. *Korean J Intern Med,* 20**,** 295-302.

SUZUKI, Y., YAMAMOTO, K., ANDO, J., MATSUMOTO, K. & MATSUDA, T. 2012. Arterial shear stress augments the differentiation of endothelial progenitor cells adhered to VEGF-bound surfaces. *Biochem Biophys Res Commun,* 423**,** 91-7.

TAKAHASHI, N., LI, F., HUA, K., DENG, J., WANG, C. H., BOWERS, R. R., BARTNESS, T. J., KIM, H. S. & HARP, J. B. 2007. Increased energy expenditure, dietary fat wasting, and resistance to diet-induced obesity in mice lacking renin. *Cell Metab,* 6**,** 506-12.

TAKEDA, K., AGUILA, H. L., PARIKH, N. S., LI, X., LAMOTHE, K., DUAN, L. J., TAKEDA, H., LEE, F. S. & FONG, G. H. 2008. Regulation of adult erythropoiesis by prolyl hydroxylase domain proteins. *Blood,* 111**,** 3229-35.

TAKEDA, K., HO, V. C., TAKEDA, H., DUAN, L. J., NAGY, A. & FONG, G. H. 2006. Placental but not heart defects are associated with elevated hypoxia-inducible factor alpha levels in mice lacking prolyl hydroxylase domain protein 2. *Mol Cell Biol,* 26**,** 8336-46.

TANG, N., MACK, F., HAASE, V. H., SIMON, M. C. & JOHNSON, R. S. 2006. pVHL function is essential for endothelial extracellular matrix deposition. *Mol Cell Biol,* 26**,** 2519-30.

TANIMOTO, K., MAKINO, Y., PEREIRA, T. & POELLINGER, L. 2000. Mechanism of regulation of the hypoxia-inducible factor-1 alpha by the von Hippel-Lindau tumor suppressor protein. *EMBO J,* 19**,** 4298-309.

TAYLOR, R. 1991. Insulin action 1991. *Clin Endocrinol (Oxf),* 34**,** 159-71.

TAZUKE, S. I., MAZURE, N. M., SUGAWARA, J., CARLAND, G., FAESSEN, G. H., SUEN, L. F., IRWIN, J. C., POWELL, D. R., GIACCIA, A. J. & GIUDICE, L. C. 1998. Hypoxia stimulates insulin-like growth factor binding protein 1 (IGFBP-1) gene expression in HepG2 cells: a possible model for IGFBP-1 expression in fetal hypoxia. *Proc Natl Acad Sci U S A,* 95**,** 10188-93.

TEN DIJKE, P. & ARTHUR, H. M. 2007. Extracellular control of TGFbeta signalling in vascular development and disease. *Nat Rev Mol Cell Biol,* 8**,** 857-69.

THATTALIYATH, B., CYKOWSKI, M. & JAGADEESWARAN, P. 2005. Young thrombocytes initiate the formation of arterial thrombi in zebrafish. *Blood,* 106**,** 118-24.

THIJSSEN, D. H., DAWSON, E. A., VAN DEN MUNCKHOF, I. C., TINKEN, T. M., DEN DRIJVER, E., HOPKINS, N., CABLE, N. T. & GREEN, D. J. 2011. Exercise-mediated changes in conduit artery wall thickness in humans: role of shear stress. *Am J Physiol Heart Circ Physiol,* 301**,** H241-6.

THISSE, C. & THISSE, B. 2008. High-resolution in situ hybridization to whole-mount zebrafish embryos. *Nat Protoc,* 3**,** 59-69.

THOMA, C. R., MATOV, A., GUTBRODT, K. L., HOERNER, C. R., SMOLE, Z., KREK, W. & DANUSER, G. 2010. Quantitative image analysis identifies pVHL as a key regulator of microtubule dynamic instability. *J Cell Biol,* 190**,** 991-1003.

THOMA, C. R., TOSO, A., GUTBRODT, K. L., REGGI, S. P., FREW, I. J., SCHRAML, P., HERGOVICH, A., MOCH, H., MERALDI, P. & KREK, W. 2009. VHL loss causes spindle misorientation and chromosome instability. *Nat Cell Biol,* 11**,** 994-1001.

TIAN, H., HAMMER, R. E., MATSUMOTO, A. M., RUSSELL, D. W. & MCKNIGHT, S. L. 1998. The hypoxia-responsive transcription factor EPAS1 is essential for catecholamine homeostasis and protection against heart failure during embryonic development. *Genes Dev,* 12**,** 3320-4.

TOBIA, C., DE SENA, G. & PRESTA, M. 2011. Zebrafish embryo, a tool to study tumor angiogenesis. *Int J Dev Biol,* 55**,** 505-9.

TOFT, P. B. 1999. Prenatal and perinatal striatal injury: a hypothetical cause of attention-deficit-hyperactivity disorder? *Pediatr Neurol,* 21**,** 602-10.

TOM, B., DE VRIES, R., SAXENA, P. R. & DANSER, A. H. 2001. Bradykinin potentiation by angiotensin-(1-7) and ACE inhibitors correlates with ACE C- and N-domain blockade. *Hypertension,* 38**,** 95-9.

TOM, B., DENDORFER, A. & DANSER, A. H. 2003. Bradykinin, angiotensin-(1-7), and ACE inhibitors: how do they interact? *Int J Biochem Cell Biol,* 35**,** 792-801.

TOPCZEWSKA, J. M., TOPCZEWSKI, J., SZOSTAK, A., SOLNICA-KREZEL, L. & HOGAN, B. L. 2003. Developmentally regulated expression of two members of the Nrarp family in zebrafish. *Gene Expr Patterns,* 3**,** 169-71.

TORNQVIST, H. E., GUNSALUS, J. R., NEMENOFF, R. A., FRACKELTON, A. R., PIERCE, M. W. & AVRUCH, J. 1988. Identification of the insulin receptor tyrosine residues undergoing insulin-stimulated phosphorylation in intact rat hepatoma cells. *J Biol Chem,* 263**,** 350-9.

TRENT, C., TSUING, N. & HORVITZ, H. R. 1983. Egg-laying defective mutants of the nematode Caenorhabditis elegans. *Genetics,* 104**,** 619-47.

TREWICK, S. C., MCLAUGHLIN, P. J. & ALLSHIRE, R. C. 2005. Methylation: lost in hydroxylation? *EMBO Rep,* 6**,** 315-20.

TUNG, J. J., TATTERSALL, I. W. & KITAJEWSKI, J. 2012. Tips, Stalks, Tubes: Notch-Mediated Cell Fate Determination and Mechanisms of Tubulogenesis during Angiogenesis. *Cold Spring Harb Perspect Med,* 2**,** a006601.

UENOYAMA, M., OGATA, S., NAKANISHI, K., KANAZAWA, F., HIROI, S., TOMINAGA, S., SEO, A., MATSUI, T., KAWAI, T. & SUZUKI, S. 2010. Protein kinase C mRNA and protein expressions in hypobaric hypoxia-induced cardiac hypertrophy in rats. *Acta Physiol (Oxf),* 198**,** 431-40.

VAN ROOIJEN, E., SANTHAKUMAR, K., LOGISTER, I., VOEST, E., SCHULTE-MERKER, S., GILES, R. & VAN EEDEN, F. 2011. A zebrafish model for VHL and hypoxia signaling. *Methods Cell Biol,* 105**,** 163-90.

VAN ROOIJEN, E., VOEST, E. E., LOGISTER, I., BUSSMANN, J., KORVING, J., VAN EEDEN, F. J., GILES, R. H. & SCHULTE-MERKER, S. 2010. von Hippel-Lindau tumor suppressor mutants faithfully model pathological hypoxia-driven angiogenesis and vascular retinopathies in zebrafish. *Dis Model Mech,* 3**,** 343-53.

VAN ROOIJEN, E., VOEST, E. E., LOGISTER, I., KORVING, J., SCHWERTE, T., SCHULTE-MERKER, S., GILES, R. H. & VAN EEDEN, F. J. 2009. Zebrafish mutants in the von Hippel-Lindau tumor suppressor display a hypoxic response and recapitulate key aspects of Chuvash polycythemia. *Blood,* 113**,** 6449-60.

VARMA, S. & COHEN, H. J. 1997. Co-transactivation of the 3' erythropoietin hypoxia inducible enhancer by the HIF-1 protein. *Blood Cells Mol Dis,* 23**,** 169-76.

VEIKKOLA, T., KARKKAINEN, M., CLAESSON-WELSH, L. & ALITALO, K. 2000. Regulation of angiogenesis via vascular endothelial growth factor receptors. *Cancer Res,* 60**,** 203-12.

VLAHAKIS, N. E., YOUNG, B. A., ATAKILIT, A. & SHEPPARD, D. 2005. The lymphangiogenic vascular endothelial growth factors VEGF-C and -D are ligands for the integrin alpha9beta1. *J Biol Chem,* 280**,** 4544-52.

WAKHLOO, A. K., LIEBER, B. B., SIEKMANN, R., EBER, D. J. & GOUNIS, M. J. 2005. Acute and chronic swine rete arteriovenous malformation models: hemodynamics and vascular remodeling. *AJNR Am J Neuroradiol,* 26**,** 1702-6.

WALMSLEY, S. R., PRINT, C., FARAHI, N., PEYSSONNAUX, C., JOHNSON, R. S., CRAMER, T., SOBOLEWSKI, A., CONDLIFFE, A. M., COWBURN, A. S., JOHNSON, N. & CHILVERS, E. R. 2005. Hypoxia-induced neutrophil survival is mediated by HIF-1alpha-dependent NF-kappaB activity. *J Exp Med,* 201**,** 105-15.

WALTENBERGER, J., CLAESSON-WELSH, L., SIEGBAHN, A., SHIBUYA, M. & HELDIN, C. H. 1994. Different signal transduction properties of KDR and Flt1, two receptors for vascular endothelial growth factor. *J Biol Chem,* 269**,** 26988-95.

WANG, G. L., JIANG, B. H., RUE, E. A. & SEMENZA, G. L. 1995. Hypoxia-inducible factor 1 is a basic-helix-loop-helix-PAS heterodimer regulated by cellular O2 tension. *Proc Natl Acad Sci U S A,* 92**,** 5510-4.

WANG, G. L. & SEMENZA, G. L. 1995. Purification and characterization of hypoxia-inducible factor 1. *J Biol Chem,* 270**,** 1230-7.

WANG, H. U., CHEN, Z. F. & ANDERSON, D. J. 1998. Molecular distinction and angiogenic interaction between embryonic arteries and veins revealed by ephrin-B2 and its receptor Eph-B4. *Cell,* 93**,** 741-53.

WANG, R., LIU, K., CHEN, L. & AIHARA, K. 2011. Neural fate decisions mediated by trans-activation and cis-inhibition in Notch signaling. *Bioinformatics,* 27**,** 3158-65.

WANG, Y., LAM, K. S., YAU, M. H. & XU, A. 2008. Post-translational modifications of adiponectin: mechanisms and functional implications. *Biochem J,* 409**,** 623-33.

WEBB, J. D., MURANYI, A., PUGH, C. W., RATCLIFFE, P. J. & COLEMAN, M. L. 2009. MYPT1, the targeting subunit of smooth-muscle myosin phosphatase, is a substrate for the asparaginyl hydroxylase factor inhibiting hypoxia-inducible factor (FIH). *Biochem J,* 420**,** 327-33.

WEINSTEIN, B. M. & LAWSON, N. D. 2002. Arteries, veins, Notch, and VEGF. *Cold Spring Harb Symp Quant Biol,* 67**,** 155-62.

WEIS, S. M. & CHERESH, D. A. 2005. Pathophysiological consequences of VEGF-induced vascular permeability. *Nature,* 437**,** 497-504.

WENGER, R. H., STIEHL, D. P. & CAMENISCH, G. 2005. Integration of oxygen signaling at the consensus HRE. *Sci STKE,* 2005**,** re12.

WIESENER, M. S., MUNCHENHAGEN, P. M., BERGER, I., MORGAN, N. V., ROIGAS, J., SCHWIERTZ, A., JURGENSEN, J. S., GRUBER, G., MAXWELL, P. H., LONING, S. A., FREI, U., MAHER, E. R., GRONE, H. J. & ECKARDT, K. U. 2001. Constitutive activation of hypoxia-inducible genes related to overexpression of hypoxia-inducible factor-1alpha in clear cell renal carcinomas. *Cancer Res,* 61**,** 5215-22.

WILKINS, S. E., HYVARINEN, J., CHICHER, J., GORMAN, J. J., PEET, D. J., BILTON, R. L. & KOIVUNEN, P. 2009. Differences in hydroxylation and binding of Notch and HIF-1alpha demonstrate substrate selectivity for factor inhibiting HIF-1 (FIH-1). *Int J Biochem Cell Biol,* 41**,** 1563-71.

WILKINS, S. E., KARTTUNEN, S., HAMPTON-SMITH, R. J., MURCHLAND, I., CHAPMAN-SMITH, A. & PEET, D. J. 2012. Factor inhibiting HIF (FIH) recognizes distinct molecular features within hypoxia-inducible factor-alpha (HIF-alpha) versus ankyrin repeat substrates. *J Biol Chem,* 287**,** 8769-81.

WILKINSON, R. N., KOUDIJS, M. J., PATIENT, R. K., INGHAM, P. W., SCHULTE-MERKER, S. & VAN EEDEN, F. J. 2012. Hedgehog signalling via a calcitonin receptor-like receptor can induce arterial differentiation independently of VEGF signalling in zebrafish. *Blood*.

WILLIAMS, C. K., SEGARRA, M., SIERRA MDE, L., SAINSON, R. C., TOSATO, G. & HARRIS, A. L. 2008. Regulation of CXCR4 by the Notch ligand delta-like 4 in endothelial cells. *Cancer Res,* 68**,** 1889-95.

WILTING, J., CHRIST, B., BOKELOH, M. & WEICH, H. A. 1993. In vivo effects of vascular endothelial growth factor on the chicken chorioallantoic membrane. *Cell Tissue Res,* 274**,** 163-72.

WONG, K., ELEGANTE, M., BARTELS, B., ELKHAYAT, S., TIEN, D., ROY, S., GOODSPEED, J., SUCIU, C., TAN, J., GRIMES, C., CHUNG, A., ROSENBERG, M., GAIKWAD, S., DENMARK, A., JACKSON, A., KADRI, F., CHUNG, K. M., STEWART, A., GILDER, T., BEESON, E., ZAPOLSKY, I., WU, N., CACHAT, J. & KALUEFF, A. V. 2010. Analyzing habituation responses to novelty in zebrafish (Danio rerio). *Behav Brain Res,* 208**,** 450-7.

WOOD, S. M., GLEADLE, J. M., PUGH, C. W., HANKINSON, O. & RATCLIFFE, P. J. 1996. The role of the aryl hydrocarbon receptor nuclear translocator (ARNT) in hypoxic induction of gene expression. Studies in ARNT-deficient cells. *J Biol Chem,* 271**,** 15117-23.

WYKOFF, C. C., PUGH, C. W., MAXWELL, P. H., HARRIS, A. L. & RATCLIFFE, P. J. 2000. Identification of novel hypoxia dependent and independent target genes of the von Hippel-Lindau (VHL) tumour suppressor by mRNA differential expression profiling. *Oncogene,* 19**,** 6297-305.

XU, A., TSO, A. W., CHEUNG, B. M., WANG, Y., WAT, N. M., FONG, C. H., YEUNG, D. C., JANUS, E. D., SHAM, P. C. & LAM, K. S. 2007. Circulating adipocyte-fatty acid binding protein levels predict the development of the metabolic syndrome: a 5-year prospective study. *Circulation,* 115**,** 1537-43.

XU, A. & VANHOUTTE, P. M. 2012. Adiponectin and adipocyte fatty acid binding protein in the pathogenesis of cardiovascular disease. *Am J Physiol Heart Circ Physiol,* 302**,** H1231-40.

YALCIN, M., AK, F., CANGUL, I. T. & ERTURK, M. 2007. The effect of centrally administered erythropoietin on cardiovascular and respiratory system of anaesthetized rats. *Auton Neurosci,* 134**,** 1-7.

YANG, J., LEDAKI, I., TURLEY, H., GATTER, K. C., MONTERO, J. C., LI, J. L. & HARRIS, A. L. 2009. Role of hypoxia-inducible factors in epigenetic regulation via histone demethylases. *Ann N Y Acad Sci,* 1177**,** 185-97.

YANG, M., CHOWDHURY, R., GE, W., HAMED, R. B., MCDONOUGH, M. A., CLARIDGE, T. D., KESSLER, B. M., COCKMAN, M. E., RATCLIFFE, P. J. & SCHOFIELD, C. J. 2011a. Factor-inhibiting hypoxia-inducible factor (FIH) catalyses the post-translational hydroxylation of histidinyl residues within ankyrin repeat domains. *FEBS J,* 278**,** 1086-97.

YANG, M., GE, W., CHOWDHURY, R., CLARIDGE, T. D., KRAMER, H. B., SCHMIERER, B., MCDONOUGH, M. A., GONG, L., KESSLER, B. M., RATCLIFFE, P. J., COLEMAN, M. L. & SCHOFIELD, C. J. 2011b. Asparagine and aspartate hydroxylation of the cytoskeletal ankyrin family is catalyzed by factor-inhibiting hypoxia-inducible factor. *J Biol Chem,* 286**,** 7648-60.

YAQOOB, N. & SCHWERTE, T. 2010. Cardiovascular and respiratory developmental plasticity under oxygen depleted environment and in genetically hypoxic zebrafish (Danio rerio). *Comp Biochem Physiol A Mol Integr Physiol,* 156**,** 475-84.

YIM, S., CHOI, S. M., CHOI, Y., LEE, N., CHUNG, J. & PARK, H. 2003. Insulin and hypoxia share common target genes but not the hypoxia-inducible factor-1alpha. *J Biol Chem,* 278**,** 38260-8.

YOHENA, T., YOSHINO, I., TAKENAKA, T., KAMEYAMA, T., OHBA, T., KUNIYOSHI, Y. & MAEHARA, Y. 2009. Upregulation of hypoxia-inducible factor-1alpha mRNA and its clinical significance in non-small cell lung cancer. *J Thorac Oncol,* 4**,** 284-90.

YU, A. Y., FRID, M. G., SHIMODA, L. A., WIENER, C. M., STENMARK, K. & SEMENZA, G. L. 1998. Temporal, spatial, and oxygen-regulated expression of hypoxia-inducible factor-1 in the lung. *Am J Physiol,* 275**,** L818-26.

YU, C. H., MOON, C. T., SUR, J. H., CHUN, Y. I., CHOI, W. H. & YHEE, J. Y. 2011. Serial expression of hypoxia inducible factor-1alpha and neuronal apoptosis in hippocampus of rats with chronic ischemic brain. *J Korean Neurosurg Soc,* 50**,** 481-5.

YVAN-CHARVET, L., EVEN, P., BLOCH-FAURE, M., GUERRE-MILLO, M., MOUSTAID-MOUSSA, N., FERRE, P. & QUIGNARD-BOULANGE, A. 2005. Deletion of the angiotensin type 2 receptor (AT2R) reduces adipose cell size and protects from diet-induced obesity and insulin resistance. *Diabetes,* 54**,** 991-9.

ZAGZAG, D., KRISHNAMACHARY, B., YEE, H., OKUYAMA, H., CHIRIBOGA, L., ALI, M. A., MELAMED, J. & SEMENZA, G. L. 2005. Stromal cell-derived factor-1alpha and CXCR4 expression in hemangioblastoma and clear cell-renal cell carcinoma: von Hippel-Lindau loss-of-function induces expression of a ligand and its receptor. *Cancer Res,* 65**,** 6178-88.

ZEHETNER, J., DANZER, C., COLLINS, S., ECKHARDT, K., GERBER, P. A., BALLSCHMIETER, P., GALVANOVSKIS, J., SHIMOMURA, K., ASHCROFT, F. M., THORENS, B., RORSMAN, P. & KREK, W. 2008. PVHL is a regulator of glucose metabolism and insulin secretion in pancreatic beta cells. *Genes Dev,* 22**,** 3135-46.

ZELZER, E., LEVY, Y., KAHANA, C., SHILO, B. Z., RUBINSTEIN, M. & COHEN, B. 1998. Insulin induces transcription of target genes through the hypoxia-inducible factor HIF-1alpha/ARNT. *EMBO J,* 17**,** 5085-94.

ZENG, Q., LI, S., CHEPEHA, D. B., GIORDANO, T. J., LI, J., ZHANG, H., POLVERINI, P. J., NOR, J., KITAJEWSKI, J. & WANG, C. Y. 2005. Crosstalk between tumor and endothelial cells promotes tumor angiogenesis by MAPK activation of Notch signaling. *Cancer Cell,* 8**,** 13-23.

ZHANG, F. L., SHEN, G. M., LIU, X. L., WANG, F., ZHAO, Y. Z. & ZHANG, J. W. 2011. Hypoxia-inducible factor 1-mediated human GATA1 induction promotes erythroid differentiation under hypoxic conditions. *J Cell Mol Med*.

ZHANG, L., LI, L., LIU, H., PRABHAKARAN, K., ZHANG, X., BOROWITZ, J. L. & ISOM, G. E. 2007. HIF-1alpha activation by a redox-sensitive pathway mediates cyanide-induced BNIP3 upregulation and mitochondrial-dependent cell death. *Free Radic Biol Med,* 43**,** 117-27.

ZHANG, N., FU, Z., LINKE, S., CHICHER, J., GORMAN, J. J., VISK, D., HADDAD, G. G., POELLINGER, L., PEET, D. J., POWELL, F. & JOHNSON, R. S. 2010. The asparaginyl hydroxylase factor inhibiting HIF-1alpha is an essential regulator of metabolism. *Cell Metab,* 11**,** 364-78.

ZHENG, X., LINKE, S., DIAS, J. M., GRADIN, K., WALLIS, T. P., HAMILTON, B. R., GUSTAFSSON, M., RUAS, J. L., WILKINS, S., BILTON, R. L., BRISMAR, K., WHITELAW, M. L., PEREIRA, T., GORMAN, J. J., ERICSON, J., PEET, D. J., LENDAHL, U. & POELLINGER, L. 2008. Interaction with factor inhibiting HIF-1 defines an additional mode of cross-coupling between the Notch and hypoxia signaling pathways. *Proc Natl Acad Sci U S A,* 105**,** 3368-73.

ZHONG, H., DE MARZO, A. M., LAUGHNER, E., LIM, M., HILTON, D. A., ZAGZAG, D., BUECHLER, P., ISAACS, W. B., SEMENZA, G. L. & SIMONS, J. W. 1999. Overexpression of hypoxia-inducible factor 1alpha in common human cancers and their metastases. *Cancer Res,* 59**,** 5830-5.

ZWEIFEL, M. E., LEAHY, D. J., HUGHSON, F. M. & BARRICK, D. 2003. Structure and stability of the ankyrin domain of the Drosophila Notch receptor. *Protein Sci,* 12**,** 2622-32.